Studies on megakaryopoiesis and platelet function

Meinders, M.

Publication date
2015
Document Version
Final published version

SUMMARY

Platelets are blood circulating specialized subcellular fragments, which are produced by megakaryocytes. Platelets are essential for hemostasis and wound healing but also play a role in non-hemostatic processes such as the immune response or cancer metastasis. Considering the immediate precursors of platelets, normal megakaryocyte development is essential for normal platelet function. Although much is known about platelet development, some aspects of platelet production remain poorly understood.

Megakaryopoiesis is a complex process whereby the multipotent erythroid/megakaryocyte progenitors that commit their fate from hematopoietic stem cells (HSCs) differentiate into megakaryocytes. During maturation, megakaryocytes undergo several dramatic phenotypical changes including polyploidization and the development of a demarcation membrane system. The purpose of this thesis is to further elucidate novel mechanisms and aspects involved in megakaryopoiesis and the effect they have on platelet function, and how to assess with newly developed tests platelet functional characteristics.

STUDIES ON MEGAKARYOPOIESIS AND PLATELET FUNCTION — *Marjolein Meinders*

Studies on

MEGAKARYOPOIESIS and PLATELET FUNCTION

MARJOLEIN MEINDERS

Studies on MEGAKARYOPOIESIS and PLATELET FUNCTION

MARJOLEIN MEINDERS

The research described in this thesis was performed in the Department of Blood Cell Research, Sanquin Research supported by and Landsteiner Laboratory, Amsterdam Medical Centre, University of Amsterdam, Amsterdam, The Netherlands.

The research described in this thesis was financially supported by Centre for Translational Molecular Medicine, Innovative Coagulation Diagnostics.

Cover
Molecular structure of Platelet Factor 4 (pf4). Mice expressing the cre-lox system with pf4, are proven to be an effective tool for generating megakaryocyte lineage-restricted specific-targeted mutants.

ISBN: 978-94-6295-197-6

Printed by
Uitgeverij BOXPress

Cover design & Layout
Jenny Schavemaker, Studio Kopzorg

Financial support was granted by:
Sanquin Blood Supply Foundation, Amsterdam
Scil animal care company B.V. Oostelbeers

Studies on megakaryopoiesis and platelet function

ACADEMISCH PROEFSCHRIFT

ter verkrijging van de graad van doctor

aan de Universiteit van Amsterdam

op gezag van de Rector Magnificus

prof. dr. D.C. van den Boom

ten overstaan van een door het College voor Promoties ingestelde commissie,

in het openbaar te verdedigen in de Agnietenkapel

op dinsdag 16 juni 2015, te 12.00 uur

door Marjolein Meinders

geboren te Oldenzaal

PROMOTIECOMMISSIE

Promotor:	**Prof. dr. T.W. Kuijpers** Universiteit van Amsterdam
Copromotor:	**Dr. L. Gutiérrez** Sanquin Research
Overige leden:	**Prof. dr. J.C.M. Meijers** Universiteit van Amsterdam
	Prof. dr. C.E. van der Schoot Universiteit van Amsterdam
	Prof. dr. J.J. Voorberg Universiteit van Amsterdam
	Dr. A.B. Meijer Universiteit van Amsterdam
	Prof. dr. J.W.M Heemskerk Universiteit Maastricht
	Prof. dr. J.N.J. Philipsen Erasmus Universiteit Rotterdam

Faculteit der Geneeskunde

OH
O
OH
O
HN
OH
O
O
HN
O
NH
O
O
NH
O
HN
H2N
OH
O
H
N
O
N
H
N
HN
O

TABLE OF CONTENTS

Chapter 1

INTRODUCTION

INTRODUCTION

Platelets are anucleated cells that circulate in the blood, whose primary function is to maintain the body hemostasis and actively participate in wound healing (Figure 1). The first evidence that platelets are essential for normal hemostasis dates back from the early 1900. In this report it was written: "A patient with severe thrombocytopenia is administered in a hospital with bleeding tendencies. After whole blood transfusion, the platelet count increased and bleeding episodes diminished." This was the first official record that low platelet counts were responsible for hemorrhage and prolonged bleeding time.[1] Since then, much research has been done which improved our knowledge about the function and development of platelets.

Figure 1. Scanning electron microscope images of resting, partially activated, and fully activated human platelets

Scanning electron microscope images of resting, partially activated, and fully activated human platelets (from left to right) from "Platelets in pulmonary physiology an pathology" by Kroll et al.[2]

It was much later that the platelet cellular origin was discovered: i.e. the megakaryocyte (Figure 2).[3] Megakaryocytes develop from the hematopoietic stem cells (HSCs) through a set of remarkable phenotypical changes also known as megakaryopoiesis.[4] The regulation of megakaryopoiesis and platelet function is a widely investigated field of research.

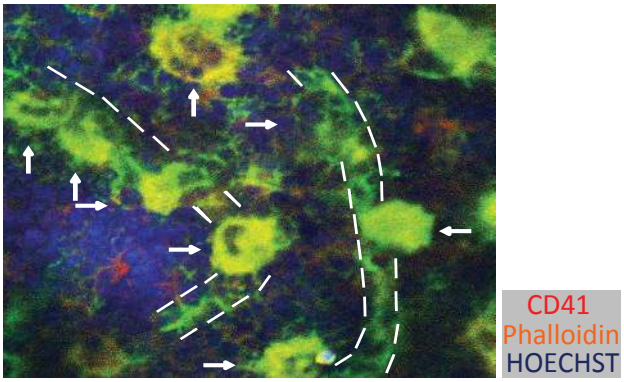

Figure 2. Megakaryocyte in the bone marrow

Picture depicting megakaryocytes (by arrow) within the bone marrow. Megakaryocytes are located near the vessels (dashed). Nuclei are blue. The bone marrow of these mice were flushed, cut into 7 µm coupes and stained with CD41-PE, CD62P-FITC and Hoechst-PB.

HEMATOPOIETIC STEM CELLS AND THEIR NICHES

All blood cells develop from hematopoietic stem cells (HSCs) in the bone marrow, through the commitment of HSCs towards more specialized cell types, including the megakaryocyte, which will ultimately produce platelets. The process of HSCs differentiating into a megakaryocyte is called megakaryopoiesis, and the final process of platelet production is referred to as thrombopoiesis.

Till and McCulloch were the first who showed that bone marrow contained HSCs, which had the capacity to give rise to multiple blood cells and had the ability of self-renewal.[5] HSCs are generated during embryonic development, and the first HSCs within the embryo are located in the Aorta-Gonad-Mesonephros (AGM) region, where they give rise to the first blood cells of embryo origin.[6;7] During embryogenesis, HSCs migrate through various hematopoietic locations, including the fetal liver, the spleen, and ultimately colonize the bone marrow around birth. The migration of HSCs during embryogenesis is commonly seen in many species including flies, amphibians, fish, birds, rodents and humans. In mammalian, the optimal niche for adult hematopoiesis is the bone marrow, which is occupied around birth.[7] Noteworthy, in adults, HSCs can be found in the blood stream in response to stress signals including injury and inflammation.[8;9] It is thought that these stress circulating HSCs, migrate towards the spleen or liver to reside during hematopoietic stress and give rise to an extra hematopoietic production, in a process that is called stress hematopoiesis.[10]

Although HSC location, development and migration in mouse are in many aspects similar to human, one fundamental difference is apparent, in particular after birth. Under normal conditions in humans, hematopoiesis occurs in the bone marrow, whereas after birth in the mouse hematopoiesis is sustained in the bone marrow and the spleen.[11] However, the steady state splenic contribution to the total

hematopoietic pool is different from that of the bone marrow, and is limited mainly to the erythroid and megakaryocytic lineages. Under steady state conditions, lineage-committed progenitors instead of HSCs give rise to these two lineages that are found in the spleen.
Because the bone marrow is the only site of human hematopoiesis and represents the primary site for HSC-derived platelet development in mouse too, most research has focused on the architecture of the bone marrow and the influence it has on HSC development.

Bone marrow
The bone marrow cellular compartment can be divided into two, the hematopoietic cells and the stromal cells.[12] Although the HSCs produce the blood cells, Trentin *et al* demonstrated that stromal cells play an active role in the regulation and differentiation of HSCs.[13] The bone marrow has distinct niches where HSCs reside and this influences the balance between quiescent and cycling HSCs. Although still under debate, the bone marrow has been subdivided into two main niches. The osteoblastic or endosteal niche (which contains the quiescent HSCs), and the vascular niche (which leads to expansion and egress of the HSCs, i.e. cycling HSCs).[14;15] These niches can be recognized and characterized by the presence of a specific balance of cytokines and chemokines, which have the capability of retaining or activating the HSCs. A chemokine involved in HSC migration is CXCL12, also known as SDF-1, which is the ligand of CXCR4.[16] CXCL12 is constitutively produced in the bone marrow by stromal cells and it is a potent regulator of HCS migration.[17] On the other hand, cytokines involved in promoting quiescence include angiopoietin and thrombopoietin.[10] Besides stromal cells, chemokines and cytokines, mature hematopoietic cells, like megakaryocytes, are also known to have a regulatory role in HSC development.[18] This regulation can be both direct, by influencing TPO levels in the bone marrow, i.e. nursing the neighboring HSC,[19] or indirect, by stimulating osteoclast and plasma cell proliferation.[20] Although the different bone marrow niches are recognized by most scientists and there is supportive evidence of their active role, a comprehensive knowledge of all the interactions occurring and needed for proper hematopoiesis at these niche sites is still missing.

Spleen
Although the bone marrow is the primary site of hematopoiesis, extramedullary hematopoiesis can occur in the spleen under hematopoietic stress (and as mentioned before, in the mouse it sustains a part of the hematopoietic production even in the steady state).
Splenic HSCs or multipotent progenitors home to the splenic sinusoid niche, which is comparable to the perivascular niche in the bone marrow. The lack of osteoclasts and osteoblasts in the spleen, and therefore the lack of osteoblastic/endosteal niches, however, suggest that HSCs or MPPs in the spleen might portray a different behavior and differentiation profile compared to bone marrow HSCs.[10] It is important to note, that many of the studies reporting on splenic HSCs, were performed on neonatal mice, and it seems that the splenic HSC pool is reduced or eradicated upon development into adulthood, while committed progenitors persist.

MEGAKARYOPOIESIS

Megakaryopoiesis is the process by which HSC develop into a mature megakaryocyte ready to produce platelets. This process is highly regulated and complicated whereby the megakaryocytes undergo several remarkable phenotypical changes.
The HSCs progressively differentiate into multipotent progenitors (MPPs), followed by megakaryocyte-erythroid progenitors (MEPs), which can mature into either erythrocytes or megakaryocytes. Before megakaryocytes are ready to produce platelets, they go through several phenotypical changes, including increase in size, polyploidization, formation of a demarcation membrane system and the acquisition to package cargo into granules. All these changes are necessary to ultimately produce 100 billion functional platelets each day.[21]

Endomitosis and polyploidization
Megakaryocyte progenitors divide normally, until a specific point in which they undergo endomitosis and become polyploid.[22] Endomitosis is a process whereby DNA replication takes place without cell division.[23] Although the number of endomitotic cycles my range between 2-6 resulting in 4N-64N megakaryocytes, the majority of megakaryocytes undergo three endomitotic cycles.[24]
Although ploidy levels do not correlate with platelet production (as exemplified by the fact that ploidy levels of megakaryocytes at fetal stages are lower than at adult stages), a nonlinear correlation was found in a study in humans between megakaryocyte ploidy and mean platelet volume, where they showed that bone marrow megakaryocytes with an increased ploidy status produce platelets with an increased MPV.[25] However, no other studies have been able to confirm these results, and the exact mechanisms that would link these to parameters remain unknown.[26]

Granules
Platelets contain functional protein cargos that are compartmentalized in three different types of granules, i.e. α-granules, dense granules and lysosomes.[27] Release of these protein cargos upon activation is necessary for the hemostatic and non-hemostatic functions of platelets. These granules contain cargos that have been synthesized by megakaryocytes, or endocytosed by either maturing megakaryocytes or circulating platelets.
α-granules are the most abundant type of granules comprising roughly 10% of the platelet volume. They contain a wide variety of coagulation/adhesive proteins, growth factors and protease inhibitors, involved in both primary and secondary hemostatic mechanisms.[28] These proteins are acquired by endogenous protein synthesis or taken up via endocytosis and pinocytosis.[29] Besides proteins involved in hemostasis, α-granules also contain several membrane proteins that are critical for platelet function including integrin αIIbß3, P-selectin and GPVI. The multi-functional diversity of α-granular proteins are required for promotion of effective local hemostasis, inflammation and ultimately wound repair.[30]
Dense granules or dense bodies are less abundant with approximately 3 to 8 granules per platelet.[31] These granules are involved in activation and contain serotonin, ATP, ADP, calcium, and pyrophosphate.[31] Platelets release their content upon acti-

vation, sustaining thrombus formation amplification signals.[32]
Lysosomes contain digestive enzymes which become active under acidic conditions. The function of lysosomes in platelets remains unknown, although it is thought that acid phosphatase is a procoagulant factor released by activated platelets.[27]

Demarcation membrane system (DMS)
During megakaryopoiesis, one of the most striking transformations is the development of the demarcation membrane system (DMS) also named the invaginated membrane system (IMS) (Figure 3). This extensive network of membrane channels was first reported by Kautz and Marsh and is necessary to increase the membrane content to ultimately give rise to 4000 platelets per megakaryocyte.[33;34] It is already incipiently detected in pro-megakaryocytes but more prominent in mature megakaryocytes.
The DMS develops from the plasma membrane, located between the lobes of the nucleus and it is linked to the cell surface through a tubular membrane connection.[34] Golgi complexes are responsible for further expansion of the extra membrane content.

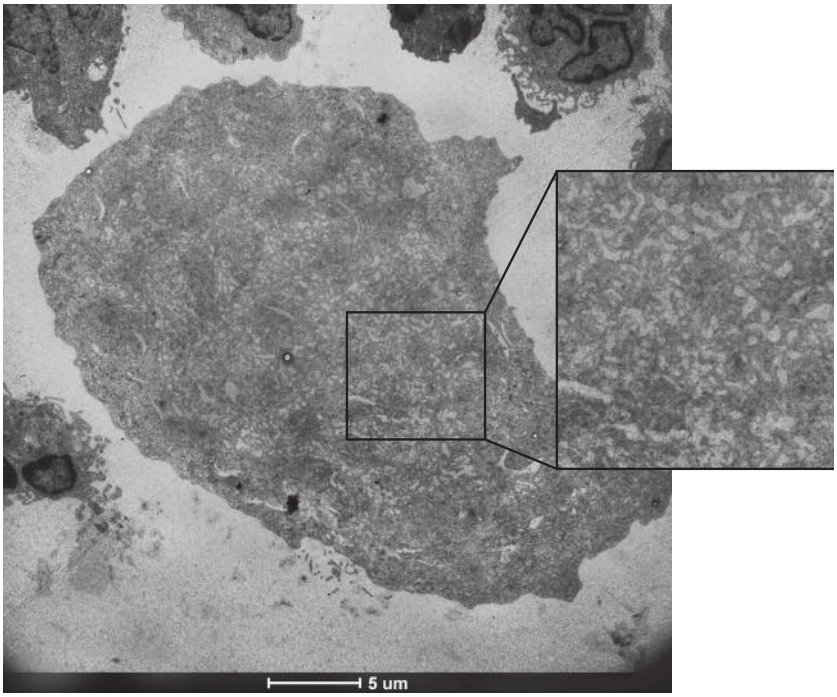

Figure 3. Electron microscopy (EM) picture of a megakaryocyte presenting with fully mature demarcation membrane system

During megakaryopoiesis one of the most striking changes is the development of a demarcation membrane system (DMS), whereby the membrane content is increased creating a highly organized membrane system. The DMS is clearly visible in this cultured mouse megakaryocyte by EM.

CYTOKINES INVOLVED IN HEMATO/MEGAKARYOPOIESIS

Megakaryopoiesis, like other hematopoietic cell lineage differentiation programs, depends on signals received by the HSC, which will induce the commitment towards committed progenitors in order to fulfill the organism needs. These signaling cues are hormones and cytokines that are produced from different sources and synergistically govern HSC differentiation.

Thrombopoietin (TPO)

TPO was first described in 1958,[35] but it was not until 1994 that is was firstly purified.[36] TPO supports the survival and development of immature megakaryocytes, induces their maturation, and stimulates platelet production.[37;38] This hormone is mainly produced by the liver but it is also produced in the kidney, bone marrow stromal cells and megakaryocytes themselves. This notion is supported by the fact that liver failure is often accompanied by thrombocytopenia, due to the stall in TPO liver-production.[37]

The constitutively synthesized TPO enters the circulation, where it binds to its receptor c-MPL, which is present on HSCs, megakaryocytic precursors and megakaryocytes, but also on platelets. Platelets sequester free TPO in plasma, internalize and degrade a portion of the bound TPO, leaving only a small basal level of TPO in the blood stream; in this way, the normal rate of platelet production from megakaryocytes is maintained through the platelet production level itself. A decrease in platelet number, for example, results in higher free TPO levels in plasma, which then induce megakaryocyte proliferation, maturation and ultimately platelet production (Figure 4).[39]

Recently, a secondary mechanism which induces TPO production has been elucidated. Grozovsky *et al* have demonstrated that aged platelets lose sialic acid and thereby are recognized by the Ashwell-Morell receptor in hepatocytes. Binding to this receptor induces TPO production via the JAK/STAT pathway.[40]

Upon binding of TPO to c-MPL receptor present on HSCs and megakaryocytic precursors, three signal transduction pathways are activated including MAPK (mitogen-activated protein kinase), PI3K-AKT (phosphoinositol-3-kinase/AKT) and JAK-STAT (Janus kinase-signal transducer and activator of transcription).[41] By activating these signaling pathways, TPO alone is able to increase megakaryocyte size, increase ploidy status, induce the production of the demarcation membrane system, induce platelet granule production and induce the expression of lineage-specific markers such as glycoprotein GPIb, part of the von Willebrand Factor (VWF) receptor complex and αIIbß3 integrin.[42]

Although TPO is necessary for megakaryocyte maturation, platelet formation and release appear to be TPO-independent and it remains elusive which components are responsible for this final step. This notion is supported by studies in mice, where loss of cMPL or TPO was not enough to abolish completely platelet production[43]. However, a number of other factors have been studied in relation to its contribution to megakaryopoiesis, which are summarized below.

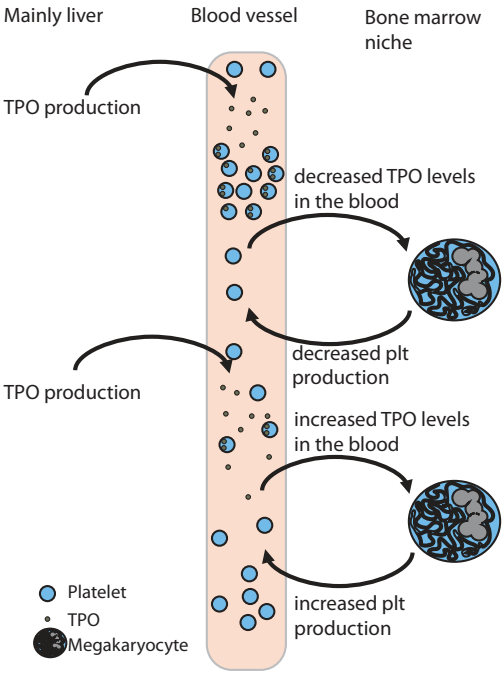

Figure 4. Schematic view of the TPO/platelet production feedback mechanism

Schematic representation of the balance between TPO levels in the blood and platelet production.
TPO is produced mainly by the liver at a constant level and enters the blood flow. Platelets endocytose free TPO from the blood flow thereby decreasing the TPO levels. This decrease in TPO levels reduces megakaryopoiesis and platelet production resulting in a decrease in platelet numbers in the blood.
The decreased numbers of platelets subsequently results in higher levels of free TPO in plasma thereby stimulating megakaryopoiesis and platelet production.

1

Interleukin 11 (IL-11)

IL-11 is a stromal cell-derived cytokine that has multiple effects on the hematopoietic and non-hematopoietic system.[44] The most pronounced effect is, however, on megakaryopoiesis and platelet production. IL-11 acts through IL-11R, which consists of an α chain and a gp130 common subunit.[45] IL-11 administration to thrombocytopenic mice show a rapid increase in peripheral blood platelet count. After IL-11 treatment an increase in megakaryocyte number and ploidy can be observed additionally.[46]

Stromal cell-derived factor-1 (SDF-1) and Fibroblast growth factor-4 (FGF-4)

SDF-1 (CXCL12) and FGF-4 are chemokines regulating megakaryopoiesis in a TPO-independent manner. In *Tpo* or *c-Mpl* knockout mice, administration of SDF-1 and FGF4 can nearly normalize the platelet count.[47] SDF-1 acts through its receptor CXCR4, and FGF-4 through FGFR-4.[48]

Treatment in vitro with FGF-4 leads to the enlargement of megakaryocytes, increased ploidy status, increased demarcation membrane formation, increased GPIIb/IIIa expression and an increase in platelet like particle release.[49]

Stem Cell Factor (SCF)
SCF, also known as 'steel factor' or 'kit ligand', acts through the so-called c-Kit receptor. Although by itself its effect is under debate, it is known to enhance the function of TPO in megakaryopoiesis and platelet production.[50] SCF is produced by virtually every tissue, and its blood levels do not vary with any blood cell counts.[51] Mice defective in SCF suffer from severe thrombocyotopenia.[51]

THROMBOPOIESIS

Although it has been universally accepted that platelets develop from megakaryocytes, the mechanism by which platelets are released from the megakaryocytes is still under debate. Four models have been proposed throughout the last years which include platelet budding, cytoplasmic fragmentation, the lung theory and proplatelet formation theory (Figure 5).

Platelet budding
One of the first theories considering platelet formation was platelet budding. Hereby platelets would pinch off from the megakaryocyte membrane. This theory was based on scanning electron micrographs, but a closer look at the fragments formed, indicated that these were not platelets,[52;53] thereby eliminating this theory as mechanism for platelet formation.

Cytoplasmic fragmentation via the demarcation membrane system (DMS)
This theory was based on the observation that maturing megakaryocytes increased their membrane content, the DMS, whereby defined territories were observed.[54] By an extensive internal membrane reorganization process the platelets would develop and, due to massive fragmentation of the megakaryocyte, individual platelets would be formed.[54] This theory was subsequently dismissed by Haley *et al*, based on phase-contrast microscopically observations.[55]

Lung theory
Aschoff *et al* first identified megakaryocytes in the lungs, and subsequent studies have identified megakaryocytes in the lungs of rabbits, rats and mice.[56;57] He proposed the hypothesis that megakaryocytes originate in the bone marrow, migrate through the endothelial furrows in marrow vessels into the circulation and are carried to the lungs where they are trapped in the pulmonary capillary or sinusoid bed. Through blood flow mechanical forces, they form long extensions which will ultimately form the platelets.[57] Although this theory has convincing evidence, the critical point remains to be whether the shear in pulmonary vessels is favorable enough to induce platelet production.

Proplatelet theory

Currently, the most widely accepted mechanism is the proplatelet theory.[21] This theory was introduced by Becker and DeBruyn[58] and states that megakaryocytes form long cytoplasmic processes called proplatelets.[21] The mechanism of proplatelet formation is therefore highly dependent on the megakaryocyte cytoskeleton proper functioning.

The proplatelets function as an assembly line, whereby individual platelets can be recognized as platelet-size swellings along the thin filaments. These processes can extend into the bone marrow vascular sinusoids, were individual platelets are released by shear stress caused by the blood flow.[21]

The release of proplatelets is described to be a two-step process. First, the impact of blood shear forces helps separating proplatelet fragments from the megakaryocytes, named preplatelets, as described by Junt *et al*.[59] These preplatelets are a fragment of a proplatelet, which turns on itself and has the appearance of a headphone. There are two hypotheses how these preplatelets develop into mature platelets. Thon *et al* stated that the circulating preplatelets form mature platelets by fast rounds of abscissions.[60] However, Howell *et al* showed that preplateles become trapped in the microcapillaries of the lung and due to shear forces the preplatelets convert into mature platelets.[61]

Although *in vivo* vcproplatelet production has already been observed in 1969 by Behnke *et al*[62], and recently with multiphoton intravital microscopy by Junt *et al*[59] we have insufficient understanding of the signals that trigger and regulate proplatelet formation and ultimately platelet production.

ß1-tubulin is the main tubulin isoform in megakaryocytes and most abundant in proplatelets. However, mice lacking ß1-tubulin, which are unable to form proplatelets, still have circulating platelets.[63] This suggests that although proplatelet formation is probably the main contributing process favoring platelet production, it is not an essential one.

Although substantial progress has been made in the recent years on the mechanism that regulates megakaryopoiesis, many questions have remained unanswered, including which are the regulators of proplatelet formation and platelet release.

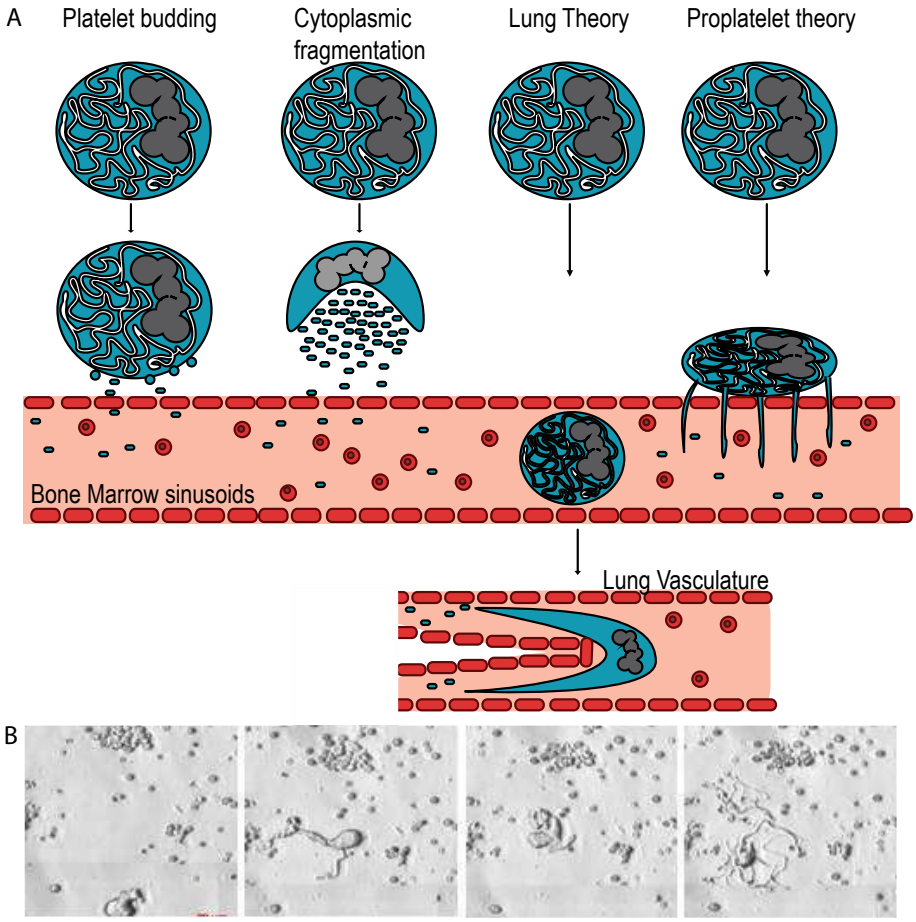

Figure 5. Schematic overview of platelet production theories

A) Scheme depicting the four main platelet formation theories through history. On the left the platelet budding theory is depicted, whereby individual platelets are released from the megakaryocytes. The cytoplasmic fragmentation theory presumes that the megakaryocyte disintegrates in the bone marrow, thereby producing thousands of platelets at once. The lung theory states that the complete megakaryocytes will migrate to the lung vasculature, where it will get stuck. Shear stress will, subsequently release individual platelets from the megakaryocyte. Currently the widely accepted platelet production theory is depicted on the far right. Following this theory, megakaryocytes migrate to the bone marrow vessel where they will protrude long extensions (i.e. proplatelets) through the vessel wall. Subsequently the shear stress will release individual platelets (through a preplatelet stage).

B) A series of still pictures of a megakaryocyte forming proplatelets

TRANSCRIPTION FACTORS AND MEGAKARYOPOIESIS

A complex network of transcription factors regulates the differentiation of HSCs into MEPs and, ultimately, megakaryocytes. Transcription factors recognize a specific motif in the promoter region of genes. By binding this motif they activate or suppress the expression of a specific set of genes and thereby contributing to the lineage-specific cell differentiation.[64]
Transcription factors involved in megakaryopoiesis include RUNX1, FLI1, TAL1, GATA1, NF-E2, SP1 and SP3, amongst others.[65]

Runt-related transcription factor 1(Runx1)
In mice, Runx1, previously known in humans as AML1, is constitutively expressed in all hematopoietic lineages, except for mature erythrocytes, and is critical for megakaryopoiesis.[20] Runx1 is known to regulate cytokine receptors, cytokines and megakaryocyte-specific genes like Pf4.[66] Runx1-deficient mice die in utero around day 12.5 due to a lack of definitive hematopoiesis.[22] Although Runx1 is necessary in the initiation of adult hematopoiesis, continuous expression is not required for the maintenance of HSCs in adult mice.[67]
Besides its role in early hematopoiesis, Runx1 is essential in megakaryocyte differentiation.[24] Megakaryocyte conditional knockout mice show an increase in megakaryocyte numbers, but they seem to be underdeveloped.[24] They are small, show a decrease in ploidy and an underdeveloped demarcation membrane system.[24]
Heterozygous germline mutations in human *RUNX1* lead to a familial platelet disorder with a predisposition to acute myeloid leukemia.[25] Patients suffer from thrombocytopenia with an impaired platelet function.

Friend leukemia virus integration 1 (Fli1)
Fli1 is a member of the ETS transcription factor family and has an activating effect when bound to its DNA motif.[26] It is involved in vasculogenesis, hematopoiesis and cell adhesion.[68] whereby it activates genes including those encoding VE-CAD,[69] ICAM[70;71] and megakaryocyte-specific genes encoding αIIb, GpIX, von Willebrand factor and Pf4.[30-33]
Mice generated with a homozygous germline mutation in *Fli1* are not viable after E12.5 due to internal hemorrhaging. Furthermore, fetal liver-derived megakaryocytes cultured ex-vivo are underdeveloped.[68]
Hemizygous loss of *FLI1* in humans leads to Jacobsen Syndrome, causing thrombocytopenia due to a maturation blockade during megakaryopoiesis that leads to the accumulation of small-sized megakaryocytes.[72]

T-cell acute lymphocytic leukemia 1 (Tal1)
In mouse, Tal1, also known in humans as SCL, is part of the helix-loop-helix family of transcription factors and is involved at several levels in the hematopoietic hierarchy.[73] It can both function directly by binding to its DNA motif, or indirectly by forming a complex with different transcription factors.[74]
Although direct targets remain unclear, megakaryocyte-specific *Tal1* knockout mice show that it is critically required for key aspects of megakaryocytic develop-

ment including megakaryocyte proliferation, polyploidization and the formation of a demarcation memebrane.[37] In addition, these mice show that Tal1 is involved in platelet formation but not function.
Patients have been identified in which SCL is inappropriately expressed leading to T-cell acute lymphoblastic leukemia (T-ALL).[75] Although these patients suffer from severe T-cell abnormalities, they seem not to have any defect in megakaryopoiesis or platelet function.[75]

Nuclear factor-erythroid 2 (Nfe2)
In mice, Nfe2 is a transcription factor expressed in erythroid, megakaryocytes and mast cells, similar to human NFE2. It is thought to have a prominent role in the last step of megakaryopoiesis by directly regulating ß1-tubulin, and when knocked-out, reduction of ß1-tubulin leads to a decreased platelet production.[37] Mouse models indicate that a complete loss of Nfe2 protein results in megakaryocytes that are unable to form platelets resulting in absolute thrombocytopenia.[41]
Interestingly, in contrast to most transcription factors where loss results in the ablation in one or more blood cell lineages, Nfe2 seems specific to megakaryocyte maturation.[76] In humans, genetic aberrations in *NFE2* have only been identified thus far as somatic mutations, associated with polycythemia vera, essential thrombocytosis and myelofibrosis.

Gata-binding factor 1 (Gata1)
Gata1 is a zinc finger transcription factor highly expressed in multipotent progenitors, erythroid cells, mast cells, dendritic cells and megakaryocytes.[64] It is one of the first transcription factors characterized involved in hematopoiesis and it is widely investigated in both human and mouse.[77]
Mouse models and point mutations in the human genome have given us insight on the function of Gata1. Since *Gata1*-null embryos die from severe anemia between embryonic day 10.5 (E10.5) and E11.5, targeted mice were generated to study in depth its contribution to different hematopoietic lineage differentiation programs.[43]
Different mouse models were generated to investigate the function of Gata1 in megakaryopoiesis. In *Gata1.05/X* heterozygous female mice, an erythroid promoter-specific knockdown of Gata1, it was shown that Gata1 was necessary for terminal differentiation of the erythroid and megakaryocytic lineages.[78] This is confirmed by hematopoietic colonies derived from the chimeric yolk sacs.[79] A targeted mutation in regulatory elements within the *Gata1* locus (ΔneoΔHS) resulted in depletion of Gata1 in megakaryocytes and eosinophils and only partially in the erythroid lineage.[80] These mice show severe macrothrombocytopenia and increased proliferation of megakaryocytes. Their platelets had a selective aggregation defected when stimulated with suboptimal concentrations of collagen, and a decreased mRNA expression of GPIb-a and GPIb-b.[81;82] Another approach to study the role of Gata1 in adult hematopoiesis consisted on using conditional inducible Cre-lox system, whereby *Gata1*-lox mice were crossed either with an interferon inducible *Mx1*-Cre or with a tamoxifen-inducible (R26-ERCre) *Cre* mice. Both mouse models confirmed the requirement of Gata1 in megakaryopoiesis in adulthood.[83]

In humans, several mutations affecting the *GATA1* gene have been described which lead to a broad spectrum of defects, including X-linked thrombocytopenia (XLT), X-linked thrombocytopenia with thalassemia (XLTT), congenital erythropoietic porphyria (CEP), and transient myeloproliferative disorder (TMD).[84] All disorders have a mutation in the amino (N)-zinc finger region of GATA1 in common, which might influence either DNA binding directly and/or the interaction with Friend of Gata1 (FOG1), leading to macrothrombocytopenia.[84] Besides these deficiencies, patients with Down syndrome are more likely to develop an acquired, i.e. somatic, *GATA1* mutation leading to a truncated form of GATA1 (GATA1s). This short GATA1 isoform increases the possibility to develop acute megakaryoblastic leukemia (AMKL).[85]
GATA1-binding motifs are abundant in the genome and can be found in the promoter region of many target genes including genes that are relevant during megakaryopoiesis, such as GPIb.[86]

Specificity Protein (Sp1 and Sp3)
Sp1 and Sp3 belong to the family of Specificity protein/Krüppel-like Factor (Sp/KLF), which recognize G-rich promoter elements (GC-box and the related GT-box) and are expressed in most mammalian cell types.[87] Sp1 and Sp3 are structurally similar, with similar affinities for the binding site, and thought that they could be redundant in function.[88]
Sp1 knockout embryos are developmentally retarded and do not survive beyond embryonic day 10.5.[89] *Sp3* null embryos develop throughout gestation but die shortly after birth due to a series of complications including defects in hematopoiesis.[50-52] Sp1/Sp3 compound heterozygous embryos are not viable and display impaired erythroid development, suggesting that a critical threshold of Sp1/Sp3 activity is required for normal embryonic development and that these two proteins have additive effects in regulating downstream target genes.[90]
In humans, SP1 and SP3 can both act as negative or positive regulators of gene expression and there are at least 12,000 Sp1/3 binding sites in the human genome.[48;54] Gene targets of SP1 and SP3 include factors involved in cell cycle progression and arrest, both pro- and anti-angiogenic factors involved in invasion and metastasis, pro- and anti-apoptotic factors involved in genomic stability, proto-oncogene and tumor suppressors.[91] Deregulation of SP1 and SP3 is observed in many cancers and diseases.[91]

Combination of transcription factors
Although single transcription factor knockout mouse models show severe effects on megakaryopoiesis, often the effects of the transcription factors are synergistic.[37] For specific megakaryocyte genes, it is known that more than one transcription factor is needed to regulate the expression of these genes. For instance, GpIX and GpIb-a need activation by both Gata1 and Fli1 for normal expression on megakaryocytes (Figure 6).[39;62]

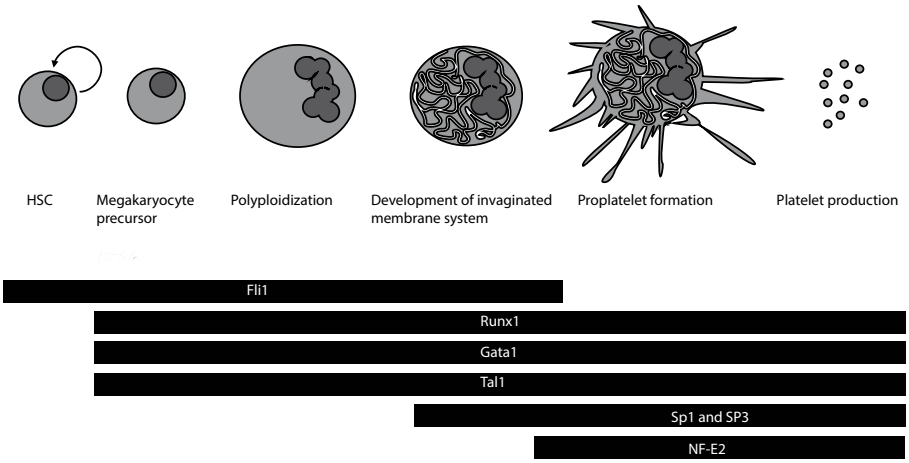

Figure 6. Summary of transcription factors involved in megakaryopoiesis and the synergistic interaction needed for megakaryocyte differentiation

The different transcription factors that are necessary during murine megakaryopoiesis are depicted and positioned at the stages of megakaryocyte differentiation where they are active.

PLATELETS

Platelets were first described in 1873[92] by Osler, when he identified and reported structures rapidly forming aggregates when removed from the blood vessels. In the early 1900 their role in hemostasis was recognized by Duke.[1] In the past years, platelets also have been recognized as effectors in inflammation and regulators in innate and adaptive immunity,[93] but their primary role is to maintain the body hemostasis. This process can be divided into two key mechanisms namely, platelet adhesion and aggregation at the site of vascular injury.

Platelet structure

Platelets are small anucleated blood cells, with a diameter of 2-5ųm and a mean cell volume of 6 to 10 femtoliters.[94] Platelets have a lifespan of 7 to 10 days and are removed from the circulation by the reticuloendothelial system, if they have not exercised their function in hemostasis or thrombus formation.[95]

The exterior of the platelets, also known as glycocalyx, is thicker than that of other blood cells, and is a dynamic structure sensing changes in the vascular compartment.[95]

The internal matrix of platelets consist of an irregular meshwork of microtubules, which support the platelet discoid shape, and an open canalicular system (OCS.)[96] The OCS serves as a pathway for transport of substances into the platelet and for discharge of α-granule products secreted during platelet activation.[97] When platelets are activated, the acto-myosin cytoskeleton constricts, whereby α-granules and dense bodies are secreted to the exterior, where they merge with the sur-

face-connected OCS.[98] Besides release of α-granules, activation initiates shape change and internal transformation, and induces a dramatic alteration in platelet shape (Figure 1).[99]
Besides the three types of secretory granules, as previously described, platelets contain glycosomes, electron-dense chains and clusters, tubular inclusions and mitochondria which are involved in energy metabolism.[98]
Since platelets do not have a nucleus, it is long thought that they are not able to produce new proteins. However, recently it has been suggested that platelets can respond to external signals through the translation of contained mRNA or degradation of proteins, since they have the machinery needed for protein translation and degradation.
During the last stages of megakaryopoieisis, an enormous increase in transcriptional activity is noted, which leads to thousands of mRNAs that can serve as templates for protein synthesis during thombopoiesis.[100] Although still under debate what the fate of these mRNAs is, there is compelling evidence that megakaryocytes transfer their mRNA to platelets.[30] The regulation of these mRNAs in thrombopoieisis remains, however, elusive.

HEMOSTASIS

The primary, and most investigated role of platelets, is their role in hemostasis, which is recognized by bleeding problems in thrombocytopenic patients.[101] Hemostasis, the process which stops bleeding, can be divided in three stages, namely localized vasoconstriction, primary hemostasis and secondary hemostasis, which ultimately leads to the formation of a permanent fibrin plug.[102]
The first response after vascular damage is a local neurogenic response of vasoconstriction mediated by endothelin. Although this potent vasoconstrictor causes a strong effect, the vasoconstriction is transient and primary hemostasis is required for bleeding to stop.[102]

Primary hemostasis
The goal of primary hemostasis is to form an initial platelet plug, which rapidly stabilizes the vascular injury. During primary hemostasis, platelets experience a set of changes including adhesion, granule release and aggregation.
Under high shear, von Willebrand Factor (VWF) is responsible for adhesion of platelets to the injured vessel wall.[103] VWF, which is secreted by platelets and endothelial cells, creates a bridge between the exposed collagen and platelets, thereby initiating a surface for platelets to bind.[101] This initial contact facilitates binding of collagen to GPVI, which induces platelet activation.[104]
Activated platelets release their α and dense granule-contents in the blood stream. The release of substrates and recognition by platelets enhances platelet activation, which creates a positive feedback loop, and results in activation of integrins, mainly αIIbβ3.[102] The activated integrin can bind to their ligand including fibrinogen, creating an initial plug.[105]

Secondary hemostasis

The goal of secondary hemostasis, also known as the coagulation cascade, is to form a stable fibrin clot at the site of vascular injury. The coagulation cascade consists of a sequence of proteolytic enzymes, activated when cleaved. Tissue factor initiates the cascade leading to the activation of fibrin, which is vital for a stable clot.[102] As explained before, the release of platelet lysosomal contents might also contribute to this secondary response, as it has been demonstrated the procoagulant role of platelet acid phosphatase.

PLATELETS AND THE IMMUNE SYSTEM

The role of platelets in the immune response has been recognized for at least four decades, but it has gained little acceptance until recently.[106] Due to their extreme high numbers in the blood and their ability to release chemo-attractants, inflammatory mediation and the ability to directly bind to bacteria, platelets are thought to play an active role in immunity.[107]

Substantial evidence places platelets at the crossroads between innate immunity and inflammation responses. Patients with severe bacterial or viral infections are thrombocytopenic, and circulating platelet-leukocyte aggregates are a hallmark feature of sepsis.[108]

Activated platelets are capable of directly binding to neutrophils leading to neutrophil degranulation and enhanced phagocytosis.[109] Furthermore, platelets are the largest source of CD40L, which induces reactive oxygen species (ROS) production, activates macrophages and induces optimal cytotoxic T cell and B cell activation in response to infection.[110] It has also been demonstrated that CD40L upregulates the expression of E-selectin, ICAM-1 and VCAM on endothelial cells and induces secretion of chemokines by these cells.[111]

Besides modulating the immune response, platelets directly participate in the immune system by capturing pathogens. They have also been suggested to induce neutrophil extracellular traps (NETs) by binding to neutrophils, and are suggested to have the capacity to phagocytose bacteria through their FcyRIIa receptor although this does not result in bacterial killing by the platelets[112] This can, as a result, lead to a pool of viable bacteria intracellular of platelets, and thereby are protected from the immune system. This could cause infective endocarditis.[113]

Platelet receptors

Receptors on the platelet surface determine the reactivity of platelets with a wide range of agonists and adhesive proteins. Most of the receptors are involved in hemostasis, whereby ligation of the receptor results in activation of the platelet or platelet adhesion to the damaged vessel wall.

The receptors can be divided by structural class, including integrins, leucine-rich repeat family receptors, seven transmembrane receptors and the immunoglobulin superfamily (Figure 7).

Integrins

Integrins are receptors involved in cellular adhesion and migration.[114] They consist of an α and ß-subunit, which are non-covalently associated. They mediate cell-cell and cell-matrix interactions and have two affinity states, namely the high affinity and low affinity. On platelets, ß3 (αIIbß3, αVß3) and ß1 (α2ß1, α5ß1, α6ß1, α8ß1) integrins are expressed, whereby αIIbß3 is the predominant protein on the platelet surface.[115]

αIIbß3 (GPIIbIIIa)

αIIbß3 is exclusively expressed on platelets and megakaryocytes, and is the major plasma membrane protein. It can bind multiple ligands, including fibrinogen, fibronectin, vitronectin, thrombospondin-1 and VWF through their RGD (Arg-Gly-Asp) peptide sequence.[116]

Binding of αIIbß3 to its ligand, mediates platelet adhesion and aggregation, but also activates a cascade of events (outside-in signaling) which leads to platelet spreading, granule secretion, stable adhesion and clot retraction.[117]

αIIbß3 receptor can have two extreme conformations: a bent state and an extended state. Hereby is the bent conformation a low affinity resting state and the extended state has a high-affinity for its ligand.[118] The intracellular signaling mechanism that induces this change, is referred to as inside-out signaling.[119] Inside-out signaling relies on the binding of Talin and Kindlins to the cytoplasmic domain of ß3, and is activated by platelet adhesion or G-protein-coupled receptors.[120]

α2ß1(GPIaIIa)

α2ß1 is the second most important platelet integrin, and is a major collagen adhesion receptor. Like αIIbß3, α2ß1 is expressed in a low-affinity state on resting platelets. Through inside-out signaling this state can change into a high-affinity state, resulting in binding to collagen. Unlike αIIbß3, α2ß1 is present on many different cell types and blocking of this receptor will not have an antithrombotic effect.[121]

Leucine-Rich Repeat family (LRR)

These receptor family members are characterized by the presence of a LRR domain, which is a structural motif that forms an α/ß horseshoe fold and is rich in leucine.[122] Two LRR receptors are present on platelets, namely the GPIb-IX-V complex and the Toll-like receptors (TLRs).

GPIb-IX-V complex

In high sheer stress condition, like in arteries and arterioles, the initial platelet adhesion to the vessel wall is dependent on GPIb-IX-V complex and its agonist von Willebrand factor (VWF).[120] Activation of this receptor initiates inside-out signaling whereby activating the integrin receptors.

Toll-like receptors (TLRs)

TLR1-9 are known to be expressed by both human and mouse platelets, although not all are functional.[123] Since TLRs are known for their function in immunity, their presence on platelets indicates that platelets have a role in immunity. TLR4

is critical for LPS-induced thrombocytopenia,[117] and new evidence suggests that platelets play a vital role in binding bacteria through TLR4 and present these to neutrophils.[124]

Seven Transmembrane Receptors (G protein-coupled receptors)
Seven transmembrane receptor family is the largest group of receptors and are ubiquitously expressed. Members of this family include receptors for hormones, neurotransmitters, and chemokines.[125] On platelets this group of receptors is well represented.[126]

Protease activation receptor (PAR)
PAR1 was the first receptor identified, and it is activated when thrombin binds to it and cleaves its amino-terminal exodomain.[127] This new N-terminus, by refolding, acts as a ligand for the receptor.[128] PAR3 responds, like PAR1, to subnanomolar concentrations of thrombin. PAR4 requires higher levels of thrombin, and PAR2 is activated by trypsin.[128]
PAR1 can activate heterotrimeric G-proteins of the G12/13, Gq and Gi/z families. Upon activation, platelet responses range from granule secretion, to integrin activation and aggregation.[129]

P2Y
The P2Y1 and P2Y12 are activated by ADP, which leads to the activation of phospholipase C (PLC). Although ADP is the first known aggregating agent, it induces mild platelet aggregation and shape change compared to other agonists.[130]

ITAM or (hemi) ITAM receptors
The immunoglobulin superfamily is involved in recognition, binding or adhesion processes and the receptors share structural features with immunoglobulins.

GPVI
GPVI is one of the members of the immunoglobulin superfamily, and is the receptor for collagen and convulxin. Convulxin, a mortipherous venom from the snake *Crotalus durissus terrificus* targets GPVI causing imminent death through activation of platelets. GPVI stimulation induces activation of Syk, which in turn initiates a downstream signaling cascade. It is suggested that GPVI has a primary role under low/no flow conditions.[131]

C-type lectin-like receptor (Clec2)
Clec-2 is a hemi-ITAM-containing receptor for podopolanin which is expressed on podocytes, lymphatic endothelial cells and megakaryocytes.[131] GpVI and Clec2 are identified to have a critical role in vascular integrity at sites of inflammation.[132] Furthermore, it has been demonstrated recently that the expression of Clec2 in platelets is required for proper lymph-blood separation during murine development.[133]

FcgRIIa
FcgRIIa is the most widely distributed Fcg receptor in nature, and is predominant-

ly expressed on neutrophils, monocytes, macrophages and platelets.[134] It is a low affinity IgG receptor and has an intracellular ITAM motif.[134] Binding to bacteria induce platelet aggregation, and it plays an important role in *αIIbß3*-mediated platelet spreading on fibrinogen.[135] However, this receptor is not present in mouse platelets.

SHARING THE SIGNALING PATHWAYS

Platelets become activated through the interaction between the agonist and its specific receptor. Although this interaction is specific, some receptors share the same components of the signal transduction pathway. For example, Clec2 and GpVI share the internal signaling pathway whereby Syk is activated, which ultimately leads to PLCg2 activation (Figure 7).[136]
Unfortunately, the internal signaling pathway of most receptors is not completely described yet.

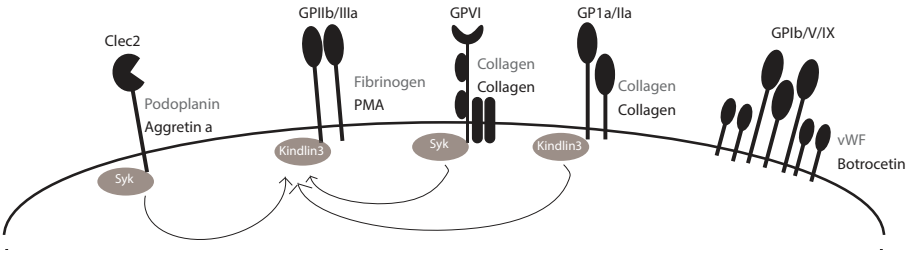

Figure 7. Overview of platelet receptors and known co-factors

Figure depicting some of the major receptors present on mouse platelets. Where Clec2 and GpVI and GpIa/IIa and GpIIb/IIIa share common internal signaling molecules, GpIb/V/IX appears to be Syk- and Kindlin3-independent.

INHERITED PLATELET DISORDERS (IPD)

As mentioned before, the production and function of platelets is a highly regulated process and mutations in genes involved at essential steps in megakaryopoiesis could lead to thrombocytopenia or platelet functional abnormalities. Patients suffering from inherited platelet disorders (IPD) typically present mucocutaeous bleeding symptoms, including easy bruising, purpura and gingival bleeding.[137]
The classification of IPDs is based according to the defective pathways or processes affected during megakaryopoiesis, i.e. defective transcriptional regulation, defective Tpo signaling, defective cytoskeletal organization, defects in platelet granule formation, defects in glycoprotein signaling and defects in G protein-coupled receptor signaling, see Figure 8.
Transcriptional regulation defects in humans include mutations in *GATA1*, *FLI1* and *RUNX1* as discussed above.

A loss of function mutation in the gene encoding the TPO receptor c-MPL leads to congenital amegakaryocytic thrombocytopenia (CAMT).[138] CAMT is an autosomal recessive disorder which presents at birth with severe thrombocytopenia and increased TPO plasma levels.[139] A defect in TPO signaling is seen in thrombocytopenia with absent radius (TAR) syndrome which is caused by a mutation in *RBM8A*.[140] TAR is relatively uncommon and characterized by hypomegakaryocytic thrombocytopenia, the absent of radii and is congenital or has an early-onset.[141]

In humans, a defect in the cytoskeletal organization could be due to a mutation in myosin heavy chain (*MYH*),[142] filamin (*FLN*)[143] or tubulin beta 1 (*TUBB1*).[144] These mutations generally induce thrombocytopenia, due to alterations in the megakaryocyte and platelet structure. MYH9-related disease (MYH9-RD) is caused by a mutation is MYH9, the gene for heavy chain of non-muscle myosin IIa, and is one of the most frequent forms of inherited thrombocytopenia. MYH9-RD causes a defect in megakaryocyte maturation and platelet formation leading to mild thrombocytopenia. It is easily diagnosed by the giant platelets in peripheral blood.[145] Filamin-A (*FLNA*) mutations can lead to a wide spectrum of disorders, and patients typically have macrothombocytopenia with enlarged α-granules and abnormalities in platelet function.[146]

IPD characterized by a defect in granule formation are generally called storage pool diseases. Next-generation sequencing identified a mutation in *NBEAL2*, leading to gray platelet syndrome (GPS).[147] GPS is identified by macrothrombocytopenia, an absence of α-granules and a varying degree of bleeding tendency.[146]

IPDs caused by mutations in glycoprotein receptors or mutations affecting the GP response include Bernard-Soulier syndrome (BSS) and platelet-type von Willebrand disease (PT-VWD).[148] PT-VWD is caused by a mutation in *GPIBA*, which could lead to increased binding to VWF and spontaneously agglutination.

The last group includes IPD due to mutations in G protein-coupled receptors, which generally lead to signaling defects.

Although due to new diagnostic tools, in recent years more diseases have been characterized which increases our understanding of platelet function and are important for the development of novel therapeutic drugs; however, a large number of patients with IPD still do not receive a genetic diagnosis. Fortunately, next-generation sequencing (NGS) technologies have become less expensive and are vastly emerging in the platelet research field. This technique can facilitate the identification of genetic defects of patients with previous unknown IPDs by exome sequencing. A limitation of this approach is, however, that causative gene defects in non-coding regions or defects in the transcription factor region are generally overlooked.[149]

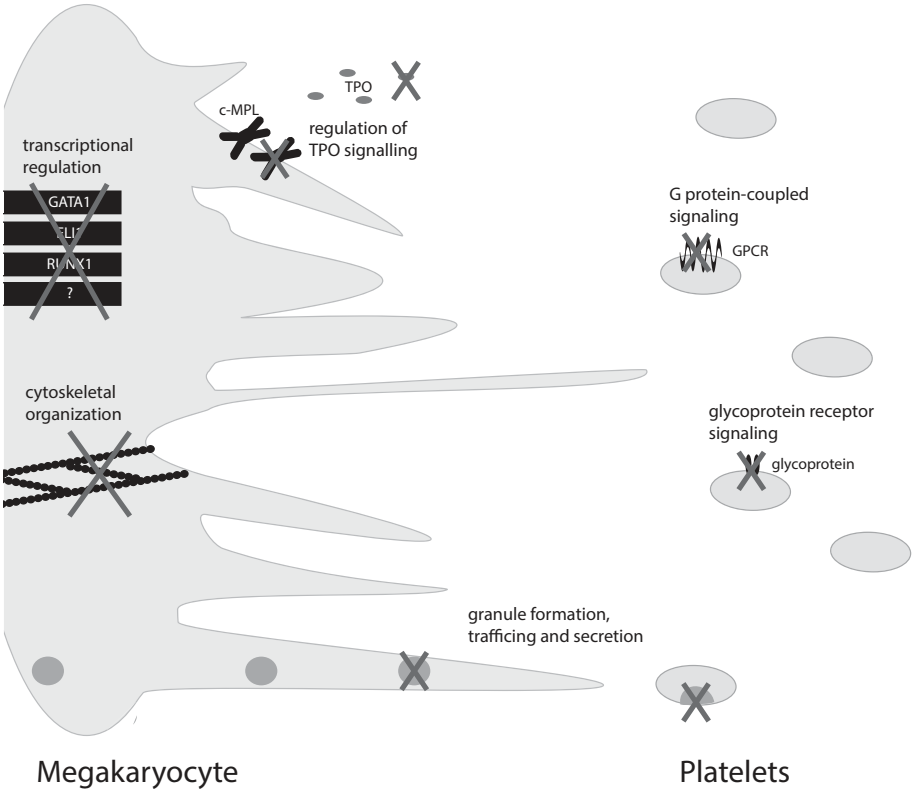

Figure 8. An overview of inherited platelet disorders (IPD)

The classification of IPD is based on the affected pathway. These include transcription factor, TPO signaling, granule formation and secretion, G protein-coupled signaling and glycoprotein receptor signaling.

	Gene name	Disorder name
Transcription factors	*GATA1*	macrothrombocytopenia with dyserythropoiesis
	FLI1	Paris-Trousseau thrombocytopenia Jacobson syndrome
	RUNX1	Familial platelet disorder
	FGFI1B	macrothrombocytopenia with dyserythropoiesis
Regulation of TPO signalling	*MPL*	Congenital amegakaryocytic thrombocytopenia
	RBM8A	Thrombocytopenia-absent radius syndrome

Cytoskeletal proteins	*MYH9*	MYH9-related diseases
	FLNA	Filaminopathy
	TUBB1	Autosomal dominant macrothrombocytopenia
	WASP	Wiskott-Aldrich syndrome
Granule formation, trafficking and/or secretion	*NBEAL2*	Gray platelet syndrome
	VSP33fB	Arthrogryposis
	HPS1, HSP3, HSP4, HSP5, HSP6, AP3B1, BLOCK1S3, BLOC1S6, DTNBP1	Hermansky Pudlak
Glycoprotein receptors and their signaling pathways	*ITGA2B*	Glanzmann thrombastenia
	GP9	Bernard Soulier Syndrome
	GP1BA	Platelet-type von Willebrand disease
	VWF	vond Willebrand disease type 2B
G-protein-coupled receptors and their signaling pathways	*TBXA2R*	Thromboxane receptor defect
	TBXAS1	Ghosal hematodiaphyseal dysplasia syndrome

Table 1. Compilation of bleeding phenotypes related to IPD

This table describes a selection of major disorders and their gene names. A full list can be found by Freson et al.[137]

PLATELET FUNCTIONAL ASSAYS

To study patients with bleeding disorders, functional tests were developed to diagnose and manage specific platelet conditions. *In vitro* platelet testing mainly involves measuring aggregation capacity or granule release, but also tests involving platelet adhesion or shape change have been developed. There are several ways to

evaluate platelet granule release, including measuring expression of P-selectin or CD63 on the platelet surface which measures the platelet extent of degranulation upon activation. Aggregation assays measures the capacity of platelets to aggregate after stimulation with specific agonists.

The first *in vivo* test used as a diagnostic tool was the bleeding time. This test was the most used screening method of platelet function till 1990.[150] Major disadvantages of this test are poor reproducibility, it is invasive, insensitive and time consuming.[150;151] Despite these shortcomings, this test is still used a first-line clinical screening tool and is particularly useful in identifying patients with severe bleeding tendencies including VWF disease and Glanzmann's thrombasthenia.[152]

In vitro aggregation assays were developed to examine platelet aggregation capacity. Light transmission aggregometry (LTA) was invented in the 1960s and is based on the decrease in light scattering when platelets form aggregates inside a cuvette through which the light passes.[150;153;154] This test requires platelet rich plasma (PRP). Platelet aggregation analysis within diluted whole blood is possible with impedance aggregometry. This method is based on the binding of platelets to two electrodes immersed in the stirring sample when a current is passed through. When an agonist is added, more platelets will bind to the electrodes and an increase in impedance is measured and correlated with platelet aggregation (Figure 9).

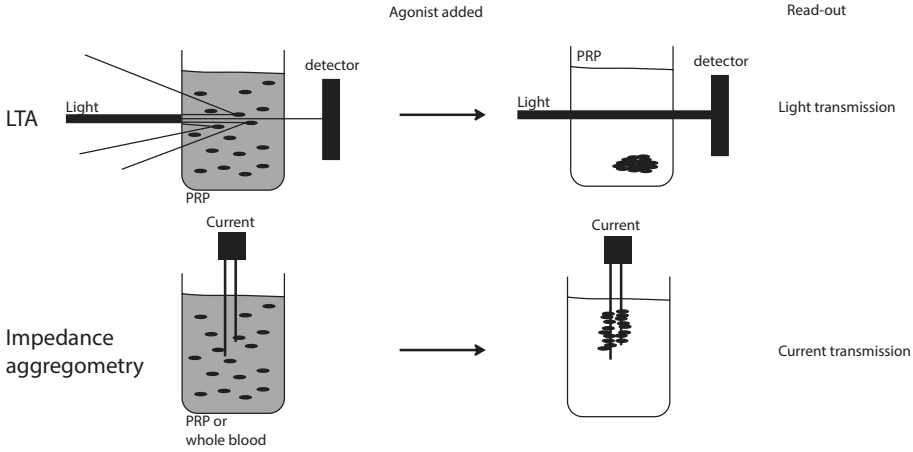

Figure 9. A schematic view of current aggregation methods used

Scheme showing how the two currently most used aggregation methods work. The LTA measures the difference of transmitted light before and after an agonist is added. Impedance aggregometry uses current to see the changes in platelet activity, whereby activated platelets reduce the current.

Common used agonists to activate the platelets include ADP, epinephrine, collagen, arachidonic acid, ristocetin, and thrombin.[155] By using these agonist and combining it with granule release assays, it is possible to characterize specific platelets disorders (table 2).[155]

Despite the vast advantages over bleeding time, which allows us to identify specific platelet deficiencies, both assays have limitations. Where LTA is poorly standardized and large amount of platelets is required for each test, making it problematic for severe thrombocytopenic patients or when working with animals, impedance aggregometry is not suitable for use with thrombocytopenic patient material.[156 157] Clearly, there is a demand for a functional test(s) that do not suffer from these limitations.

Platelet disorder	Defect in platelet function
Bernard-Soulier syndrome	abnormal adhesion
Glanzmann's thrombasthenia	absent aggregation with physiological agonists defective clot retraction
platelet type VWD	abnormal adhesion ↑ sensitivity to ristocetin
α2β1 collagen receptor	abnormal adhesion ↓ response to collagen
GPVI collagen receptor	abnormal adhesion ↓ response to collagen
P2Y12 ADP receptor	abnormal aggregation to ADP
Thrombaxane A2 receptor	absence of response to TXA2 analogues ↓ resopnse to collagen
Scott syndrome	↓procoagulant activity and microparticle release
Wiskott-Aldrich syndrome	↓ aggregation ↓ secretion
Gray platelet syndrome	empty α-granules
Quebec syndrome	abnormal aggregation with epinephrine

Table 2

Short overview of platelet disorders and their defect in platelet function measured in conventional platelet tests.[155]

SCOPE OF THE THESIS:

- To develop a new method to measure platelet aggregation using very little blood volumes, and that allows the study of the contribution of single-receptors to platelet aggregation (Chapter 2).
- To investigate the contribution of different transcription factors on megakaryocyte development and thrombopoiesis (Chapter 3 and 4).
- To study the contribution of the bone marrow and spleen megakaryopoiesis to stress megakaryopoiesis (i.e. during inflammation) (Chapter 5).

REFERENCE LIST

1. Duke WW. The relation of blood platelets to hemorrhagic disease. By W.W. Duke. JAMA 1983;250:1201-1209.
2. Kroll MH, Afshar-Kharghan V. Platelets in pulmonary vascular physiology and pathology. Pulm.Circ. 2012;2:291-308.
3. PEASE DC. An electron microscopic study of red bone marrow. Blood 1956;11:501-526.
4. Machlus KR, Italiano JE, Jr. The incredible journey: From megakaryocyte development to platelet formation. J.Cell Biol. 2013;201:785-796.
5. Till JE. Proliferation and differentiation of stem cells of the blood-forming system of the mouse. NASA CR-673. NASA Contract.Rep.NASA CR 196769-75.
6. de Bruijn MF, Speck NA, Peeters MC, Dzierzak E. Definitive hematopoietic stem cells first develop within the major arterial regions of the mouse embryo. EMBO J. 2000;19:2465-2474.
7. Mikkola HK, Orkin SH. The journey of developing hematopoietic stem cells. Development 2006;133:3733-3744.
8. Adams GB, Scadden DT. The hematopoietic stem cell in its place. Nat.Immunol. 2006;7:333-337.
9. Nervi B, Link DC, DiPersio JF. Cytokines and hematopoietic stem cell mobilization. J.Cell Biochem. 2006;99:690-705.
10. Kiel MJ, Morrison SJ. Uncertainty in the niches that maintain haematopoietic stem cells. Nat.Rev.Immunol. 2008;8:290-301.
11. Weiss L. A scanning electron microscopic study of the spleen. Blood 1974;43:665-691.
12. Kopp HG, Avecilla ST, Hooper AT, Rafii S. The bone marrow vascular niche: home of HSC differentiation and mobilization. Physiology.(Bethesda.) 2005;20:349-356.
13. Trentin JJ. Determination of bone marrow stem cell differentiation by stromal hemopoietic inductive microenvironments (HIM). Am.J.Pathol. 1971;65:621-628.
14. Kaplan RN, Psaila B, Lyden D. Niche-to-niche migration of bone-marrow-derived cells. Trends Mol.Med. 2007;13:72-81.
15. Nilsson SK, Simmons PJ. Transplantable stem cells: home to specific niches. Curr.Opin. Hematol. 2004;11:102-106.
16. Tzeng YS, Li H, Kang YL et al. Loss of Cxcl12/Sdf-1 in adult mice decreases the quiescent state of hematopoietic stem/progenitor cells and alters the pattern of hematopoietic regeneration after myelosuppression. Blood 2011;117:429-439.
17. Pelus LM, Fukuda S. Chemokine-mobilized adult stem cells; defining a better hematopoietic graft. Leukemia 2008;22:466-473.
18. Shen Y, Nilsson SK. Bone, microenvironment and hematopoiesis. Curr.Opin.Hematol. 2012;19:250-255.
19. Yoshihara H, Arai F, Hosokawa K et al. Thrombopoietin/MPL signaling regulates hematopoietic stem cell quiescence and interaction with the osteoblastic niche. Cell Stem Cell 2007;1:685-697.

20. Lemieux JM, Horowitz MC, Kacena MA. Involvement of integrins alpha(3)beta(1) and alpha(5)beta(1) and glycoprotein IIb in megakaryocyte-induced osteoblast proliferation. J.Cell Biochem. 2010;109:927-932.

21. Italiano JE, Jr. Unraveling mechanisms that control platelet production. Semin.Thromb. Hemost. 2013;39:15-24.

22. Machlus KR, Thon JN, Italiano JE, Jr. Interpreting the developmental dance of the megakaryocyte: a review of the cellular and molecular processes mediating platelet formation. Br.J.Haematol. 2014;165:227-236.

23. Ebbe S. Biology of megakaryocytes. Prog.Hemost.Thromb. 1976;3:211-229.

24. Odell TT, Jr., Jackson CW, Friday TJ. Megakaryocytopoiesis in rats with special reference to polyploidy. Blood 1970;35:775-782.

25. Bessman JD. The relation of megakaryocyte ploidy to platelet volume. Am.J.Hematol. 1984;16:161-170.

26. Zimmet J, Ravid K. Polyploidy: occurrence in nature, mechanisms, and significance for the megakaryocyte-platelet system. Exp.Hematol. 2000;28:3-16.

27. Cimmino G, Golino P. Platelet biology and receptor pathways. J.Cardiovasc.Transl.Res. 2013;6:299-309.

28. Cramer EM, Berger G, Berndt MC. Platelet alpha-granule and plasma membrane share two new components: CD9 and PECAM-1. Blood 1994;84:1722-1730.

29. Handagama PJ, George JN, Shuman MA, McEver RP, Bainton DF. Incorporation of a circulating protein into megakaryocyte and platelet granules. Proc.Natl.Acad.Sci.U.S.A 1987;84:861-865.

30. Harrison P, Cramer EM. Platelet alpha-granules. Blood Rev. 1993;7:52-62.

31. Holmsen H, Weiss HJ. Secretable storage pools in platelets. Annu.Rev.Med. 1979;30:119-134.

32. Gerrard JM, McNicol A. Platelet storage pool deficiency, leukemia, and myelodysplastic syndromes. Leuk.Lymphoma 1992;8:277-281.

33. KAUTZ J, DE MARSH QB. Electron microscopy of sectioned blood and bone marrow elements. Rev.Hematol. 1955;10:314-323.

34. Eckly A, Heijnen H, Pertuy F et al. Biogenesis of the demarcation membrane system (DMS) in megakaryocytes. Blood 2014;123:921-930.

35. Kelemen E, CSERHATI I, Tanos B. Demonstration and some properties of human thrombopoietin in thrombocythaemic sera. Acta Haematol. 1958;20:350-355.

36. Kaushansky K. Thrombopoietin the primary regulator of platelet production. Trends Endocrinol.Metab 1997;8:45-50.

37. Szalai G, LaRue AC, Watson DK. Molecular mechanisms of megakaryopoiesis. Cell Mol. Life Sci. 2006;63:2460-2476.

38. Kaushansky K. Thrombopoietin. N.Engl.J.Med. 1998;339:746-754.

39. Kuter DJ. The physiology of platelet production. Stem Cells 1996;14 Suppl 1:88-101.

40. Grozovsky R, Begonja AJ, Liu K et al. The Ashwell-Morell receptor regulates hepatic thrombopoietin production via JAK2-STAT3 signaling. Nat.Med. 2015;21:47-54.

41. Kaushansky K. The molecular mechanisms that control thrombopoiesis. J.Clin.Invest 2005;115:3339-3347.

42. Kaushansky K, Lok S, Holly RD et al. Promotion of megakaryocyte progenitor expansion and differentiation by the c-Mpl ligand thrombopoietin. Nature 1994;369:568-571.

43. Murone M, Carpenter DA, de Sauvage FJ. Hematopoietic deficiencies in c-mpl and TPO knockout mice. Stem Cells 1998;16:1-6.

44. Teramura M, Kobayashi S, Yoshinaga K, Iwabe K, Mizoguchi H. Effect of interleukin 11 on normal and pathological thrombopoiesis. Cancer Chemother.Pharmacol. 1996;38 Suppl:S99-102.

45. Gainsford T, Nandurkar H, Metcalf D et al. The residual megakaryocyte and platelet production in c-mpl-deficient mice is not dependent on the actions of interleukin-6, interleukin-11, or leukemia inhibitory factor. Blood 2000;95:528-534.

46. Burstein SA, Mei RL, Henthorn J, Friese P, Turner K. Leukemia inhibitory factor and interleukin-11 promote maturation of murine and human megakaryocytes in vitro. J.Cell Physiol 1992;153:305-312.

47. Avecilla ST, Hattori K, Heissig B et al. Chemokine-mediated interaction of hematopoietic progenitors with the bone marrow vascular niche is required for thrombopoiesis. Nat. Med. 2004;10:64-71.

48. Powers CJ, McLeskey SW, Wellstein A. Fibroblast growth factors, their receptors and signaling. Endocr.Relat Cancer 2000;7:165-197.

49. Konishi H, Ochiya T, Sakamoto H et al. Effective prevention of thrombocytopenia using adenovirus-mediated transfer of HST-11FGF-4 gene: in vivo and in vitro studies. Leukemia 1997;11 Suppl 3:530-532.

50. Zheng C, Yang R, Han Z et al. TPO-independent megakaryocytopoiesis. Crit Rev.Oncol. Hematol. 2008;65:212-222.

51. Kaushansky K. Determinants of platelet number and regulation of thrombopoiesis. Hematology.Am.Soc.Hematol.Educ.Program. 2009147-152.

52. Ihzumi T, Hattori A, Sanada M, Muto M. Megakaryocyte and platelet formation: a scanning electron microscope study in mouse spleen. Arch.Histol.Jpn. 1977;40:305-320.

53. Djaldetti M, Gilgal R, Shainberg A, Klein B, Zahavi I. SEM observations on the effect of anthracycline drugs on cultured newborn rat cardiomyocytes. Basic Res.Cardiol. 1988;83:672-677.

54. Shaklai M, Tavassoli M. Demarcation membrane system in rat megakaryocyte and the mechanism of platelet formation: a membrane reorganization process. J.Ultrastruct.Res. 1978;62:270-285.

55. Radley JM, Haller CJ. The demarcation membrane system of the megakaryocyte: a misnomer? Blood 1982;60:213-219.

56. Howell WH, Donahue DD. The production of blood platelets in the lungs. J.Exp.Med. 1937;65:177-203.

57. Weyrich AS, Zimmerman GA. Platelets in lung biology. Annu.Rev.Physiol 2013;75:569-591.

58. Becker RP, De Bruyn PP. The transmural passage of blood cells into myeloid sinusoids and the entry of platelets into the sinusoidal circulation; a scanning electron microscopic investigation. Am.J.Anat. 1976;145:183-205.

59. Junt T, Schulze H, Chen Z et al. Dynamic visualization of thrombopoiesis within bone marrow. Science 2007;317:1767-1770.

60. Thon JN, Italiano JE, Jr. Does size matter in platelet production? Blood 2012;120:1552-1561.

61. Howell WH, Donahue DD. The production of blood platelets in the lungs. J.Exp.Med. 1937;65:177-203.

62. Behnke O. An electron microscope study of the rat megacaryocyte. II. Some aspects of platelet release and microtubules. J.Ultrastruct.Res. 1969;26:111-129.

63. Lecine P, Italiano JE, Jr., Kim SW, Villeval JL, Shivdasani RA. Hematopoietic-specific beta 1 tubulin participates in a pathway of platelet biogenesis dependent on the transcription factor NF-E2. Blood 2000;96:1366-1373.

64. Tijssen MR, Ghevaert C. Transcription factors in late megakaryopoiesis and related platelet disorders. J.Thromb.Haemost. 2013;11:593-604.

65. Geddis AE. Megakaryopoiesis. Semin.Hematol. 2010;47:212-219.

66. ANEJA K, Jalagaugula G, MAO G, SINGH A, RAO AK. Mechanism of platelet factor-á4 (PF4) deficiency with RUNX1 haplodeficiency: RUNX1 is a transcriptional regulator of PF4. Journal of Thrombosis and Haemostasis 2011;9:383-391.

67. Ichikawa M, Yoshimi A, Nakagawa M et al. A role for RUNX1 in hematopoiesis and myeloid leukemia. Int.J.Hematol. 2013;97:726-734.

68. Hart A, Melet F, Grossfeld P et al. Fli-1 Is Required for Murine Vascular and Megakaryocytic Development and Is Hemizygously Deleted in Patients with Thrombocytopenia. Immunity 2000;13:167-177.

69. Gory S, Dalmon J, Prandini MH et al. Requirement of a GT box (Sp1 site) and two Ets binding sites for vascular endothelial cadherin gene transcription. J.Biol.Chem. 1998;273:6750-6755.

70. de LY, Audette M, Pelczar H, Plaza S, Baert JL. The transcription of the intercellular adhesion molecule-1 is regulated by Ets transcription factors. Oncogene 1998;16:2065-2073.

71. de LY, Audette M, Pelczar H, Plaza S, Baert JL. The transcription of the intercellular adhesion molecule-1 is regulated by Ets transcription factors. Oncogene 1998;16:2065-2073.

72. Penny LA, Dell'Aquila M, Jones MC et al. Clinical and molecular characterization of patients with distal 11q deletions. Am.J.Hum.Genet. 1995;56:676-683.

73. Lecuyer E, Hoang T. SCL: from the origin of hematopoiesis to stem cells and leukemia. Exp.Hematol. 2004;32:11-24.

74. Kassouf MT, Chagraoui H, Vyas P, Porcher C. Differential use of SCL/TAL-1 DNA-binding domain in developmental hematopoiesis. Blood 2008;112:1056-1067.

75. Begley CG, Green AR. The SCL gene: from case report to critical hematopoietic regulator. Blood 1999;93:2760-2770.

76. Shivdasani RA, Rosenblatt MF, Zucker-Franklin D et al. Transcription factor NF-E2 is required for platelet formation independent of the actions of thrombopoietin/MGDF in megakaryocyte development. Cell 1995;81:695-704.

77. Orkin SH, Shivdasani RA, Fujiwara Y, McDevitt MA. Transcription factor GATA-1 in megakaryocyte development. Stem Cells 1998;16 Suppl 2:79-83.

78. Takahashi S, Komeno T, Suwabe N et al. Role of GATA-1 in proliferation and differentiation of definitive erythroid and megakaryocytic cells in vivo. Blood 1998;92:434-442.

79. Pevny L, Lin CS, D'Agati V et al. Development of hematopoietic cells lacking transcription factor GATA-1. Development 1995;121:163-172.

80. Shivdasani RAF. A lineage selective knockout establishes the critical role of transcription factor GATA1 in megakaryocyte growth and platelet development. The EMBO Journal 1997;16:3965-3973.

81. Hughan SC, Senis Y, Best D et al. Selective impairment of platelet activation to collagen in the absence of GATA1. Blood 2005;105:4369-4376.

82. Vyas PAKJC. Consequences of GATA-1 Deficiency in Megakaryocytes and Platelets. Blood 1999;93:2867-2875.

83. Gutierrez L, Tsukamoto S, Suzuki M et al. Ablation of Gata1 in adult mice results in aplastic crisis, revealing its essential role in steady-state and stress erythropoiesis. Blood 2008;111:4375-4385.

84. Ciovacco WA, Raskind WH, Kacena MA. Human phenotypes associated with GATA-1 mutations. Gene 2008;427:1-6.

85. Wechsler J, Greene M, McDevitt MA et al. Acquired mutations in GATA1 in the megakaryoblastic leukemia of Down syndrome. Nat.Genet. 2002;32:148-152.

86. Ferreira R, Ohneda K, Yamamoto M, Philipsen S. GATA1 Function, a Paradigm for Transcription Factors in Hematopoiesis. Molecular and Cellular Biology 2005;25:1215-1227.

87. Suske G, Bruford E, Philipsen S. Mammalian SP/KLF transcription factors: bring in the family. Genomics 2005;85:551-556.

88. Li L, He S, Sun JM, Davie JR. Gene regulation by Sp1 and Sp3. Biochem.Cell Biol. 2004;82:460-471.

89. Marin M, Karis A, Visser P, Grosveld F, Philipsen S. Transcription factor Sp1 is essential for early embryonic development but dispensable for cell growth and differentiation. Cell 1997;89:619-628.

90. Kruger I, Vollmer M, Simmons DG et al. Sp1/Sp3 compound heterozygous mice are not viable: impaired erythropoiesis and severe placental defects. Dev.Dyn. 2007;236:2235-2244.

91. Li L, Davie JR. The role of Sp1 and Sp3 in normal and cancer cell biology. Ann.Anat. 2010;192:275-283.

92. Osler W. An account of certain organisms occuring in the liqour sanquinis. proc R soc lond 1874

93. Vieira-de-Abreu A, Campbell RA, Weyrich AS, Zimmerman GA. Platelets: versatile effector cells in hemostasis, inflammation, and the immune continuum. Semin. Immunopathol. 2012;34:5-30.

94. TOCANTINS LM. Historical notes on blood platelets. Blood 1948;3:1073-1082.

95. White J.G. Platelet Structure. Platelets second edition 2007

96. White JG. Effects of colchicine and Vinca alkaloids on human platelets. I. Influence on platelet microtubules and contractile function. Am.J.Pathol. 1968;53:281-291.

97. Escolar G, White JG. The platelet open canalicular system: a final common pathway. Blood Cells 1991;17:467-485.

98. White JG, Krumwiede M. Further studies of the secretory pathway in thrombin-stimulated human platelets. Blood 1987;69:1196-1203.

99. Leistikow EA. Platelet internalization in early thrombogenesis. Semin.Thromb.Hemost. 1996;22:289-294.

100. Patel SR, Hartwig JH, Italiano JE, Jr. The biogenesis of platelets from megakaryocyte proplatelets. J.Clin.Invest 2005;115:3348-3354.

101. Clemetson KJ. Platelets and primary haemostasis. Thromb.Res. 2012;129:220-224.

102. Golan D, Tashjian A, Armstron E, Armstron A. Pharmacology of hemostasis and thrombosis. 2011:

103. Bergmeier W, Piffath CL, Goerge T et al. The role of platelet adhesion receptor GPIbalpha far exceeds that of its main ligand, von Willebrand factor, in arterial thrombosis. Proc. Natl.Acad.Sci.U.S.A 2006;103:16900-16905.

104. Clemetson JM, Polgar J, Magnenat E, Wells TN, Clemetson KJ. The platelet collagen receptor glycoprotein VI is a member of the immunoglobulin superfamily closely related to FcalphaR and the natural killer receptors. J.Biol.Chem. 1999;274:29019-29024.

105. Bennett JS. Structure and function of the platelet integrin alphaIIbbeta3. J.Clin.Invest 2005;115:3363-3369.

106. Klinger MH. Platelets and inflammation. Anat.Embryol.(Berl) 1997;196:1-11.

107. Semple JW, Italiano JE, Jr., Freedman J. Platelets and the immune continuum. Nat.Rev. Immunol. 2011;11:264-274.

108. Hui P, Cook DJ, Lim W, Fraser GA, Arnold DM. The frequency and clinical significance of thrombocytopenia complicating critical illness: a systematic review. Chest 2011;139:271-278.

109. Clark SR, Ma AC, Tavener SA et al. Platelet TLR4 activates neutrophil extracellular traps to ensnare bacteria in septic blood. Nat.Med. 2007;13:463-469.

110. Elzey BD, Ratliff TL, Sowa JM, Crist SA. Platelet CD40L at the interface of adaptive immunity. Thromb.Res. 2011;127:180-183.

111. Henn V, Slupsky JR, Grafe M et al. CD40 ligand on activated platelets triggers an inflammatory reaction of endothelial cells. Nature 1998;391:591-594.

112. Cox D, Kerrigan SW, Watson SP. Platelets and the innate immune system: mechanisms of bacterial-induced platelet activation. J.Thromb.Haemost. 2011;9:1097-1107.

113. Youssefian T, Drouin A, Masse JM, Guichard J, Cramer EM. Host defense role of platelets: engulfment of HIV and Staphylococcus aureus occurs in a specific subcellular compartment and is enhanced by platelet activation. Blood 2002;99:4021-4029.

114. Bouvard D, Brakebusch C, Gustafsson E et al. Functional consequences of integrin gene mutations in mice. Circ.Res. 2001;89:211-223.

115. Ni H, Freedman J. Platelets in hemostasis and thrombosis: role of integrins and their ligands. Transfus.Apher.Sci. 2003;28:257-264.

116. Plow EF, Haas TA, Zhang L, Loftus J, Smith JW. Ligand binding to integrins. J.Biol.Chem. 2000;275:21785-21788.

117. Shattil SJ, Newman PJ. Integrins: dynamic scaffolds for adhesion and signaling in platelets. Blood 2004;104:1606-1615.

118. Takagi J, Petre BM, Walz T, Springer TA. Global conformational rearrangements in integrin extracellular domains in outside-in and inside-out signaling. Cell 2002;110:599-11.

119. Li Z, Delaney MK, O'Brien KA, Du X. Signaling During Platelet Adhesion and Activation. Arteriosclerosis, Thrombosis, and Vascular Biology 2010;30:2341-2349.

120. Moser M, Nieswandt B, Ussar S, Pozgajova M, Fassler R. Kindlin-3 is essential for integrin activation and platelet aggregation. Nat.Med. 2008;14:325-330.

121. Nuyttens BP, Thijs T, Deckmyn H, Broos K. Platelet adhesion to collagen. Thromb.Res. 2011;127 Suppl 2:S26-S29.

122. Enkhbayar P, Kamiya M, Osaki M, Matsumoto T, Matsushima N. Structural principles of leucine-rich repeat (LRR) proteins. Proteins 2004;54:394-403.

123. Semple JW, Italiano JE, Jr., Freedman J. Platelets and the immune continuum. Nat.Rev. Immunol. 2011;11:264-274.

124. Berthet J, Damien P, Hamzeh-Cognasse H et al. Human platelets can discriminate between various bacterial LPS isoforms via TLR4 signaling and differential cytokine secretion. Clin.Immunol. 2012;145:189-200.

125. Pierce KL, Premont RT, Lefkowitz RJ. Seven-transmembrane receptors. Nat.Rev.Mol.Cell Biol. 2002;3:639-650.

126. Clemetson K.J., Clemetson M. Platelet Receptors. 2007:

127. Vu TK, Hung DT, Wheaton VI, Coughlin SR. Molecular cloning of a functional thrombin receptor reveals a novel proteolytic mechanism of receptor activation. Cell 1991;64:1057-1068.

128. Coughlin SR. How the protease thrombin talks to cells. Proc.Natl Acad.Sci.U.S.A 1999;96:11023-11027.

129. De CE. Mechanisms of platelet activation by thrombin: a short history. Thromb.Res. 2012;129:250-256.

130. Cattaneo M. The platelet P2 receptors. 2007:

131. Bergmeier W, Stefanini L. Platelet ITAM signaling. Curr.Opin.Hematol. 2013;20:445-450.

132. Boulaftali Y, Hess PR, Getz TM et al. Platelet ITAM signaling is critical for vascular integrity in inflammation. J.Clin.Invest 2013;123:908-916.

133. Bertozzi CC, Schmaier AA, Mericko P et al. Platelets regulate lymphatic vascular development through CLEC-2-SLP-76 signaling. Blood 2010;116:661-670.

134. Cox D, Kerrigan SW, Watson SP. Platelets and the innate immune system: mechanisms of bacterial-induced platelet activation. J.Thromb.Haemost. 2011;9:1097-1107.

135. Boylan B, Gao C, Rathore V et al. Identification of FcgammaRIIa as the ITAM-bearing receptor mediating alphaIIbbeta3 outside-in integrin signaling in human platelets. Blood 2008;112:2780-2786.

136. Ozaki Y, Suzuki-Inoue K, Inoue O. Platelet receptors activated via mulitmerization: glycoprotein VI, GPIb-IX-V, and CLEC-2. J.Thromb.Haemost. 2013;11 Suppl 1:330-339.

137. Freson K, Wijgaerts A, van GC. Update on the causes of platelet disorders and functional consequences. Int.J.Lab Hematol. 2014;36:313-325.

138. Germeshausen M, Ballmaier M, Welte K. MPL mutations in 23 patients suffering from congenital amegakaryocytic thrombocytopenia: the type of mutation predicts the course of the disease. Hum.Mutat. 2006;27:296.

139. Geddis AE. Congenital amegakaryocytic thrombocytopenia and thrombocytopenia with absent radii. Hematol.Oncol.Clin.North Am. 2009;23:321-331.

140. Albers CA, Paul DS, Schulze H et al. Compound inheritance of a low-frequency regulatory SNP and a rare null mutation in exon-junction complex subunit RBM8A causes TAR syndrome. Nat.Genet. 2012;44:435-2.

141. Toriello HV. Thrombocytopenia-absent radius syndrome. Semin.Thromb.Hemost. 2011;37:707-712.

142. Balduini CL, Pecci A, Savoia A. Recent advances in the understanding and management of MYH9-related inherited thrombocytopenias. Br.J.Haematol. 2011;154:161-174.

143. Berrou E, Adam F, Lebret M et al. Heterogeneity of platelet functional alterations in patients with filamin A mutations. Arterioscler.Thromb.Vasc.Biol. 2013;33:e11-e18.

144. Kunishima S, Kobayashi R, Itoh TJ, Hamaguchi M, Saito H. Mutation of the beta1-tubulin gene associated with congenital macrothrombocytopenia affecting microtubule assembly. Blood 2009;113:458-461.

145. Balduini CL, Pecci A, Savoia A. Recent advances in the understanding and management of MYH9-related inherited thrombocytopenias. Br.J.Haematol. 2011;154:161-174.

146. Balduini CL, Savoia A. Genetics of familial forms of thrombocytopenia. Hum.Genet. 2012;131:1821-1832.

147. Cullinane AR, Schaffer AA, Huizing M. The BEACH is hot: a LYST of emerging roles for BEACH-domain containing proteins in human disease. Traffic. 2013;14:749-766.

148. Li R, Emsley J. The organizing principle of the platelet glycoprotein Ib-IX-V complex. J.Thromb.Haemost. 2013;11:605-614.

149. Leo VC, Morgan NV, Bem D et al. Use of next-generation sequencing and candidate gene analysis to identify underlying defects in patients with inherited platelet function disorders. J.Thromb.Haemost. 2014

150. Harrison P, Keeling D. Clinical Tests of platelet function. Platelets. 2010:

151. Lind SE. Prolonged bleeding time. Am.J.Med. 1984;77:305-312.

152. Harrison P, Lordkipanidze M. Testing platelet function. Hematol.Oncol.Clin.North Am. 2013;27:411-441.

153. BORN GV. Aggregation of blood platelets by adenosine diphosphate and its reversal. Nature 1962;194:927-929.

154. Yardumian DA, Mackie IJ, Machin SJ. Laboratory investigation of platelet function: a review of methodology. J Clin.Pathol. 1986;39:701-712.

155. Shapiro AD. Platelet function disorders. Haemophilia. 2000;6 Suppl 1:120-127.

156. Rand ML, Leung R, Packham MA. Platelet function assays. Transfus.Apher.Sci. 2003;28:307-317.

157. Zhou L, Schmaier AH. Platelet aggregation testing in platelet-rich plasma: description of procedures with the aim to develop standards in the field. Am.J.Clin.Pathol. 2005;123:172-183.

Chapter 2

A NOVEL FLOW CYTOMETRY-BASED PLATELET AGGREGATION ASSAY

Platelets and thrombopoiesis

A novel flow cytometry-based platelet aggregation assay

Blood. 2013 March 7

Marjolein Meinders, Iris M. De Cuyper, Edith van de Vijver,
Dirk de Korte, Leendert Porcelijn, Masja de Haas,
Johannes A. Eble, Karl Seeger, Sergio Rutella,
Daria Pagliara, Taco W. Kuijpers, Arthur J. Verhoeven,
Timo K. van den Berg and Laura Gutiérrez

A NOVEL FLOW CYTOMETRY-BASED PLATELET AGGREGATION ASSAY

Iris M. De Cuyper,[1] Marjolein Meinders,[1] Edith van de Vijver,[1,2] Dirk de Korte,[1] Leendert Porcelijn,[3] Masja de Haas,[4] Johannes A. Eble,[5] Karl Seeger,[6] Sergio Rutella,[7] Daria Pagliara,[7] Taco W. Kuijpers,[1,2] Arthur J. Verhoeven,[1] Timo K. van den Berg,[1] and Laura Gutiérrez.[1]

[1]Department of Blood Cell Research, Sanquin Research and Landsteiner Laboratory, and [2]Emma Children's Hospital, Academic Medical Center, Universit y of Amsterdam, The Netherlands; [3]Department of Thrombo/Leukocyte Serology, and [4]Department of Erythrocyte Serology, Sanquin Diagnostics, Amsterdam, The Netherlands; [5]Center for Molecular Medicine, Department of Vascular Matrix Biology, Excellence Cluster Cardio-Pulmonary System, Frankfurt University Hospital, Frankfurt am Main, Germany; [6]Department of Pediatric Oncology/Hematology, Otto-Heubner-Center for Pediatric and Adolescent Medicine, Charité-Universitätsmedizin, Berlin, Germany; and [7]Department of Pediatric Hematology/Oncology, IRCCS Bambino Gesù Children's Hospital, Rome, Italy.

Key Points

- FCA is a novel flow cytometry–based platelet aggregation assay that allows single receptor analysis in small volume/thrombocytopenic samples
- FCA facilitates platelet studies in experimental animal models even during gestation and allows kinetic measurements in individual animals

ABSTRACT

The main function of platelets is to maintain normal hemostasis. Inefficient platelet production and/or defective platelet function results in bleeding disorders resulting from a wide range of genetic traits and acquired pathologies. Several platelet function tests have been developed for use in the clinic and in experimental animal models. In particular, platelet aggregation is routinely measured in an aggregometer, which requires normal platelet counts and significant blood sample volumes. For this reason, the analysis of thrombocytopenic patients, infants, and animal models is problematic. We have developed a novel flow cytometry test of platelet aggregation, in which 10- to 25-fold lower platelet counts or sample volumes can be used, either of platelet-rich plasma or whole blood from human subjects or mice. This setup can be applied to test in small assay volumes the influence of a variety of stimuli, drugs, and plasma factors, such as antibodies, on platelet aggregation. The presented principle stands as a novel promising tool, which allows analysis of platelet aggregation in thrombocytopenic patients or infants, and facilitates studies in platelets obtained from experimental animal models without the need of special devices but a flow cytometer. (Blood. 2013;121(10):e70-e80)

INTRODUCTION

Platelets are the blood cells responsible for maintaining hemostasis. In addition, more recently, platelets have also been implicated, among others, in the regulation of immune responses, cancer metastasis, vascular development, and angiogenesis.[1-6] Different aspects of platelet function relevant for hemostasis (ie, platelet adhesion, activation, and aggregation) can be tested in vitro.[7,8] Adhesion and activation parameters can be extrapolated from the analysis of relevant plasma proteins, surface marker expression, granular content and release, and signaling pathways.[7,8] However, the only truly functional platelet tests used to date, such as the bleeding time (which is losing popularity)[9-11] and light transmission aggregometry (LTA), have major methodological limitations.[8,12-19]

LTA relies on the measurement of light transmission through a cuvette filled with platelet-rich plasma (PRP) placed between a light source and a photocell. This test is based on the decrease in light scattering upon addition of a platelet agonist resulting from the increased number of platelet aggregates. As a result, the turbidity of the sample decreases and the light transmission detected by the photocell increases.[12,13] In view of the variations in methodology and output, efforts have been undertaken to standardize LTA conditions.[14,15] Based on these comparative studies, it was recommended to perform the test with freshly isolated PRP and not to adjust the platelet counts. However, a negative result of a standard LTA on thrombocytopenic patients with PRP platelet numbers below $50x10^6$/mL deviates from normal and cannot be interpreted as indicative for a defect in platelet aggregation. LTA therefore requires a significant sample volume to obtain enough PRP to be tested.[16-18] This renders the analysis of samples from infants suspected of platelet aggregation defects very difficult. It is also not suitable for use in lipemic blood samples.[8,19] Moreover, to perform 1 aggregometry test with mouse blood with the conventional aggregometer, a single mouse has to be euthanized to obtain enough material.[20] Kinetic studies in the same animal are thus impossible. Furthermore, LTA requires a specific device to measure aggregation. The generalized use of citrate as anticoagulant has an additional drawback, because due to the calcium ion concentration changes, the response to certain agonists increases.[8] In general, LTA remains poorly reproducible and standardized between different laboratories,[14-16,21] is labor intensive, and does not simulate primary hemostasis because it uses PRP instead of whole blood.[8]

Platelet aggregation analysis within diluted whole blood is possible with impedance aggregometry. This method is based on the binding of platelets to 2 electrodes immersed in the stirring sample when a current is passed through it. When an agonist is added, more platelets will bind to the electrodes, and the extent and increase in impedance is measured and correlated with platelet aggregation. Although this method can be used in lipemic blood samples, it is not suitable for use with thrombocytopenic patient material.[19] Clearly, there is a demand for a functional test that does not suffer from these limitations.

We have developed a novel flow cytometry assay that allows the detection of platelet aggregates with small blood volumes and low platelet numbers. In brief, 2 portions of platelets from the same donor either washed or within the whole blood

context are labeled with different fluorochromes and, after mixing and upon appropriate stimulation, analyzed for the formation of double-colored aggregates by flow cytometry. The protocol allows the detection of small aggregates after agonist incubation, as opposed to the gross aggregate formation required for LTA. This characteristic allows sensitive dissection of platelet receptor function when combining agonists and antagonists in the assay. In addition, the assay renders studies on the influence of plasma and/or drugs on platelet aggregation more straightforward and affordable. We also present a whole blood aggregation option that can be used with very small blood volumes. In combination with conventional surface marker analysis by flow cytometry and classical assays, this method represents a highly promising tool for platelet function tests in human as well as in animal models without the requirement for specialized equipment other than a flow cytometer.

MATERIALS AND METHODS

Preparation of human washed platelets

Whole blood collected in EDTA, heparin, or citrate was centrifuged for 15 minutes at 210 g, and the PRP fraction was collected. Platelets were washed twice with sequestrine buffer (17.5 mM Na_2HPO_4, 8.9 mM Na_2EDTA, 154 mM NaCl, pH 6.9, containing 0.1% [wt/vol] bovine serum albumin) by centrifuging them 5 minutes at 2310g. Platelets were resuspended to a final concentration of $50x10^6$ plt/mL in HEPES medium (132 mM NaCl, 6 mM KCl, 1 mM $MgSO_4$, 1.2 mM KH_2PO_4, 20 mM HEPES, pH 7.4, containing 5 mM glucose). The study was approved by our institute medical ethics committee in accordance with the 1964 Declaration of Helsinki.

Labeling human washed platelets

Platelets were labeled with 0.1 μM carboxyfluorescein diacetate succinimidyl ester (CFSE; Molecular Probes, Eugene, OR) or with 1.6 μM PKH26 (Sigma-Aldrich, St. Louis, MO) for 15 minutes at room temperature. The labeling was stopped by adding pooled CPD plasma from healthy AB^+ donors to a final concentration of 20% (vol/vol).

Labeling human platelets in whole blood

Whole blood was incubated with 1:100 dilution of CD31-Pacific Blue (eBiosciences, San Diego, CA) or CD31-FITC (BD Biosciences, San Jose, NJ) for 15 min at room temperature. After washing twice with 2x volume sequestrine buffer + 0.1% bovine serum albumin 5 minutes at 2250g, whole blood was resuspended to the same starting volume in HEPES medium containing 20% (vol/vol) AB^+ pool CPD plasma.

Preparation of mouse washed platelets and collection of embryonic blood

Mouse whole blood was taken by orbital, cheek, or heart puncture and collected in heparinized mouse blood collection tubes. The whole blood was diluted with 2x volume HEPES medium. Diluted blood was centrifuged 15 minutes at 50g, and the collected PRP was diluted further in HEPES medium to a final concentration of $50x10^6$ plt/mL.

Mouse embryonic blood was collected as described: the blood of 8 to 15 13.5 days post coitum embryos was collected in approximately 8 mL of heparin–phosphate-buffered saline and filtered through a 40-µm cell strainer.[22] All animal experiments were approved by the local ethical review committee.

Staining of mouse platelets in PRP and whole blood

Mouse PRP or whole blood was incubated with 1:100 dilution of CD9-APC and CD31-PECy7 or CD9-PE monoclonal antibodies (moAbs) (Abcam, Cambridge, UK) for 15 minutes at room temperature. In whole blood samples, an additional staining with 1:100 Ter119-PerCP-Cy5.5 (Ly-76) (eBiosciences) was performed to stain definitive erythrocytes (optional). When staining embryonic blood, antibodies were used in a 1:1000 concentration in a volume of 4 mL. After incubation, samples were centrifuged 5 minutes at 2250g (2x for whole blood samples) and resuspended in HEPES medium supplemented with 2% (vol/vol) heparin mouse plasma or 2% (vol/vol) AB^+ pool CPD plasma to a concentration of $50x10^6$ plt/mL in the case of PRP, and with 5% to 10% plasma to 100 to $300x10^6$ plt/mL in the case of whole blood or embryonic blood.

Flow cytometry–based platelet aggregation assay

Preincubation of human samples

Differently labeled washed platelets or whole blood samples were mixed 1:1, and 0.1x volume of healthy donor AB^+ pool CPD plasma, supplemented with 20 µM D-phenylalanyl-L-prolyl-L-arginine chloromethyl ketone (thrombin inhibitor, PPACK; Calbiochem, Merck Group, Darmstadt, Germany) was added to citrate anticoagulated samples. Alternatively, EDTA anticoagulated samples were supplemented with 1x volume healthy or patient EDTA plasma, 1 mM $MgCl_2$, and 20 µM PPACK. Samples were incubated with or without antagonists at 37°C while shaking at 700 rpm for 15 minutes. As antagonists, we used 0.5 µg/mL tirofiban (αIIbβ3 integrin inhibitor Aggrastat; Merck, Whitehouse Station, NJ) or 10 µg/mL moAb LIA 1/2.1 (β1 integrin chain blocking moAb).[23] After the incubation, 3 mM $CaCl_2$ was added when performing the assay with washed platelets.

Preincubation of mouse samples

The 2 populations of labeled washed plateletsor whole blood were mixed 1:1 and then preincubated for 15 min at 37°C while shaking at 600 rpm. As antagonists we used 5 µg/mL tirofiban (Aggrastat), 20 µg/mL CD29 β1 integrin blocking moAb (Ha2/5; BD Pharmingen, San Diego, CA), 12.5µM Bay (Syk inhibitor IV; Bay-61-3606; Calbiochem), and 5 µg/mL JAQ1 (GPVI blocking moAb, M011-0; Emfret Analytics, Eibelstadt, Germany).

Activation

Preincubated human platelets were activated with 100 ng/mL phorbol myristate acetate (PMA, Sigma-Aldrich), 10 µg/mL type-I collagen (Horm; Nycomed Arzneimittel GmbH, M¨unchen, Germany), 300 µM Aggretin A,[24] or 1.5 mg/mL ristocetin (Biopool; Trinity Biotech Plc, Bray, Co Wincklow, Ireland) at 37°C while shaking at 1000 rpm. Preincubated mouse platelets were activated with 10 µg/

mL type-I collagen or 10 µg/mL botrocetin (Sigma-Aldrich) at 37°C while shaking at 1000 rpm or with 100 ng/mL PMA or 75 to 300 µM Aggretin A at 37°C while shaking at 700 rpm. At different times, samples were fixed by addition of 9x volume of 0.5% (vol/vol) formaldehyde (Polysciences Inc., Warrington, NJ, methanol-free) in phosphate-buffered saline.

Measurement
Fixed samples were measured by flow cytometry (LSRII 1HTS, BD Biosciences) and analyzed with BD FACS DIVA software (BD Biosciences) or FlowJo version 9.2 software (Tree Star, inc). Alternatively, samples were measured with the ImageStream^X (Amnis, Seattle, WA).

Quantification
For analysis, a quadrant was set in the dot plot of respective channels on non-stimulated platelets. The appearance of double-colored events in the upper right quadrant (Q2) was quantified as percentage of total amount of labeled events (Q1+Q2+Q4) at every time point analyzed:

$$\% \text{ double-colored events} = [Q2/(Q1+Q2+Q4)]x100$$

The decrease in total single-colored events at a given time point relative to the t=0 sample can be calculated as follows and is an indirect measurement of the aggregation of platelets:

$$\% \text{ single-colored eventst}_{t=x} = [(Q1+Q4)_{t=x}/(Q1+Q4)_{t=0}]x100$$

The average size of the aggregates at a given time point can be calculated as follows, although this is a relative or indicative measurement, and should not be taken into consideration when the Q2 event number falls below 100 or when the sum of single-colored events at a given time is higher than the sum of the single events at t=0:

$$\text{Average events-aggregate}_{t=x} = [(Q1+Q4)_{t=0} - (Q1+Q4)_{t=x}] / Q2_{t=x}$$

Measurements and calculations were made with mouse samples as described previously after gating out Ter119$^+$ cells or including all cells in the analysis.

Light transmission aggregometry
Platelets were centrifuged for 5 minutes at 2310g and resuspended to a final concentration of 25x10^7 plt/mL in 40% (vol/vol) HEPES medium, 10% (vol/vol) CPD, and 50% (vol/vol) EDTA healthy donor plasma, supplemented with 1 mM $MgCl_2$ and 20 µM PPACK. The stained and unstained platelets were incubated 15 minutes at 37°C while shaking at 600 rpm. A Lumi-aggregation module Series 1000B (Payton Scientific, Buffalo, NY) was attached to a linear recorder and set on slight stirring (800 rpm) at 37°C. The baseline was set with 450 µL of 40% (vol/vol) HEPES medium, 10% (vol/vol) CPD, and 50% (vol/vol) EDTA plasma. Cuvettes containing

450 µL of stained or unstained samples were measured and after stabilization of the signal, 3 mM $CaCl_2$ was added. After restabilization of the signal, incubations were activated with either 100 ng/mL PMA or 10 µg/mL type-I collagen and light transmission was recorded over time.

Statistical analysis
Two-tailed Welch's t test analysis (2 samples unequal variance) was performed when indicated.

RESULTS

Labeling of platelets does not affect platelet morphology or function
To enable measurement of platelet aggregation by detection of double-colored events in a flow cytometer, human or mouse platelets were labeled with two different fluorochromes, either CFSE (a green fluorescent dye labeling the cytosol) and PKH26 (a red fluorescent dye labeling the plasma membrane) or with conjugated antibodies. The conditions of these labeling protocols did not affect the scatter characteristics or the morphology of the platelets as judged by light microscopy of formaldehyde-fixed samples (data not shown).
To exclude a possible effect of the labeling procedure on platelet aggregation, labeled platelets were employed in a standard LTA assay and their response toward collagen was compared with that of unlabeled platelets. The labeling with the 2 fluorescent dyes or with conjugated antibodies had a negligible effect on human and mouse platelet aggregation (Figure 1A). Therefore we proceeded with this labeling option to develop our flow cytometry-based platelet aggregation assay (FCA).

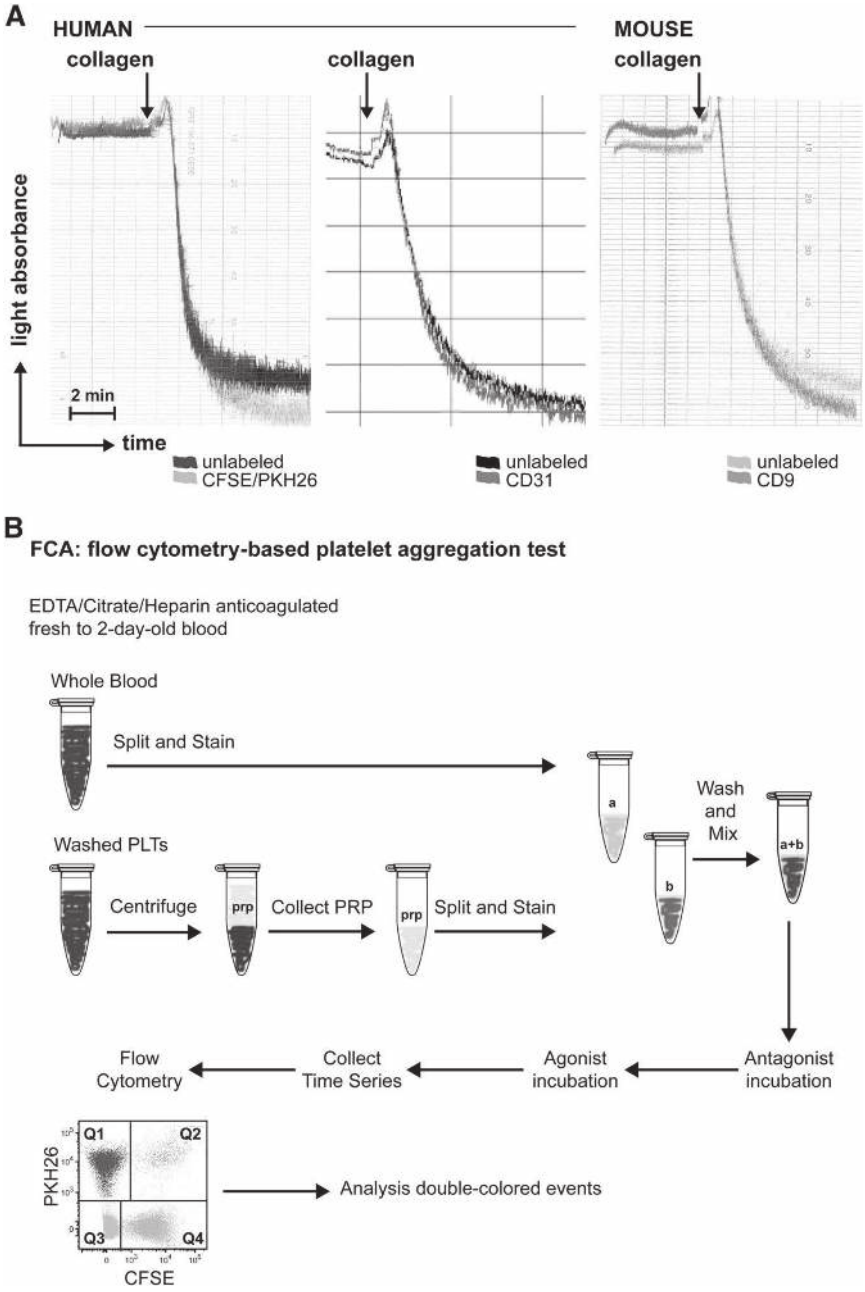

Figure 1. Effect of fluorescent labeling on platelet aggregation.

A) Light transmission aggregometry upon collagen stimulation of human platelets unlabeled or labeled with PKH26/CFSE (left), CD31 (middle), or mouse platelets unlabeled or labeled with CD9 (right).

B) Simplified scheme of FCA.

FCA allows assessment of single receptor function in samples with low starting volume or platelet number

We first isolated platelets from PRP, labeled them with either CFSE or PKH26, and mixed them 1:1 as described in "Materials and methods." Platelet mixtures were stimulated and fixed at different times to measure the kinetics of aggregate formation by flow cytometry (Figure 1B). Upon stimulation with PMA (which activates the fibrinogen receptor αIIbβ3 integrin), the percentage of double-colored events (Figure 2A, Q2) increased over time and their forward scatter/side scatter positioning shifted compared with single platelets (Figure 2A). We measured with ImageStream^X our aggregation time series to visualize the single-colored platelets or double-colored aggregates (Figure 2B), which are small (2 to 15 platelets on average, data not shown, and supplemental Table 1). This characteristic made us investigate whether our test would allow studying the contribution of single receptors at the onset of aggregate formation.

We used a combination of stimuli and antagonists well-characterized for their specificity. As stimuli we used PMA, collagen (which binds to both α2β1 integrin and GPVI, which will in turn activate αIIbβ3 and α2β1 integrins),[25,26] Aggretin A (which binds to CLEC-2 and will in turn activate αIIbβ3 integrin through a Syk-dependent mechanism),[24,27,28] and ristocetin (which binds to and changes the conformation of von Willebrand factor-A, subsequently activating glycoprotein [GP] Ib). When using antagonists, we preincubated the platelets with tirofiban, a peptide antagonist of αIIbβ3 integrin, or LIA, a moAb directed against β1 integrin.[23,29] As expected, tirofiban completely inhibited aggregate formation induced by PMA and Aggretin A, whereas LIA did not interfere with aggregation (Figure 2C) because PMA and Aggretin A both induce αIIbβ3-dependent aggregation. The decrease in single-colored events and the average size of aggregates remained unaltered in the presence of LIA (supplemental Table 1). In case of collagen stimulation, tirofiban did not exert an inhibitory effect on the aggregation kinetics, whereas LIA decreased by 75% the collagen-mediated aggregation (Figure 2C). However, tirofiban preincubation affected the size of aggregates and consequently the reduction in single-colored events (supplemental Table 1). This suggests that collagen-mediated aggregation requires functional α2β1 instead of αIIbβ3 integrin at the onset of aggregation and that αIIbβ3 integrin contributes to aggregate size and stability in a second wave. Aggregation induced by ristocetin was not inhibited by either tirofiban or LIA; neither were the aggregate size nor the decrease in single-colored events affected in the presence of the antagonists used (Figure 2C and supplemental Table 1). In conclusion, FCA of human washed platelets allows, in comparison with LTA, a distinction between α2β1 and αIIbβ3 integrin function that can be dissected by stimulating the platelets with either collagen (α2β1-mediated) or PMA (αIIbβ3-mediated), a feature that we have shown previously to distinguish the aggregopathy of Glanzmann thrombasthenia and leukocyte adhesion deficiency (LAD)-III patient-derived platelets.[30,31]

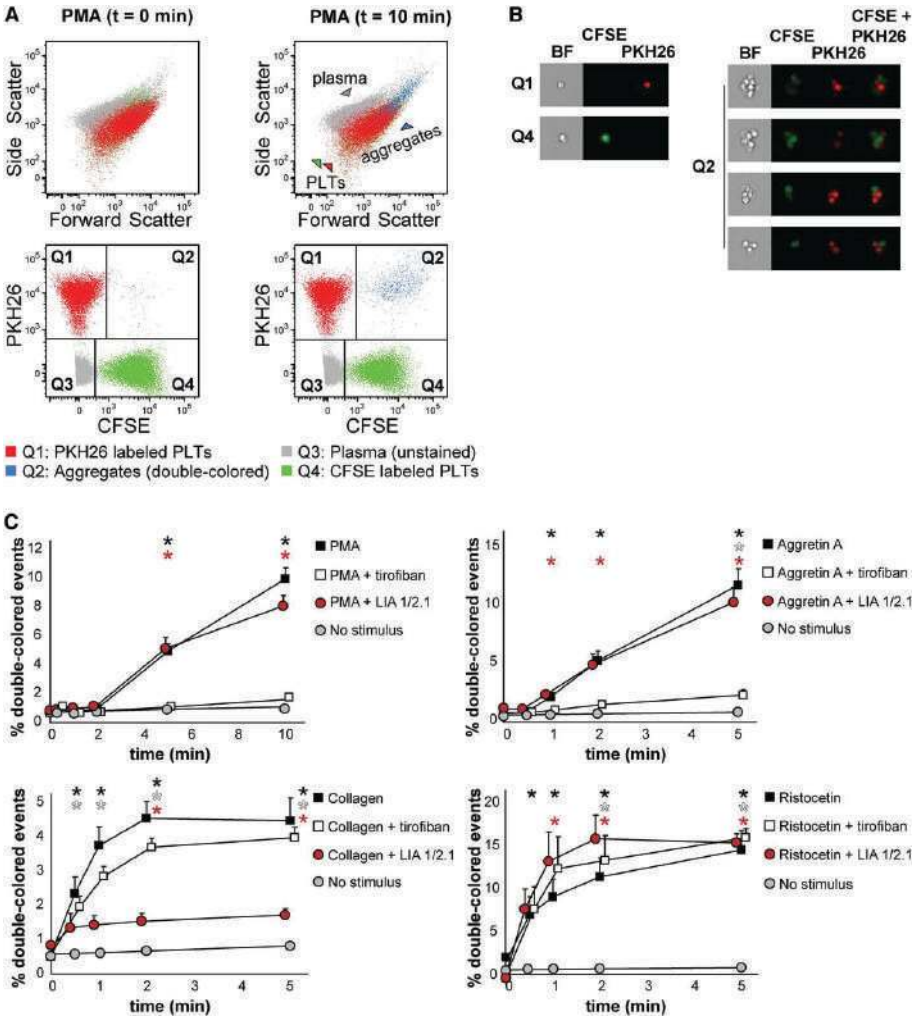

Figure 2. Human platelet aggregation test with washed platelets.

A) Dot plots depicting platelets labeled with CFSE or PKH26 mixed in 1:1 ratio as measured by flow cytometry before addition of PMA (t = 0 min, left) or upon PMA stimulation (t = 10 min, right). Platelets stained with PKH26 are enclosed in quadrant Q1. Platelets stained with CFSE are enclosed in quadrant Q4. Double-colored events in quadrant Q2 represent aggregates before and after stimulation by PMA. All populations are plotted against the forward and side scatter and indicated by colored arrowheads. PLT, platelet.

B) Images of single-stained platelets from quadrants Q1 and Q4 or aggregates from quadrant Q2 obtained with ImageStreamX are depicted next to the respective dot plots. BF, bright field.

C) Platelets were labeled with CFSE or PKH26 and mixed in 1:1 ratio before stimulation. Aggregation was measured by flow cytometry in time after stimulation with PMA, collagen, Aggretin A, or ristocetin alone or in the

presence of either the integrin β3 inhibitor tirofiban or blocking anti-integrin β1 antibody LIA 1/2.1. Average and standard error of the mean are depicted, n > 3. Non-stimulated labeled platelets are shown as baseline for spontaneous aggregation. Colored asterisks at each data point indicate statistical significance with the unstimulated control (P < .05).

FCA allows testing platelet function in small volumes of whole blood

We next set out to optimize FCA for whole blood samples, with the intention to analyze platelet function in small volumes of whole blood. This is necessary when the clinical profile does not allow sampling the large volumes of blood required for proper PRP collection, as occurs with newborns, infants, or thrombocytopenic patients. For this purpose, we used antibodies directed against surface markers present on platelets, but not on red cells, that will not interfere with platelet aggregation. After testing several possibilities (data not shown), we selected CD31 as specified in "Materials and methods." In Figure 3, we show representative data of whole blood platelet aggregation kinetics when using CD31-FITC and CD31-Pacific Blue as antibodies.

Upon stimulation with ristocetin, the percentage of double-colored events (Figure 3A, Q2) increased over time, and their forward scatter/side scatter positioning shifted compared with single platelets (Figure 3A). Red blood cells were detected in Q3, where other cells and plasma components are also distributed (Figure 3A).

Stimulation with PMA, collagen, Aggretin A, and ristocetin resulted in detectable platelet aggregation measured either directly (increase in double-colored events relative to total colored events, Figure 3B) or indirectly (decrease in single-colored events, supplemental Table 2). The aggregate size (events/aggregate) is equal (ristocetin) or larger with the same stimulus when performing the aggregation assay with whole blood in comparison with washed platelets (supplemental Tables 1 and 2).

We have previously shown that FCA allows the distinction between the aggregopathy of Glanzmann thrombasthenia vs LAD-III patients in washed platelets,[31] based on the collagen-induced α2β1-dependent aggregation present in Glanzmann but absent in LAD-III platelets. Therefore, we aimed to validate our method in whole blood samples from Glanzmann thrombasthenia and LAD-III patients. As shown in Figure 3C, platelets from Glanzmann thrombasthenia and LAD-III patients respond normally to stimulation by ristocetin as compared with platelets from healthy controls, set to 100%. LAD-III platelets have an equally reduced response to collagen and PMA, whereas Glanzmann platelets have a better response to collagen than to PMA (Figure 3C and supplemental Table 2), confirming previous results and suggesting that the still-functional α2β1 integrin in Glanzmann platelets could explain the less severe bleeding phenotype of Glanzmann patients when compared with LAD-III patients.[30,31]

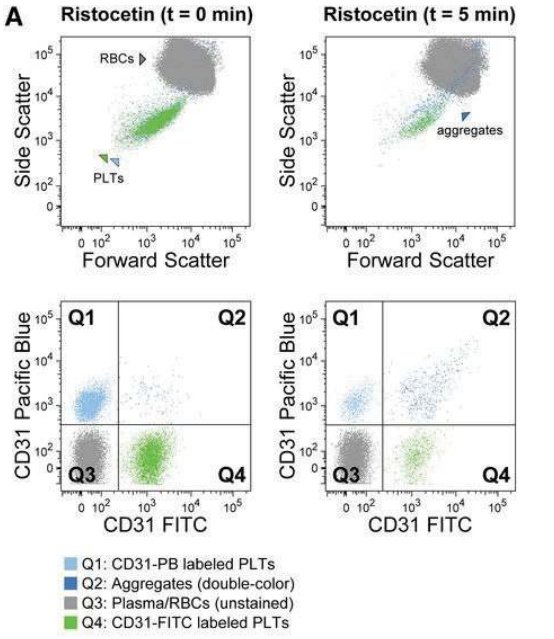
A
Ristocetin (t = 0 min)
Ristocetin (t = 5 min)
RBCs
PLTs
aggregates
Side Scatter
Forward Scatter
Q1
Q2
Q3
Q4
CD31 Pacific Blue
CD31 FITC
Q1: CD31-PB labeled PLTs
Q2: Aggregates (double-color)
Q3: Plasma/RBCs (unstained)
Q4: CD31-FITC labeled PLTs

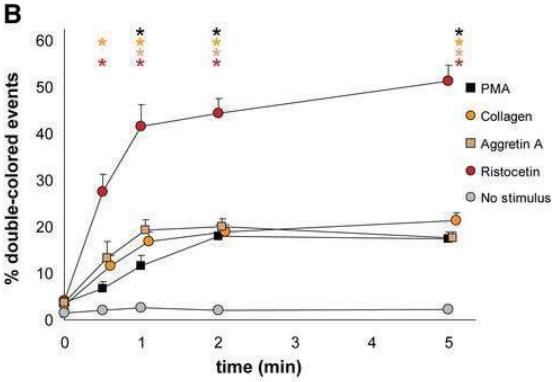
B
% double-colored events
time (min)
PMA
Collagen
Aggretin A
Ristocetin
No stimulus

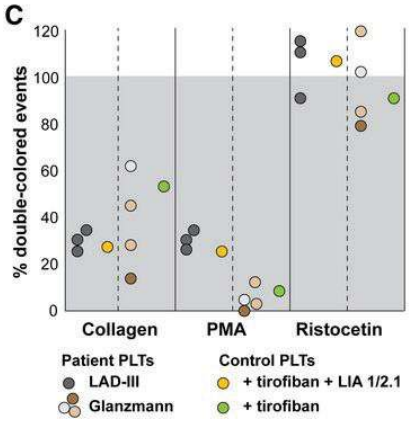
C
% double-colored events
Collagen
PMA
Ristocetin
Patient PLTs
LAD-III
Glanzmann
Control PLTs
+ tirofiban + LIA 1/2.1
+ tirofiban

Figure 3. Human platelet aggregation test with whole blood

Platelets were labeled with CD31-Pacific Blue or CD31-FITC and mixed in 1:1 proportion prior to stimulation.

A) Representative dot plots before and after platelet aggregation upon stimulation with ristocetin. All populations (unstained, single-stained platelets and double-colored aggregates) are plotted against the forward and side scatter and indicated by colored arrowheads. PLT, platelet; RBC, red blood cell.

B) Aggregation was measured by flow cytometry in time after stimulation with PMA, collagen, Aggretin A, and ristocetin. Average and standard error of the mean are depicted, n > 3. Non-stimulated labeled platelets are shown as baseline for spontaneous aggregation. Colored asterisks at each data point indicate statistical significance with the unstimulated control ($P < .05$).

C) Whole blood platelet aggregation analysis performed with blood from Glanzmann thrombasthenia and LAD-III patients upon collagen, PMA, or ristocetin stimulation. Note that Glanzmann platelets respond about half normally to collagen but not to PMA, whereas in LAD-III patients, collagen and PMA-induced aggregation is equally reduced. Control platelets were incubated with tirofiban (β3 integrin inhibitor) or tirofiban 1 LIA 1/2.1 (integrin β1 blocking moAb) to mimic the phenotype of Glanzmann thrombasthenia and LAD-III variant patients, respectively.

FCA allows testing the effect of platelet autoantibodies in plasma

There is a plethora of conditions in which platelet autoantibodies are generated or induced in a patient. It is relevant to the clinic to know not only the molecule recognized by the autoantibodies, but also to test their effect on platelet function. We have tested the plasma of immune thrombocytopenic purpura patients with persisting skin bleedings after splenectomy in spite of increased platelet counts and compared them with platelets from healthy donors. These patients produce strong reactive autoantibodies against αIIbβ3 integrin, which might result in altered platelet function.

We used ristocetin as a αIIbβ3-independent agonist as a positive control for the quality of the plasma and the platelets. As can be seen, most of the plasma samples induced a comparable or even a better response than did the healthy plasma controls, which were set to 100%. The increased response to ristocetin in some of these patient plasma samples (Figure 4, left) could be explained by increased levels of von Willebrand factor (data not shown), as occurs generally in thrombocytopenic patients.[32-34] When stimulated with PMA, 2 patient plasma samples reduced aggregation by 10%, 2 patient plasma samples reduced aggregation by 35%, and 1 patient's plasma did not affect the PMA-induced aggregation (Figure 4, right). One of the plasmas slightly increased and another decreased up to 80% both responses. The inhibitory effect of αIIbβ3 integrin autoantibodies on platelet aggregation is known for acquired Glanzmann thrombasthenia patients, with a primary coagulation defect in spite of (near) normal platelet counts.[35] This inhibitory effect exists in some immune thrombocytopenic purpura patients that, next to the thrombocytopenia, further impairs the primary coagulation. Clearly, this effect can be characterized by FCA.

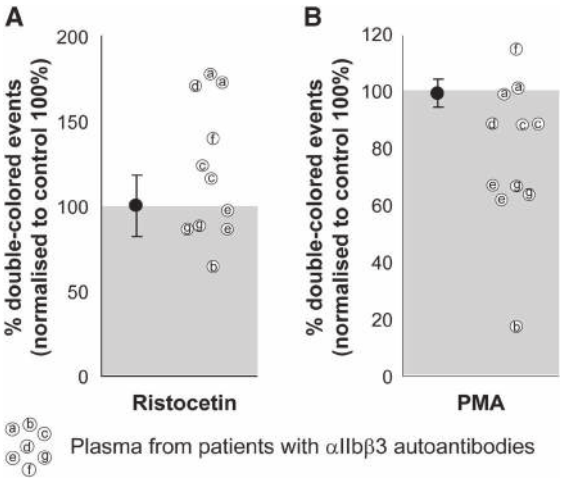

Figure 4. Effect of plasma on human platelet aggregation test

The plasma from patients with confirmed αIIbβ3 integrin autoantibodies was used with matched blood group, healthy donor platelets labeled with either CFSE or PKH26 and mixed in 1:1 ratio before stimulation. Ristocetin stimulation (left) was used as a control of the plasma quality because GPIb-induced platelet aggregation is independent of αIIbβ3 integrin function. PMA stimulation (right) was used to test the potential inhibitory effects of patient autoantibodies on αIIbβ3 integrin function. Aggregation percentages were normalized to those obtained with the same platelets incubated with healthy EDTA pool plasma (set to 100%) and either agonist. Average and standard deviation are depicted for the group of control plasmas on each condition, n = 4. Some of the patient plasmas were tested in 2 independent experiments.

FCA allows testing small volumes of mouse PRP and adult and embryonic whole blood

Mouse models are increasingly used to unravel platelet function mechanisms at the genetic level or in preclinical studies. However, assessing platelet function in small rodents requires in most cases euthanizing an animal for a single test. This precludes kinetic measurements in individual animals. For the same reason, the analysis of platelet function during the mouse fetal stages is very difficult. We therefore set out to validate our FCA method with mouse washed platelets, whole blood, and embryonic blood.

We tested mouse platelet aggregation upon PMA, collagen, Aggretin A, and botrocetin (which induces platelet aggregation in mice by activating GPIb, as does ristocetin with human platelets), and we employed several antagonists to each stimulation, ie, tirofiban, CD29 (α2β1 integrin blocking moAb), Bay (Syk inhibitor), and JAQ1 (GPVI inhibitor) (Figure 5 and supplemental Table 3). As shown in Figure 5A, PMA-induced aggregation was only inhibited by tirofiban, which confirms that this stimulus is αIIbβ3-dependent. Collagen-induced aggregation depends on functional GPVI and α2β1 integrin, Syk signaling, and, as opposed to human platelets in this assay, it depends on functional αIIbβ3 integrin (Figure 5B). Aggretin A–induced aggregation was dependent on functional αIIbβ3 integrin and Syk signaling,

as has been previously described (Figure 5C,E).[24,28] Botrocetin-induced aggregation was in our assay not influenced by any of the antagonists used (Figure 5D). Figure 5E depicts an example of the aggregation kinetics upon stimulation with Aggretin A: the percentage of double-colored events (Q2) increased over time and their forward scatter/side scatter positioning shifted compared with single platelets.

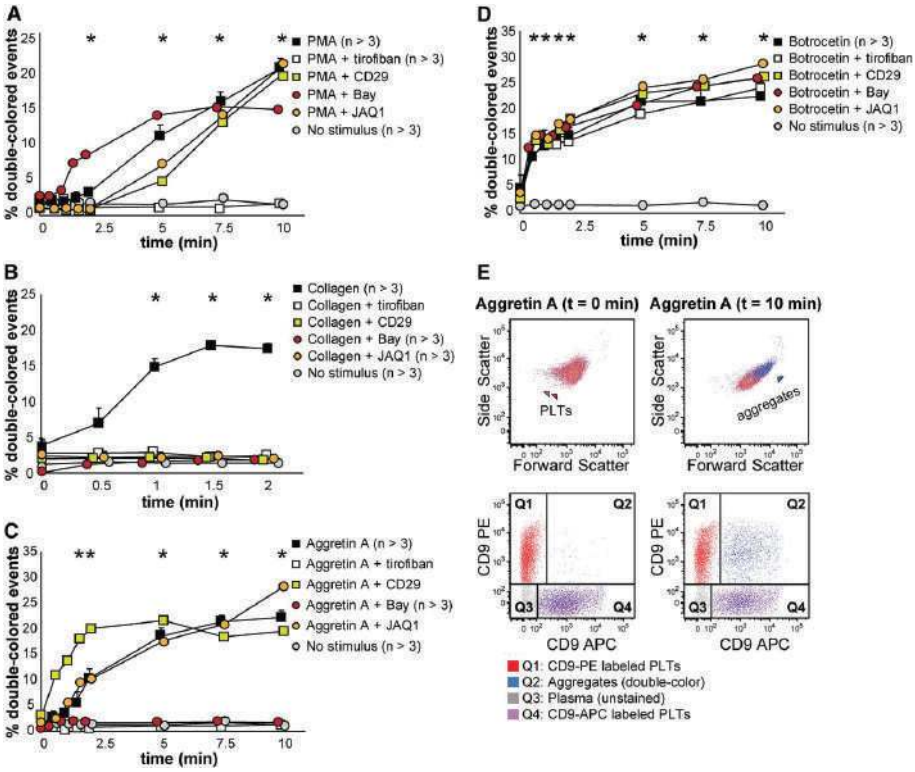

Figure 5. Mouse platelet aggregation test with washed platelets

Platelets were labeled with CD9-PE or CD9-APC and mixed in 1:1 ratio before stimulation. Aggregation was measured by flow cytometry in time after stimulation with PMA (A), collagen (B), Aggretin A (C), and botrocetin (D). Average and standard error of the mean are depicted when indicated, n > 3. Colored asterisks at each data point indicate statistical significance with the unstimulated control (P<.05). Representative data out of at least 5 independent experiments are depicted. We combined the agonists with the following antagonists: tirofiban (integrin β3 inhibitor), blocking anti-CD29 antibody (integrin β1), Bay (Syk inhibitor), and JAQ1 (GPVI blocking antibody). (E) An example of the gating used after flow cytometry analysis is depicted. Note the increase in events in Q2 after stimulation with Aggretin A. All populations are plotted against the forward and side scatter and indicated by colored arrowheads. PLT, platelets.

Next, we aimed to detect mouse platelet aggregation in whole blood samples. Optionally, it is possible to exclude erythroid blood cells by using Ter119-PerCPCy5.5 antibodies and gating the Ter119- population before the analysis of double-colored events. Upon stimulation with collagen, the percentage of double-colored events (Figure 6A, Q2) increased over time and their forward scatter/side scatter positioning shifted compared with single platelets (Figure 6A). Red blood cells were detected in Q3, where other cells and plasma components are also included (Figure 6A). As shown in Figure 6B, mouse platelet aggregation induced by PMA, collagen, Aggretin A, and botrocetin can be reliably measured in whole blood. As occurs with human platelets, the average events/aggregate is larger with the same stimulus when the aggregation test is performed in whole blood than with PRP-derived platelets (supplemental Tables 3 and 4). Summarizing, FCA allows platelet function analysis with a very small volume of blood (ie, 40-80 μL of blood are needed for testing 4 agonists with 4 aggregation time points per agonist), thus allowing time studies within the same animal in the context of clinical treatments or developmental studies.

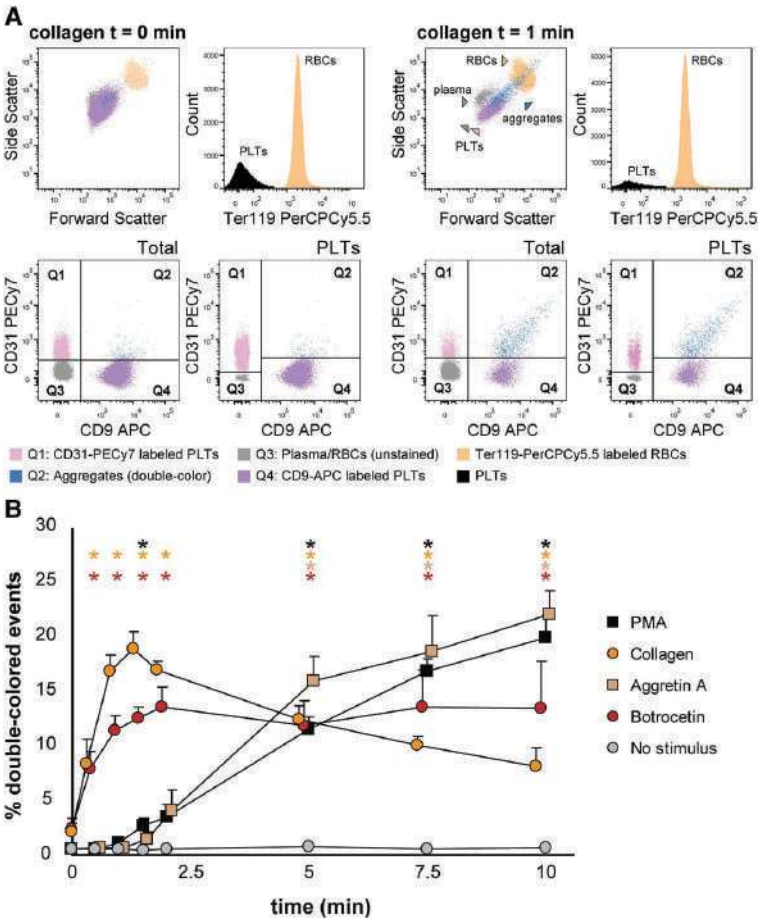

Figure 6. Mouse platelet aggregation test with whole blood

Platelets were labeled with CD9-APC or CD9-PE and mixed in 1:1 ratio before stimulation. Aggregation was measured by flow cytometry in time after stimulation with PMA, collagen, Aggretin A, and botrocetin. Average and standard error of the mean are depicted, n > 3.

A) An example of the gating strategy used after flow cytometry analysis. Ter1192 cells were selected to calculate double-colored events by plotting them against PE/APC channels. The same dot plot is shown for total events. Note the increase in events in Q2 after stimulation with collagen. Q1-Q4 and RBC populations are plotted against the forward and side scatter and indicated by colored arrowheads. PLT, platelets; RBC, red blood cells.

B) Time course of double-colored events upon stimulation with PMA, collagen, Aggretin A, and botrocetin. Non-stimulated labeled platelets are shown as baseline for spontaneous aggregation. Colored asterisks at each data point indicate statistical significance with the unstimulated control ($P < .05$).

Finally, we aimed to measure platelet aggregation of mouse embryonic platelets within the whole embryonic blood context. We collected 13.5 days post coitum embryonic blood, stained the platelets, and performed the aggregation test as described in "Materials and methods." As shown in Figure 7, we could detect platelet aggregation when activating the platelets with the 4 agonists used (ie, PMA, collagen, Aggretin A, and botrocetin), although the response to collagen stimulation was very low. This low collagen response of embryonic platelets has been previously described in porcine and human platelets,[36,37] and it might be occurring also with mouse platelets during ontogeny. Because the marker we use to label platelets (CD9) is also expressed by primitive erythroid cells (primitive red blood cells, Figure 7A), we performed an extra gating of CD9-positive cells (PE or APC gates) and selected single platelets as forward scatter low. We did not perform an equal selection from the Q2 gate of aggregates, because aggregates shift to higher forward scatter values. We conclude that FCA allows the study of platelet function during the ontogeny of the mouse (Figure 7 and supplemental Table 5), a clearly advantageous functional application when it is of interest to measure platelet aggregation defects in case of mouse models that do not get to term.

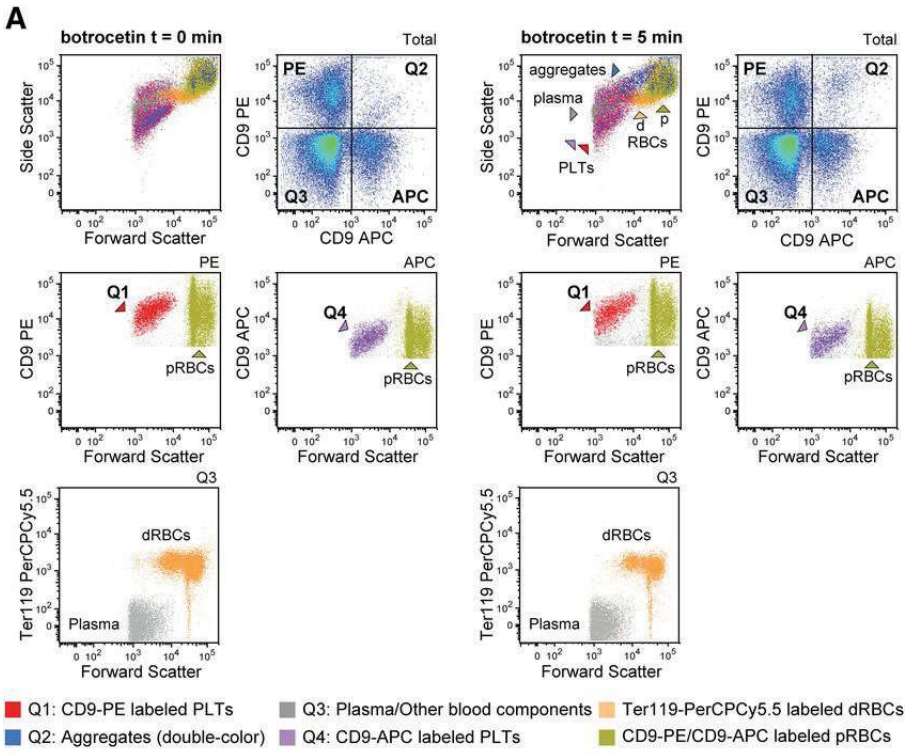
A
botrocetin t = 0 min
botrocetin t = 5 min
Total
Side Scatter
Forward Scatter
CD9 PE
CD9 APC
PE
APC
Q1
Q2
Q3
Q4
aggregates
plasma
PLTs
RBCs
d
p
pRBCs
dRBCs
Plasma
Ter119 PerCPCy5.5
Q1: CD9-PE labeled PLTs
Q2: Aggregates (double-color)
Q3: Plasma/Other blood components
Q4: CD9-APC labeled PLTs
Ter119-PerCPCy5.5 labeled dRBCs
CD9-PE/CD9-APC labeled pRBCs

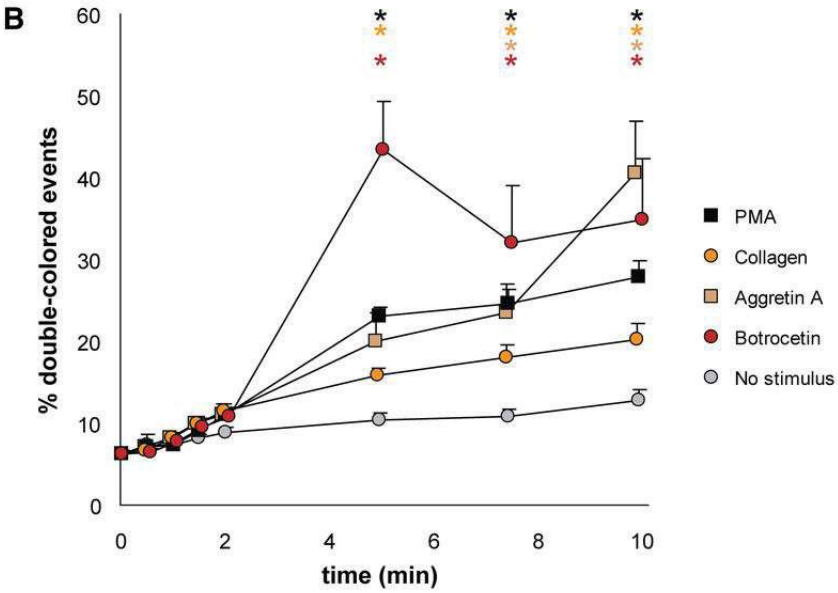
B
% double-colored events
time (min)
PMA
Collagen
Aggretin A
Botrocetin
No stimulus

Figure 7. Mouse platelet aggregation test with embryonic whole blood

Platelets were labeled with CD9-APC or CD9-PE and mixed in 1:1 ratio before stimulation. Aggregation was measured by flow cytometry in time after stimulation with PMA, collagen, Aggretin A, and botrocetin. Average and standard error of the mean are depicted, n > 3.

A) An example of the gating strategy used after flow cytometry analysis. CD9-PE or CD9-APC positive cells (gates APC or PE) were plotted against the forward scatter to select platelets (forward scatter low, named Q1 or Q4 to follow the nomenclature used in the formulas given in "Materials and methods") or primitive RBC that are also CD9-positive (forward scatter high, pRBC). Note the increase in events in Q2 after stimulation. Within the double-negative gate Q3, Ter119 marked dRBC and the rest were components of blood and plasma that are negative for all markers used (plasma). All these populations are plotted against the forward and side scatter and indicated by colored arrowheads. d, definitive; p, primitive; PLT, platelets; RBC, red blood cells.

B) Time course of double-colored events upon stimulation with PMA, collagen, Aggretin A, and botrocetin. Non-stimulated labeled platelets are shown as baseline for spontaneous aggregation. Colored asterisks at each data point indicate statistical significance with the unstimulated control ($P < .05$).

DISCUSSION

We have developed a sensitive test for platelet aggregation that we have named FCA. The protocol is based on the fluorescent labeling of platelets with 2 different dyes or fluorochrome-conjugated antibodies, and subsequent measurement of double-colored events on a flow cytometer, as adapted from previous aggregation assays of neutrophils and lymphocytes.[38] The labeling procedure did not affect platelet aggregation as measured by LTA and as shown in equivalent unstimulated time point samples measured by FCA.

It should be noted that the percentage of double-colored events underestimates the true number of aggregated platelets, because it counts aggregates of >2 platelets as a single event, and it excludes small aggregates containing -by chance- platelets with 1 label only. The contribution of the first phenomenon can be estimated from the number of platelets disappearing from the single-colored population. This indirect calculation (single-colored events disappearing) can be useful when using high platelet counts, but also in whole blood FCA because platelet aggregation with other blood cell types can result in much bigger aggregates that are not detected. Nevertheless, when performing FCA with washed platelets, we recommend maintaining a low platelet concentration (10-50x10^6/mL), because it allows the study of individual receptor function with a larger time response window. Whole blood FCA works optimally with higher platelet numbers (up to 300x10^6/mL), although it is sensitive enough with counts as low as 10x10^6/mL.

When assaying the function of washed human platelets, the formation of double-colored events was completely inhibited by the peptide antagonist tirofiban when using PMA as stimulus, as expected. With collagen as stimulus, the aggrega-

tion response appeared not to be dependent on αIIbβ3 integrin, because this aggregation failed to be inhibited by tirofiban. This was an unexpected result because collagen is known to trigger multiple synergistic pathways via multiple receptors, which would merge on αIIbβ3 integrin activation, required for aggregate formation.[39] On the other hand, the binding of soluble collagen to activated platelets has been shown to be dependent on α2β1 integrin.[40] In support of this notion, we observed that the response after collagen stimulation in our assay was strongly inhibited by LIA, which is directed against α2β1 integrin. This antibody did not interfere with the aggregation responses elicited by PMA or ristocetin. As more specifically developed in a separate study,[31] this particular characteristic brings about a novel feature of FCA: whereas the readout of classical aggregometry is dependent on αIIbβ3 integrin function upon collagen stimulus (ie, large aggregates), we can now distinguish between aggregation mediated by αIIbβ3 or α2β1 integrin because we are able to measure the early onset of aggregate formation. This feature allowed us to distinguish the aggregopathy accompanying Glanzmann thrombasthenia (αIIbβ3 integrin/fibrinogen receptor absent, α2β1 integrin functional) and the aggregopathy accompanying LAD-III (both integrins inactive), because we could still detect collagen-induced aggregates in Glanzmann thrombasthenia but not in LAD-III platelets.[31] Furthermore, tirofiban preincubation affected the size of collagen-induced aggregates and consequently the reduction in single-colored events. This suggests that collagen-mediated aggregation requires functional α2β1 integrin instead of αIIbβ3 integrin at the onset of aggregation and that αIIbβ3 integrin contributes to aggregate size and stability in a second wave. Translated to a physiological context, collagen-induced FCA probably represents the platelet adhesion to and aggregation on the damaged blood vessel wall, which also involves primarily interaction with α2β1 followed by αIIbβ3 mediated amplification. Of note, whereas PMA, collagen, Aggretin A, and ristocetin can be used in 1- to 2-day-old blood samples, other agonists such as ADP or thrombin receptor agonist peptide 6 (data not shown) perform properly only in fresh samples.

In case of whole blood aggregation, we detected a higher percentage of double-colored events when compared with aggregation of washed platelets. In addition, we detected platelet–red cell aggregates and platelet–mononuclear cell aggregates, which contribute also to clot formation in vivo (data not shown). Thus, many more different parameters have to be taken into account when measuring platelet aggregation in whole blood than is the case with washed platelets. This is the reason why dissection of single receptor function is more straight-forward in the washed platelet setup than in whole blood, because aggregation to other cell types might mask the function of a specific receptor at the onset of aggregate formation. We additionally have observed an important contribution of αIIbβ3 integrin in the collagen-induced aggregation process in the whole blood context (Figure 3C). In concordance with this, when assaying the function of Glanzmann thrombasthenia and LAD-III patients in whole blood, we could still distinguish between the two aggregopathies; however, Glanzmann platelets aggregated 50% of control platelets upon collagen stimulation, as opposed to the normal aggregation levels we detected in washed platelet samples.[31]

We have shown that FCA allows not only the detection of intrinsic defects in platelet aggregation, but can also be used to detect blocking autoantibodies present in plasma and directed against platelet membrane antigens. With the same philosophy, FCA can be used to test chemical libraries or drugs, in small volumes of multiple samples on a large scale, thereby reducing the costs. This is potentially very relevant for screening studies for the development of novel hemostatic drugs, but also for patient-directed antiplatelet therapy monitoring.[41,42] In addition, FCA can be applied to study platelet aggregation induced by bacteria or bacteria–platelet binding in washed platelets or whole blood. Relevant in the context of transfusion monitoring, platelet–blood cell interactions can be also potentially measured by FCA. We further validated FCA for use with mouse platelets, either washed or in the whole blood context, and also fetal platelets in the embryonic blood context. We used botrocetin instead of ristocetin to induce GPIb-mediated platelet aggregation, because ristocetin is known to be unable to induce mouse platelet agregation.[43,44] We noted that collagen-induced aggregation always required αIIbβ3 integrin function in mouse platelets, either washed or in the whole blood context, in contrast to what we found in human platelets. This could be due to species evolutionary divergence.[45] The β3-independent collagen-induced platelet aggregation in human washed platelets is a process that occurs during a very small time window at physiological conditions, and the signaling cascade toward αIIbβ3 integrin seems to be much faster in the mouse platelets. When analyzing the function of fetal platelets, we observed a very low response upon collagen stimulation, as has been described for human and porcine platelets.[36,37] Thus, this "fetal platelet dysfunction" appears conserved among species.

In conclusion, we provide a novel flow cytometry-based platelet aggregation assay that we have termed FCA, which can be performed with small starting volumes or low numbers of platelets. In combination with conventional surface marker analysis by flow cytometry and classical assays, FCA stands as a promising tool for the diagnosis of platelet defects, for screening of drug effects on platelet function, and for studies in animal models.

ACKNOWLEDGMENTS

The authors are grateful to Dr F. Sánchez-Madrid (Universidad Autónoma de Madrid, Spain) for providing moAb LIA1/2.1, and to Dr P.W. Kamphuisen and Dr M. Peters (Academic Medical Centre, Amsterdam, The Netherlands), as well as Dr Ö. Sanal and Dr M. Çetin (Hacepette University, Ankara, Turkey) for providing patient material. The authors thank Prof. D. Roos for critically reading the manuscript.

This work was supported by the Landsteiner Foundation for Blood Transfusion Research (grant 0619) (T.W.K. and E.v.d.V.), Sanquin Blood Supply, grant number PPOC-08-004 (I.M.D.C.), the Center for Translational Molecular Medicine program Innovative Coagulation Diagnostics (I.M.D.C., M.M.), The Netherlands Organization for Scientific Research (863.09.012) (L.G.), and the Deutsche Forschungsgemeinschaft (Eb177/9-1) (J.A.E.).

Authorship

Contribution: I.M.D.C. and M.M. designed and performed experiments and analyzed data; E.v.d.V. performed experiments; D.d.K. designed experiments and wrote the paper; L.P., M.d.H., J.A.E., K.S., S.R., and D.P. provided material and participated in discussions; T.W.K. designed experiments and wrote the paper; A.J.V. designed experiments and wrote the paper; T.K.v.d.B. designed experiments and wrote the paper; and L.G. designed and performed experiments, analyzed data and wrote the paper.

Conflict-of-interest disclosure

The authors declare no competing financial interests.

The current affiliation for A.J.V. is the Department of Medical Biochemistry, Academic Medical Centre, University of Amsterdam, The Netherlands.

Correspondence

Laura Gutiérrez, Department of Blood Cell Research, Sanquin Research and Landsteiner Laboratory, Academic Medical Center, University of Amsterdam, Plesmanlaan 125, 1066 CX Amsterdam, The Netherlands; e-mail: l.gutierrez@sanquin.nl.

REFERENCE LIST

1. Leslie M. Cell biology. Beyond clotting: the powers of platelets. Science 2010;328(5978):562-564.
2. Gay LJ, Felding-Habermann B. Contribution of platelets to tumour metastasis. Nat Rev Cancer 2011;11(2):123-134.
3. Feng W, Madajka M, Kerr BA, et al. A novel role for platelet secretion in angiogenesis: mediating bone marrow-derived cell mobilization and homing. Blood 2011;117(14):3893-3902.
4. Semple JW, Italiano JE Jr, Freedman J. Platelets and the immune continuum. Nat Rev Immunol 2011;11(4):264-274.
5. Ma AC, Kubes P. Platelets, neutrophils, and neutrophil extracellular traps (NETs) in sepsis. J Thromb Haemost 2008;6(3):415-420.
6. Uhrin P, Zaujec J, Breuss JM, et al. Novel function for blood platelets and podoplanin in developmental separation of blood and lymphatic circulation. Blood 2010;115(19):3997-4005.
7. Brass L. Understanding and evaluating platelet function. Hematology Am Soc Hematol Educ Program 2010;2010:387-396.
8. Picker SM. In-vitro assessment of platelet function. Transfus Apheresis Sci 2011;44(3):305-319.
9. Rodgers RP, Levin J. Bleeding time: a guide to its diagnostic and clinical utility. Arch Pathol Lab Med 1990;114(12):1187-1188.
10. Rodgers RP, Levin J. A critical reappraisal of the bleeding time. Semin Thromb Hemost 1990;16(1):1-20.
11. Rodgers RP, Levin J. Bleeding time revisited. Blood 1992;79(9):2495-2497.
12. Yardumian DA, MackieI J, Machin SJ. Laboratory investigation of platelet function: a review of methodology. J Clin Pathol 1986;39(7):701-712.
13. Born GV. Aggregation of blood platelets by adenosine diphosphate and its reversal. Nature 1962;194:927-929.
14. Breddin HK. Can platelet aggregometry be standardized? Platelets 2005;16(3-4):151-158.
15. Linnemann B, Schwonberg J, Mani H, et al. Standardization of light transmittance aggregometry for monitoring antiplatelet therapy: an adjustment for platelet count is not necessary. J Thromb Haemost 2008;6(4):677-683.
16. Moffat KA, Ledford-Kraemer MR, Nichols WL, et al; North American Specialized Coagulation Laboratory Association. Variability in clinical laboratory practice in testing for disorders of platelet function: results of two surveys of the North American Specialized Coagulation Laboratory Association. Thromb Haemost 2005;93(3):549-553.
17. Price EA, Hayward CP, Moffat KA, et al. Laboratory testing for heparin-induced thrombocytopenia is inconsistent in North America: a survey of North American specialized coagulation laboratories. Thromb Haemost 2007;98(6):1357-1361.
18. Harrison P. Assessment of platelet function in the laboratory. Hamostaseologie 2009;29(1):25-31.

19. Rand ML, Leung R, Packham MA. Platelet function assays. Transfus Apheresis Sci 2003;28(3):307-317.

20. Johnson EN, Brass LF, Funk CD. Increased platelet sensitivity to ADP in mice lacking platelet-type 12-lipoxygenase. Proc Natl Acad Sci USA 1998;95(6):3100-3105.

21. Hayward CP, Moffat KA, Raby A, et al. Development of North American consensus guidelines for medical laboratories that perform and interpret platelet function testing using light transmission aggregometry. Am J Clin Pathol 2010;134(6):955-963.

22. Gutiérrez L, Lindeboom F, Langeveld A, et al. Homotypic signalling regulates Gata1 activity in the erythroblastic island. Development 2004;131(13):3183-3193.

23. Campanero MR, Arroyo AG, Pulido R, et al. Functional role of alpha 2/beta 1 and alpha 4/beta 1 integrins in leukocyte intercellular adhesion induced through the common beta 1 subunit. Eur J Immunol 1992;22(12):3111-3119.

24. Suzuki-Inoue K, Fuller GL, García A, et al. A novel Syk-dependent mechanism of platelet activation by the C-type lectin receptor CLEC-2. Blood 2006;107(2):542-549.

25. Tandon NN. Jamieson GA. Role of GPIV as a platelet receptor for collagen adhesion. Prog Clin Biol Res 1988;283:315-318.

26. Saelman EU, Nieuwenhuis HK, Hese KM, et al. Platelet adhesion to collagen types I through VIII under conditions of stasis and flow is mediated by GPIa/IIa (alpha 2 beta 1-integrin). Blood 1994;83(5):1244-1250.

27. Bergmeier W, Bouvard D, Eble JA, et al. Rhodocytin (aggretin) activates platelets lacking alpha(2)beta(1) integrin, glycoprotein VI, and the ligand-binding domain of glycoprotein Ibalpha. J Biol Chem 2001;276(27):25121-25126.

28. Finney BA, Schweighoffer E, Navarro-Núñez L, et al. CLEC-2 and Syk in the megakaryocytic/platelet lineage are essential for development. Blood 2012;119(7):1747-1756.

29. Peñas PF, Gómez M, Buezo GF, et al. Differential expression of activation epitopes of beta1 integrins in psoriasis and normal skin. J Invest Dermatol 1998;111(1):19-24.

30. McGregor L, Hanss M, Sayegh A, et al. Aggregation to thrombin and collagen of platelets from a Glanzmann thrombasthenic patient lacking glycoproteins IIb and IIIa. Thromb Haemost 1989;62(3):962-967.

31. van de Vijver E, De Cuyper IM, Gerrits AJ, et al. Defects in Glanzmann thrombasthenia and LAD-III (LAD-1/v) syndrome: the role of integrin ⊠1 and ⊠3 in platelet adhesion to collagen. Blood 2012;119(2):583-586.

32. Casonato A, Fabris F, Boscaro M, et al. Increased factor VIII/vWf levels in patients with reduced platelet number. Blut 1987;54(5):281-288.

33. Hanss M, Ville D, Dechavanne M. Increased plasma tissue-type plasminogen activator levels in patients with chronic thrombocytopenia. Haemostasis 1990;20(6):341-346.

34. Nilsson TK, Sondell KM, Norberg BO, et al. Plasma levels of endothelial-derived haemostatic factors in autoimmune thrombocytopenia and haemolytic anaemia. J Intern Med 1990;228(3):249-252.

35. Porcelijn L, Huiskes E, Maatman R, et al. Acquired Glanzmann's thrombasthenia caused by glycoprotein IIb/IIIa autoantibodies of the immunoglobulin G1 (IgG1), IgG2 or IgG4 subclass: a study in six cases. Vox Sang 2008;95(4):324-330.

36. Pandolfi M, Astedt B, Cronberg L, et al. Failure of fetal platelets to aggregate in response to adrenaline and collagen. Proc Soc Exp Biol Med 1972;141(3):1081-1083.

37. Olutoye OO, Alaish SM, Carr ME Jr, et al. Aggregatory characteristics and expression of the collagen adhesion receptor in fetal porcine platelets. J Pediatr Surg 1995;30(12):1649-1653.

38. Kuypers TW, Koenderman L, Weening RS, et al. Continuous cell activation is necessary for stable interaction of complement receptor type 3 with its counter-structure in the aggregation response of human neutrophils. Eur J Immunol 1990;20(3):501-508.

39. Nuyttens BP, Thijs T, Deckmyn H, Broos K. Platelet adhesion to collagen. Thromb Res 2011;127(Suppl 2):S26-S29.

40. Jung SM, Moroi M. Platelets interact with soluble and insoluble collagens through characteristically different reactions. J Biol Chem 1998;273(24):14827-14837.

41. Seidel H, Rahman MM, Scharf RE. Monitoring of antiplatelet therapy. Current limitations, challenges, and perspectives. Hamostaseologie 2011;31(1):41-51.

42. Scharf RE, Rahman MM, Seidel H. The impact and management of acquired platelet dysfunction. Hamostaseologie 2011;31(1):28-40.

43. Ware J, Russell SR, Marchese P, et al. Expression of human platelet glycoprotein Ib alpha in transgenic mice. J Biol Chem 1993;268(11):8376-8382.

44. Ware J, Russell S, Ruggeri ZM. Cloning of the murine platelet glycoprotein Ibalpha gene highlighting species-specific platelet adhesion. Blood Cells Mol Dis 1997;23(2):292-301.

45. Smyth SS, Tsakiris DA, Scudder LE, et al. Structure and function of murine alphaIIbbeta3 (GPIIb/IIIa): studies using monoclonal antibodies and beta3-null mice. Thromb Haemost 2000;84(6):1103-1108.

% single-colored events													
		PMA			Collagen			Aggretin A			Ristocetin		
min	no stimulus		+T	+ LIA		+T	+ LIA		+T	+ LIA		+T	+ LIA
0	100	100	100	100	100	100	100	100	100	100	100	100	100
1	92	102	101	97	100	112	105	95	95	98	75	76	66
2	90	103	98	102	83	99	102	93	95	91	44	37	41
5	88	94	103	85	54	79	99	73	91	70	26	24	23
10	95	58	105	63	29	53	90	58	86	52	17	14	13

average number of events/aggregate													
		PMA			Collagen			Aggretin A			Ristocetin		
min	no stimulus		+T	+ LIA		+T	+ LIA		+T	+ LIA		+T	+ LIA
0	nd	2	nd	2	0	nd	nd	1	1	nd	3	2	4
1	nd	2	4	nd	2	0	nd	2.1	2.8	2.6	7	9	8
2	nd	2	nd	2	7	3	1	3.5	2.5	3.8	17	15	20
5	nd	7	nd	6	21	8	4	8.2	2.5	9.7	45	57	67

Supplementary Table 1

Calculation of the percentage of reduction in single-colored events and average size of aggregates (events/aggregate) in the human PRP flow cytometry platelet aggregation test (Figure 2), as explained in the Materials and Methods section. Representative data out of at least five independent experiments are depicted. Nd: not determined due to low double-colored events or no decrease in single-colored events. T, tirofiban.

% single-colored events											
		PMA			Collagen			Aggretin A	Ristocetin		
min	no stimulus		Glanz	LAD		Glanz	LAD			Glanz	LAD
0	100	100	100	100	100	100	100	100	100	100	100
0.5	128	59	102	89	23	53	73	45	28	24	37
1	101	35	128	80	8	46	63	34	15	13	23
2	105	19	128	111	5	38	64	25	7	1	16
5	116	6	124	84	5	36	71	20	7	7	5

average number of events/aggregate											
		PMA			Collagen			Aggretin A		Ristocetin		
min	no stimulus		+T	+ LIA		+T	+ LIA	+T	+ LIA	+T	+ LIA
0.5	nd	0	nd	nd	19	nd	nd	4.1	10	9.9	1.1
1	nd	5	nd	nd	47	nd	nd	5.6	12	1.7	1.5
2	nd	9	nd	nd	55	nd	nd	10.6	34	76.6	4.3
5	nd	48	nd	nd	49	nd	nd	14.3	20	22.1	5

Supplementary Table 2

Calculation of the percentage of reduction in single-colored events and average size of aggregates (events/aggregate) in the human whole blood flow cytometry platelet aggregation test (Figure 3). Representative data out of at least five independent experiments are depicted. Glanz, Glanzmann Thrombasthenia platelets; LAD, LAD-III platelets.

% single-colored events											
		PMA					Collagen				
min	no stimulus		+ T	+ CD29	+ Bay	+ JAQ1		+ T	+ CD29	+ Bay	+ JAQ1
0	100	100	100	100	100	100	100	100	100	100	100
0.5	100	92	104	100	93	99	89	99	98	100	114
1	100	94	103	95	94	94	69	97	96	100	113
1.5	99	91	103	92	92	92	60	91	97	96	111
2	100	97	103	103	98	102	58	99	98	101	112
5	100	76	103	85	78	83					
7.5	99	58	101	68	62	67					
10	101	49	97	56	48	54					

average number of events/aggregate											
		PMA					Collagen				
min	no stimulus		+ T	+ CD29	+ Bay	+ JAQ1		+ T	+ CD29	+ Bay	+ JAQ1
0.5	nd	2.1	nd	nd	nd	nd	1.5	nd	nd	nd	nd
1	nd	3	nd	nd	nd	nd	3.7	nd	nd	nd	nd
1.5	nd	2.8	nd	nd	nd	nd	4.8	nd	nd	nd	nd
2	nd	nd	nd	nd	nd	nd	7.4	nd	nd	nd	nd
5	nd	1.6	nd	nd	2.2	nd					
7.5	nd	3.7	nd	nd	4	nd					
10	nd	4.9	nd	1.2	8.8	1.2					

Supplementary Table 3

Calculation of the percentage of reduction in single-colored events and average size of aggregates (events/aggregate) in the mouse PRP flow cytometry platelet aggregation test (Figure 5). Representative data out of at least five independent experiments are depicted. Nd: not determined due to low double-colored events or no decrease in singlecolored events. T, tirofiban.

% single-colored events					
min	**no stimulus**	**PMA**	**Collagen**	**Aggretin A**	**Botrocetin**
0	100	100	100	100	100
0.5	98	102	100	101	103
1	100	94	77	99	100
1.5	95	76	54	97	87
2	100	70	40	88	72
5	100	51	25	76	18
7.5	101	47	29	63	13
10	101	47	21	55	10
average number of events/aggregate					
min	**no stimulus**	**PMA**	**Collagen**	**Aggretin A**	**Botrocetin**
0.5	nd	nd	nd	nd	nd
1	nd	nd	1.5	3.7	1.2
1.5	nd	1.3	4.1	1.6	4
2	nd	4.05	7.5	2.3	9.8
5	nd	4.33	17.3	8.5	99.8
7.5	nd	16.9	18.4	10.7	148.3
10	nd	20.4	26.1	32.9	243.6

Supplementary Table 4

Calculation of the percentage of reduction in single-colored events and average size of aggregates (events/aggregate) in the mouse whole blood flow cytometry platelet aggregation test (Figure 6). Representative data out of at least five independent experiments are depicted. Nd: not determined due to low double-colored events or no decrease in singlecolored events.

% single-colored events					
min	**no stimulus**	**PMA**	**Collagen**	**Aggretin A**	**Botrocetin**
0	100	100	100	100	100
0.5	102	86	100	81	111
1	106	87	96	86	114
1.5	105	83	92	81	111
2	98	82	89	77	109
5	87	48	67	59	30
7.5	81	37	56	38	23
10	74	32	51	21	21
average number of events/aggregate					
min	**no stimulus**	**PMA**	**Collagen**	**Aggretin A**	**Botrocetin**
0.5	nd	5	nd	5.9	1
1	nd	4.2	4.5	4.3	nd
1.5	nd	4	4.7	2.4	nd
2	nd	2.3	4.8	2.6	nd
5	1	3.4	5.8	2.8	4.5
7.5	2	4.6	4.9	4.5	9.3
10	2	4.9	5	7.4	9.2

Supplementary Table 5

Calculation of the percentage of reduction in single-colored events and average size of aggregates (events/aggregate) in the mouse fetal whole blood flow cytometry platelet aggregation test (Figure 7). Representative data out of at least five independent experiments are depicted. Nd: not determined due to low double-colored events or no decrease in single-colored events.

Chapter 3

SP1/SP3 TRANSCRIPTION FACTORS IN MEGAKARYOPOIESIS

Sp1/Sp3 transcription factors regulate hallmarks of megakaryocyte maturation, and platelet formation and function

Blood. 2014 December

Marjolein Meinders, Divine I. Kulu, Harmen J.G. van de Werken,
Mark Hoogenboezem, Hans Janssen, Rutger W.W. Brouwer,
Wilfred F.J. van Ijcken, Erik-Jan Rijkers, Jeroen A.A. Demmers,
Imme Krüger, Timo K. van den Berg, Guntram Suske,
Laura Gutiérrez and Sjaak Philipsen

SP1/SP3 TRANSCRIPTION FACTORS REGULATE HALLMARKS OF MEGAKARYOCYTE MATURATION, AND PLATELET FORMATION AND FUNCTION

Marjolein Meinders[1,8], Divine I. Kulu[2,8], Harmen J.G. van de Werken[2], Mark Hoogenboezem[3], Hans Janssen[4], Rutger W.W. Brouwer[5], Wilfred F.J. van Ijcken[5], Erik-Jan Rijkers[6], Jeroen A.A. Demmers[6], Imme Krüger[7], Timo K. van den Berg[1], Guntram Suske[7], Laura Gutiérrez[1,9] and Sjaak Philipsen[2,9].

[1]Dept. Blood Cell Research, Sanquin Research and Landsteiner Laboratory, Academic Medical Centre (AMC), University of Amsterdam (UvA), 1066CX Amsterdam, the Netherlands; [2]Dept. Cell Biology, Erasmus MC, 3015CE Rotterdam, the Netherlands; [3]Dept. Molecular Cell Biology, Sanquin Research and Landsteiner Laboratory, Academic Medical Centre (AMC), University of Amsterdam (UvA), 1066CX Amsterdam, the Netherlands; [4]Division of Cell Biology, The Netherlands Cancer Institute (NKI), 1006BE Amsterdam, the Netherlands; [5]Center for Biomics, Erasmus MC, 3015CE Rotterdam, the Netherlands; [6]Proteomics Center, Erasmus MC, 3015CE Rotterdam, the Netherlands; [7]Institute of Molecular Biology and Tumor Research, Philipps-University Marburg, Germany; [8]Co-first authors; [9]Co-senior and corresponding authors.

Running Head: Sp1/Sp3 transcription factors in megakaryopoiesis
Abstract (200 words): 198
Manuscript (max 4000 words): 3994
Figures: 7
References (Max 100): 78
Supplemental Methods: 1
Supplemental Figures and Legends: 6
Supplemental Tables: 3
Videos: 8

ABSTRACT

Sp1 and Sp3 belong to the Specificity proteins (Sp)/Krüppel-like transcription factor family. They are closely related, ubiquitously expressed and recognize G-rich DNA motifs. They are thought to regulate generic processes such as cell cycle and growth control, metabolic pathways and apoptosis. Ablation of Sp1 or Sp3 in mice is lethal, and combined haploinsufficiency results in hematopoietic defects during the fetal stages. Here, we show that in adult mice conditional pan-hematopoietic (Mx1-Cre) ablation of either Sp1 or Sp3 has minimal impact on hematopoiesis, while the simultaneous loss of Sp1 and Sp3 results in severe macrothrombocytopenia. This occurs in a cell-autonomous manner as shown by megakaryocyte-specific (Pf4-Cre) double knockout mice. We employed flow cytometry, cell culture and electron microscopy and show that although megakaryocyte numbers are normal in bone marrow and spleen, they display a less compact demarcation membrane

system and a striking inability to form proplatelets. Through megakaryocyte transcriptomics and platelet proteomics we identified several cytoskeleton-related proteins and downstream effector kinases, including Mylk, that were downregulated upon Sp1/Sp3 depletion, providing an explanation for the observed defects in megakaryopoiesis. Supporting this notion, selective Mylk inhibition by ML7 affected proplatelet formation and stabilization and resulted in defective ITAM receptor-mediated platelet aggregation.

Key Words

Sp transcription factor, macrothrombocytopenia, megakaryopoiesis, platelets, Mylk.

Key Points

- FMegakaryocyte-specific Sp1/Sp3 dKO mice display macrothrombocytopenia and platelet dysfunction, due to defects in megakaryocyte maturation
- Selective Mylk inhibition by ML7 affects proplatelet formation and stabilization and ITAM receptor-mediated platelet aggregation

INTRODUCTION

Platelets are the blood cells responsible for maintaining the body hemostasis and, in humans, ~10^{11} platelets are produced by megakaryocytes daily.[1] Megakaryopoiesis is the process whereby hematopoietic progenitor cells differentiate into mature megakaryocytes, which produce platelets in a process known as thrombopoiesis.[2,3] This takes place at sites of primary hematopoiesis, i.e. the bone marrow and, in mice, also in the spleen.[4] The hormone thrombopoietin (TPO), produced by the liver, regulates platelet production. TPO levels in plasma are inversely proportional to the megakaryocyte/platelet mass.[5] Megakaryocyte differentiation is characterized by highly specialized cellular changes including endomitosis (leading to polyploid cells), accumulation of alpha and dense granules and development of a demarcation membrane system (DMS), which is required as a membrane reservoir to produce large numbers of platelets.[2,3] Mature megakaryocytes migrate towards the proximity of blood vessels through which they protrude cytoplasmic microtubule-rich extensions into the blood stream, known as proplatelets, from which platelets are shed.[6] Coordinated interactions between the membrane, cytoskeletal machinery and intracellular signaling are essential for proplatelet formation.[3] These events are accompanied by extensive transcription and protein synthesis and defects in one or more of these processes lead to qualitative or quantitative defects in platelets.[3,7,8] Acquired or congenital thrombocytopenias, i.e. low platelet counts,[9] are caused by increased platelet destruction[10] or by decreased platelet production.[7,11,12] The causative mutations for some of the congenital thrombocytopenias, which present with bleeding symptoms, have been identified: i.e. Glanzmann Thrombasthenia, Ber-

nard-Soulier Syndrome (BSS).[7,12-14] However, an increasing number of congenital thrombocytopenias of unknown etiology, asymptomatic with respect to bleeding, are currently diagnosed due to the routine use of automated blood counting.[9] Increasing efforts worldwide are aimed at identifying the molecular mechanisms regulating megakaryopoiesis, including transcriptional programs, since not only coding mutations but also mutations in regulatory regions of genes could be involved in the development of inherited thrombocytopenias.[15]

Many studies have already pinpointed several transcription factors that play an essential role in megakaryopoiesis, such as GATA1,[7,12,16-19] GFI1B,[20] RUNX1,[21] FLI1, NFE2 and TAL1.[15,22-24]

Sp1 and Sp3 belong to the family of Specificity protein/Krüppel-like Factor (Sp/KLF), which recognize G-rich promoter elements (GC-box and the related GT-box) and are expressed in most mammalian cell types investigated to date.[25,26] *Sp1* knockout embryos are developmentally retarded and do not survive beyond embryonic day 10.5.[27] *Sp3 null* embryos die shortly after birth due to complications including defects in hematopoiesis.[28-30] Sp1/Sp3 compound heterozygous embryos are not viable and display impaired erythroid development, suggesting that a critical threshold of Sp1/Sp3 activity is required for normal embryonic development and that these two proteins have additive effects in regulating downstream target genes.[31]

To understand the role of Sp1 and Sp3 in the adult hematopoietic system, we generated mice with conditional knockout alleles for Sp1 and Sp3 which we crossed with the inducible pan-hematopoietic Cre line, *Mx1-Cre*.[32] Sp1/Sp3 double knockout animals showed a dramatic reduction in the number of circulatory platelets. Based on these findings, we used the *Pf4-Cre* line, which allows for gene excision in the megakaryocytic lineage,[33] to investigate a cell-autonomous role of Sp1 and Sp3 in megakaryocyte and platelet development. Megakaryocyte-specific Sp1/Sp3 double knockout mice display macrothrombocytopenia and platelet dysfunction. We studied megakaryopoiesis and platelet function in these mice, and combined genome-wide transcriptomics and proteomics in order to reveal deregulated genes and their function during megakaryopoiesis.

METHODS

Mice

Mice were maintained in the Erasmus MC (EDC) or the Netherlands Cancer Institute (NKI) animal care facilities under specific pathogen-free conditions. All animal experiments were approved by the Erasmus MC and NKI Animal Ethics Committee.

Blood analysis

Blood was drawn by submandibular vein or heart puncture, and collected in heparin-coated vials. Blood parameters were determined on a scil Vet abc Plus+ instrument (Viernheim, Germany). Platelet rich plasma (PRP) was separated by centrifuging the blood 15 min at 50 G. TPO levels in plasma were measured by mouse TPO immunoassay (R&D; Minneapolis, MN, USA).

Platelet function assays

Flow chamber perfusion

Platelets were washed from PRP and 10^8 platelets were resuspended in 200 µl of platelet-free blood + plasma 1:1 ($5x10^8$ platelets/mL), which was perfused over a micro-slide (0.1 Luer, Ibidi; Martinsried, Germany) coated with 100 µl/mL collagen (Horm, Nycomed Arzneimittel; Munich, Germany) under arterial shear conditions (1500 m/s). Thrombi were labelled with 200 µl 2 nM CFSE in PBS (Invitrogen, Life Technologies; Carlsbad, CA, USA), and images were taken at 20X magnification with an EVOS fluorescent microscope (AMG, Life Technologies). Coverage of adhered platelets was quantified using ImageJ software (8 images per sample).

Flow cytometry based platelet aggregation assay (FCA)

FCA was performed as described.[34] See Supplemental Methods.

Tail bleeding time

Non-anesthetized mice were placed in a restraining device and 5 mm of the distal tail was cut. The tail was immersed in PBS at 37°C and bleeding time was measured from the moment of transection until first arrest of bleeding. If bleeding did not cease observation was stopped at 120 seconds.

Flow cytometry

See Supplemental Methods.

Histology

Spleen samples and HEPES-flushed bone marrow from mouse femora were embedded in Tissue-Tek® (EMS; Hatfield, PA, USA) and snap-frozen in liquid nitrogen. Bone marrow sections (5 µm) were cut using a cryostat and were subsequently stained with CD41-PE (BD Biosciences; San Diego, CA, USA), CD31-FITC (R&D) and Phalloidin-CF633 (Biotium; Hayward, CA, USA). Pictures were taken using a LSM510 confocal microscope equipped with an axiocam MRm (Zeiss; Oberkochen, Germany). Acetylcholinesterase staining on spleen sections was performed as described previously.[35]

In vitro culture

Bone marrow explants: proplatelet formation assay

As previously described[36] and specified in Supplemental Methods.

Bone marrow-derived megakaryocyte cultures

Bone marrow single cell suspension was made by straining crushed femora through a 40 µm filter (BD Biosciences) and cultured in StemSpan (Stem Cell technologies; Vancouver, Canada) supplemented with 10% heat-inactivated fetal calf serum, Penicillin/Streptavidin, 2% low density lipoprotein (Sigma-Aldrich; St. Louis, MO, USA), 50ng/ml recombinant human SCF, 20 ng/ml TPO and 1 unit/mL Erythropoietin at a concentration of $2x10^6$ cells/ml. Cells were washed at day 2 and 4 and an increasing concentration of TPO was added, i.e. 50 ng/mL at day 2 and 100 ng/mL at day 4. At day 7 the cells were harvested.

Electron microscopy
Cultured megakaryocytes were fixed in Karnovsky's fixative. Post-fixation was done with 1% Osmiumtetroxide in 0.1 M cacodylate buffer. After washing, the pellets were stained *en bloc* with Ultrastain 1 (Leica; Wetzlar, Germany), followed by ethanol dehydration series. Finally, megakaryocytes were embedded in a mixture of DDSA/NMA/Embed-812 (EMS), sectioned and stained with Ultrastain 2 (Leica) and analyzed with a Philips CM10 electron microscope (FEI company; Hillsboro, OR, USA).

RNA and Protein
See Supplemental Methods.

Statistical Analysis
We represent average and standard error of the mean (SEM) of at least three mice per genotype unless otherwise indicated. We applied two-tailed Student's *t*-tests to calculate statistical significance. * $P < .05$; ** $P < .005$; *** $P < .001$.

RESULTS

Sp1::Sp3 dKO mice are macrothrombocytopenic with normal plasma TPO levels
In order to evaluate the contribution of the Sp1/Sp3 transcription factors to adult hematopoiesis, *Sp1*$^{fl/fl}$::*Sp3*$^{fl/fl}$ mice were crossed with *Mx1-Cre* mice[32] and treated with polyinosinic:polycytidylic acid (poly I:C) as described previously.[16] *Mx1-Cre*::*Sp1*$^{fl/fl}$::*Sp3*$^{fl/fl}$ (Mx1-Cre::dKO) mice displayed decreased white blood cell and platelet numbers, while *Sp1*$^{fl/fl}$::*Sp3*$^{fl/fl}$ (WT^{lox}) mice or single KO mice did not (Figure 1A-C). These results suggest an essential redundant role for Sp1/Sp3 in megakaryopoiesis. To further investigate this, and to establish that the observed thrombocytopenia was an intrinsic effect of Sp1/Sp3 deletion in the megakaryocytic lineage, we crossed the *Sp1*$^{fl/fl}$::*Sp3*$^{fl/fl}$ with *Pf4-Cre* mice.[33] For reasons of clarity, we will refer to the *Sp1*$^{fl/fl}$::*Sp3*$^{fl/fl}$ control mice as WT^{lox}, and the *Pf4-Cre*::*Sp1*$^{fl/fl}$::*Sp3*$^{fl/fl}$ mice as double knockout (dKO) in the remainder of this paper. Survival of all lines generated was not affected up to 180 days, and they did not display spontaneous bleeding or any other major pathology. The mean blood platelet count was reduced by 60% and the mean platelet volume was increased 1.5 fold in dKO when compared to WT^{lox} mice, while red blood cells and white blood cells were not affected (Figure 1D-E). This data shows that dKO mice suffer from macrothrombocytopenia.
TPO levels in plasma of dKO and WT^{lox} mice were similar (Figure 1F), suggesting that the macrothrombocytopenia is not due to a defect in TPO production and that the total megakaryocyte/platelet mass is not altered.

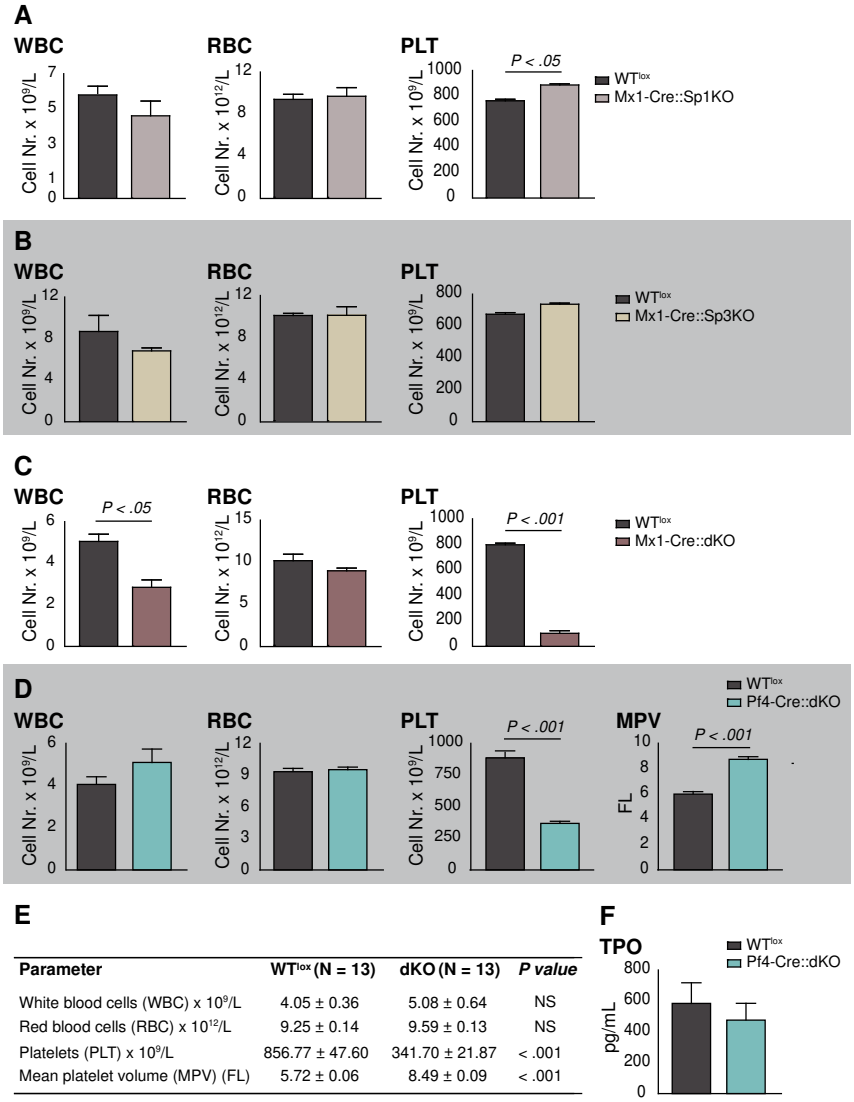

E

Parameter	WT^{lox} (N = 13)	dKO (N = 13)	*P value*
White blood cells (WBC) x 10^9/L	4.05 ± 0.36	5.08 ± 0.64	NS
Red blood cells (RBC) x 10^{12}/L	9.25 ± 0.14	9.59 ± 0.13	NS
Platelets (PLT) x 10^9/L	856.77 ± 47.60	341.70 ± 21.87	< .001
Mean platelet volume (MPV) (FL)	5.72 ± 0.06	8.49 ± 0.09	< .001

Figure 1. Sp1::Sp3 dKO mice display macrothrombocytopenia with unaltered megakaryocyte/platelet mass

A) Blood parameters of Mx1-Cre::Sp1KO and WT^{lox} mice at 12 weeks of age and after poly IC treatment.
B) Blood parameters of Mx1-Cre::Sp3KO and WT^{lox} mice at 12 weeks of age and after poly IC treatment.
C) Blood parameters of Mx1-Cre::dKO and WT^{lox} mice at 12 weeks of age and after poly IC treatment.
D) Blood parameters of Pf4-Cre::dKO and WT^{lox} mice at 12 weeks of age (n=13).
E) Table summarizing the blood parameters of Pf4-Cre::dKO and WT^{lox} mice corresponding to D.
F) TPO levels in plasma of dKO and WT^{lox} mice (n=13).

Normal number, ploidy and distribution of megakaryocytes in bone marrow and spleen of dKO mice

Flow cytometry analysis was performed to determine the percentage of megakaryocytes at consecutive differentiation stages (Figure S1A) in the bone marrow and spleen. In both tissues, no differences in the percentage of megakaryocyte precursors were noticed in dKO mice when compared to WT^{lox} animals. Furthermore, the total cell numbers of bone marrow and spleen were not altered (Figure 2A-B). Histological analysis of spleen sections using acetylcholinesterase staining to visualize megakaryocytes revealed no overt differences in their distribution and numbers within the splenic red pulp (Figure S1B). Collectively, this strongly suggests that commitment and expansion of megakaryocytes is not affected in dKO mice, and neither is TPO responsiveness.

We next analyzed the ploidy status of bone marrow and spleen megakaryocytes by flow cytometry, using CD41 and CD42b to phenotypically identify respectively megakaryocytes and megakaryocytes enriched at a more advanced differentiation stage, but no significant differences were observed between dKO and WT^{lox} mice (Figure 2C-D and Figure S2).

Megakaryocyte location next to arterioles and sinusoids is a sign of proper migration.[37-39] Therefore, fluorescence microscopy was used to examine the distribution of megakaryocytes in bone marrow cryosections, which was not affected between dKO and WT^{lox} mice (Figure 2E).

Figure 2. Megakaryocyte differentiation, location and ploidy status are not affected in dKO mice

A and B) Percentage of megakaryocytes at consecutive stages of differentiation (I-V, as detailed in Figure S1) of nucleated bone marrow and spleen cells, and total bone marrow and spleen cell counts.

C and D) Ploidy staining of CD41-positive bone marrow and spleen megakaryocytes (as detailed in Figure S2).

E) Representative images of bone marrow cryosections, immuno-stained with CD41-PE (megakaryocytes), CD31-FITC (megakaryocytes and endothelial cells) and Phalloidin-CF633 (actin) to visualize their location and proximity to blood vessels in the bone marrow. Low and high magnifications are shown.

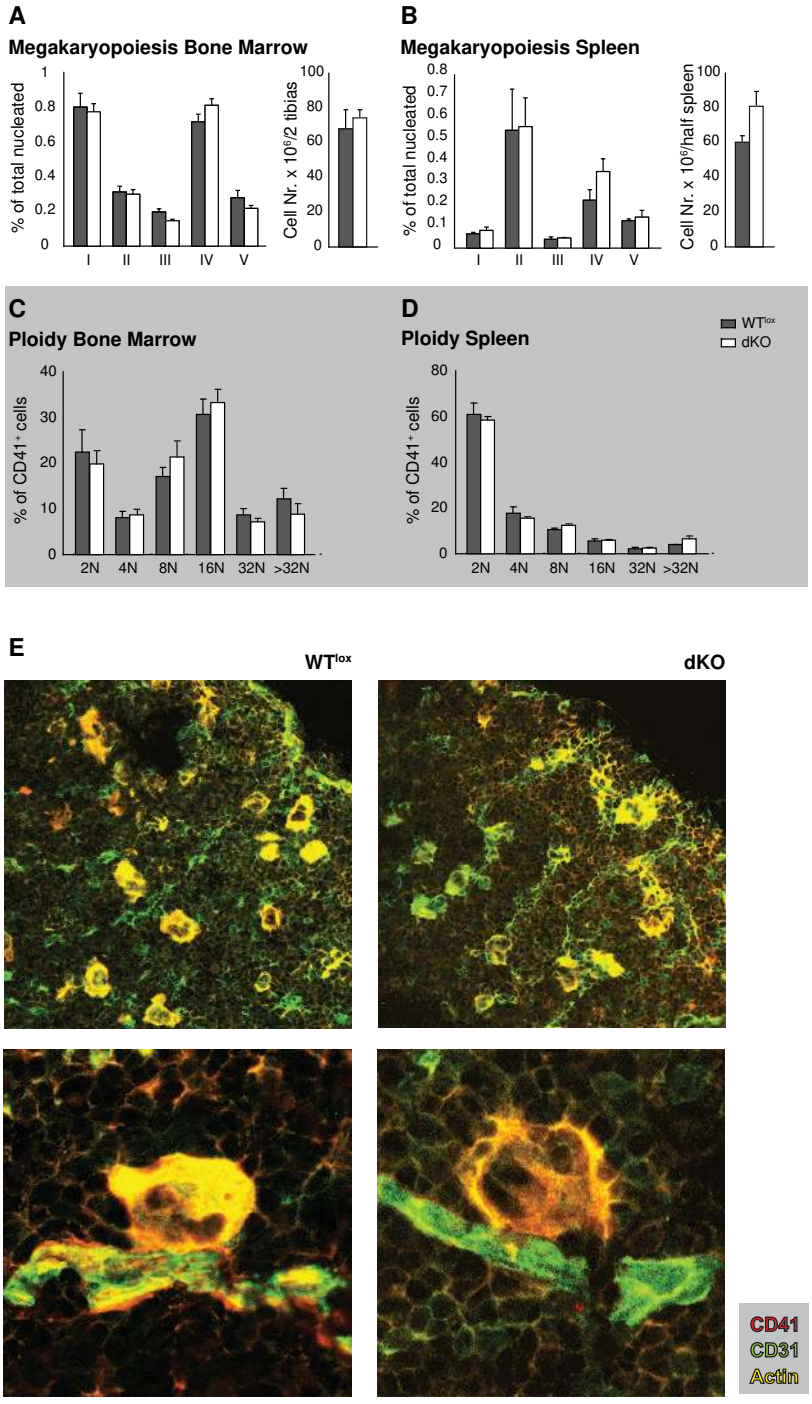
A
Megakaryopoiesis Bone Marrow
% of total nucleated
Cell Nr. x 10⁶/2 tibias
I II III IV V
B
Megakaryopoiesis Spleen
% of total nucleated
Cell Nr. x 10⁶/half spleen
I II III IV V
C
Ploidy Bone Marrow
% of CD41⁺ cells
2N 4N 8N 16N 32N >32N
D
Ploidy Spleen
WTlox
dKO
% of CD41⁺ cells
2N 4N 8N 16N 32N >32N
E
WTlox
dKO
CD41
CD31
Actin

dKO megakaryocytes display aberrant DMS and proplatelet formation

We next used electron microscopy to study the demarcation membrane system (DMS) of cultured bone marrow-derived megakaryocytes, harvested at day 7. While in WT^{lox} cultures most of the megakaryocytes showed an intricate, compact and well developed DMS, dKO megakaryocytes were highly heterogeneous regarding DMS morphology. Some of the dKO megakaryocytes displayed an apparently normal DMS, but the majority contained a very loose DMS or large vacuolar spaces in their cytoplasm (Figure 3A and Figure S3). Such a defect likely leads to impaired proplatelet formation and will therefore affect platelet production.

To investigate the capacity of megakaryocytes to form proplatelets, an *ex vivo* bone marrow explant method was used.[36] In dKO explants the same number of megakaryocytes appeared in the periphery after 6 hours when compared to WT^{lox} explants, but proplatelet production was severely impaired (Figure 3B, Figure S4 and Videos 1-3). Collectively, the aberrant DMS and severely reduced ability to form proplatelets offer an explanation for the macrothrombocytopenia observed in dKO mice.

Figure 3. dKO megakaryocytes display an aberrant DMS and are incapacitated to form proplatelets

A) Electron microscope images of bone marrow-derived cultured megakaryocytes. Representative pictures are shown. WT^{lox} megakaryocytes display a normal compact DMS, while dKO megakaryocytes present with an abnormal less compact DMS, or even larger vacuolar cytoplasmic structures. See Figure S3 for additional pictures.

B) Left: micrograph of the periphery of a bone marrow explant (contour indicated by dashed line). A megakaryocyte (MK) in the center of the image has formed proplatelets (ProPLTs, arrowheads). Such MKs with ProPLTs are counted as one unit, and the percentage of units with proplatelets of total counted megakaryocytes is depicted (bar graph on the right). See Videos 1-3 showing WT megakaryocytes forming proplatelets and Figure S4 for explant still images.

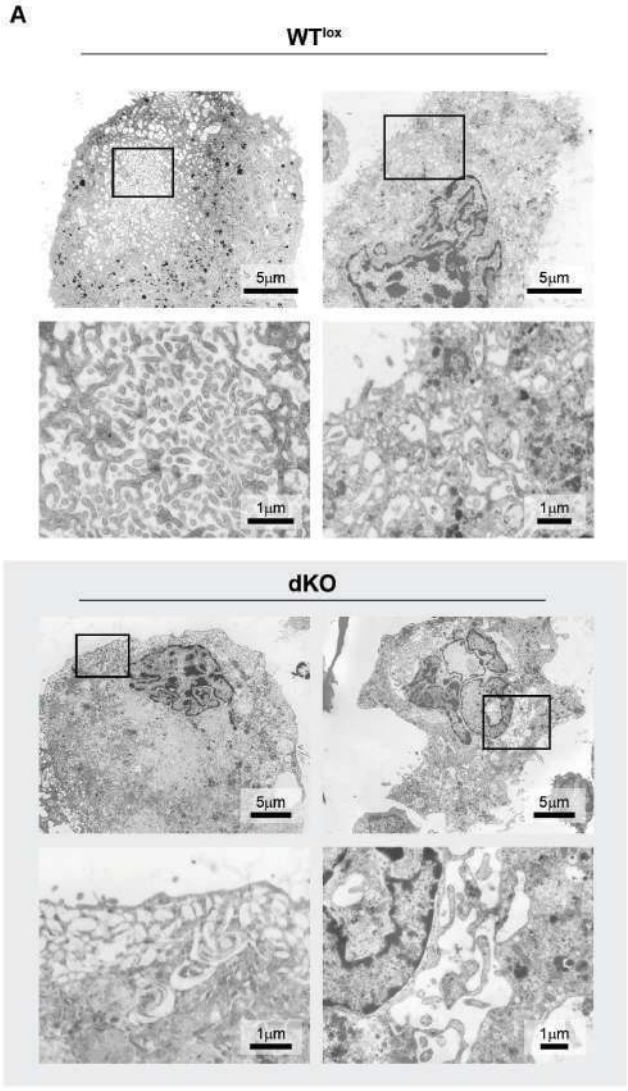
A
WTlox
5µm
5µm
1µm
1µm
dKO
5µm
5µm
1µm
1µm

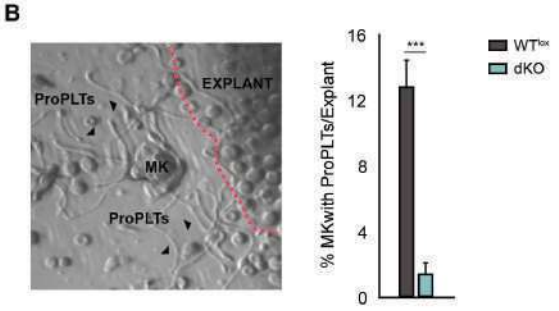
B
ProPLTs
EXPLANT
MK
ProPLTs
% MKwith ProPLTs/Explant
16
12
8
4
0
***
WTlox
dKO

dKO mice display impaired platelet function

Since thrombocytopenias are often accompanied by platelet dysfunction,[14] we decided to study platelet function in dKO mice. Platelets recognize different substrates at damaged vessel walls including collagen and von Willebrand factor (vWF), which are recognized by a2b1 integrin/GPVI and vWF receptor respectively, leading to platelet activation and thrombus formation, which is ultimately dependent on fibrinogen binding via aIIbb3 integrin.[34,40] We evaluated the capacity of dKO platelets to form thrombi *in vitro* by perfusing reconstituted blood containing equal number of platelets over a collagen-coated surface at physiological flow rates. dKO platelets had a profoundly reduced capacity to form thrombi when compared to WT^{lox} platelets, as measured by coverage of platelet thrombi (Figure 4A). Similarly, the tail bleeding time was increased in dKO when compared to WT^{lox} mice (Figure 4B).

Next, we used a flow cytometry-based platelet aggregation test (FCA) to study the contribution of specific platelet receptors to platelet aggregation.[34] Isolated platelets were stimulated with the agonists PMA (which activates the fibrinogen receptor aIIbb3 integrin), Botrocetin (which activates the vWF receptor), Aggretin A (which activates the Clec2 receptor) and Convulxin (which activates GPVI).[34,40] We observed that the aggregation capacity of dKO platelets was decreased compared to WT^{lox} platelets. However, whereas PMA and Convulxin caused a decrease in maximum activation but comparable aggregation kinetics in dKO when compared to WT^{lox} platelets, the responses to Aggretin A and Botrocetin were almost completely abrogated (Figure 4C).

Figure 4. Platelets from dKO mice are dysfunctional

A) Left: micrographs of collagen-coated slides after perfusion of WT^{lox} and dKO reconstituted blood containing the same number of platelets. The average coverage measured as green fluorescence over the total surface was quantitated with J Image software.

B) Tail bleeding time of WT^{lox} and dKO mice is depicted. (C) Flow cytometry-based platelet aggregation assay (FCA) shows the aggregation capacity of platelets when stimulated with different agonists. * $P < .05$; ** $P < .01$; *** $P < .001$.

C) Flow cytometry-based platelet aggregation assay (FCA) shows the aggregation capacity of platelets when stimulated with different agonists.

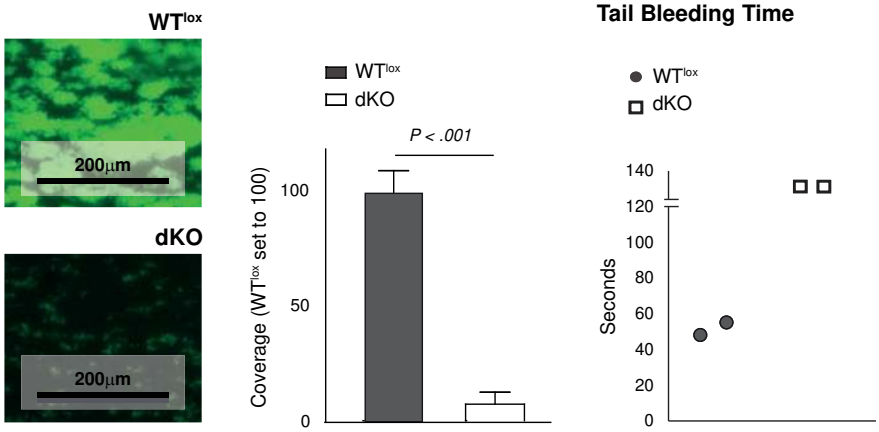
WTlox
200μm
dKO
200μm
WTlox
dKO
P < .001
Coverage (WTlox set to 100)
100
50
0
Tail Bleeding Time
WTlox
dKO
Seconds
140
120
100
80
60
40
20
0

C

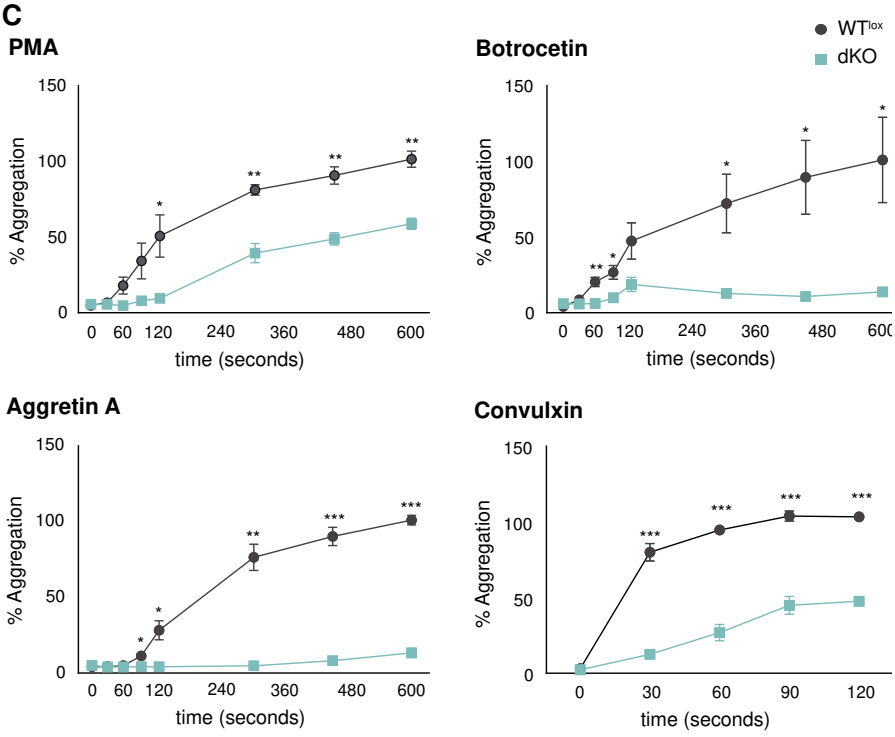
PMA
Botrocetin
WTlox
dKO
% Aggregation
150
100
50
0
0 60 120 240 360 480 600
time (seconds)
Aggretin A
Convulxin
0 30 60 90 120

Analysis of the megakaryocyte transcriptome and platelet proteome in dKO mice

To identify Sp1/Sp3 potential target genes affected in dKO mice and relevant for megakaryopoiesis, bone marrow-derived megakaryocytes were isolated from dKO and WT^{lox} cultures and their transcriptomes were analyzed by RNA-Seq (Figure 5, Figure S5 and Table S1). In parallel, the protein content of freshly isolated dKO and WT^{lox} platelets was analyzed by mass spectrometry (Figure 6, Figure S6 and Tables S2-3).

RNA-Seq analysis revealed 833 differentially expressed genes in dKO megakaryocytes (FDR < .01, Figure 5A, Figure S5 and Table S1). Gene ontology term enrichment analysis revealed a number of pathways specifically affected, such as microtubule polymerization, necrosis, metabolism, transcription, granule transport and hemostasis (Figure S5). Transcription factor binding motif (Homer) analysis on the promoters of the dKO deregulated genes identified the Sp binding site motif with the lowest *P*-value ($P = 10^{-8}$) in dKO downregulated genes, suggesting that they might be direct Sp1/Sp3 targets (Figure 5B). This was not the case when examining the enriched binding motifs of dKO upregulated genes, i.e. Six1, GFY or Ets1 transcription factors, that were enriched with a much higher *P*-value ($P = 10^{-3}$) (Figure 5C). This suggests that globally, Sp1 and Sp3 are activators of transcription in megakaryocytes.

Figure 5. Megakaryocyte RNA-Seq

A) Hierarchical clustered heat map with scaled Z-score color key of normalized counts of 833 differentially expressed genes in three WT^{lox} and three dKO samples. Samples with the same genotype are indicated by black (WT^{lox}) and red (dKO) horizontal bars; gene clusters are indicated by red (upregulated in dKO) and cyan (downregulated in dKO) vertical bars.

B) Transcription factor binding sites enrichment detected, using HOMER, in promoters of 454 downregulated genes in dKO with a threshold *FDR* < .01.

C) Transcription factor binding sites enrichment detected, using HOMER, in promoters of 379 upregulated genes in dKO with a threshold *FDR* < .01.

A

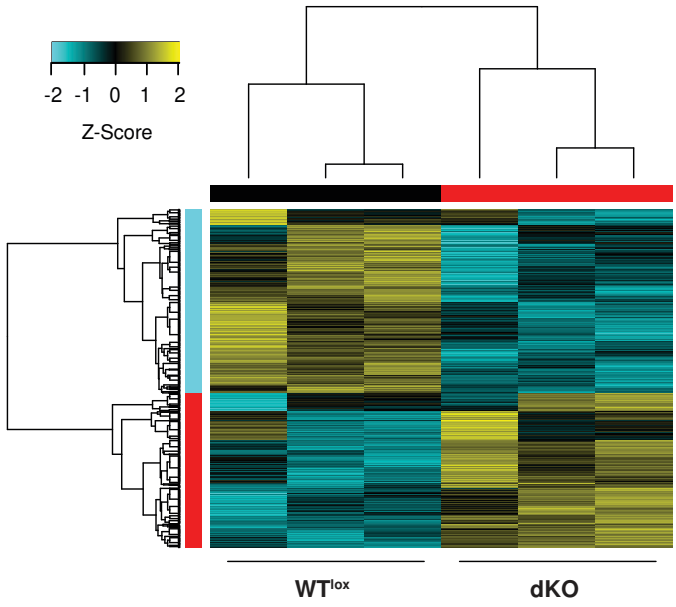

B

Rank	Motif	Name	*P*	% Target	% Background
1		Sp1	10^{-8}	48.43	34.25
2		Klf4	10^{-7}	32.53	21.12
3		Klf1	10^{-2}	10.84	6.99
4		Olig2 (bHLH)	10^{-2}	26.99	21.34
5		Srebp1a (HLH)	10^{-2}	4.82	2.67

DOWNREGULATED GENES: Target Sequences = 415; Background Sequences = 24218

C

Rank	Motif	Name	*P*	% Target	% Background
1		Six1	10^{-3}	5.71	2.42
2		GFY	10^{-2}	8.25	4.21
3		Ets1	10^{-2}	34.29	26.56

UPREGULATED GENES: Target Sequences = 315; Background Sequences = 26463

To complement the RNA-Seq data we examined the proteome of platelets. We identified 85 proteins differentially expressed in dKO platelets of which 63 where downregulated (FDR < .25; Figure 6A, Figure S6 and Tables S2-3). The functions of the differentially expressed proteins were linked to cell metabolism, cytoskeleton rearrangement, receptor signaling, and protein folding. As indicated in Figure S6 and Table S3, 40% of these proteins have been reported previously as potential Sp1/Sp3 target genes or their gene promoters contain G-rich SP binding sites. Furthermore, a number of these proteins have been previously identified as essential during megakaryopoiesis and for platelet function, i.e. Myh9, Flna, Rasgrp2, Fermt3, Src and Syk.[7,12,41-45] Deregulation of these proteins could readily explain the defective megakaryocyte DMS and proplatelet formation and the platelet dysfunction observed in dKO mice.

We next compared the RNA-Seq and proteomics datasets to identify the transcripts/proteins with identical signatures (Figure S6C and Figure 6B). As shown in Figure 6B, only 4 hits shared the same overlapping signature with an FDR < .1 in both datasets, i.e. Add3 (Adducin gamma, involved in assembly of the spectrin-actin network), Alox12 (Arachidonate 12-Lipoxygenase, involved in the production and metabolism of fatty acid hydroperoxides), Mylk (Myosin light chain kinase) and Rasgrp2 (RAS Guanyl Releasing Protein 2 -Calcium And DAG-Regulated-, which functions in platelet aggregation through integrin inside-out signaling). Amongst these 4 proteins, Alox12 appears to fully require Sp1/Sp3 transcription factors, since it was amongst the top 20 downregulated genes in dKO megakaryocytes and we could not detect any peptides in dKO platelets (Tables S1-3). We validated downregulation of these factors in dKO megakaryocytes (mRNA, by RT-qPCR) and in platelets (protein, by western blotting) (Figure S6D).

Figure 6. Platelet proteomics with integrative RNA-Seq analysis

A) Hierarchical clustered heat map with scaled Z-score color key of log2 transformed Label Free Quantification (LFQ) intensities of 85 differentially expressed proteins in four WT^{lox} and four dKO platelet lysate samples. Samples with the same genotype are indicated by black (WT^{lox}) and red (dKO) horizontal bars and protein expression clusters are indicated by red (upregulated in dKO) and cyan (downregulated in dKO) vertical bar.

B) Scatterplot of differentially expressed proteins in platelets (mass spectrometry) and differentially expressed genes in megakaryocytes (RNA-Seq) in dKO samples with n=106.

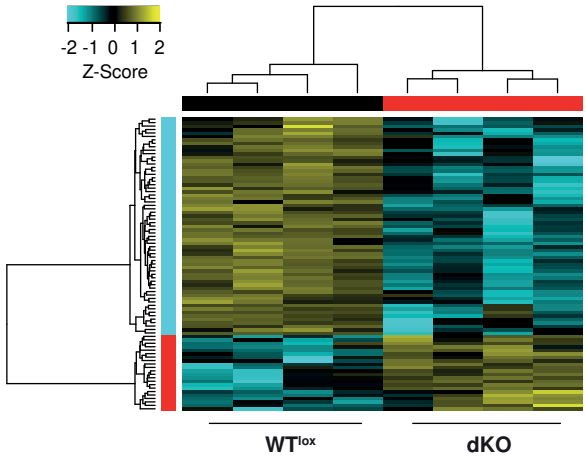

B

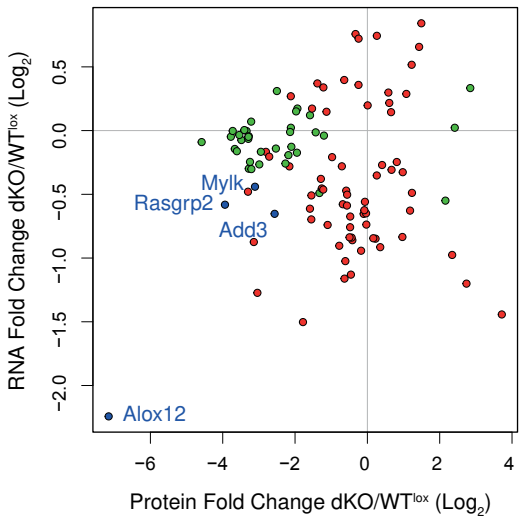

- RNA FDR < .1
- Protein FDR < .1
- RNA FDR < .1 + Protein FDR < .1

Selective Mylk inhibition by ML7 affects proplatelet formation and stabilization, and interferes with ITAM receptor-induced platelet aggregation

Myosin light chain kinase (Mylk) was one of the targets with highest score on signature overlap and significantly downregulated in megakaryocytes (mRNA) and platelets (protein). We could map the peptide coverage to the previously reported MYLK isoform 3,[46] which is translated from an alternative start codon present on exon 16, corroborating previous data reporting that this is the major Mylk isoform present in platelets.[47-49] The RNA-Seq data also confirms that megakaryocytes mainly express this isoform (Figure 7A). The promoter governing the transcription of this isoform contains G-rich elements (Sp binding sites; Figure 7A). Mylk phosphorylates myosin regulatory light chains to facilitate myosin interaction with actin filaments to produce contractile activity, and as such it represents a potential essential factor during proplatelet formation and platelet activation. It is known that myosin light chain phosphorylation has a modulatory role on platelet activation.[50] Interestingly, it has been recently reported from studies in morphant zebrafish that Mylk1a (a thrombocyte enriched Mylk orthologue) is required for thrombus formation,[51] however, its function during megakaryopoiesis in mammals has not been studied in detail.

We performed bone marrow explant cultures in the presence of the selective Mylk inhibitor ML7[52] at different concentrations, and examined proplatelet formation after 6 hours. Addition of 20mM ML7 resulted in almost complete inhibition of proplatelet formation (Figure 7B). Surprisingly, when we added ML7 once proplatelets had been formed, we observed complete retraction of the proplatelets, as opposed to DMSO controls (Videos 4-7). These results suggest that Mylk is required for proplatelet formation, but also for proplatelet stabilization. Since Mylk requires and is activated by Ca^{2+}/Calmodulin,[48] we next applied EDTA to megakaryocytes in our explants once proplatelets had been formed in order to interfere with Ca^{2+} signaling. Interestingly, we observed complete proplatelet retraction due to extracellular Ca^{2+} sequestration (Video 8). This suggests that Ca^{2+} signaling is required and can modulate proplatelet stabilization, using Mylk as one of its downstream effector kinases.

We next applied ML7 to WT platelets that were induced to aggregate in the presence of PMA, Botrocetin, Aggretin A or Convulxin. We observed a marked inhibition of aggregation induced by Aggretin A and Convulxin in the presence of ML7, but not to aggregation induced by the other agonists used (Figure 7C), suggesting that Mylk is necessary downstream the platelet ITAM-receptors Clec-2 and GPVI, which are known to invite Ca^{2+}/Calmodulin via PLCg to execute its complete signaling.[53]

In summary, we conclude that the ubiquitous Sp1/Sp3 transcription factors are required for proper platelet production and function. Depletion of Sp1/Sp3 in the megakaryocytic lineage results in deregulation of a number of proteins with well-known functions in megakaryopoiesis, such as Myh9, Rasgrp2, Syk and Flna, resulting in megakaryocyte terminal maturation defects, macrothrombocytopenia and platelet malfunction. Furthermore, Alox12 transcription absolutely requires Sp1/Sp3 transcription factors, and we identified Mylk as a potential Sp1/Sp3 target. We show that Mylk inhibition by ML7 affects proplatelet formation and stabilization, and interferes with platelet ITAM receptor-dependent signaling functions.

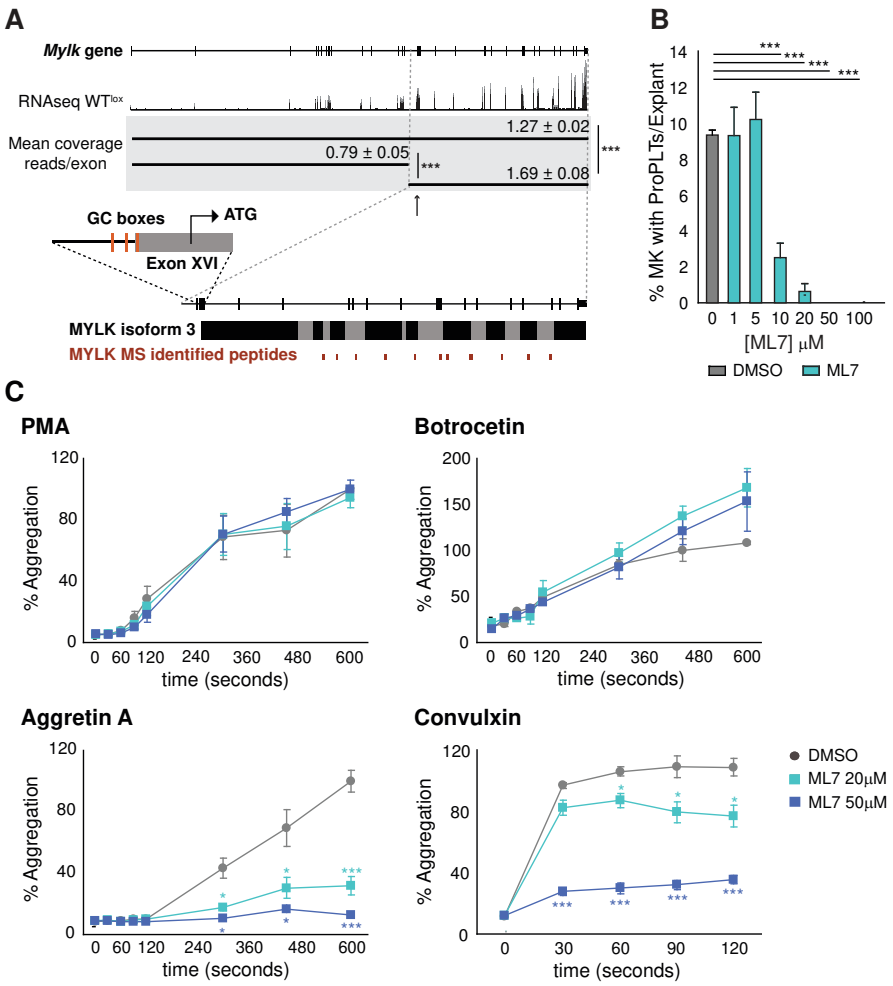

Figure 7. Selective Mylk inhibition by ML7 affects proplatelet formation and stabilization, and interferes with platelet Clec-2 and GPVI downstream signaling

A) Graphic representation of *Mylk* gene, Mylk isoform 3, and the peptide coverage identified in dKO platelets corresponding to Mylk isoform 3. Sp GC-rich binding sites are depicted on the promoter region upstream the Mylk isoform 3 ATG starting codon.

B) Explant assay performed with WT mice after addition of Mylk inhibitor ML7 at different concentrations or DMSO. The percentage of megakaryocytes with proplatelets of total counted megakaryocytes per explant is depicted. ** $P < .01$. See Videos 4-7 showing that ML7 inhibition of Mylk after proplatelet formation results in proplatelet retraction.

C) Flow cytometry based platelet aggregation assay (FCA) of WT platelets pre-incubated with either DMSO or ML7. * $P < .05$; *** $P < .001$.

DISCUSSION

This study shows the intrinsic effect of loss of transcription factors Sp1 and Sp3 during megakaryopoiesis and on platelet function in adult mice. Upon ablation of Sp1 and Sp3 in megakaryocytes, DMS development and proplatelet formation are defective, leading to severe macrothrombocytopenia and platelet dysfunction in dKO mice.

Transcriptomics analysis on dKO megakaryocytes revealed ~800 differentially expressed genes. G-rich Sp binding motifs were enriched only in the promoters of downregulated genes, suggesting that globally Sp1/Sp3 are activators of transcription in megakaryocytes. G-rich Sp binding motifs were not enriched in the subset of upregulated genes, suggesting that their promoters might be regulated, for example, by other transcription factors affected by loss of Sp1/Sp3. Notably, Sp7 is increased significantly (Log_2 Fold Change = 1.2803; FDR < .01), which could provide some compensatory regulatory functions. Amongst the differentially expressed genes, many are involved in cell metabolism. However, a large proportion of affected genes/proteins are known to play an essential role during megakaryopoiesis or in platelet function.

Treatment of patients with Mithramycin, an anti-neoplastic antibiotic that binds to GC-rich regions in the DNA and interferes with Sp transcription factor activity, results in thrombocytopenia and bleeding.[54,55] Furthermore, from our proteomics analysis, we identified two alpha-granule proteins significantly downregulated in dKO platelets, i.e. Pros1 (S protein) and F13a1. In humans, mutations in the regulatory region of these genes specifically affecting a GC-rich Sp DNA binding motif, result in deficiency of PROS1 and F13A1 respectively.[56,57] ALOX12, a RUNX1 target gene,[58] is severely reduced in dKO megakaryocytes and platelets. ALOX12 and F13A1 are both downregulated in patients bearing CBFA2/RUNX1 mutations and presenting macrothrombocytopenia.[59] In addition, these patients show deficiencies in the activity of PKCq, PLCb2 and MYLK.[60] It is possible that in our dKO mice specific transcription factor complexes, which are finely orchestrated during normal megakaryopoiesis, i.e. Runx1/Sp1/Sp3, are disturbed.

A number of proteins essential for megakaryopoiesis and/or platelet function are significantly downregulated in dKO platelets. For example, Myh9, Flna, Calpn2, Fermt3, Rasgrp2, Syk, Src,[7,8,12,41,44,61] and proteins involved in cytoskeletal rearrangements or in the folding of cytoskeletal proteins. Some of them have been previously reported to be directly regulated by Sp1, such as Flna,[62] or contain G-rich motifs on their promoters. MYH9 patients have a defect in megakaryocyte DMS and proplatelet formation, but also in migration.[8] We do not observe a defect in migration of dKO megakaryocytes based on their distribution in bone marrow cryosections, indicating that the remaining level of Myh9 is sufficient to support this process. Megakaryocyte-specific Flna knockout mice are severely macrothrombocytopenic and platelets have altered signaling through aIIbb3 integrin, GPVI and Clec-2 receptors.[42,43] These characteristics correlate with those observed in our dKO mice, indicating that reduced Flna expression contributes to the defects observed in dKO platelets. It has been reported that Flna-deficient platelets have a decreased expression of GP1ba.[63] Although in our proteomics data we observed downregula-

tion of GP1ba, it did not reach significance (Log_2 Fold Change = -0.4; FDR = .7). Of note, platelets of dKO mice have lowered levels of Flna, but not complete absence of the protein. Furthermore, the simultaneous downregulation of Flna, Lyn, Src and Syk explain the platelet aggregation defect upon stimulation with Botrocetin, i.e. defective vWF receptor function.[64,65]

Our data suggest that Mylk is necessary for proplatelet formation and stabilization in megakaryocytes, and that Mylk is required for Clec-2 and GPVI downstream signaling. In human platelets it is known that Mylk inhibition with a blocking agent leads to decreased shape change upon stimulation with Convulxin,[66] which activates GPVI, and that ML7 inhibition interferes with Convulxin and collagen induced aggregation,[67] corroborating our results.

Mylk is an effector kinase highly dependent on Ca^{2+}/Calmodulin signaling.[48] Recently, it has been characterized how the Store-Operated Ca^{2+} Entry (SOCE) functions in megakaryocytes,[68] highlighting the different spatio-temporal levels and effects of intracellular and extracellular Ca2+ signaling during megakaryopoiesis.[68,69] When we applied EDTA to sequester extracellular Ca^{2+} once proplatelets had formed in bone marrow explants, we observed similarly proplatelet retraction as when we applied ML7 Mylk inhibitor, supporting the notion that Ca^{2+} signaling regulates the process of proplatelet formation. Of note, sequestration of the intracellular Ca^{2+} pool with BAPTA does not affect proplatelet formation,[70] which makes SOCE mechanism and extracellular Ca^{2+} more relevant. Our findings seem to contradict previous studies in which another Mylk inhibitor enhances proplatelet formation.[71] However, not only the inhibitor used is different; it is performed on human $CD34^+$ *in vitro* derived megakaryocytes, while we analyze the effects of Mylk inhibition on *in vivo* matured murine megakaryocytes, within the native bone marrow tissue. It is not clear whether both inhibitors target the complete array of Mylk functions, and it has been suggested that Mylk phosphorylates other substrates than myosin light chain.[72,73] In accordance with our findings, manipulation of upstream/activating components of the Ca^{2+}/Calmodulin pathway have been previously linked to deficits on proplatelet formation in mouse models, i.e. PKC, PLC.[69,70,74] It is important to acknowledge that microtubule dynamics might be fine-tuned in a more complex way, and alterations on this process result in the same readout, i.e. proplatelet retraction. For example, inhibition of serine/threonine phosphatases 1/2A by Calyculin A also results in proplatelet retraction.[75] Proplatelet production and progression require the growth of microtubules at the plus-ends, but also the sliding of microtubules.[76,77] Microtubule sliding is Ca^{2+} dependent, requires actomyosin complex formation, is restricted to available dynein, and it is blocked when inhibiting Mylk with ML7.[78] Proplatelet retraction has been observed previously *in vitro* in the presence of microtubule destabilizing agents,[77] however, the notion that Mylk might be required for the formation and stabilization of proplatelets suggests that not only microtubule sliding is essential to the process, but that proplatelet formation is potentially reversible *in vivo*, depending on Ca^{2+} signaling cues.

It is remarkable that the ubiquitously expressed Sp1/Sp3 transcription factors control such specific processes in the highly specialized megakaryocytes, while we did not observe the expected defects in generic housekeeping functions thought to be

regulated by Sp1/Sp3. Further studies will aim at the individual contribution of the differentially expressed genes and the Sp1/Sp3 – transcription factor interaction network during megakaryopoiesis. Such knowledge may contribute to the identification of causative mutations in the increasing group of macrothrombocytopenias of unknown etiology.[15]

ACKNOWLEDGMENTS

This study was funded by the Center for Translational Molecular Medicine (CTMM, www.ctmm.nl), project Innovative Coagulation Diagnostics (INCOAG, grant 01C-201), and the Dutch Heart Foundation. HvdW was supported by the Netherlands Genomics Initiative (NGI Zenith 93511036); DIK and SP received support from the Landsteiner Foundation for Blood Transfusion Research (LSBR 1040), the Netherlands Organization for Scientific Research (NWO / ZonMw TOP 40-00812-98-08032, 40-00812-98-12128 and DN 82-301), and EU fp7 Specific Cooperation Research Project THALAMOSS (306201); JAAD and E-JR were supported by the Netherlands Proteomics Center. We thank Prof. J. Eble for kindly providing Aggretin A.

Author contributions

MM, DIK and LG designed and performed experiments, analyzed data and wrote the paper; SP designed experiments, analyzed data and wrote the paper; HJGvdW and WvIJ analyzed data and wrote the paper; TKvdB reviewed the paper and participated in discussions; MH and HJ performed experiments; RWWB, E-JR and JAAD analyzed data; IK and GS designed and generated the Sp3 lox mouse line.

Conflict-of-interest disclosure

The authors declare no competing financial interests.

REFERENCE LIST

1. Bluteau D, Lordier L, Di Stefano A, et al. Regulation of megakaryocyte maturation and platelet formation. J Thromb Haemost. 2009;7 Suppl 1:227-234.
2. Geddis AE. Megakaryopoiesis. Semin Hematol. 2010;47(3):212-219.
3. Italiano JE, Jr. Unraveling mechanisms that control platelet production. Semin Thromb Hemost. 2013;39(1):15-24.
4. Schmitt A, Guichard J, Masse JM, Debili N, Cramer EM. Of mice and men: comparison of the ultrastructure of megakaryocytes and platelets. Exp Hematol. 2001;29(11):1295-1302.
5. Kuter DJ. The physiology of platelet production. Stem Cells. 1996;14 Suppl 1:88-101.
6. Junt T, Schulze H, Chen Z, et al. Dynamic visualization of thrombopoiesis within bone marrow. Science. 2007;317(5845):1767-1770.
7. Geddis AE. Inherited thrombocytopenias: an approach to diagnosis and management. Int J Lab Hematol. 2013;35(1):14-25.
8. Pecci A, Bozzi V, Panza E, et al. Mutations responsible for MYH9-related thrombocytopenia impair SDF-1-driven migration of megakaryoblastic cells. Thromb Haemost. 2011;106(4):693-704.
9. Cines DB, Bussel JB, McMillan RB, Zehnder JL. Congenital and acquired thrombocytopenia. Hematology Am Soc Hematol Educ Program. 2004:390-406.
10. Kistangari G, McCrae KR. Immune thrombocytopenia. Hematol Oncol Clin North Am. 2013;27(3):495-520.
11. Schiodt FV, Balko J, Schilsky M, et al. Thrombopoietin in acute liver failure. Hepatology. 2003;37(3):558-561.
12. Balduini CL, Savoia A, Seri M. Inherited thrombocytopenias frequently diagnosed in adults. J Thromb Haemost. 2013;11(6):1006-1019.
13. Nurden P, Debili N, Coupry I, et al. Thrombocytopenia resulting from mutations in filamin A can be expressed as an isolated syndrome. Blood. 2011;118(22):5928-5937.
14. Nurden P, Nurden AT. Congenital disorders associated with platelet dysfunctions. Thromb Haemost. 2008;99(2):253-263.
15. Tijssen MR, Ghevaert C. Transcription factors in late megakaryopoiesis and related platelet disorders. J Thromb Haemost. 2013;11(4):593-604.
16. Gutierrez L, Tsukamoto S, Suzuki M, et al. Ablation of Gata1 in adult mice results in aplastic crisis, revealing its essential role in steady-state and stress erythropoiesis. Blood. 2008;111(8):4375-4385.
17. Vyas P, Ault K, Jackson CW, Orkin SH, Shivdasani RA. Consequences of GATA-1 deficiency in megakaryocytes and platelets. Blood. 1999;93(9):2867-2875.
18. Freson K, Matthijs G, Thys C, et al. Different substitutions at residue D218 of the X-linked transcription factor GATA1 lead to altered clinical severity of macrothrombocytopenia and anemia and are associated with variable skewed X inactivation. Hum Mol Genet. 2002;11(2):147-152.

19. Shimizu R, Engel JD, Yamamoto M. GATA1-related leukaemias. Nat Rev Cancer. 2008;8(4):279-287.

20. Stevenson WS, Morel-Kopp MC, Chen Q, et al. GFI1B mutation causes a bleeding disorder with abnormal platelet function. J Thromb Haemost. 2013;11(11):2039-2047.

21. Ichikawa M, Yoshimi A, Nakagawa M, Nishimoto N, Watanabe-Okochi N, Kurokawa M. A role for RUNX1 in hematopoiesis and myeloid leukemia. Int J Hematol. 2013;97(6):726-734.

22. Fujita R, Takayama-Tsujimoto M, Satoh H, et al. NF-E2 p45 is important for establishing normal function of platelets. Mol Cell Biol. 2013;33(14):2659-2670.

23. McCormack MP, Hall MA, Schoenwaelder SM, et al. A critical role for the transcription factor Scl in platelet production during stress thrombopoiesis. Blood. 2006;108(7):2248-2256.

24. Stockley J, Morgan NV, Bem D, et al. Enrichment of FLI1 and RUNX1 mutations in families with excessive bleeding and platelet dense granule secretion defects. Blood. 2013;122(25):4090-4093.

25. Suske G, Bruford E, Philipsen S. Mammalian SP/KLF transcription factors: bring in the family. Genomics. 2005;85(5):551-556.

26. Gollner H, Bouwman P, Mangold M, et al. Complex phenotype of mice homozygous for a null mutation in the Sp4 transcription factor gene. Genes Cells. 2001;6(8):689-697.

27. Marin M, Karis A, Visser P, Grosveld F, Philipsen S. Transcription factor Sp1 is essential for early embryonic development but dispensable for cell growth and differentiation. Cell. 1997;89(4):619-628.

28. Bouwman P, Gollner H, Elsasser HP, et al. Transcription factor Sp3 is essential for post-natal survival and late tooth development. EMBO J. 2000;19(4):655-661.

29. van Loo PF, Bouwman P, Ling KW, et al. Impaired hematopoiesis in mice lacking the transcription factor Sp3. Blood. 2003;102(3):858-866.

30. van Loo PF, Mahtab EA, Wisse LJ, et al. Transcription factor Sp3 knockout mice display serious cardiac malformations. Mol Cell Biol. 2007;27(24):8571-8582.

31. Kruger I, Vollmer M, Simmons DG, Elsasser HP, Philipsen S, Suske G. Sp1/Sp3 compound heterozygous mice are not viable: impaired erythropoiesis and severe placental defects. Dev Dyn. 2007;236(8):2235-2244.

32. Kuhn R, Schwenk F, Aguet M, Rajewsky K. Inducible gene targeting in mice. Science. 1995;269(5229):1427-1429.

33. Tiedt R, Schomber T, Hao-Shen H, Skoda RC. Pf4-Cre transgenic mice allow the generation of lineage-restricted gene knockouts for studying megakaryocyte and platelet function in vivo. Blood. 2007;109(4):1503-1506.

34. De Cuyper IM, Meinders M, van de Vijver E, et al. A novel flow cytometry-based platelet aggregation assay. Blood. 2013;121(10):e70-80.

35. Shimizu R, Ohneda K, Engel JD, Trainor CD, Yamamoto M. Transgenic rescue of GATA-1-deficient mice with GATA-1 lacking a FOG-1 association site phenocopies patients with X-linked thrombocytopenia. Blood. 2004;103(7):2560-2567.

36. Eckly A, Strassel C, Cazenave JP, Lanza F, Leon C, Gachet C. Characterization of megakaryocyte development in the native bone marrow environment. Methods Mol Biol. 2012;788:175-192.

37. Lichtman MA, Chamberlain JK, Simon W, Santillo PA. Parasinusoidal location of megakaryocytes in marrow: a determinant of platelet release. Am J Hematol. 1978;4(4):303-312.

38. Pitchford SC, Lodie T, Rankin SM. VEGFR1 stimulates a CXCR4-dependent translocation of megakaryocytes to the vascular niche, enhancing platelet production in mice. Blood. 2012;120(14):2787-2795.

39. Tavassoli M, Aoki M. Localization of megakaryocytes in the bone marrow. Blood Cells. 1989;15(1):3-14.

40. Rivera J, Lozano ML, Navarro-Nunez L, Vicente V. Platelet receptors and signaling in the dynamics of thrombus formation. Haematologica. 2009;94(5):700-711.

41. Eckly A, Rinckel JY, Laeuffer P, et al. Proplatelet formation deficit and megakaryocyte death contribute to thrombocytopenia in Myh9 knockout mice. J Thromb Haemost. 2010;8(10):2243-2251.

42. Ozaki Y, Suzuki-Inoue K, Inoue O. Platelet receptors activated via mulitmerization: glycoprotein VI, GPIb-IX-V, and CLEC-2. J Thromb Haemost. 2013;11 Suppl 1:330-339.

43. Falet H, Pollitt AY, Begonja AJ, et al. A novel interaction between FlnA and Syk regulates platelet ITAM-mediated receptor signaling and function. J Exp Med. 2010;207(9):1967-1979.

44. Stefanini L, Bergmeier W. CalDAG-GEFI and platelet activation. Platelets. 2010;21(4):239-243.

45. Kuijpers TW, van de Vijver E, Weterman MA, et al. LAD-1/variant syndrome is caused by mutations in FERMT3. Blood. 2009;113(19):4740-4746.

46. Yin F, Hoggatt AM, Zhou J, Herring BP. 130-kDa smooth muscle myosin light chain kinase is transcribed from a CArG-dependent, internal promoter within the mouse mylk gene. Am J Physiol Cell Physiol. 2006;290(6):C1599-1609.

47. Dabrowska R, Hartshorne DJ. A Ca2+-and modulator-dependent myosin light chain kinase from non-muscle cells. Biochem Biophys Res Commun. 1978;85(4):1352-1359.

48. Hathaway DR, Adelstein RS. Human platelet myosin light chain kinase requires the calcium-binding protein calmodulin for activity. Proc Natl Acad Sci U S A. 1979;76(4):1653-1657.

49. Hathaway DR, Eaton CR, Adelstein RS. Regulation of human platelet myosin light chain kinase by the catalytic subunit of cyclic AMP-dependent protein kinase. Nature. 1981;291(5812):252-256.

50. Saitoh M, Naka M, Hidaka H. The modulatory role of myosin light chain phosphorylation in human platelet activation. Biochem Biophys Res Commun. 1986;140(1):280-287.

51. Tournoij E, Weber GJ, Akkerman JW, et al. Mlck1a is expressed in zebrafish thrombocytes and is an essential component of thrombus formation. J Thromb Haemost. 2010;8(3):588-595.

52. Makishima M, Honma Y, Hozumi M, Sampi K, Hattori M, Motoyoshi K. Induction of differentiation of human leukemia cells by inhibitors of myosin light chain kinase. FEBS Lett. 1991;287(1-2):175-177.

53. Watson SP, Herbert JM, Pollitt AY. GPVI and CLEC-2 in hemostasis and vascular integrity. J Thromb Haemost. 2010;8(7):1456-1467.

54. Kennedy BJ. Metabolic and toxic effects of mithramycin during tumor therapy. Am J Med. 1970;49(4):494-503.

55. Yamreudeewong W, Henann NE, Fazio A, Rangaraj U. Possible severe thrombocytopenia associated with a single dose of plicamycin. Ann Pharmacother. 1992;26(11):1369-1373.

56. Sanda N, Fujimori Y, Kashiwagi T, et al. An Sp1 binding site mutation of the PROS1 promoter in a patient with protein S deficiency. Br J Haematol. 2007;138(5):663-665.

57. Wang W, Huang L, Ma Q, et al. Homozygous intronic mutation leading to inefficient transcription combined with a novel frameshift mutation in F13A1 gene causes FXIII deficiency. J Hum Genet. 2011;56(6):460-463.

58. Kaur G, Jalagadugula G, Mao G, Rao AK. RUNX1/core binding factor A2 regulates platelet 12-lipoxygenase gene (ALOX12): studies in human RUNX1 haplodeficiency. Blood. 2010;115(15):3128-3135.

59. Sun L, Gorospe JR, Hoffman EP, Rao AK. Decreased platelet expression of myosin regulatory light chain polypeptide (MYL9) and other genes with platelet dysfunction and CBFA2/RUNX1 mutation: insights from platelet expression profiling. J Thromb Haemost. 2007;5(1):146-154.

60. Nurden A, Nurden P. Advances in our understanding of the molecular basis of disorders of platelet function. J Thromb Haemost. 2011;9 Suppl 1:76-91.

61. Leon C, Eckly A, Hechler B, et al. Megakaryocyte-restricted MYH9 inactivation dramatically affects hemostasis while preserving platelet aggregation and secretion. Blood. 2007;110(9):3183-3191.

62. D'Addario M, Arora PD, Ellen RP, McCulloch CA. Interaction of p38 and Sp1 in a mechanical force-induced, beta 1 integrin-mediated transcriptional circuit that regulates the actin-binding protein filamin-A. J Biol Chem. 2002;277(49):47541-47550.

63. Jurak Begonja A, Hoffmeister KM, Hartwig JH, Falet H. FlnA-null megakaryocytes prematurely release large and fragile platelets that circulate poorly. Blood. 2011;118(8):2285-2295.

64. Falati S, Edmead CE, Poole AW. Glycoprotein Ib-V-IX, a receptor for von Willebrand factor, couples physically and functionally to the Fc receptor gamma-chain, Fyn, and Lyn to activate human platelets. Blood. 1999;94(5):1648-1656.

65. Liu J, Pestina TI, Berndt MC, Jackson CW, Gartner TK. Botrocetin/VWF-induced signaling through GPIb-IX-V produces TxA2 in an alphaIIbbeta3- and aggregation-independent manner. Blood. 2005;106(8):2750-2756.

66. Riondino S, Gazzaniga PP, Pulcinelli FM. Convulxin induces platelet shape change through myosin light chain kinase and Rho kinase. Eur J Biochem. 2002;269(23):5878-5884.

67. Toth-Zsamboki E, Oury C, Cornelissen H, De Vos R, Vermylen J, Hoylaerts MF. P2X1-mediated ERK2 activation amplifies the collagen-induced platelet secretion by enhancing myosin light chain kinase activation. J Biol Chem. 2003;278(47):46661-46667.

68. Di Buduo CA, Moccia F, Battiston M, et al. The importance of calcium in the regulation of megakaryocyte function. Haematologica. 2014;99(4):769-778.

69. Larson MK, Watson SP. A product of their environment: do megakaryocytes rely on extracellular cues for proplatelet formation? Platelets. 2006;17(7):435-440.

70. Larson MK, Watson SP. Regulation of proplatelet formation and platelet release by integrin alpha IIb beta3. Blood. 2006;108(5):1509-1514.

71. Chang Y, Aurade F, Larbret F, et al. Proplatelet formation is regulated by the Rho/ROCK pathway. Blood. 2007;109(10):4229-4236.

72. Xu J, Gao XP, Ramchandran R, Zhao YY, Vogel SM, Malik AB. Nonmuscle myosin light-chain kinase mediates neutrophil transmigration in sepsis-induced lung inflammation by activating beta2 integrins. Nat Immunol. 2008;9(8):880-886.

73. Ikebe M, Reardon S, Fay FS. Primary structure required for the inhibition of smooth muscle myosin light chain kinase. FEBS Lett. 1992;312(2-3):245-248.

74. Rojnuckarin P, Kaushansky K. Actin reorganization and proplatelet formation in murine megakaryocytes: the role of protein kinase calpha. Blood. 2001;97(1):154-161.

75. Tamaru S, Kitajima K, Nakano T, et al. Calyculin A retraction of mature megakaryocytes proplatelets from embryonic stem cells. Biochem Biophys Res Commun. 2008;366(3):763-768.

76. Patel SR, Richardson JL, Schulze H, et al. Differential roles of microtubule assembly and sliding in proplatelet formation by megakaryocytes. Blood. 2005;106(13):4076-4085.

77. Radley JM, Haller CJ. The demarcation membrane system of the megakaryocyte: a misnomer? Blood. 1982;60(1):213-219.

78. Yvon AM, Gross DJ, Wadsworth P. Antagonistic forces generated by myosin II and cytoplasmic dynein regulate microtubule turnover, movement, and organization in interphase cells. Proc Natl Acad Sci U S A. 2001;98(15):8656-8661.

SUPPLEMENTARY MATERIAL AND METHODS

Mice

Generation of Sp1 and Sp3 targeting constructs and homologous recombination in ES cells

The *Sp1* and *Sp3* targeting constructs were constructed using standard cloning procedures, as described in Kulu et al (manuscript in preparation). In brief, the mouse *Sp1* gene is located on chromosome 15 and contains 7 exons. Deleting exons 6 and 7 removes the C-terminal part of the protein including the entire DNA binding domain resulting in an Sp1 *null* mutation.[1,2] We constructed an *Sp1* conditional targeting vector by introducing two loxP sites flanking exons 6 and 7 of the *Sp1* gene, and inserted a *LacZ-Neo* fusion gene under the control of the *PGK* promoter downstream of the last exon, in the antisense direction. Cre-induced recombination between the two loxP sites would result in the deletion of exons 6 and 7 thereby creating an *Sp1 null* allele (Scheme 1).

To target the mouse Sp3 gene, a vector was constructed with two loxP sites flanking exon 4, and the adjacent selection marker (*sa-IRES-lacZ-Neo*) was flanked by FRT sites (Scheme 2). In this way, the *LacZ-Neo* fusion gene is expressed under the control of the endogenous *Sp3* promoter.[3] The orientation and functionality of the loxP and FRT sites in the targeting vector was verified in *E. coli* strains expressing Cre- or Flp recombinase.[4]

The targeting vectors were linearized with Not1 and transfected into E14 ES cells. After Gancyclovir counter selection and G418 resistance selection, clones were picked and analyzed for homologous recombination events. Positive clones that had retained both loxP sites were karyotyped, and clones with the correct karyotype were used to generate chimeric mice. Cre-induced recombination between the two loxP sites introduces a frameshift after exon 4 excision.

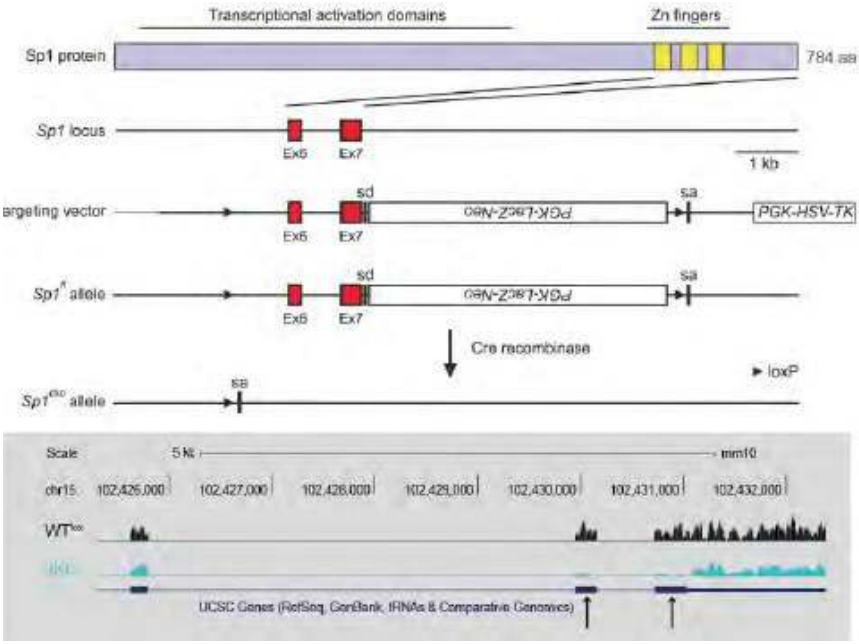

Scheme 1. Generation of mice with floxed Sp1 alleles and recombination in dKO cultured megakaryocytes as shown by RNA-Seq profiling

Schematic drawing of the strategy to create the allele used for Cre-mediated conditional knockout of the Sp1 gene. The PGK-HSV-TK cassette is deleted upon homologous recombination and was used for counter-selection to enrich for ES cell clones with homologous recombination events. The PGK-LacZ-Neo is inserted in the opposite transcriptional orientation relative to Sp1, and flanked by splice donor (sd) and acceptor (sa) sites. Sp1 exons are numbered Ex6 and Ex7. The zinc fingers are indicated as yellow boxes, exons are represented by red boxes. The panel below depicts UCSC browser RNA-Seq profiles of WT^{lox} and dKO representative samples, where absence of transcription of exons 6 and 7 is observed in the dKO sample. The mean coverage of reads per base of the deleted exons divided by the mean coverage of reads per base of Gapdh exon 5 was calculated and resulted in 1 ± 0.235 in WT^{lox} and 0.07 ± 0.06 in dKO samples ($P < .005$).

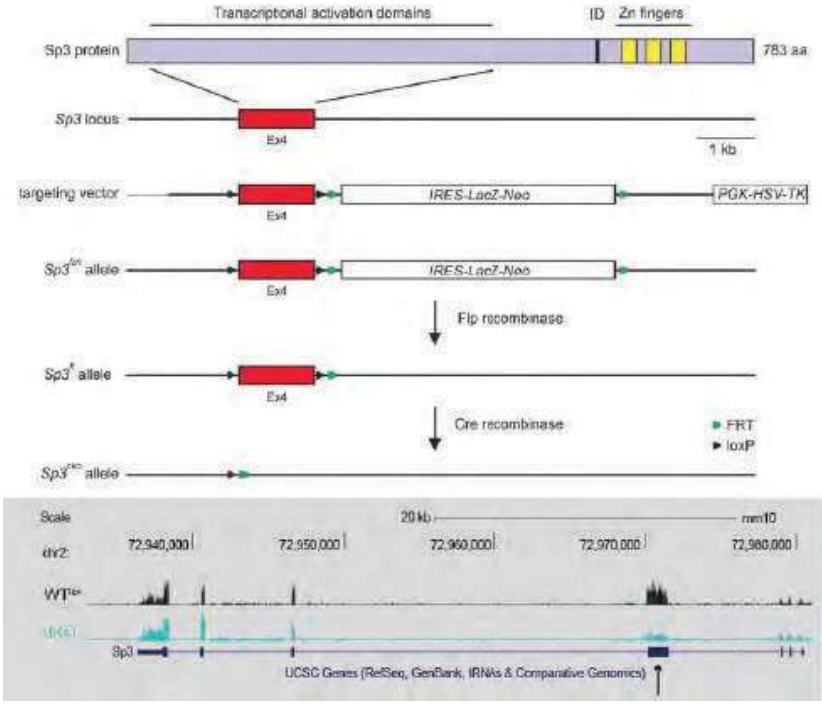

Scheme 2. Generation of mice with floxed Sp3 alleles and recombination in dKO cultured megakaryocytes as shown by RNA-Seq profiling

Schematic drawing of the strategy to create the allele used for Cre-mediated conditional knockout of the Sp3 gene. Flp recombinase was used to remove the IRES-LacZ-Neo selection cassette, leaving exon 4 (Ex4) flanked by loxP sites. ID = inhibitory domain. Other details are as for Scheme 1. The panel below depicts UCSC browser RNA-Seq profiles of WT^{lox} and dKO representative samples, where absence of transcription of exon 4 is observed in the dKO. sample. The mean coverage of reads per base of the deleted exon divided by the mean coverage of reads per base of Gapdh exon 5 was calculated and resulted in 1 ± 0.323 in WT^{lox} and 0.14 ± 0.048 in dKO samples ($P < .05$).

Correctly targeted ES cell clones were injected into C57BL/6 blastocysts to generate chimeric animals. Chimeric males, as judged by coat color, were mated to C57BL/6 females and germline transmission was scored by coat color. F1 animals were genotyped for the presence of the targeted *Sp1* or *Sp3* allele and positive animals were selected for further breeding. To delete the IRES-lacZ-Neo cassette from the targeted *Sp3* locus, animals were bred to the *Rosa26-Flp* line.[5] Animals carrying floxed *Sp1* or *Sp3* alleles were bred to homozygosity and crossed with the *Mx1-Cre*[6] or *Pf4-Cre* lines.[7,8] Additional rounds of breeding resulted in compound mice homozygous for the floxed *Sp1* and *Sp3* alleles, with or without the *Mx1-Cre* or *Pf4-Cre* alleles.

Induction of Sp1 and Sp3 deletion by activation of Mx1-Cre

Mx1-Cre::Sp1fl/fl::Sp3fl/fl and control $Sp1^{fl/fl}$::$Sp3^{fl/fl}$ animals were injected intraper-

itoneally with polyriboinosinic polyribocytidylic acid/PBS (25 μg/g body weight) every other day for a total of 5 days (3 poly I:C injections).[9] The mice were allowed to recover from the induced interferon response for at least 3 weeks before being analyzed.

Platelet function assays

Flow cytometry based platelet aggregation assay (FCA)

FCA was performed as described.[10] In short, CD9-APC (Abcam; Cambridge, UK) and CD9-PE (Abcam) labeled platelets were mixed 1:1 and preincubated 10 minutes at 37°C 700 RPM in the presence of 2% mouse plasma. When indicated, platelets were preincubated with 20 μM or 50 μM Mylk inhibitor (ML7 hydrochloride, # 4310, Tocris Bioscience, Bristol, UK). As agonists, we used 100 ng/mL phorbol myristate acetate (PMA; Sigma-Aldrich; St. Louis, MO, USA), 10 μg/mL Botrocetin (Sigma-Aldrich), 10 μg/mL collagen, 0.5 μg/ml Convulxin (Santa Cruz; Dallas, TX, USA) or 30 nM Aggretin A (a kind gift of Prof. Dr. Johannes A. Eble). Timed samples fixed in 0.5% formaldehyde/PBS were measured on an LSRII + HTS or Canto flow cytometer and analyzed for double-colored events by FACSDiva Version 6.1 software (BD Biosciences; San Jose, CA, USA).

Flow cytometry

Megakaryocyte phenotyping

Bone marrow and spleen single cell suspensions were stained with a cocktail of antibodies. Antibodies used were CD61-FITC, CD41-PE, KIT PerCPCy5.5, (BD Biosciences); CD42a-FITC, CD42b-DL649, CD42c-FITC, CD42d-FITC (Emfret; Eibelstadt, Germany); CD31 PECy7 (Abcam). Incubations were performed at 4°C during 20 min, after which cells were washed and resuspended in PBS/1%BSA containing 1:10000 Hoechst staining for dead/live discrimination.

Megakaryocyte ploidy measurements

Mouse bone marrow single cell suspensions were incubated with CD41-PE and CD42b- DL649 for 20 min on ice in PBS/1%BSA. Cells were then washed with PBS/1%BSA and spun at 1000 rpm for 5 min. Cells were resuspended in Cytofix/Cytoperm solution (Cytofix/Cytoperm, BD Biosciences) and incubated 10 min at room temperature. Cells were spun at 1000 rpm for 5 min, resuspended 1X Perm-Wash solution containing 50 mg/mL Hoechst 33342, 0.1% Triton X-100 and 50 mg/mL RNaseA and incubated for 30 min at 37oC. Megakaryocytes were identified as CD41-positive or CD42b-positive cells and Hoechst 33342 staining intensity was used as a measure of DNA ploidy. Samples were measured on a flow cytometer (LSR-II or Canto, BD Biosciences) and analyzed with FlowJo software (Ashland, OR, USA).

In vitro culture of bone marrow-derived megakaryocytes

Bone marrow explants: proplatelet formation assay

As previously described.[11] In these explant cultures, mature megakaryocytes already present in the bone marrow migrate to the periphery of the explant, and within six hours they start producing proplatelets. In brief, bone marrows from dKO and WT^{lox} mice were obtained by flushing femurs with HEPES buffer (132

mM NaCl, 20 mM HEPES, 6 mM KCL, 1 mM $MgSO_4$, 1.2 mM K_2HPO_4, pH 7.4). The marrows were cut in transverse sections of 1 mm and placed in an incubation chamber containing HEPES buffer. Each chamber contained 4 bone marrow fragments and was maintained at 37°C for 6 hr. Megakaryocytes at the periphery of the tissue were observed under a phase contrast microscope (Axiovert or EVOS, 20x objective; Life Technologies, Carlsbad, CA, USA) coupled to a video camera. Tiled scans were taken every hour. Cells were classified as megakaryocytes without proplatelets and megakaryocytes with proplatelets. Three mice per genotype were analyzed, including 3 explant sections per mouse. When indicated, 1-100 μM ML7 Mylk inhibitor or the equivalent volume of DMSO was added at the onset of the explant or after proplatelet formation. When indicated, 2 mM Ethylenediaminetetraacetic acid (EDTA) was added to the explant.

RNA

RNA extraction

CD61-FITC, CD41-PE and CD49b-Pacific blue triple positive cells were sorted from megakaryocyte cultures on a FACS ARIA (BD Biosciences) and used for RNA extraction using Trizol (Ambion, Life Technologies).

Megakaryocyte RNA sequencing

RNA-Seq was performed at the Erasmus MC Center for Biomics (Rotterdam, The Netherlands) according to manufacturer's instructions (Illumina; San Diego, CA, USA) and using the TruSeq RNA sample prep kit v2. Briefly, polyA containing mRNA molecules were purified using poly-T oligo attached magnetic beads. Following purification, the mRNA was fragmented into ~200 bp fragments using divalent cations under elevated temperature. The cleaved RNA fragments were copied into first strand cDNA using reverse transcriptase and random primers. This was followed by second strand synthesis using DNA polymerase I and RNaseH treatment. These cDNA fragments were end repaired, a single A base was added and Illumina adaptors were ligated. The products were purified and size selected on gel and enriched by PCR. The PCR products were purified by Qiaquick PCR purification and used for cluster generation according to the Illumina cluster generation protocols (www.illumina.com). The sample was sequenced for 36bp on a HiSeq2000 and demultiplexed using Narwhal.[12] The reads were aligned using Tophat version 2.0.8[13] against the UCSC mm10 reference genome, using Ensembl genes.gtf version 73.[14] For dKO RNA we obtained 57.5 million reads, of which 82.6 % aligned back to the reference genome, for WT^{lox} RNA we obtained 55.1 million reads with 82.3 % alignment (Figure S3).

RNA-Seq analysis

Raw counts were measured with htseq-count version 0.5.4. using -m union -s no -a 20 as settings.[15] The counted data were normalized by the size factor of the libraries. The differentially expressed genes were called using a generalized linear negative binomial model with controlling the effect of the RNA sample preparation date. The calculations were performed by the DESeq2 R package.[16] The False Discover Rate (FDR) was calculated with Benjamini Hochberg method[17] and the

threshold value was set to 0.01. After blind variance stabilizing transformation of the normalized counts, the differentially expressed genes were used to calculate the pairwise Spearman's rank correlation (r_s) coefficient matrices and the subsequent dissimilarity matrices ($1 - r_s$) for both genes and samples. The Euclidean distances of the dissimilarity matrices were used to apply hierarchical clustering with average linkage. The normalized gene expression data were scaled by row (Z-score) and subsequently plotted in a heat map using R (R Core Team (2014)). These dataset is available with Accession Number GSE5870.
Gene Ontology (GO) and Kyoto Encyclopedia of Genes and Genomes (KEGG) gene- enrichment analyses were carried out with the GO-stat package[18] using a conditional hypergeometrical test for over-representing Ensembl Gene IDs with a threshold *p* value of 0.01 and 0.05, respectively.
HOMER software suite was used, with default settings, to identify enrichment of known motifs in promoters of differentially regulated genes.[19]

RT-qPCR Analysis
Total RNA (1 µg) was converted to cDNA using SuperScript II reverse transcriptase according to the manufacturer's instructions (Life Technologies). Expression levels of mRNAs were analyzed by quantitative real-time PCR (qPCR) using SYBR green on a Applied Biosystems StepOne RT-qPCR system (Life Technologies). All reactions were performed in duplicate. Gene expression levels were calculated with the $2^{-\Delta_{CT}}$ method.[20] Target gene expression was normalized to Gapdh expression. Primers used were as follows:

Gapdh
5'-CCTGCCAAGTATGATGACAT-3' and 5'-GTCCTCAGTGTAGCCCAAG-3';
Alox
12 5'-TTCAGTTGCTTACTCGGGC-3' and 5'-CATACCTGGCAGTGACTTCC-3';
Add3
5'-AGCGTTACAGCAGATTGCG-3' and 5'-TTTCTCCCTTCACATACGAGG-3';
Mylk
5'-TGTCTCATTCTGGAAGCGG-3' and 5'-GCTGTAACTCAGGCAAGGATTAG-3';
Rasgrp2
5'-TCAGTTGCCAAGCCTAAGC-3' and 5'-TGAGATAAGGGAAGTTGCCC-3'.

Protein
Platelet lysates and Western blotting
Around 10^9 platelets were lysed in 500 mL RIPA buffer (150 mM NaCl, 1% NP-40, 0.5% Deoxycholate, 0.1% SDS, 50 mM Tris HCL, pH 7.5). Antibodies used were Alox12 (sc-27359, Santa Cruz), Add3 (17585-1-AP, Proteintech; Chicago, IL, USA), Rasgrp2 (PA5- 28865, Pierce antibodies; Rockford, IL, USA), Mylk (21642-1-AP, Proteintech) and Anti- Gapdh (MAB374, Merck Millipore; Darmstadt, Germany), and secondary antibodies IRDye 680 goat anti-mouse IgG, IRDye 680 goat anti-rabbit IgG, IRDye 800 donkey anti- goat IgG and IRDye 800CW donkey anti-mouse IgG (926-32220, 926-32221, 926-32214 and 926-32212, respectively, LI-COR Biosciences; Lincoln, NE, USA). Western blot membranes were quantified using Odyssey LI-COR Imaging system. Alternatively, secondary antibodies against rabbit or mouse IgG conjugat-

ed to horseradish peroxidase were purchased from GE Healthcare (NA934V and NA931V, respectively; Little Chalfont, UK). Enhanced chemoluminescence (ECL) was performed to develop the blots as described by the manufacturer (Supersignal West Dura #34075, ThermoFisher Scientific; Waltham, MA, USA).

Mass spectrometry analysis

Proteins were separated on SDS-PAGE and processed for mass spectrometry analysis. Peptides were separated using a reverse-phase C18 Acclaim PepMap RSLC (75 ìm × 150 mm, 2 m particles) at a flow rate of 300 nl/min using a one-hour linear gradient from 0.05% acetic acid (v/v) to 0.05% (v/v) acetic acid and 35% (v/v) acetonitrile employing a Dionex Ultimate 3000 RSLC. Once separated, the peptides were directly sprayed into an LTQ Orbitrap XL mass spectrometer (Thermo Scientific).

Proteomics data analysis

The raw mass spectrometry data were analyzed with MaxQuant software version 1.5.0.0[21] using default settings and Label Free Quantification (LFQ).[22] The peptides were identified by searching against the UniProt mouse taxonomy database release 2014_04.[23]

The Protein Groups table generated by MaxQuant software was filtered for contaminants (except for platelet proteins Tpm2 and Pfn1), reverse hits and only-identified-by modification-site hits. Moreover only proteins that were identified by more than one peptide and with at least one unique peptide were used. The LFQ intensities values were log2 transformed and used to determine, at protein level, the genes that are differentially expressed. We imputed missing values similarly as the Perseus software package of MaxQuant, that is, by sampling a normal distribution based on the estimated mean and standard deviation (SD) of each sample, while the mean was shifted with 1.8 x SD and the SD was multiplied by 0.3. Subsequently, we kept proteins that were identified at least twice in the WT^{lox} or dKO samples. Two-tailed Student's *t*-tests were applied for each identified protein with multiple testing correction using the Benjamini Hochberg method.[17]

Heat map of differentially expressed proteins was plotted similar to the RNA-Seq data (see RNA-Seq analysis) with the same settings, but using Pearson's correlation coefficient and an FDR of < 0.25 as threshold value instead.

Computational analysis of RNA-Seq and proteomics datasets

Proteomics data were merged with RNA-Seq data by the Ensembl Gene IDs and MaxQuant Majority protein IDs, which were converted into Ensembl Gene IDs using biomaRt.[24] We selected the entries with the lowest *p* value in the proteomics data if the Majority protein ID converted to multiple Ensembl Gene IDs. The statistical package R was used for calculations and plotting of the data (R Core Team (2014).

All graphics were designed QIAGEN's Ingenuity Pathway Analysis (IPA®, QIAGEN Redwood City, www.qiagen.com/ingenuity). Sp1 binding sites on promoters of differentially expressed proteins were identified using SABiosciences (QIAGEN, http://www.sabiosciences.com/chipqpcrsearch.php, choosing mouse as species and Sp1 as transcription factor), or otherwise Sp regulation of target proteins reported elsewhere is indicated in Table S3 (PMID).

REFERENCE LIST

1. Kruger I, Vollmer M, Simmons DG, Elsasser HP, Philipsen S, Suske G. Sp1/Sp3 compound heterozygous mice are not viable: impaired erythropoiesis and severe placental defects. Dev Dyn. 2007;236(8):2235-2244.
2. Marin M, Karis A, Visser P, Grosveld F, Philipsen S. Transcription factor Sp1 is essential for early embryonic development but dispensable for cell growth and differentiation. Cell. 1997;89(4):619-628.
3. Mountford P, Zevnik B, Duwel A, et al. Dicistronic targeting constructs: reporters and modifiers of mammalian gene expression. Proc Natl Acad Sci U S A. 1994;91(10):4303-4307.
4. Buchholz F, Angrand PO, Stewart AF. A simple assay to determine the functionality of Cre or FLP recombination targets in genomic manipulation constructs. Nucleic Acids Res. 1996;24(15):3118-3119.
5. Farley FW, Soriano P, Steffen LS, Dymecki SM. Widespread recombinase expression using FLPeR (flipper) mice. Genesis. 2000;28(3-4):106-110.
6. Kuhn R, Schwenk F, Aguet M, Rajewsky K. Inducible gene targeting in mice. Science. 1995;269(5229):1427-1429.
7. Calaminus SD, Guitart AV, Sinclair A, et al. Lineage tracing of Pf4-Cre marks hematopoietic stem cells and their progeny. PLoS One. 2012;7(12):e51361.
8. Tiedt R, Schomber T, Hao-Shen H, Skoda RC. Pf4-Cre transgenic mice allow the generation of lineage- restricted gene knockouts for studying megakaryocyte and platelet function in vivo. Blood. 2007;109(4):1503-1506.
9. Gutierrez L, Tsukamoto S, Suzuki M, et al. Ablation of Gata1 in adult mice results in aplastic crisis, revealing its essential role in steady-state and stress erythropoiesis. Blood. 2008;111(8):4375-4385.
10. De Cuyper IM, Meinders M, van de Vijver E, et al. A novel flow cytometry-based platelet aggregation assay. Blood. 2013;121(10):e70-80.
11. Eckly A, Strassel C, Cazenave JP, Lanza F, Leon C, Gachet C. Characterization of megakaryocyte development in the native bone marrow environment. Methods Mol Biol. 2012;788:175-192.
12. Brouwer RW, van den Hout MC, Grosveld FG, van Ijcken WF. NARWHAL, a primary analysis pipeline for NGS data. Bioinformatics. 2012;28(2):284-285.
13. Kim D, Pertea G, Trapnell C, Pimentel H, Kelley R, Salzberg SL. TopHat2: accurate alignment of transcriptomes in the presence of insertions, deletions and gene fusions. Genome Biol. 2013;14(4):R36.
14. Flicek P, Amode MR, Barrell D, et al. Ensembl 2014. Nucleic Acids Res. 2014;42(Database issue):D749-755.
15. Anders S, Pyl PT, Huber W. HTSeq – A Python framework to work with high-throughput sequencing data. BioRxiv; 2014.
16. Anders S, Huber W. Differential expression analysis for sequence count data. Genome Biol. 2010;11(10):R106.

17. Benjamini Y, Hochberg Y. Controlling the false discovery rate: a practical and powerful approach to multiple testing. Roy Statist Soc Ser B (Methodological). 1995;57:289-300.

18. Falcon S, Gentleman R. Using GOstats to test gene lists for GO term association. Bioinformatics. 2007;23(2):257-258.

19. Heinz S, Benner C, Spann N, et al. Simple combinations of lineage-determining transcription factors prime cis-regulatory elements required for macrophage and B cell identities. Mol Cell. 2010;38(4):576-589.

20. Schmittgen TD, Livak KJ. Analyzing real-time PCR data by the comparative C(T) method. Nat Protoc.2008;3(6):1101-1108.

21. Cox J, Mann M. MaxQuant enables high peptide identification rates, individualized p.p.b.-range mass accuracies and proteome-wide protein quantification. Nat Biotechnol. 2008;26(12):1367-1372.

22. Cox J, Hein MY, Luber CA, Paron I, Nagaraj N, Mann M. MaxLFQ allows accurate proteome-wide label- free quantification by delayed normalization and maximal peptide ratio extraction. Mol Cell Proteomics. 2014.

23. UniProt C. Activities at the Universal Protein Resource (UniProt). Nucleic Acids Res. 2014;42(Database issue):D191-198.

24. Durinck S, Spellman PT, Birney E, Huber W. Mapping identifiers for the integration of genomic datasets with the R/Bioconductor package biomaRt. Nat Protoc. 2009;4(8):1184-1191.

A Flow Cytometry

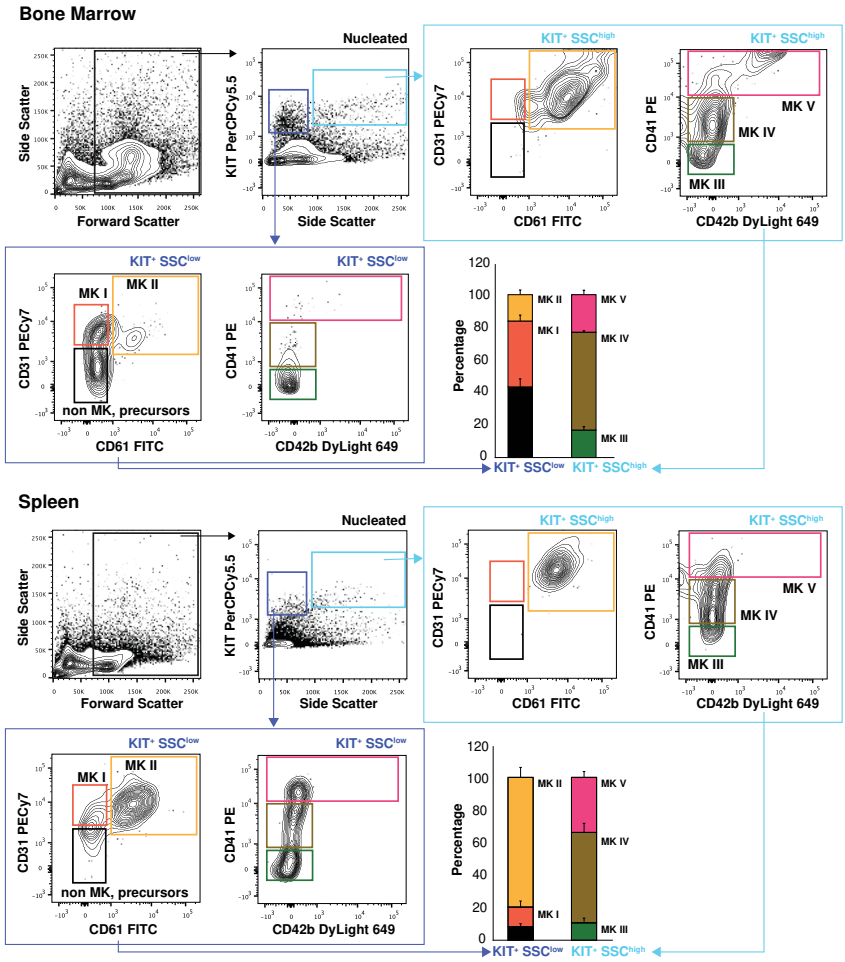

B Spleen Histology
AChE staining

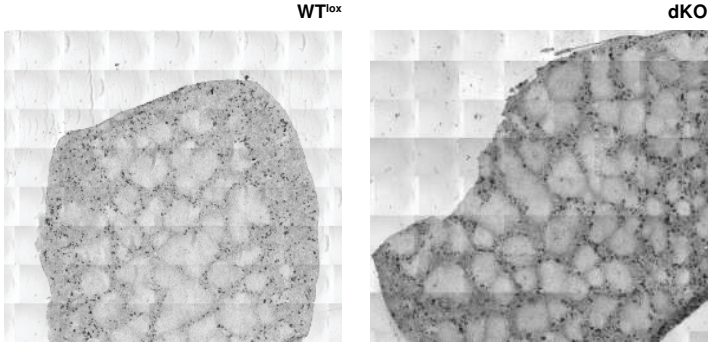

Figure S1. Characterization of megakaryopoiesis in vivo: flow cytometry and histology

A) Gating strategy to identify megakaryocytes (MK) at consecutive stages of differentiation in bone marrow and spleen. We attempted to subdivide stages of megakaryocyte maturation based on surface marker expression, despite the overlapping expression of many of these throughout megakaryocyte differentiation. The upper panels show the gating strategy in WT^{lox} bone marrow, and the lower panels show the gating strategy in WT^{lox} spleen.
First, KIT positive cells were subdivided in side scatter (SSC) low (dark blue) or high (light blue). The $KIT^{+}SSC^{low}$ cell population contains early MK precursors, amongst other hematopoietic precursors. This population was further gated against CD31 and CD61, which are early markers during megakaryocyte maturation, and subdivided as double negative $KIT^{+}SSC^{low}CD31^{-}CD61^{-}$ (containing hematopoietic precursors and non-megakaryocytic cells -black-), $KIT^{+}SSC^{low}CD31^{+}CD61^{-}$ (MK I, -orange-) and $KIT^{+}SSC^{low}CD31^{+}CD61^{+}$ (MK II, -yellow-). When the $KIT^{+}SSC^{low}$ population is plotted against CD41 and CD42b, which mark generally more mature megakaryocytes, most of the cells are still negative for both. The $KIT^{+}SSC^{high}$ population should contain mostly more mature megakaryocytes (and possibly mast cells), and therefore, they are all double positive for CD31 and CD61 (markers used to distinguish earlier megakaryocyte progenitors in the SSC^{low} gate). The $KIT^{+}SSC^{high}$ population was further gated as $KIT^{+}SSC^{high}CD41^{-}CD42b^{-}$ (MK III, -green-), $KIT^{+}SSC^{high}CD41^{dim}CD42b^{-/dim}$ (MK IV, - brown-), and $KIT^{+}SSC^{high}CD41^{+}CD42b^{dim/+}$ (MK V, -pink-).
The gating strategy for the spleen is the same, and it shows the difference in the differentiation status of spleen MK compared to bone marrow MK: most of the splenic $KIT^{+}SSC^{low}$ cells are double positive for CD31 and CD61, and they start expressing CD41 and $CD42b^{dim}$, while in bone marrow there is a higher prevalence of the MK I population, and many double negative cells (other hematopoietic precursors) that are not present in spleen.

B) Representative composite images of whole spleen sections from dKO and WT^{lox} mice stained for acetylcholinesterase activity, which labels mature megakaryocytes. No overt differences are observed regarding red pulp/white pulp histology or distribution and number of MK in WT^{lox} and dKO spleens.

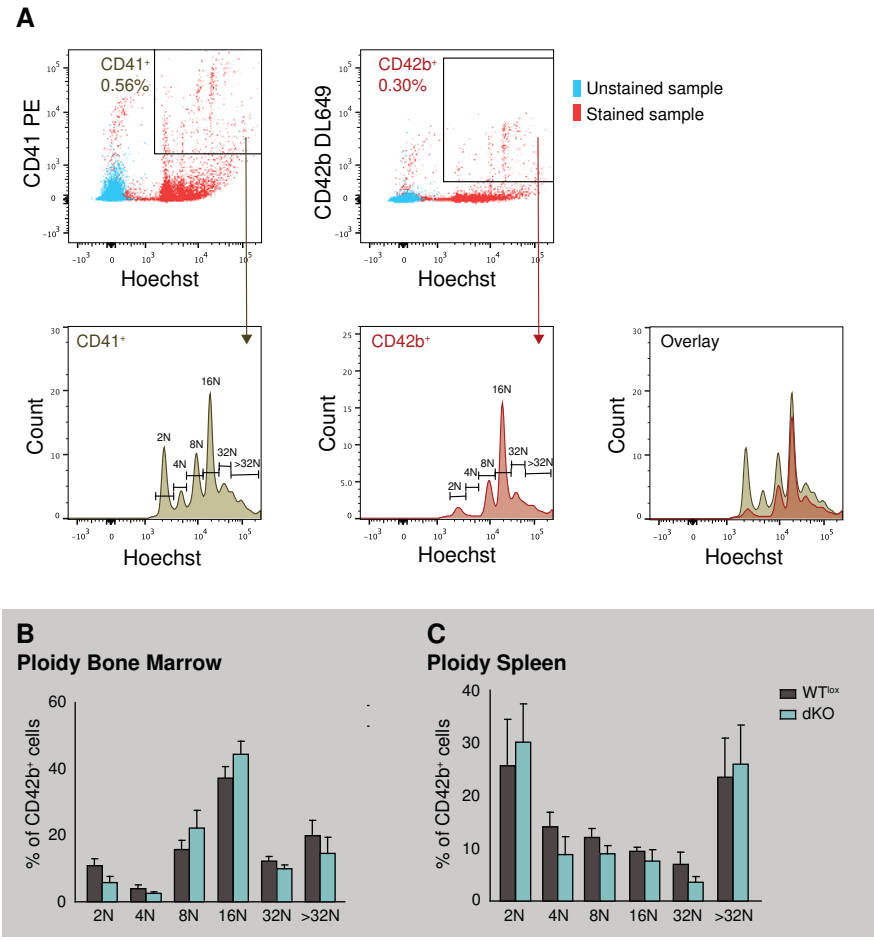

Figure S2. Characterization of megakaryopoiesis in vivo: flow cytometry ploidy analysis

A) Gating strategy for ploidy measurements, bone marrow samples from WT^{lox} mice are depicted. The ploidy status of $CD41^+$ (megakaryocytes) and $CD42b^+$ (enriched for more mature megakryocytes) was measured by the Hoechst staining. In bone marrow, 16N is the most frequent megakaryocyte ploidy status. Note that the majority of 2N megakaryocytes are CD42b-negative.

B-C) Bar graphs depicting the ploidy status of $CD42b^+$ cells in bone marrow and spleen.

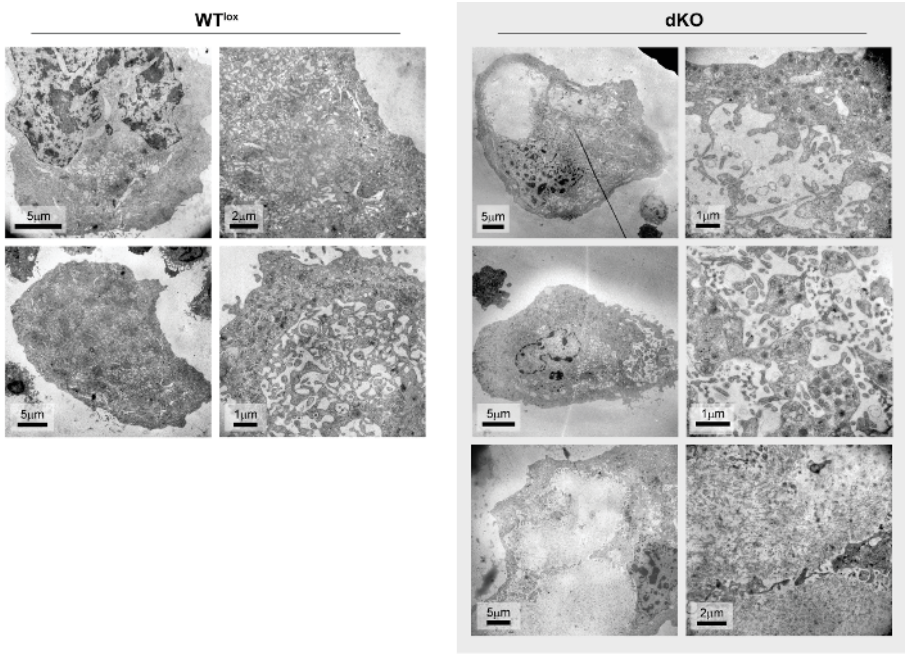

Figure S3. dKO megakaryocytes display an aberrant DMS

Electron microscope images of bone marrow-derived cultured WT^{lox} and dKO megakaryocytes. Complements Figure 3A.

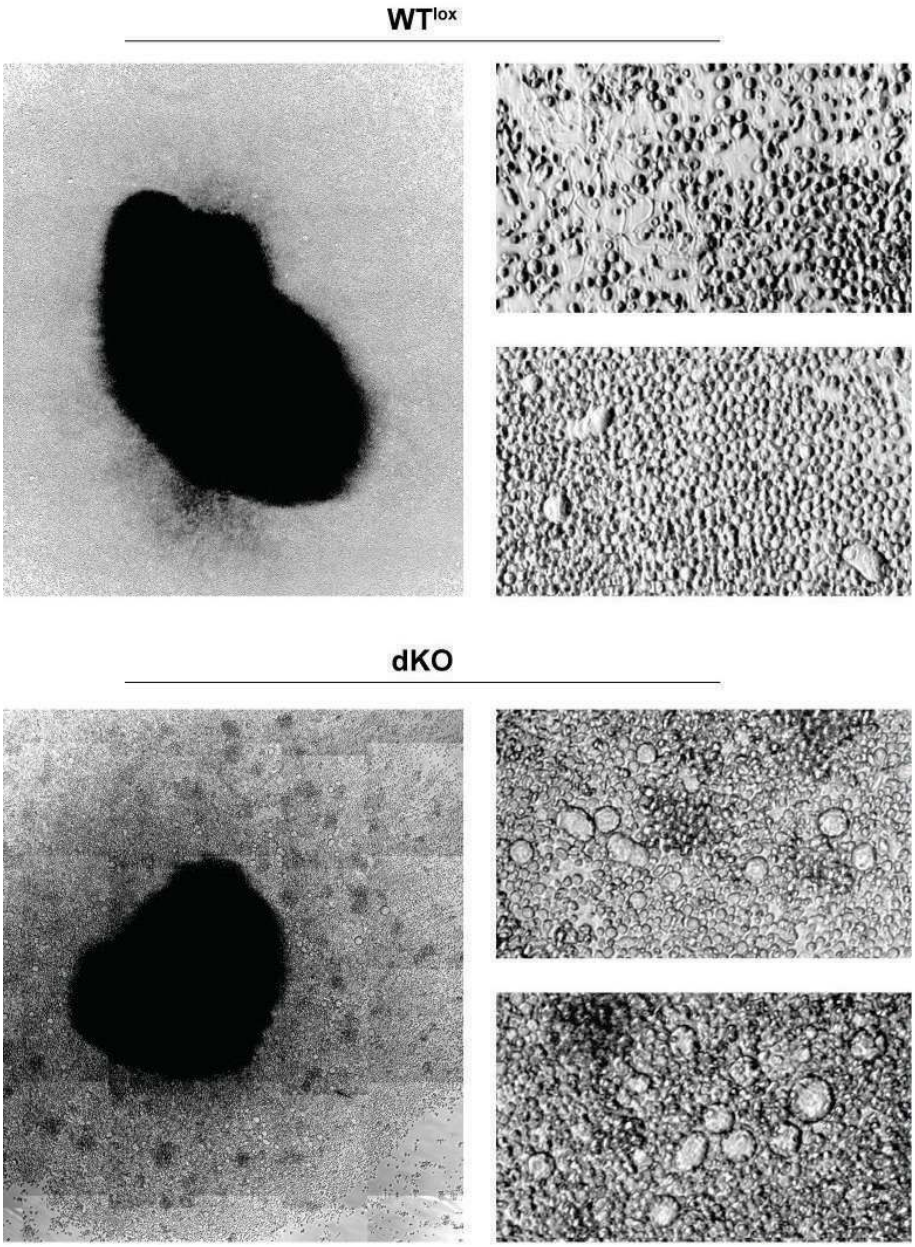

Figure S4. dKO megakaryocytes are incapacitated to form proplatelets

Representative pictures of WT^{lox} (upper panel) and dKO (lower panel) bone marrow explants with zoomed-in areas. This shows that dKO megakaryocytes are present at the periphery of the explant, but they do not produce proplatelets and maintain a round shape. In contrast, most of the WT^{lox} megakaryocytes are undergoing shape changes or have produced proplatelets. Complements Figure 3B.

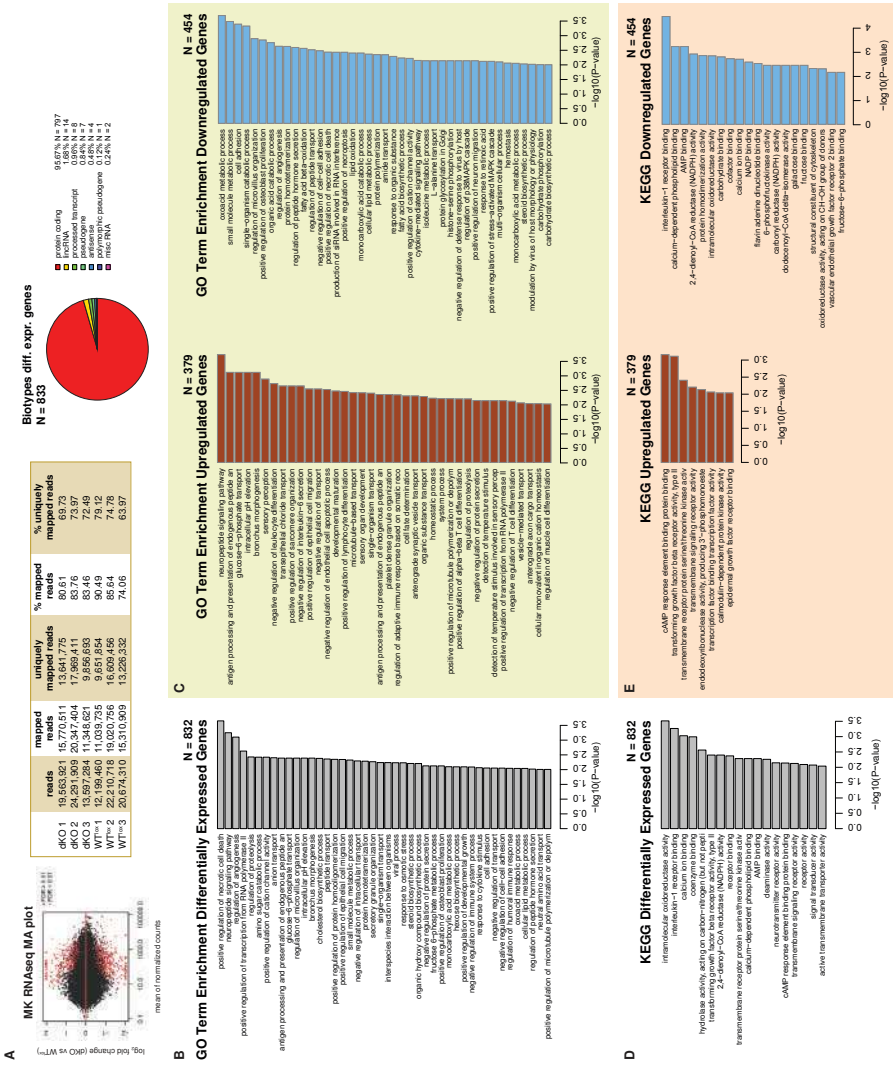

Figure S5. Megakaryocyte RNA-Seq

A) On the left, MA-plot of the mean normalized gene count versus the $\log_2$ fold changes of dKO over WT^{lox}. Genes are plotted as closed black circles. 833 genes with an adjusted *p*-value (FDR) < 0.01 are colored red. Genes that fall out of the window boundaries of -2 or 2 $\log_2$ fold change are plotted as open triangles. Center, table summarizing RNA-Seq results, and on the right biotypes pie chart.

B-C) Enrichment of biological processes Gene Ontology (GO) terms in differentially regulated genes (gray bars), and genes which are downregulated (blue bars) or upregulated (brown bars) in dKO megakaryocytes.

D-E) Results of enrichment analysis similar to B-C on Kyoto Encyclopedia of Genes and Genomes database (KEGG).

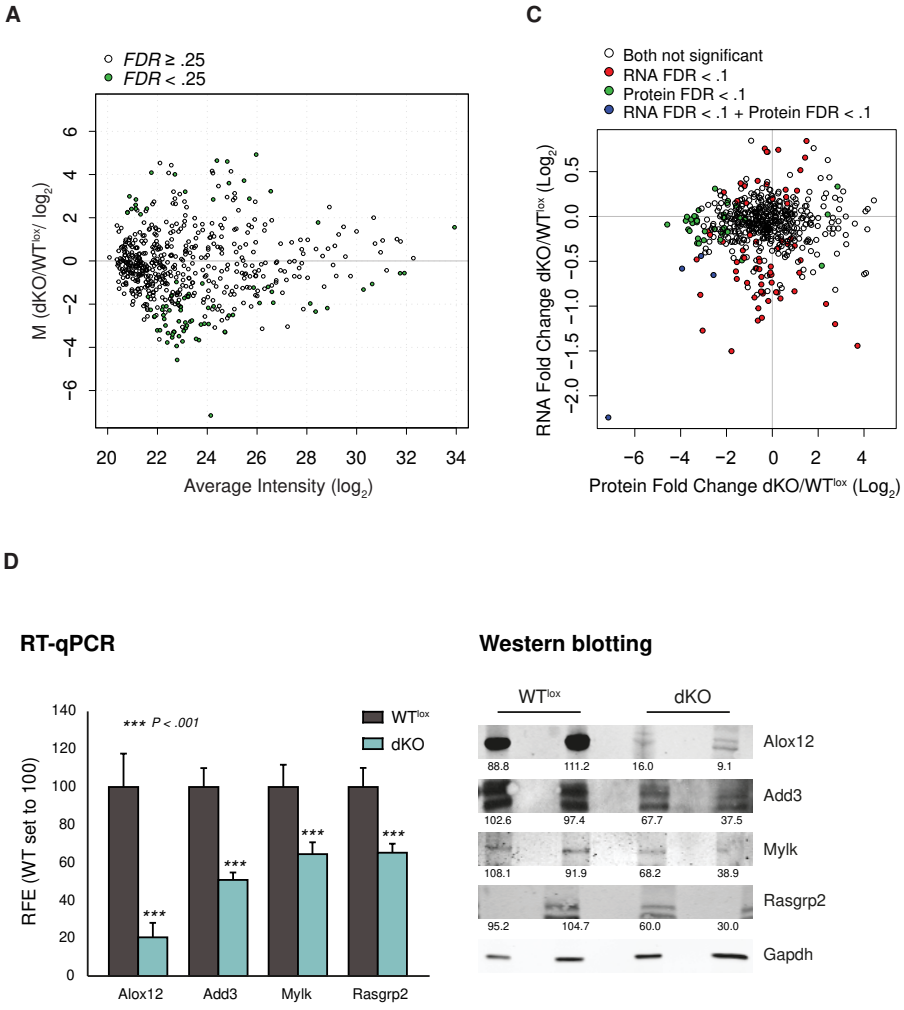

Figure S6. Platelet proteomics.

A) MA-plot of the average normalized spectral counts from WT^{lox} and dKO platelets shows significantly deregulated proteins (FDR < 0.25).
B) Scheme of differentially expressed proteins in dKO platelet lysates.
C) Scatterplot of differentially expressed proteins in platelets (mass spectrometry) and differentially expressed genes in megakaryocytes (RNA-Seq) in dKO samples with N =527.
D) Validation of downregulated genes with identical signature in mRNA of cultured bone marrow derived megakaryocytes (by RT-qPCR, left bar graph), and in protein lysates of platelets (by western blotting, right panel). Numbers displayed below each band represent quantitation against Gapdh.

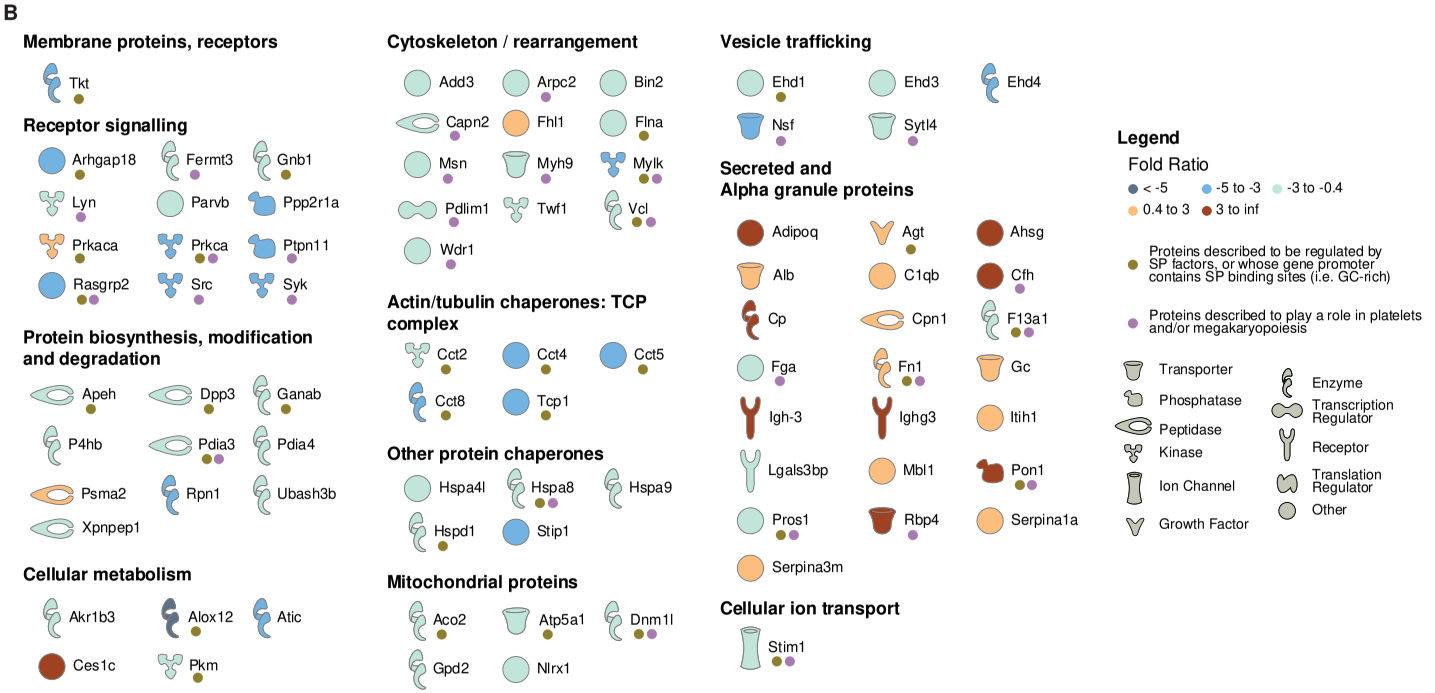
B
Membrane proteins, receptors
Tkt
Receptor signalling
Arhgap18
Fermt3
Gnb1
Lyn
Parvb
Ppp2r1a
Prkaca
Prkca
Ptpn11
Rasgrp2
Src
Syk
Protein biosynthesis, modification and degradation
Apeh
Dpp3
Ganab
P4hb
Pdia3
Pdia4
Psma2
Rpn1
Ubash3b
Xpnpep1
Cellular metabolism
Akr1b3
Alox12
Atic
Ces1c
Pkm
Cytoskeleton / rearrangement
Add3
Arpc2
Bin2
Capn2
Fhl1
Flna
Msn
Myh9
Mylk
Pdlim1
Twf1
Vcl
Wdr1
Actin/tubulin chaperones: TCP complex
Cct2
Cct4
Cct5
Cct8
Tcp1
Other protein chaperones
Hspa4l
Hspa8
Hspa9
Hspd1
Stip1
Mitochondrial proteins
Aco2
Atp5a1
Dnm1l
Gpd2
Nlrx1
Vesicle trafficking
Ehd1
Ehd3
Ehd4
Nsf
Sytl4
Secreted and Alpha granule proteins
Adipoq
Agt
Ahsg
Alb
C1qb
Cfh
Cp
Cpn1
F13a1
Fga
Fn1
Gc
Igh-3
Ighg3
Itih1
Lgals3bp
Mbl1
Pon1
Pros1
Rbp4
Serpina1a
Serpina3m
Cellular ion transport
Stim1
Legend
Fold Ratio
< -5
-5 to -3
-3 to -0.4
0.4 to 3
3 to inf
Proteins described to be regulated by SP factors, or whose gene promoter contains SP binding sites (i.e. GC-rich)
Proteins described to play a role in platelets and/or megakaryopoiesis
Transporter
Phosphatase
Peptidase
Kinase
Ion Channel
Growth Factor
Enzyme
Transcription Regulator
Receptor
Translation Regulator
Other

Chapter 4

SYK TRANSCRIPTION IS DIRECTLY REGULATED BY GATA1 IN MOUSE MEGAKARYOCYTES

SYK TRANSCRIPTION IS DIRECTLY REGULA-TED BY GATA1 IN MOUSE MEGAKARYOCYTES

M. Meinders[1], M. Hoogenboezem[2], M.R. Scheenstra[1], T.K. van den Berg[1], T.W. Kuijpers[1,3] and L. Gutiérrez[1,4]

[1]Dept. of Blood Cell Research, Sanquin Research and Landsteiner Laboratory, Academic Medical Centre (AMC), University of Amsterdam (UvA), Amsterdam, the Netherlands; [2]Dept. of Molecular Cell Biology, Sanquin Research and Landsteiner Laboratory, AMC, UvA, Amsterdam; [3]Emma Children's Hospital, Academic Medical Centre (AMC), UvA, Amsterdam; [4]Senior and corresponding author.

Running Head: Gata1 regulates megakaryocyte Syk transcription
Abstract (150 words): 150
Manuscript (max 1200 words): 1199
Figures: 2
References (Max 25): 25

ABSTRACT

During hematopoiesis, transcriptional programs are essential for the commitment and differentiation of progenitors into the different blood lineages. GATA1 is a transcription factor expressed in several hematopoietic lineages and essential for proper erythropoiesis and megakaryopoiesis. Megakaryocyte-specific genes, such as *GP1BA*, are known to be directly regulated by GATA1. Mutations in GATA1 can lead to dyserythropoietic anemia and *pseudo* gray-platelet syndrome. Selective loss of Gata1 expression in adult mice results in macrothrombocytopenia with platelet dysfunction, characterized by an excess of immature megakaryocytes. To specifically analyze the function of Gata1 in mature committed megakaryocytes, we generated Gata1-Lox|Pf4-Cre mice, which are macrothrombocytopenic with platelet dysfunction, consistently with previous findings. Interestingly, these mice present a misbalance of the multipotent progenitor compartment and an additional aberrant megakaryocyte differentiation stage. Furthermore, we show that Gata1 directly regulates the transcription of Syk, a tyrosine kinase that functions downstream of Clec2 and GPVI receptors in megakaryocytes and platelets.

Key Words

Gata1, megakaryopoiesis, hematopoietic stem cells, transcription, Syk.

Key Points

- Gata1 loss in megakaryocytes results in aberrant megakaryocyte differentiation and impacts the balance of hematopoietic progenitors.
- Gata1 regulates the transcription of Syk in megakaryocytes.

INTRODUCTION

Gata1 is a critical transcription factor for the differentiation of erythroid cells, eosinophils, mast cells and megakaryocytes.[1] It belongs to the GATA family of zinc-finger transcription factors and is located on the X-chromosome. In humans, mutations in GATA1 may lead to X-linked thrombocytopenia and/or anemia.[2-5] Besides congenital mutations, patients with Down syndrome are more likely to develop acquired somatic GATA1 mutations leading to a truncated form of GATA1 increasing the risk at acute megakaryoblastic leukemia (AMKL).[6] As a transcription factor it binds to the W(A/T)GATAR(A/G) motif and regulates the expression of essential genes during megakaryopoiesis, i.e. *GP1BA*, *GP1BB* and *MPL*.[7-11]
Gata1 knockout mice die around day E10.5 of gestation due to severe anemia[12] and conditional ablation of Gata1 has shown its requirement in the erythro-megakaryocytic lineages in adult mice.[13] Mice with targeted mutations on the Gata1 promoter affecting its expression, such as Gata-1.05/X female mice and ΔneoΔHS mice, display macrothrombocytopenia and increased proliferation of megakaryocytes.[14, 15] Collagen and vWF platelet responses are defective in ΔneoΔHS platelets, similarly to what occurs in patients carrying a GATA1 mutation.[5, 9, 16]
We generated Gata1-Lox|Pf4-Cre mice in order to specifically study the consequences of Gata1 depletion in committed megakaryocytes.[17, 18] Consistent with previous findings, late ablation of Gata1 in the megakaryocytic lineage resulted in macrothrombocytopenia and platelets that are functionally impaired. We show that these mice present a misbalance of their multipotent progenitor compartment and an additional aberrant megakaryocyte differentiation stage. Furthermore, Gata1 directly regulates the transcription of Syk, a pivotal tyrosine kinase that functions downstream of Clec2 and GPVI receptors in megakaryocytes and platelets.

METHODS

Mouse

Gata1-lox mice[17] were crossed with PF4-cre mice[18] and maintained in the Dutch Cancer Center (NKI) animal facility under specific pathogen-free conditions and following the institutional ethical committee guidelines.

Blood analysis and platelet functional assays

Blood was drawn by heart puncture and collected in heparin-coated vials (Sarstedt, Nümbrecht, Germany). Blood parameters were determined on a scil Vet abc Plus+. FCA was performed as described.[19]

Flow cytometry

Platelets or bone marrow single cell suspensions were stained for flow cytometry analysis as previously described.[20, 21] Antibodies used were: CD61-FITC, CD41-PE, Sca1-PECy7, CD34-FITC, Lin-cocktail-APC, CD16/CD32-PE, cKit-PerCP (BD Pharmingen, Oxford, United Kingdom), Clec2–FITC (AbD Serotec, Kidlington, United Kingdom), CD42a-FITC, CD42b-DL649, CD42c-FITC (Emfret, Wurzburg,

Germany), GPVI-PE (R&D, Abingdon, United Kingdom), CD9-PE, CD31-PECy7 (Abcam, Cambridge United Kingdom), CD49b-PB (BioLegend, San Diego, CA).

Bone marrow-derived megakaryocyte cultures
Megakaryocyte cultures were performed as previously described.[20, 21]

RNA
$CD61^+$ $CD41^+$ $CD49b^+$ cells were sorted from megakaryocyte cultures on a FACS ARIA (BD Bioscience) and used for RNA extraction using Trizol (Ambion, Life Technologies). cDNA was prepared from 1mg RNA with Superscript III first strand (Invitrogen). Expression levels of mRNAs were analyzed by quantitative real-time PCR (qPCR) using SYBR green on a Applied Biosystems StepOne RT-qPCR system (Life Technologies). All reactions were performed in triplo. Gene expression levels were calculated with the $2^{-\Delta CT}$ method.[22] Target gene expression was normalized to Gapdh expression. Primers used were:

Gata1
5'-CAGTCCTTTCTTCTCTCCCAC-3'and 5'-GCTCCACAGTTCACACACT-3';
PU1
5'-TCTTCACCTCGCCTGTCTT-3' and 5'-TCCAGTTCTCGTCCAAGCA-3';
Syk
5'-TCACAACAGGAAGGCACAC-3' and 5'-GAGTGGTAATGGCAGAGGTC-3';
Gapdh
5'-CCTGCCAAGTATGATGACAT-3' and 5'-GTCCTCAGTGTAGCCCAAG-3'.

Protein
Approximately 10^9 platelets were lysed in 500 ml RIPA buffer (150 mM NaCl, 1% NP-40, 0.5% Deoxycolate, 0.1% SDS, 50 mM Tris HCL, pH 7.5). Proteins were separated by SDS-PAGE gel electrophoresis and transferred to PVDF membranes and incubated following standard procedures. Antibodies used were Anti-Gata1 (sc-265, Santa Cruz), Anti-Syk (sc-573, Santa Cruz), Anti-Gapdh (MAB374, Merck Millipore), and secondary antibodies IRDye 680 goat anti-mouse IgG and IRDye 800CW donkey anti-mouse IgG (926-32220 and 926-32212, respectively, LI-COR Biosciences). Western blot membranes were quantified using Odyssey LI-COR Imaging system.

Chromatin Immunoprecipitation (ChIP)
Chromatin Immunoprecipitations were performed as previously described[23] using anti-Gata1 antibody (ab11963, Abcam) and protein A magnetic beads (10002D, Life Technologies). Enrichment was measured by qPCR. Primers used were:

Syk
5'-TCACAACAGGAAGGCACAC-3'and 5'-GAGTGGTAATGGCAGAGGTC-3';
Gp1ba
5'-GCTGATAAGAGCCTTTGCC-3' and 5'-GGGAGGAAATGACAACCTG-3;
Cd9
5'-ACCGTGCTCAACTAAGTGCG-3'and 5'-AGATTCCCGAGGCAAGTCTG-3'.

Statistical Analysis

We represent average and standard error of the mean (SEM) of at least three mice per genotype or experiments unless otherwise indicated. We applied two-tailed Student's *t*-tests to calculate statistical significance.

RESULTS AND DISCUSSION

To investigate the role of Gata1 in late megakaryopoiesis, Gata1-lox|Pf4-Cre mice were generated.[17, 18] We refer to these mice as Gata1cKO^{MK}, and to control Gata1-lox littermates as WT^{lox}. Gata1 mRNA expression was reduced to 20% in Gata1cKO^{MK} cultured megakaryocytes (Figure 1A). Consistent with previous reports,[9, 14, 24] Gata1cKO^{MK} mice suffer from severe macrothrombocytopenia (Figure 1B).

Misbalance of multipotent progenitors in the bone marrow of Gata1cKO^{MK} mice

Surface marker expression analysis of the hematopoietic compartment in the bone marrow revealed that Gata1cKO^{MK} mice display a misbalance in hematopoietic progenitors, i.e. an increase in the total number of lineage^{-}|Sca-1^{+}|Kit+ (LSK) hematopoietic stem cells (HSC) and myeloid progenitors (MP), mainly due to an increase in common myeloid progenitor (CMP) cells (Figure 1C). This suggests that the chronic low platelet production affects the early hematopoietic compartment.

Aberrant megakaryocyte maturation in Gata1cKO^{MK} mice

We next characterized the various megakaryopoiesis differentiation stages in the bone marrow, ranging from stage I-V from immature to mature.[21] Compared to WT^{lox} littermates, and as previously reported, we identified a shift towards more immature megakaryocytes in the bone marrow, i.e. a relative increase in population I and a decrease in populations IV-V (Figure 1D), which was accompanied by an increase in low ploidy 2N-CD41^{+} megakaryocytes in Gata1cKO^{MK} mice (Figure 1E). Interestingly, we identified an additional subpopulation exclusively in the Gata1cKO^{MK} megakaryocytes, indicated as II+, in which MKs with low SSC characteristics express higher (inappropriate) levels of CD61.

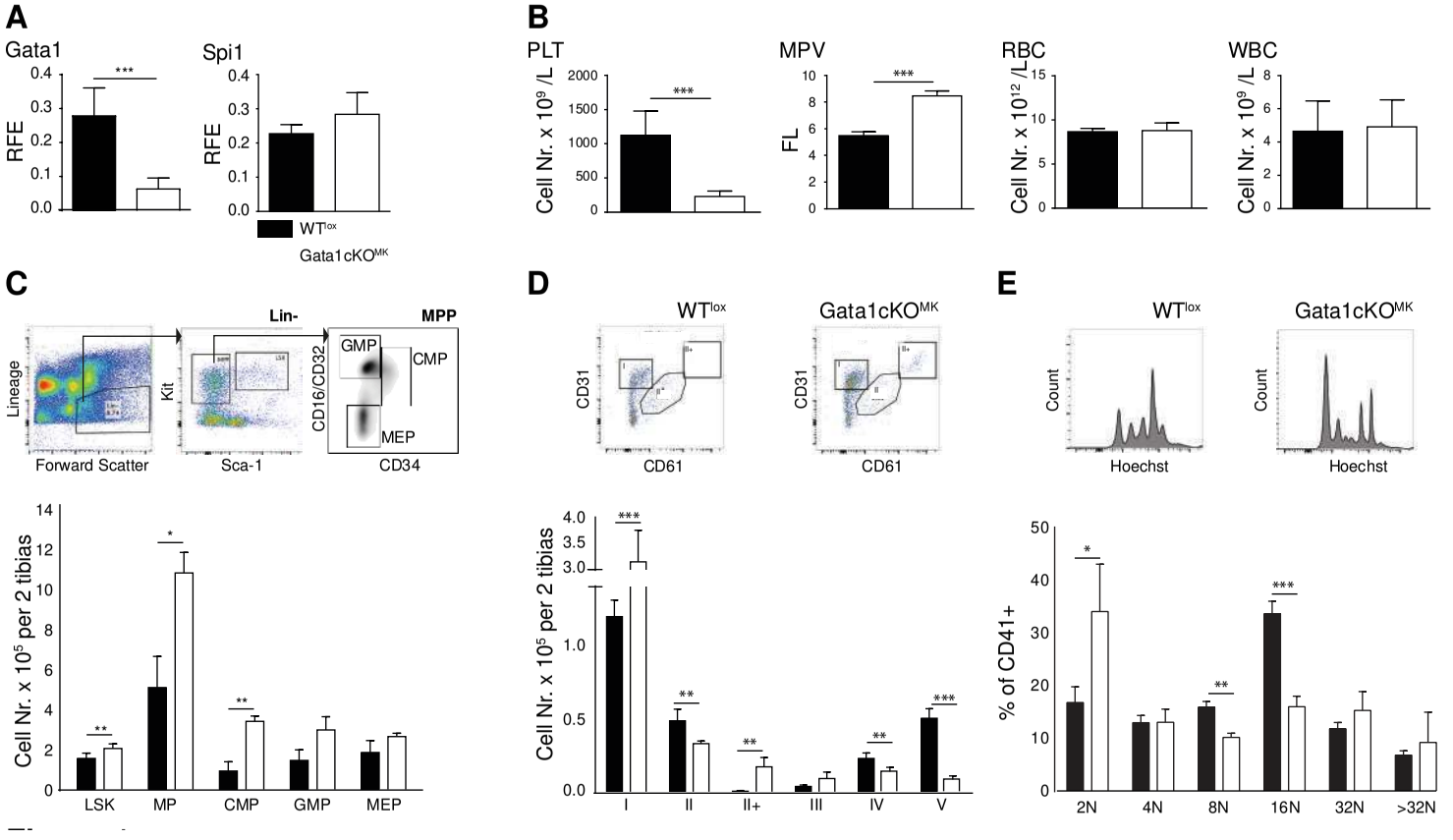
A
Gata1
Spi1
RFE
***
WTlox
Gata1cKOMK
B
PLT
MPV
RBC
WBC
Cell Nr. x 10^9 /L
FL
Cell Nr. x 10^12 /L
C
Lin-
MPP
GMP
CMP
MEP
Lineage
Kit
CD16/CD32
Forward Scatter
Sca-1
CD34
Cell Nr. x 10^5 per 2 tibias
LSK
MP
CMP
GMP
MEP
D
WTlox
Gata1cKOMK
CD31
CD61
I
II
II+
III
IV
V
E
Count
Hoechst
% of CD41+
2N
4N
8N
16N
32N
>32N

Figure 1. Gata1cKOMK mice display severe macrothrombocytopenia with defects in the hematopoietic early precursor compartment and aberrant megakaryopoiesis

A) Gata1 and PU.1 (Spi1) mRNA expression levels in Gata1cKOMK and WT^{lox} cultured megakaryocytes. PU.1 levels are normal in Gata1cKOMK mice.
B) Blood parameters of Gata1cKOMK and WT^{lox} mice at 8 – 12 weeks of age. PLT, platelets; MPV, mean platelet volume; RBC, red blood cells; WBC, white blood cells.
C) Absolute number of the stem cell and committed progenitor compartment, gating strategy is depicted on top. LSK, Lin-|Sca-1+|Kit+ cells; MP (Lin-|Sca-1-|Kit+), multipotent progenitors; CMP (MP gate – CD34+|CD16/CD32mid), common myeloid progenitor; GMP (MP gate – CD34-|CD16/CD32+), granulocyte-monocyte progenitor; MEP (MP gate – CD34-|CD16/CD32-), megakaryocyte-erythroid progenitor.
D) Absolute cell number of bone marrow megakaryocytes at consecutive stages of differentiation.21 The dot plot depicts the extra population, named II+ found exclusively in Gata1cKOMK bone marrow.
E) Ploidy staining of Gata1cKOMK and WT^{lox} bone marrow CD41+ megakaryocytes.

Malfunction of Gata1cKO^{MK} platelets

We next measured platelet aggregation by flow cytometry[19] and observed that upon stimulation with aggretin (Clec2 agonist), collagen (GPVI and α2ß1 agonist), convulxin (GPVI agonist), and botrocetin (GPIb/V/IX agonist) platelet aggregation responses were severely reduced, whereas responses were mildly affected when stimulated with PMA (PKC agonist that triggers αIIbß3 integrin-dependent aggregation; Figure 2A).[5, 9, 16] The reduced aggregation capacity upon stimulation with botrocetin and collagen could be explained by the decreased expression of their receptors as previously reported (CD42b and CD49b; Figure 2B). Interestingly, the expression of Clec2 was normal, and that of GPVI only minimally affected, which could therefore not explain the prominent reduction in aggregation when stimulated with convulxin or aggretin. Since GPVI and Clec2 receptors share Syk-dependent signaling pathways,[25] we next investigated whether Syk expression could be affected in Gata1cKO^{MK} MKs.

Syk transcription is regulated by Gata1

Syk mRNA and protein expression levels were reduced in cultured sorted Gata1cKO^{MK} megakaryocytes (Figure 2C), suggesting that Gata1 could regulate its expression. We identified a WGATAR binding site ≈ 600bp upstream of the *Syk* gene start codon and performed Gata1 ChIP experiments on WT^{lox} and Gata1cKO^{MK} MKs (as background control) to elucidate whether Gata1 interacts directly with the *Syk* promoter. We took as positive control a GATA+ amplicon (≈-300bp) at the *Gp1ba* promoter (known Gata1 target) and as a negative control a GATA– amplicon (≈-600bp) at the *Cd9* promoter. Gata1 ChIP results show enrichment at the GATA site in the *Syk* promoter in WT^{lox} MK, similarly to the positive control, while it does not enrich above background at the GATA- site in the *Cd9* promoter. These data support the notion that Syk is a direct Gata1 target in megakaryocytes and explain the GPVI/Clec2 aggregation defects shown in Gata1 KO mice.

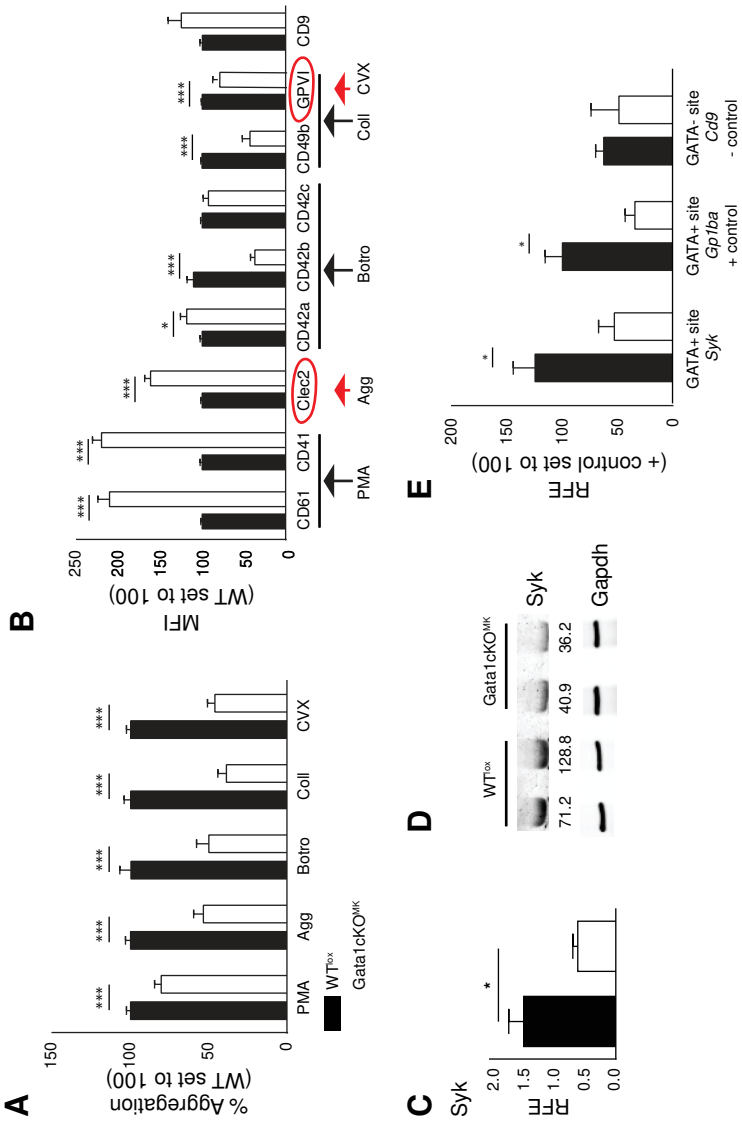

Figure 2. Gata1cKOMK platelets show a Syk-dependent defect upon activation: Gata1 regulates Syk expression

A) Flow cytometry-based platelet aggregation assay (FCA) shows the aggregation capacity of platelets when stimulated with different agonists. Gata1cKOMK and WT^{lox} platelets were studied. PMA, phorbol myristate acid; Agg, aggretin; Botro. Botrocetin; Coll, collagen; CVX, convulxin.

B) MFI of receptors expressed on Gata1cKOMK platelets, relative expression of a given receptor in WT^{lox} platelets was set to 100. For clarification: CD61 (Itgb3), CD41 (Itga2b), CD42a (GPIX), CD42b (Gp1ba), CD42c (Gp1bb), CD49b (Itga2).

C) Syk mRNA expression levels in Gata1cKOMK and WT^{lox} cultured megakaryocytes measured by qRT-PCR.
D) Syk protein levels in Gata1cKOMK and WT^{lox} platelets, analyzed by Western blotting. Syk expression level normalized to loading control Gapdh is indicated, setting the average expression levels of Syk in WT^{lox} platelets to 100.
E) Chromatin immunoprecipitation (ChIP) assay shows Gata1 binding to the Syk promoter in WT^{lox} compared to Gata1cKOMK (background control) cultured megakaryocytes. A GATA+ site on the promoter of the known target Gp1ba (CD42b) was used as positive control and a GATA– site on the promoter of Cd9 was used as negative control.

ACKNOWLEDGEMENTS

This study was funded by the Center for Translational Molecular Medicine (CTMM, www.ctmm.nl), project Innovative Coagulation Diagnostics (INCOAG, grant 01C-201), and the Dutch Heart Foundation. We thank Prof. J. Eble for kindly providing aggretin.

Author contribution
MM designed and performed experiments, analyzed data and wrote the manuscript; MH and MRS performed experiments; TKvdB and TWK participated in discussions and reviewed the manuscript; LG designed and performed experiments, analyzed data and wrote the manuscript.

Conflict-of-interest disclosure
The authors declare no competing financial interests.

REFERENCE LIST

1. Weiss, M.J. & Orkin, S.H. GATA transcription factors: key regulators of hematopoiesis. Experimental hematology 23, 99-107 (1995).
2. Freson, K. et al. Platelet characteristics in patients with X-linked macrothrombocytopenia because of a novel GATA1 mutation. Blood 98, 85-92 (2001).
3. Mehaffey, M.G., Newton, A.L., Gandhi, M.J., Crossley, M. & Drachman, J.G. X-linked thrombocytopenia caused by a novel mutation of GATA-1. Blood 98, 2681-2688 (2001).
4. Nichols, K.E. et al. Familial dyserythropoietic anaemia and thrombocytopenia due to an inherited mutation in GATA1. Nature genetics 24, 266-270 (2000).
5. White, J.G. & Thomas, A. Platelet structural pathology in a patient with the X-linked GATA-1, R216Q mutation. Platelets 20, 41-49 (2009).
6. Wechsler, J. et al. Acquired mutations in GATA1 in the megakaryoblastic leukemia of Down syndrome. Nature genetics 32, 148-152 (2002).
7. Ludlow, L.B. et al. Identification of a mutation in a GATA binding site of the platelet glycoprotein Ibbeta promoter resulting in the Bernard-Soulier syndrome. The Journal of biological chemistry 271, 22076-22080 (1996).
8. Martin, D.I. & Orkin, S.H. Transcriptional activation and DNA binding by the erythroid factor GF-1/NF-E1/Eryf 1. Genes & development 4, 1886-1898 (1990).
9. Vyas, P., Ault, K., Jackson, C.W., Orkin, S.H. & Shivdasani, R.A. Consequences of GATA-1 deficiency in megakaryocytes and platelets. Blood 93, 2867-2875 (1999).
10. Yamaguchi, Y., Zon, L.I., Ackerman, S.J., Yamamoto, M. & Suda, T. Forced GATA-1 expression in the murine myeloid cell line M1: induction of c-Mpl expression and megakaryocytic/erythroid differentiation. Blood 91, 450-457 (1998).
11. Visvader, J.E., Elefanty, A.G., Strasser, A. & Adams, J.M. GATA-1 but not SCL induces megakaryocytic differentiation in an early myeloid line. The EMBO journal 11, 4557-4564 (1992).
12. Fujiwara, Y., Browne, C.P., Cunniff, K., Goff, S.C. & Orkin, S.H. Arrested development of embryonic red cell precursors in mouse embryos lacking transcription factor GATA-1. Proceedings of the National Academy of Sciences of the United States of America 93, 12355-12358 (1996).
13. Gutierrez, L. et al. Ablation of Gata1 in adult mice results in aplastic crisis, revealing its essential role in steady-state and stress erythropoiesis. Blood 111, 4375-4385 (2008).
14. Shivdasani, R.A., Fujiwara, Y., McDevitt, M.A. & Orkin, S.H. A lineage-selective knockout establishes the critical role of transcription factor GATA-1 in megakaryocyte growth and platelet development. The EMBO journal 16, 3965-3973 (1997).
15. Takahashi, S. et al. Arrest in primitive erythroid cell development caused by promoter-specific disruption of the GATA-1 gene. The Journal of biological chemistry 272, 12611-12615 (1997).
16. Hughan, S.C. et al. Selective impairment of platelet activation to collagen in the absence of GATA1. Blood 105, 4369-4376 (2005).
17. Lindeboom, F. et al. A tissue-specific knockout reveals that Gata1 is not essential for Sertoli cell function in the mouse. Nucleic acids research 31, 5405-5412 (2003).

18. Tiedt, R., Schomber, T., Hao-Shen, H. & Skoda, R.C. Pf4-Cre transgenic mice allow the generation of lineage-restricted gene knockouts for studying megakaryocyte and platelet function in vivo. Blood 109, 1503-1506 (2007).

19. De Cuyper, I.M. et al. A novel flow cytometry-based platelet aggregation assay. Blood 121, e70-80 (2013).

20. Drabek, K. et al. The microtubule plus-end tracking protein CLASP2 is required for hematopoiesis and hematopoietic stem cell maintenance. Cell reports 2, 781-788 (2012).

21. Meinders, M. et al. Sp1/Sp3 transcription factors regulate hallmarks of megakaryocyte maturation, and platelet formation and function. Blood (2014).

22. Schmittgen, T.D. & Livak, K.J. Analyzing real-time PCR data by the comparative C(T) method. Nature protocols 3, 1101-1108 (2008).

23. Borg, J. et al. Haploinsufficiency for the erythroid transcription factor KLF1 causes hereditary persistence of fetal hemoglobin. Nature genetics 42, 801-805 (2010).

24. Takahashi, S. et al. Role of GATA-1 in proliferation and differentiation of definitive erythroid and megakaryocytic cells in vivo. Blood 92, 434-442 (1998).

25. Watson, S.P., Herbert, J.M. & Pollitt, A.Y. GPVI and CLEC-2 in hemostasis and vascular integrity. Journal of thrombosis and haemostasis : JTH 8, 1456-1467 (2010).

Chapter 5

PLATELET PRODUCTION AND FUNCTION DURING HEMATOPOIETIC STRESS EPISODES

PLATELET PRODUCTION AND FUNCTION DURING HEMATOPOIETIC STRESS EPISODES

M. Meinders[1], M. Hoogenboezem[2], M.R. Scheenstra[1], I. M. De Cuyper[1], T.K. van de Berg[1], M.A. Nolte[3], T.W. Kuijpers[1,4] and L. Gutiérrez[1]

[1]Dept. Blood Cell Research, Sanquin Research and Landsteiner Laboratory, Academic Medical Centre (AMC), University of Amsterdam (UvA), 1066CX Amsterdam, the Netherlands; [2]Dept. Molecular Cell Biology, Sanquin Research and Landsteiner Laboratory, Academic Medical Centre (AMC), University of Amsterdam (UvA), 1066CX Amsterdam, the Netherlands; [3]Sanquin Research, Department of Hematopoiesis, Amsterdam, The Netherlands; Landsteiner Laboratory, Academic Medical Centre, University of Amsterdam, Amsterdam, The Netherlands; [4]Dept. Pediatric Hematology, Immunology and Infectious Disease, Emma Children's Hospital, AMC, Amsterdam, University of Amsterdam, The Netherlands.

ABSTRACT

Hematopoietic stem cells (HSCs) are unique self-renewing cells generating all hematopoietic cell lineages through commitment to multipotent progenitors (i.e. multipotency). The hematopoietic output varies through ontogeny, as does the site of hematopoietic production in the fetal liver and spleen during gestation and bone marrow after birth. It is known that during hematopoietic stress, extramedullary hematopoiesis occurs at the sites that were active during ontogeny: i.e. spleen and liver. Mouse megakaryocytes, the platelet progenitors which descend from HSCs, reside in both the bone marrow and the spleen during steady state conditions. Their contribution to the total circulating platelet mass by each megakaryocyte pool is, however, different, with the bone marrow megakaryocytes producing the vast majority of platelets.

Here we studied the impact of different types of hematopoietic stress on HSC differentiation, megakaryopoiesis, thrombopoiesis and platelet function in several experimental models. We show that platelets produced under conditions of hematopoietic stress have a distinct aggregation profile compared to steady state platelets. Especially during stress hematopoiesis inducing severe thrombocytopenia, we identified a subpopulation of spleen-derived platelets expressing high levels of CD42b, which were absent in splenectomized mice upon induction of stress hematopoiesis. We also observed a different skewing on the HSC/progenitor populations depending on the primary demand of the stress response. Although the spleen plays an active role during hematopoietic stress responses, we also show that this organ is not vital for platelet count recovery upon induced hematopoietic stress.

INTRODUCTION

Hematopoietic stem cells (HSCs) are quiescent cells with unique features including multipotency and self-renewal capacity. In 1961 Till and McCulloch were the first who showed that a single HSC could yield multilineage descendants while preserving the multipotency of the mother cell.[1] Later on, Dexter *et al* proved that stromal

cells were required for the maintenance of primitive hematopoietic cells *ex vivo*.[2] These were the first clues that hematopoiesis depends on both HSCs and their environment, *i.e.* the niche or stroma.

The first self-sustainable HSCs identified during embryogenesis arise in the Aorta-Gonad-Mesonephros (AGM) during midgestation.[3] Subsequently, these HSCs translocate to the fetal liver and spleen to relocate just before birth to the primary postnatal hematopoietic niche, i.e. the bone marrow.[4] The hematopoietic output differs during development, i.e. in the fetal stages it is mainly erythroid, while in adulthood it is mainly myeloid. This is conditioned by the site of hematopoiesis and the demands during ontogeny/development.

Although HSC development and migration in mouse is in many respects similar to human HSCs, one fundamental difference in the postnatal adult steady state could be observed. While human HSCs and progenitors can only be found in the bone marrow, mouse hematopoietic progenitors reside both in the bone marrow and the spleen.[17;18] However, during hematopoietic stress, extramedullary splenic hematopoiesis can be observed in both human and mice.[19] Hematopoietic stress can be caused by bleeding episodes, infection, inflammation or congenital hematopoietic disorders resulting in thrombocytopenia, anemia or leukopenia. These stress episodes induce the quick release of pooled stored cells into the circulation and progenitors increase their production rate.[20]

Megakaryocytes are large polyploid cells which reside in humans mainly in the bone marrow. They arise from HSCs through consecutive differentiation steps leading to multipotent progenitors (MPP), common myeloid progenitors (CMP), and the megakaryocyte-erythroid progenitor (MEP), which can develop into megakaryocytes to ultimately produce platelets.[23] The vast majority of megakaryocytes reside in the bone marrow, although, in mice, a substantial number of megakaryocytes can also be found in the spleen.

In this article we investigate different types of stress hematopoiesis, i.e. acute and chronic inflammatory response and platelet depletion. We study the impact of such stress types on the HSC/progenitor compartment in the bone marrow, on megakaryopoiesis and on platelet production and function. We show that platelets from stress models display a distinct aggregation profile compared to healthy steady state platelets. We show a subpopulation of platelets with high CD42b expression that derives from the spleen, especially on those models inducing severe thrombocytopenia, as confirmed on splenectomized mice who lack that population upon induced stress hematopoiesis. We also demonstrate that despite the spleen has an active role on the stress hematopoiesis response, it is not a vital organ for platelet count recovery upon induced stress hematopoiesis.

RESULTS

To determine the effect of stress hematopoiesis on the HSCs/multipotent progenitor compartment, megakaryopoiesis, platelet production and function, three different hematopoietic stress models were used.

First, an acute inflammatory response was induced by injecting LPS intravenous-

ly into wild type (WT) mice, i.e. mimicking sepsis, which results in mild thrombocytopenia.[29] Secondly, we used a mouse platelet depletion model by injecting anti-CD42b antibody intravenously in WT mice, which results in severe thrombocytopenia.[30] Thirdly, CD70Tg mice were used as an established model of sterile chronic inflammation. These mice constitutively express CD70 on B cells leading to T cell activation, with subsequent high INF-y production, which results in anemia and severe thrombocytopenia.[31]

All three models displayed a distinct alteration on platelet number. LPS injection induced a mild reduction in platelet numbers after 48hr (45% reduction compared to WT littermates) without altering the mean platelet volume (MPV), and platelet number was normalized at day 4 (Figure 1). CD42b antibody-mediated platelet depletion caused a dramatic decline in platelet number with an increased MPV (97% reduction of platelet number within two days after injection), which normalized at day 4 and MPV was restored by day 7 (Figure 1). CD70Tg mice suffer from severe thrombocytopenia, with platelets counts reduced to 20% compared to WT littermates and an increased MPV (Figure 1).

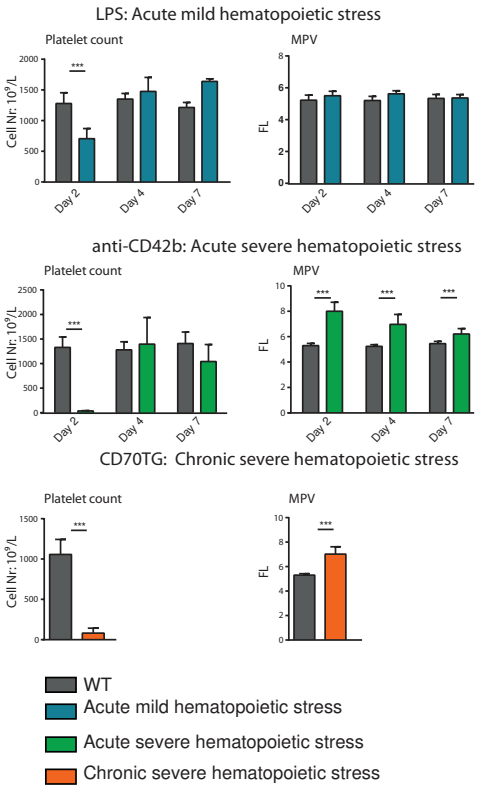

Figure 1. Platelet count and mean platelet volume of the three hematopoietic stress models. Acute severe and mild hematopoietic stress is shown in time.

In addition, we studied megakaryopoiesis and platelet aggregation upon stress hematopoiesis in the three mouse models at the respective time-points of recovery in platelet number and/or volume to assess the function of newly formed platelets in each specific model; *i.e.* under acute inflammation condition (LPS injection) at day 4 after injection, and severe platelet depletion (CD42b antibody injection) at day 7 after injection. CD70Tg mice (chronic inflammation model), which show no recovery of platelet counts, were analyzed between 8-12 weeks of age. In the remainder of this article, the LPS model is referred to as acute mild hematopoietic stress, the platelet depletion model as acute severe hematopoietic stress, and the chronic inflammation model as chronic severe hematopoietic stress (Table 1).

Acute mild hematopoietic stress mouse model

Impact of acute mild hematopoietic stress on the HSCs/multipotent progenitor compartments

We investigated the hematopoietic progenitor compartment in the bone marrow by using phenotyping by flow cytometry (Figure 2A). In this way we can identify Lin-|Sca-1+|Kit+ (LSK) HSCs cells, multipotent myeloid progenitors (MP, Lin-|Kit+|Sca-1-), common myeloid progenitors (CMP, within MP, 2.4G2+|CD34+), granulocyte macrophage progenitors (GMP, within MP, 2.4G2+|CD34-) and megakaryocyte erythroid progenitors (MEP, within MP, 2.4G2-|CD34-) based on surface marker expression (see Figure 2A for gating strategy).

Mice subjected to acute mild hematopoietic stress displayed a slight increase of MPs with no alteration in the LSK compartment. Furthermore, the balance between GMPs and MEPs was shifted towards GMPs, probably due to an increased demand of myeloid cells, required for the inflammatory response induced by the LPS injection (Figure 2A). This shift could explain the thrombocytopenia seen in these mice; however we cannot exclude an increased turnover of platelets during inflammation causing their numbers to drop.

Determination of megakaryocyte maturation status after induction of acute mild hematopoietic stress

Megakaryocyte maturation was determined based on receptor expression profile and ploidy status. Five consecutive stages of megakaryocyte maturation could be identified, as previously described, whereby subtype I contains the most immature and V the most mature megakaryocytes.[32] Although a direct link between ploidy status and maturation has yet to be determined, it is generally accepted that megakaryocytes increase their DNA during maturation.[33] Ploidy status was determined on these megakaryocytes by PI staining. We thus identified a higher proportion of immature megakaryocytes in the bone marrow, shown by both maturation status and reduced polyploidization in mice suffering from acute mild hematopoietic stress (Figure 2B-C). This could be due to hyperproliferation of committed immature megakaryocytes or due to a blockade in terminal differentiation of megakaryocytes. Although we cannot exclude the possibility that HSCs differentiate into megakaryocytes, this scenario is unlikely since the balance seen in MPs is favored towards GMPs vs MEPs. Therefore we think that the accumulation of immature megakaryocytes is probably due to a direct effect of the inflammation response on the committed megakaryocytes.

Functional analysis of platelets produced under acute mild hematopoietic stress conditions

Platelet functionality was tested by a novel platelet aggregation method (FCA) (Chapter 1).[34] This assay allows us to study the contribution of individual receptor pathways to platelet aggregation whereby isolated platelets were stimulated with the agonists PMA (which activates the fibrinogen receptor αIIbβ3 integrin), botrocetin (which activates the vWF receptor), aggretin (which activates the Clec2 receptor and signals via Syk to activate both αIIbβ3 and α2β1), collagen (which activates α2β1 integrin and GPVI) or convulxin (which activates only GPVI).

Only a decrease in aggregation capacity was observed after activation with aggretin (Figure 2D). To determine whether the defect was caused by a decreased receptor expression, the surface expression of Clec2 was measured (Figure 2E). We show that these platelets have an increased expression of this receptor indicating that the defect is not caused by decreased receptor expression, suggesting an alteration in the internal signaling pathway.

Summarizing, mice suffering from acute mild hematopoietic stress, have alteration in their HSC differentiation, megakaryopoiesis and platelet function. To investigate if the severity of hematopoietic stress increased the displayed phenotype, the same assays were performed on the acute severe hematopoietic stress model.

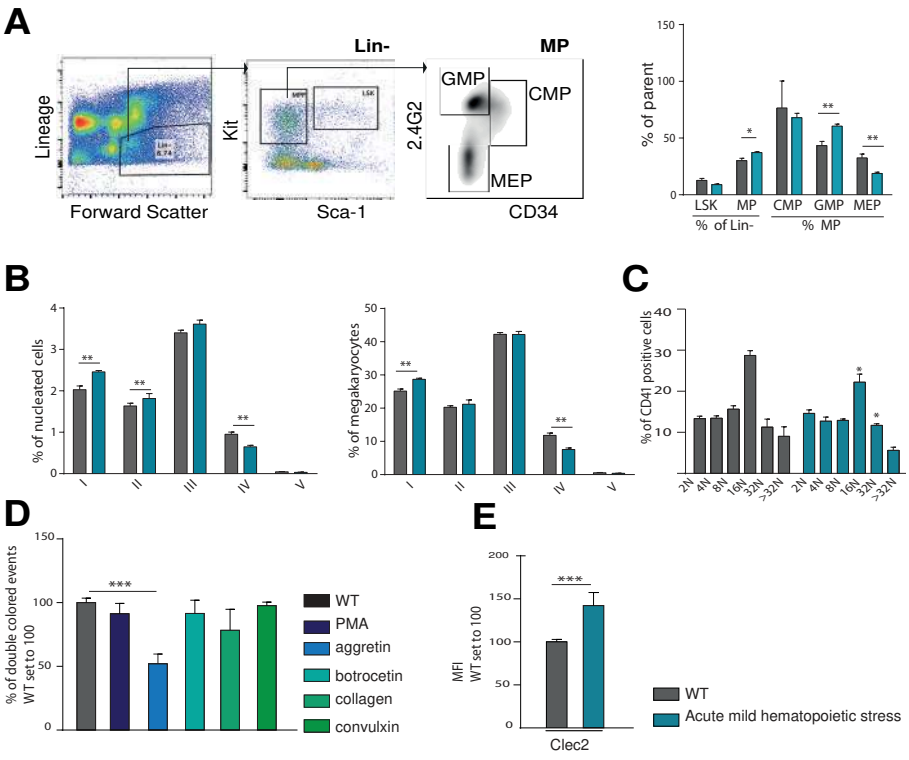

Figure 2. Acute mild hematopoietic stress model shows alteration in their HSC differentiation, megakaryopoiesis and platelet function.

A) Flow cytometry analysis of the stem cell and committed progenitor compartment, gating strategy is depicted on the right. LSK, $Lin^-|Sca\text{-}1^+|Kit^+$ cells; MP ($Lin^-|Sca\text{-}1^-|Kit^+$), multipotent myeloid progenitors; CMP (MP gate – $CD34^+|2.4G2+|^{mid}$), common myeloid progenitor; GMP (MP gate – $CD34^-|2.4G2+|^+$), granulocyte-monocyte progenitor; MEP (MP gate – $CD34^-|2.4G2+|^-$), megakaryocyte-erythroid progenitor.
B) Percentage of megakaryocytes at consecutive stages of differentiation.[32] The left graph shows bone marrow megakaryocyte percentage form nucleated cells. The right graph shows the percentage of megakaryocytes from total megakaryocytes.
C) Ploidy staining of bone marrow and spleen $CD41^+$ megakaryocytes.
D) Flow cytometry-based platelet aggregation assay (FCA) shows the aggregation capacity of platelets when stimulated with different agonists
E) MFI of Clec2 expressed on platelets, setting expression in WT platelets to 100.

Acute severe hematopoietic stress mouse model

Impact of acute severe hematopoietic stress on the HSCs/multipotent progenitor compartments

As previous described, these mice have a dramatic decline in platelet number after CD42b injection, inducing severe macrothrombocytopenia (Figure 1). We investigated the hematopoietic progenitor compartment in the bone marrow by using phenotyping by flow cytometry as described above (Figure 2A). No changes in the LSK or MP compartment were identified in these mice. However, within the MPs, the balance between GMPs and MEPs is shifted towards MEPs, probably due to the primary increased demand for platelets (Figure 3A).

Determination of megakaryocyte maturation status after induction of acute severe hematopoietic stress

Identification of megakaryocyte maturation based on receptor expression profile revealed more immature phenotype, as confirmed by the ploidy, *i.e.* the majority of megakaryocytes had a ploidy of 8N instead of 16N (Figure 3B-C). Interestingly, these mice showed an increase in mature spleen megakaryocytes which suggests that the severe acute thrombocytopenia induced by platelet depletion stimulates the proliferation of spleen megakaryocytes in order to increase platelet output from this pool.

Functional analysis of platelets produced under acute severe hematopoietic stress conditions

Platelet function was determined by FCA, as described above. Platelets produced under severe hematopoietic stress showed a decreased aggregation capacity after stimulation with aggretin when compared to steady state platelets, and in a comparable manner to platelets from the acute mild hematopoietic stress mouse model. Besides, these platelets have a decreased aggregation capacity when stimulated with convulxin, but not to collagen, indicating that GPVI responses are also affected in these platelets (Figure 3D). Flow cytometry analysis of Clec2 (receptor for aggretin) and GPVI (receptor for convulxin) surface expression showed no alteration

compared to steady state platelets (Figure 3E). However, an increase in CD42b (receptor for botrocetin) on a subpopulation of platelets, was observed (Figure 3F). This indicates that during severe hematopoietic stress two distinct populations of platelets are produced which could have a different precursor. We next analysed the expression of CD42b in BM and spleen megakaryocytes in the BM and spleen. We observed that spleen megakaryocytes express higher levels of CD42b upon stress hematopoiesis, suggesting that the population of CD42b^{high} platelets might derive from splenic megakaryocytes (Figure 3F).

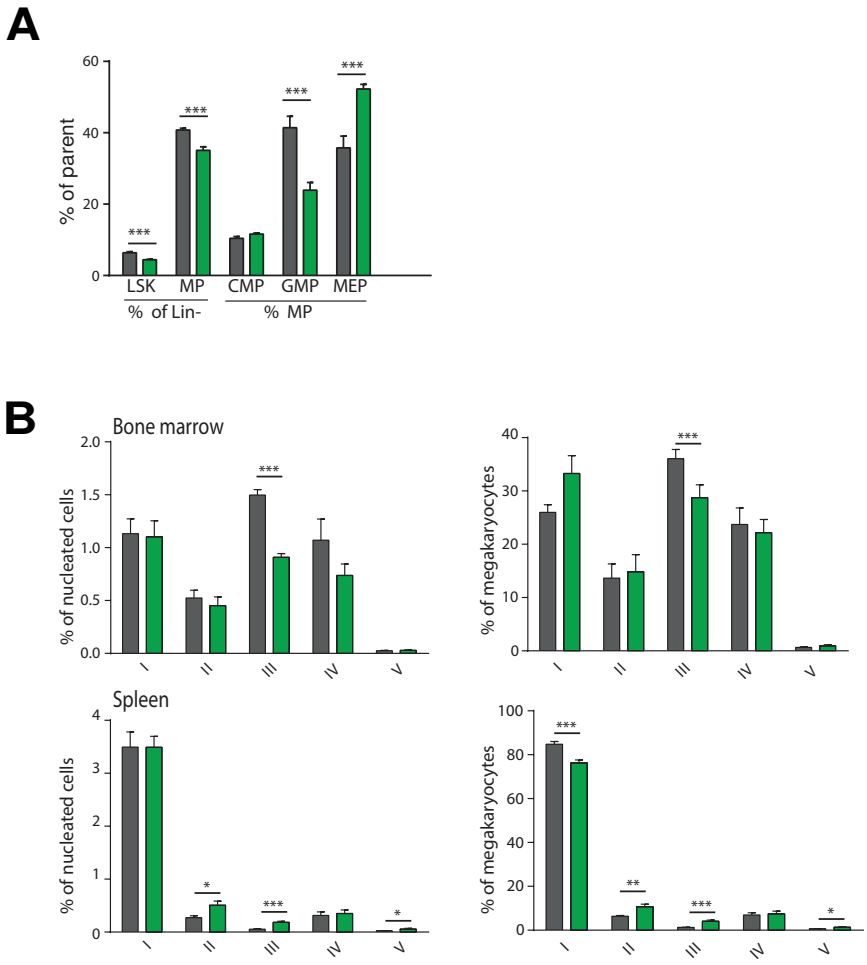

Figure 3. Acute severe hematopoietic stress model shows alteration in their HSC differentiation, megakaryopoiesis and platelet function.

A) Flow cytometry analysis of the stem cell and committed progenitor compartment.

B) Percentage of megakaryocytes at consecutive stages of differentiation. The top left graph shows bone marrow megakaryocyte percentage form

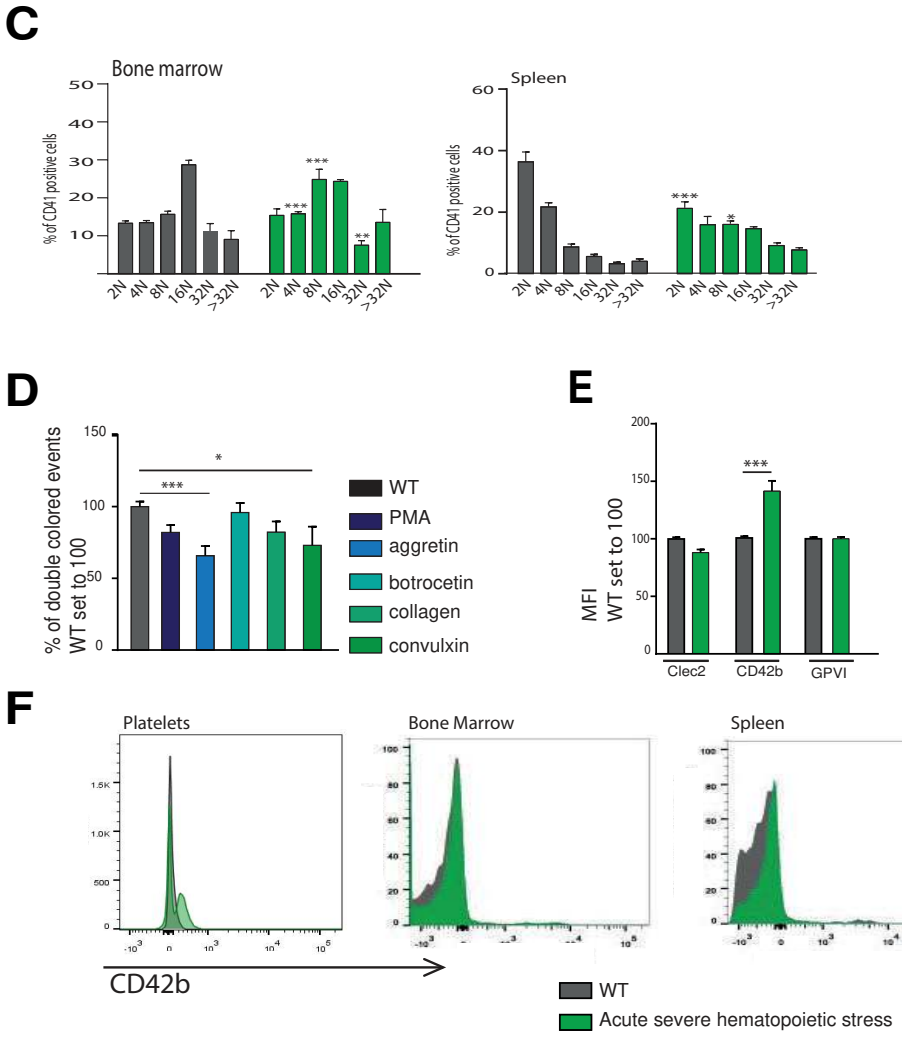

nucleated cells. The top right graph shows the percentage of bone marrow megakaryocytes from total megakaryocytes. The bottom left graph shows shows splenic megakaryocyte percentage form nucleated cells. The bottom right graph shows the percentage of splenic megakaryocytes from total megakaryocytes.[32]

C) Ploidy staining of bone marrow and spleen CD41+ megakaryocytes.

D) Flow cytometry-based platelet aggregation assay (FCA) shows the aggregation capacity of platelets when stimulated with different agonists

E) MFI of Clec2, CD24b and GPVI expressed on platelets, expression on WT platelets was set to 100.

F) Flow cytometry analysis of CD42b expression on platelets, and in bone marrow and spleen megakaryocytes.

The functional differences in platelet aggregation under severe and mild hematopoietic stress conditions indicates that the severity and type of the hematopoietic stress influences the platelet phenotype, *i.e.* platelet depletion or acute inflammation. We therefore set out to investigate the impact of chronic inflammation on HSC differentiation, megakaryopoiesis and platelet function.

Chronic severe stress hematopoietic mouse model

Impact of chronic hematopoietic stress on the HSCs/multipotent progenitor compartments

To investigate HSC differentiation in our chronic severe hematopoietic model, a different gating strategy was used since the long term severe hematopoietic stress dramatically altered the expression of Sca1, making it impossible to use the staining strategy mentioned above. To define HSCs and multipotent progenitor (MPP) cells were first gated as Lin-|Kit+. Next, a subdivision was made based on CD150 and CD48 whereby CD48-|CD150- are defined as MPPs and CD48-|CD150+ as HSC (see Figure 4A for gating strategy). These mice display a dramatic reduction in MPPs, created by severe long term hematopoietic stress causing exhaustion of the multipotent progenitors (Figure 4A).[35] Taken together, we conclude that the character of the stress, and the primary demand of platelets influences the multipotent progenitor compartment and its output, and that chronic hematopoietic stress situations can lead to exhaustion of the bone marrow progenitor pool.

Determination of megakaryocyte maturation status under chronic severe hematopoietic stress

We observed that the megakaryocyte differentiation profile was altered in the bone marrow of CD70Tg mice, with a significant increase at stage III of total nucleated cells. When calculating the megakaryocyte differentiation stages of total megakaryocytes, there was a clear differentiation defect in stage V in CD70Tg mice, indicating that although more megakaryocytes are found in the bone marrow of CD70TG mice, a bigger percentage of megakaryocytes in these mice are immature (Figure 4B).
The spleen showed an increase in megakaryocyte population III as seen in the bone marrow megakaryocytes of these mice. Interestingly an increase in population V was noted, which could indicate that these megakaryocytes are more mature. Accordingly, an increase in megakaryocytes with a lower ploidy status was measured in the bone marrow, i.e. an increase in 2N and 4N and reduction in 16N. In the spleen, the 2N ploidy status was slightly reduced, and the 8N slightly increased (Figure 4C). The decrease in ploidy status was noted in all three hematopoietic stress models, which could indicate that these megakaryocytes are less mature, or that in proportion, those megakaryocytes with lower ploidy are driven to divide instead of undergoing endomitosis.

Functional analysis of platelets produced under chronic severe hematopoietic stress conditions

Platelets produces under chronic severe hematopoietic stress conditions also have a severe aggregation defect, which is independent of the agonist used (Figure 4D). Since these platelets have an increased size, it could be argued that these platelets

are younger and the defect is due to increased turn-over and younger age of the platelets.
This could mean that when platelets are subject to long periods of stress severely alter their aggregation capacity (or are produced altered). Platelets produced under acute stress conditions only change specific responses, whereby a difference is noted between severe and moderate thrombocytopenia.
Comparable to platelet produced under acute severe hematopoietic stress, an increase in CD42b (subunit of the vWF receptor, activated by botrocetin) on a subpopulation of platelets, was observed (Figure 4F), similarly to what occurred in the acute severe stress hematopoiesis model (Figure 3F). This indicates that during severe hematopoietic stress two distinct populations of platelets are produced which could have a different precursor. Bone marrow and splenic megakaryocytes were tested for their receptor profile while no subdivision was made between the differentiation stadia of these megakaryocytes. Bone marrow megakaryocytes had a similar receptor expression profile during hematopoietic stress compared to steady state condition. In contrast, splenic megakaryocytes displayed an increased expression of CD42b on their surface after hematopoietic stress episodes (Figure 4F). This suggests that the pool of platelets expressing high levels of CD42b derives from the spleen.
Previous reports show that during hematopoietic stress, platelet production relocates from the bone marrow to the splenic niche. The increased expression of CD42b on splenic megakaryocytes and the identified CD42b^{high} subpopulation of platelets present under hematopoietic stress suggest that the location of hematopoiesis (partly) shifts during severe hematopoietic stress to the spleen, thereby confirming this hypothesis.
Taken together, this indicates that platelets can alter their responsiveness depending on the severity of thrombocytopenia and the duration of the hematopoietic stress. Alterations induced by the different hematopoietic stress models are summarized in Table 1.

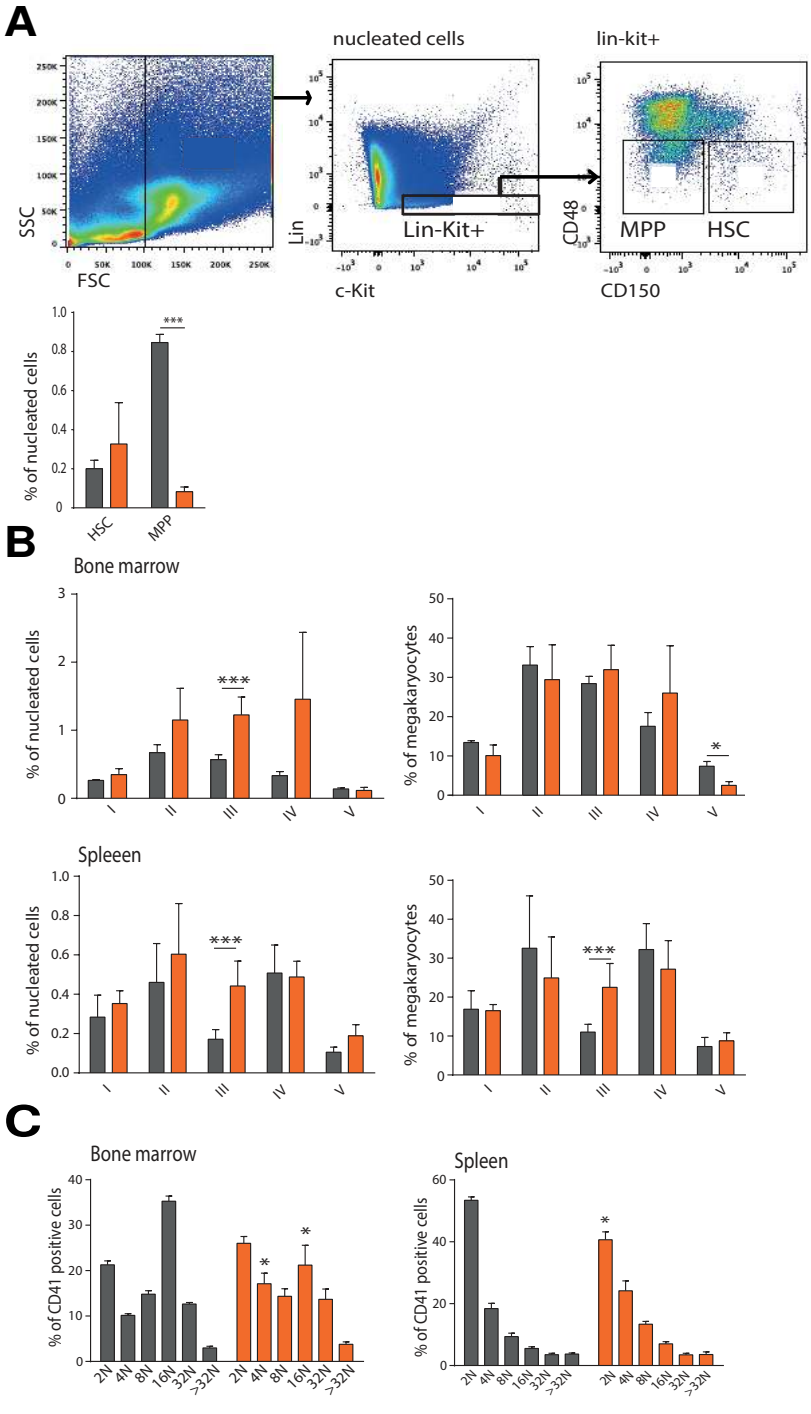
A
nucleated cells
lin-kit+
SSC
FSC
Lin
Lin-Kit+
c-Kit
CD48
MPP
HSC
CD150
% of nucleated cells
HSC
MPP
B
Bone marrow
% of nucleated cells
% of megakaryocytes
Spleeen
C
Bone marrow
Spleen
% of CD41 positive cells
2N
4N
8N
16N
32N
>32N

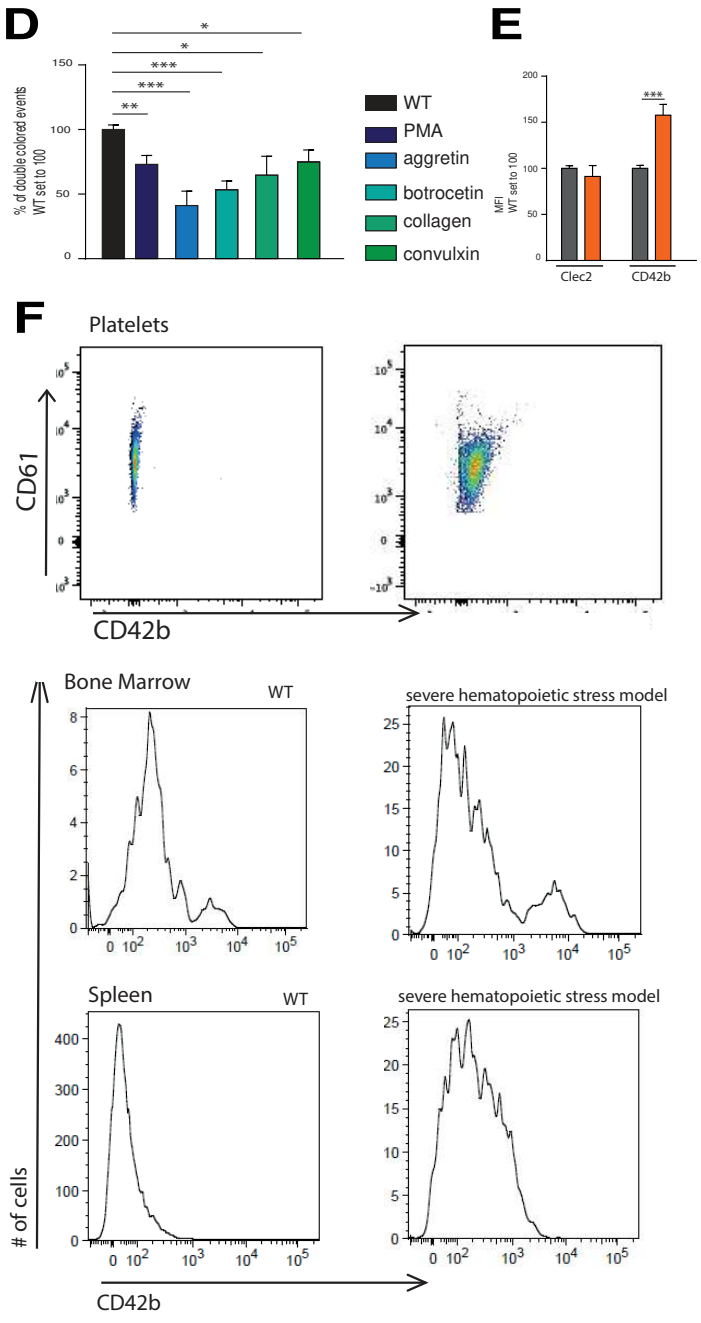

Figure 4. Chronic severe hematopoietic stress model shows alteration in their HSC differentiation, megakaryopoiesis and platelet function.

A) Flow cytometry analysis of the stem cell and committed progenitor compartment, gating strategy is depicted on top. Flow cytometry analysis

of the stem cell and committed progenitor compartment depicted below.

B) Percentage of megakaryocytes at consecutive stages of differentiation. The top left graph shows bone marrow megakaryocyte percentage form nucleated cells. The top right graph shows the percentage of bone marrow megakaryocytes from total megakaryocytes. The bottom left graph shows shows splenic megakaryocyte percentage form nucleated cells. The bottom right graph shows the percentage of splenic megakaryocytes from total megakaryocytes..[32]
C) Ploidy staining of bone marrow and spleen $CD41^{+}$ megakaryocytes.
D) Flow cytometry-based platelet aggregation assay (FCA) shows the aggregation capacity of platelets when stimulated with different agonists
E) MFI of Clec2 and CD24b expressed on platelets, expression on WT platelets was set to 100.
F) Flow cytometry analysis of CD42b expression on platelets, and in bone marrow and spleen megakaryocytes.

The role of the spleen in stress hematopoiesis: acute hematopoietic stress in splenectomized mice

During severe hematopoietic stress, a subpopulation of platelets expressing CD-$42b^{high}$ was observed. We performed the same analysis in splenectomized mice upon the induction of acute severe stress hematopoiesis, in our platelet depletion mouse model.

Blood parameters were determined 2, 4 and 7 days after induction of stress (Figure 5A). Although recovery is similar between splenectomized mice and non-operated littermates, an increase in platelet number is noted at day 5 after injection. The increase is most likely due to splenectomy and lacking thereof of the normal platelet clearance performed by the spleen. The MPV was similar between WT and splenectomized mice (Figure 5A).

Impact of splenectomy and acute hematopoietic stress on the HSCs/multipotent progenitor compartments

The distribution of hematopoietic progenitors was determined in the bone marrow after splenectomy with or without the induction of hematopoietic stress (Figure 5B). When WT mice were splenectomized, a decreased percentage of MPs was observed, although the changes seen in WT versus severe hematopoietic stress conditions were similar. This indicates that during stress episodes, the bone marrow has enough capacity to compensate for acute changes in hematopoietic output or an alternative extramedullary occupied.

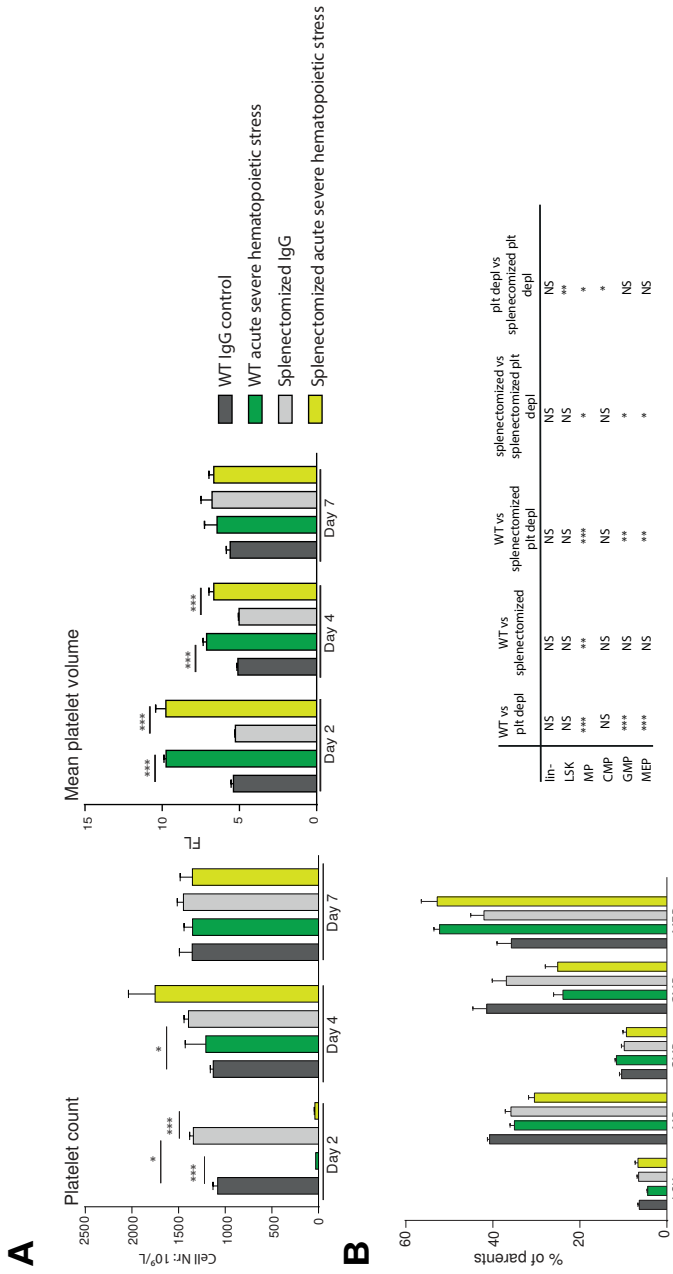

Figure 5. Effect of severe hematopoietic stress on megakaryopoiesis in splenectomized mice

A) Platelet count and mean platelet volume of splenectomized mice and with or without the induction of acute severe hematopoietic stress.

B) Flow cytometry analysis of the stem cell and committed progenitor compartment.

Determination of megakaryocyte maturation status in splenectomized mice under acute severe hematopoietic stress

When comparing the differentiation status of megakaryocytes, a similar trend was observed between acute severe hematopoietic stress conditions and splenectomized mice suffering from severe hematopoietic stress conditions, i.e. a decrease in differentiation status of subtype III and IV (Figure 6A). This trend could be explained by the sudden demand of platelets, reducing the amount of more mature megakaryocytes. Besides a similar pattern in differentiation, the ploidy status of megakaryocytes form severe hematopoietic stressed mice with or without splenectomy, was also comparable (Figure 6B). These data indicate that under acute hematopoietic stress conditions, bone marrow megakaryopoiesis does not seem to be affected by the removal of the spleen.

Functional analysis of platelets in splenectomized mice under acute hematopoietic stress conditions

While platelets produced under severe hematopoietic stress have an increased expression of CD42b, splenectomized mice experiencing severe hematopoietic stress expressed a reduced amount of CD42b on their platelets, which would support the notion that it is mainly those platelets produced in the spleen that have an overall increased expression of CD42b (Figure 6C).

The ability to form aggregates was measured by FCA, showing that platelets formed under hematopoietic stress (WT or splenectomized mice) had a decreased capacity to form aggregates when stimulated with aggretin and convulxin. Additionally, splenectomized mice suffering from severe hematopoietic stress also showed a defect in aggregation when stimulated with PMA or botrocetin. This indicates that both the location of platelet production and the induction of hematopoietic stress alter the platelet capacity to respond to different agonists (Figure 6D).

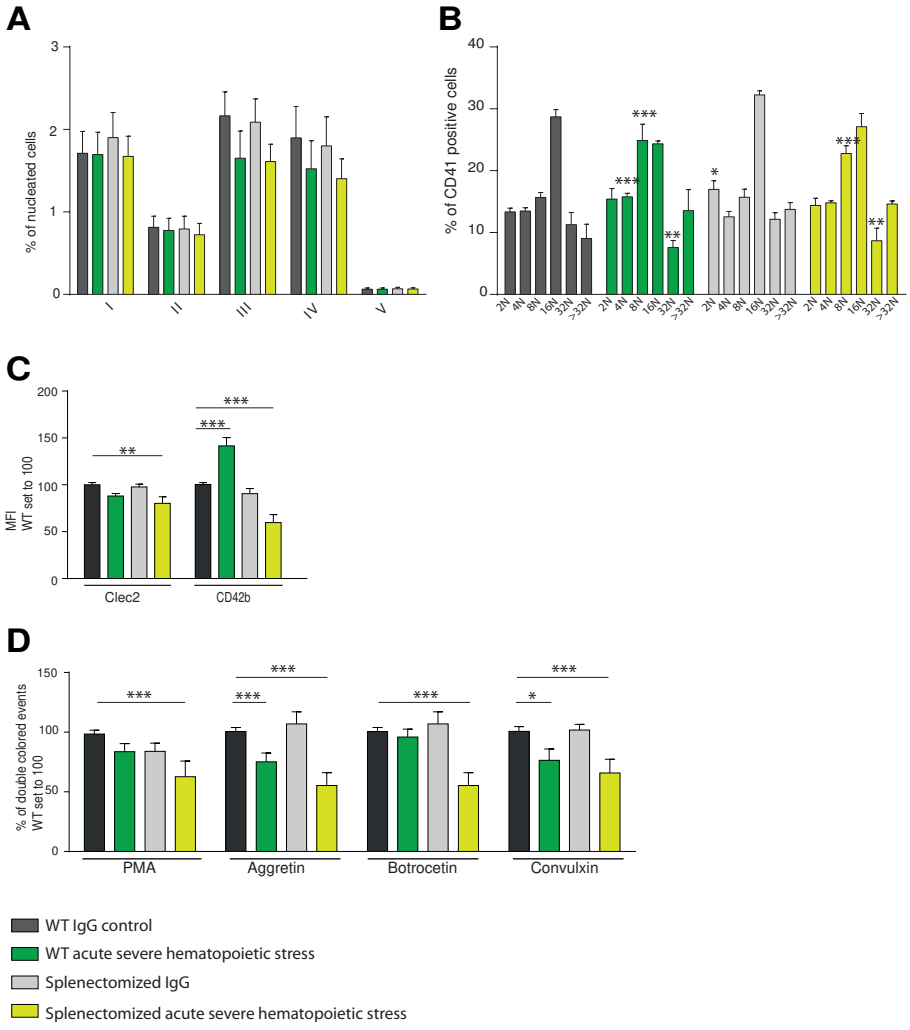

Figure 6. Effect of severe hematopoietic stress on megakaryopoiesis and platelet function in splenectomized mice

A) Percentage of megakaryocytes at consecutive stages of differentiation.[32]

B) Ploidy staining of bone marrow CD41⁺ megakaryocytes.

C) MFI of Clec2 and CD42b expressed on platelets produced under acute sever hematopoietic stress, relative expression of a given receptor in WT IgG control platelets was set to 100.

D) Flow cytometry-based platelet aggregation assay (FCA) shows the aggregation capacity of platelets when stimulated with different agonists.

	Acute mild hematopoietic stress	Acute severe hematopoietic stress	Chronic servere hematopoietic stress
Platelet count	Mild thrombocytopenia	Severe macrothom-bocytopenia	Severe macrothom-bocytopenia
	Slight increase in MPPs Shift towards GMPs	Shift towards MEPs	Reduction of MPPs
HSC / progenitor differentiation **Megakaryopoiesis**	Increased proportion of immature megakaryocytes	Increased proportion of immature megakaryocytes	Increase in total megakaryocyte number decrease in maturation
Ploidy status **Aggregation capacity**	Decrease in ploidy status	Decrease in ploidy status	Decrease in ploidy status
Receptor expression	Decrease aggregation capacity when stimulated with: - aggretin	Decrease aggregation capacity when stimulated with: - aggretin - convulxin	Decrease aggregation capacity when stimulated with: - aggretin - convulxin - PMA - botrocetin

	Splenectomized	Splenectomized with acute stress hematopoietic stress
Platelet count	Slight increased platelet count	Severe macrothombocytopenia
HSC / progenitor differentiation **Megakaryopoiesis**	No changes	Shift towards MEPs
	No changes	Increased proportion of immature megakaryocytes
Ploidy status	No changes	Decrease in ploidy status
Aggregation capacity	No changes	Decrease aggregation capacity when stimulated with: - aggretin - convulxin - PMA - botrocetin
Receptor expression	No changes	Decrease expression of CD42b and Clec2

Table 1 phenotypical changes induced by different stress episodes.

A summary of the phenotypical changes in the HSC compartment, megakaryopoiesis and platelet function induced by different hematopoietic stress models.

DISCUSSION

This study shows that different types of hematopoietic stress, either chronic or acute, severe or mild, which in all cases results in thrombocytopenia increases splenic platelet production and the platelets produced under these circumstances have a distinct functional phenotype. We were interested if platelet production and function was altered due to different types of hematopoietic stress episodes, and if production location alters platelet function.

HSCs are first responders to infection and inflammation since direct stimulation of HSCs with LPS induces a skewing of MPs towards GMP commitment.[38] The data from our acute inflammation model, confirms this conclusion. The platelet depletion model induces severe thrombopoietic stress, skewing MPs to MEPs indicating that investigation of the bone marrow department could give important clues of the origin of stress. The chronic inflammation model studied here displayed severe exhaustion of MPPs, in concordance with what previously described by de Bruin *et al*,[35;39] Concluding, depending on the primary demand upon each sort of hematopoietic stress, *i.e.* chronic or acute, the impact on the HSCs/multipotent myeloid progenitor compartment is manifested in a different way, i.e. there is an increase in GMP in the chronic stress model (i.e. inflammation primary cause of the stress) and an increase in MEP in the acute severe hematopoietic stress model (platelet depletion as a primary cause of stress).

Our method of determining the maturity status of megakaryocytes creates new insight in the distribution and maturation of megakaryocytes upon acute, or chonic thrombopoietic stress cues. Where acute thrombocytopenia causes a trend towards more immature megakaryocytes with a decreased ploidy status, chronic severe thrombocytopenia results in a differentiation arrest and the accumulation of megakaryocytes at mid-differentiation. This indicates that during acute hematopoietic stress, immature megakaryocytes are more prone to divide and mature to increase their platelet output, creating a relative increase in the immature megakaryocyte pool. During chronic thrombocytopenic conditions, on the other hand, it seems that megakaryopoietic differentiation is arrested and can no longer cope with the platelet production demands.

The increased contribution of splenic megakaryocytes in total platelet production was confirmed by receptor expression. We observed upregulation of CD42b on a subpopulation of platelets produced under hematopoietic stress and on splenic megakaryocytes but not on BM megakaryocytes. This subpopulation of CD42b^{high} platelets was only identified in mouse models which were subjected to severe hematopoietic stress. Furthermore, we observed that splenectomized mice suffering from severe hematopoietic stress did not have the CD42b^{high} platelet subpopulation, indicating that the contribution of splenic megakaryocytes to platelet pro-

duction is increased during hematopoietic stress, depends on the severity of the thrombocytopenia and that the spleen megakaryocytes produce platelets with a higher expression of CD42b. A question that remains unanswered is whether the increased platelet production in the spleen is due to increased megakaryocyte proliferation or an increased migration of megakaryocyte progenitors from the bone marrow to the spleen.

During embryogenesis, the fetal liver is the primary site for hemato/megakaryopoiesis, and it seems likely that under severe stress conditions, the liver could supplement as a secondary site for platelet production. Although data suggests this could be a plausible explanation, more research is necessary to confirm this hypothesis. In any case, CD42b^{high} platelets do not appear in splenectomized mice (acute response) and it would only apply to chronic stress whether they do appear from additional extramedullary sites like the liver.

Besides their function in hemostasis, platelets are known to be involved in the immune continuum.[40] We hypothesize that hematopoietic stress conditions induces the production of platelet with an altered phenotype to increase their immunological function. CD42b is part of the GPI/V/IX complex whose main function is binding to vWF,[41] and recently it has been described that CD42b is critical for leukocyte invasion at atheromatous lesions.[42] Increased expression of CD42b on platelets could thus increase the migratory capacity of leukocytes during inflammation. Splenectomy mice suffering from severe hematopoietic stress showed a decreased CD42b expression on their platelet surface which indicates that these platelets are less capable to induce leukocyte invasion and thereby are more susceptible to infections. In humans, splenectomized patients have an increased risk of infections, but to which extent such mechanism may play a role in neutrophil extravasation is necessary to corroborate this conclusion.[37]

Besides the alteration of CD42b expression on the surface of platelets, we noted that platelets produced under severe hematopoietic stress conditions have a decreased aggregation capacity when stimulated with either aggretin or convulxin. Platelets formed under hematopoietic stress respond less to these agonists, which may also decrease the vascular integrity at sites of inflammation hence contributing to neutrophil extravasation.[43 44] Whether platelets are produced differently, or become differently 'primed' in the circulation upon hematopoietic stress responses needs to be further elucidated.

Splenectomized patients are known to have increased platelet activity, resulting in an increased risk of thrombosis whereas our mice did not show any sign of platelet hyperactivation.[37] On the contrary, we observed that in splenectomized mice undergoing hematopoietic stress, platelets have a lower response upon botrocetin stimulation. The higher expression of CD42b in the platelets produced by the spleen as evidenced here, might be responsible for maintaining proper platelet hemostatic function when thrombocytopenia is sensed (to balance platelet counts with responsiveness at first). While we did not observe hyperactivation, we could speculate that this mechanism and stress-platelet production in the absence of the spleen might lead to unwanted platelet hyperactivity and subsequent thrombotic events. Of note, our mice were examined 4 weeks after surgery, whereas patients can develop thrombosis years after surgery.

In conclusion, we confirm that the spleen is not an essential hematopoietic organ. Although in WT mice the spleen participates in stress megakaryopoiesis, following acute stress episodes in splenectomized mice platelet output did not alter, indicating that, the spleen is not essential to sustain platelet production. The platelets produced by the spleen are different and express high levels of CD42b, which may exert an as yet unidentified function under certain stress responses.

EXPERIMENTAL PROCEDURES

Mice

Mice were generated and maintained in the Netherlands Cancer Institute (NKI) or AMC animal care facility under specific pathogen-free conditions. Animal experiments were approved by the NKI Animal Ethics Committee. Acute infection was induced by injecting LPS 5 μg/g body weight (sigma).
For platelet depletion 2μg/g body weight CD42b antibody was intravenously injected (Emfret analytics), as a control C301 antibody was injected (Emfret analytics).

Splenectomy

Mice were anesthetized with isofluorane via a face mask and placed on a 37°C mat to maintain core temperature. Hair was removed from the left flank and a longitudinal incision (10–15 mm) was made through the skin and a 10 mm incision in the peritoneal wall was made. The splenic arteries and efferent veins were ligated with sterilized 6-0 silk sutures separately by looping the sutures through the mesentery. The mesentery and connective tissue were cut and the spleen removed. Abdominal muscle incisions and skin were closed using sterilized 6-0 absorbable sutures separately.

Blood analysis

Blood was drawn by heart puncture, and collected in heparin-coated vials. Blood parameters were determined on a scil Vet abc Plus+ instrument. Platelet rich plasma was separated by centrifuging the blood 15 min at 50g.

Platelet function assays

Flow cytometry based platelet aggregation assay (FCA)

FCA was performed as described.[34] In short, CD9-APC (Abcam) and CD9-PE (Abcam) labeled platelets were mixed 1:1 and preincubated 10 minutes at 37°C 700 RPM in the presence of 2% mouse plasma. As agonists, we used 100 ng/mL phorbol myristate acetate (PMA; Sigma-Aldrich), Botrocetin 10mg/mL (Sigma-Aldrich), convulxin 0.5mg/ml (Santa Cruz) or 30 nM aggretin (a kind gift of Prof. Dr. Johannes A. Eble). Timed samples fixed in 0.5% formaldehyde/PBS were measured on an LSRII + HTS flow cytometer and analyzed for double-colored events by FACSDiva Version 6.1 software (BD Biosciences).

Flow cytometry

HSC multipotent progenitor compartment, megakaryocyte and platelet phenotyping

Platelets or bone marrow single cell suspensions were stained for flow cytometry

analysis. Antibodies used were: CD61-FITC, CD41-PE, Sca1-PECy7, CD34-FITC, Lin-cocktail-APC, CD16/CD32-PE, cKit-PerCP, CD150-PE CD48-APC-Cy7 (BD Pharmingen, Oxford, United Kingdom), Clec2–FITC (AbD Serotec, Kidlington, United Kingdom), CD42a-FITC, CD42b-DL649, CD42c-FITC (Emfret, Wurzburg, Germany), GPVI-PE (R&D, Abingdon, United Kingdom), CD9-PE, CD31-PECy7 (Abcam, Cambridge United Kingdom), CD49b-PB (BioLegend, San Diego, CA).
Platelets were incubated with antibodies at room temperature for 10 minutes and diluted 10-fold with PBS/1%BSA before measuring; bone marrow cells were incubated with antibodies on ice, after which cells were washed and resuspended in PBS/1%BSA before measuring.

Megakaryocyte ploidy measurements
Mouse bone marrow single cell suspensions were incubated with CD41-PE for 20min on ice in PBS/1%BSA. Cells were then washed with PBS/1%BSA and spun at 1000 rpm for 5 min. Cells were resuspended in Cytofix/Cytoperm solution (Cytofix/Cytoperm, BD Biosciences) and incubated 10 min at room temperature. Cells were spun at 1000 rpm for 5 min, resuspended 1X PermWash solution containing 50 mg/mL Hoechst 33342, 0.1% Triton X-100 and 50 mg/mL RNaseA and incubated for 30 min at 37°C. Megakaryocytes were identified as CD41-positive staining intensity was used as a measure of DNA ploidy. Samples were measured on a flow cytometer (LSR-II, BD Biosciences) and analyzed with FlowJo software.

Statistical Analysis
We represent average and standard error of the mean (SEM) of at least 3 mice per genotype unless otherwise indicated. We applied 2-tailed student's T-tests to calculate statistical significance. * $p < 0.05$; ** $p < 0.005$; *** $p < 0.001$.

ACKNOWLEDGEMENTS

This study was funded by the Center for Translational Molecular Medicine (CTMM, www.ctmm.nl), project Innovative Coagulation Diagnostics (INCOAG, grant 01C-201), and the Dutch Heart Foundation. We thank Prof. J. Eble for kindly providing aggretin and Sulima Geerman for assistance with the CD70Tg mice.

Author contribution:
MM designed and performed experiments, analyzed data and wrote the manuscript; MH, MS and IdC performed experiments; TKvdB and TWK participated in discussions and reviewed the manuscript; LG designed and performed experiments, analyzed data and wrote the manuscript.

REFERENCE LIST

1. Till JE, McCulloch EA. A direct measurement of the radiation sensitivity of normal mouse bone marrow cells. 1961. Radiat.Res. 2012;178:AV3-AV7.
2. Morrison SJ, Scadden DT. The bone marrow niche for haematopoietic stem cells. Nature 2014;505:327-334.
3. Dzierzak E, Speck NA. Of lineage and legacy: the development of mammalian hematopoietic stem cells. Nat.Immunol. 2008;9:129-136.
4. Morrison SJ, Scadden DT. The bone marrow niche for haematopoietic stem cells. Nature 2014;505:327-334.
5. Mikkola HK, Orkin SH. The journey of developing hematopoietic stem cells. Development 2006;133:3733-3744.
6. Anthony BA, Link DC. Regulation of hematopoietic stem cells by bone marrow stromal cells. Trends Immunol. 2014;35:32-37.
7. Kiel MJ, Morrison SJ. Uncertainty in the niches that maintain haematopoietic stem cells. Nat.Rev.Immunol. 2008;8:290-301.
8. Kopp HG, Avecilla ST, Hooper AT, Rafii S. The bone marrow vascular niche: home of HSC differentiation and mobilization. Physiology.(Bethesda.) 2005;20:349-356.
9. He N, Zhang L, Cui J, Li Z. Bone marrow vascular niche: home for hematopoietic stem cells. Bone Marrow Res. 2014;2014:128436.
10. Mackie EJ. Osteoblasts: novel roles in orchestration of skeletal architecture. Int.J.Biochem.Cell Biol. 2003;35:1301-1305.
11. Sacchetti B, Funari A, Michienzi S et al. Self-renewing osteoprogenitors in bone marrow sinusoids can organize a hematopoietic microenvironment. Cell 2007;131:324-336.
12. Arai F, Hirao A, Ohmura M et al. Tie2/angiopoietin-1 signaling regulates hematopoietic stem cell quiescence in the bone marrow niche. Cell 2004;118:149-161.
13. Yoshihara H, Arai F, Hosokawa K et al. Thrombopoietin/MPL signaling regulates hematopoietic stem cell quiescence and interaction with the osteoblastic niche. Cell Stem Cell 2007;1:685-697.
14. Purton LE, Scadden DT. The hematopoietic stem cell niche. 2008
15. He N, Zhang L, Cui J, Li Z. Bone marrow vascular niche: home for hematopoietic stem cells. Bone Marrow Res. 2014;2014:128436.
16. Butler JM, Nolan DJ, Vertes EL et al. Endothelial cells are essential for the self-renewal and repopulation of Notch-dependent hematopoietic stem cells. Cell Stem Cell 2010;6:251-264.
17. Weiss L. A scanning electron microscopic study of the spleen. Blood 1974;43:665-691.
18. Morita Y, Iseki A, Okamura S et al. Functional characterization of hematopoietic stem cells in the spleen. Exp.Hematol. 2011;39:351-359.
19. O'Malley DP, Kim YS, Perkins SL et al. Morphologic and immunohistochemical evaluation of splenic hematopoietic proliferations in neoplastic and benign disorders. Mod.Pathol. 2005;18:1550-1561.

20. Smith C. Hematopoietic stem cells and hematopoiesis. Cancer Control 2003;10:9-16.

21. O'Neill HC, Griffiths KL, Periasamy P et al. Spleen as a site for hematopoiesis of a distinct antigen presenting cell type. Stem Cells Int. 2011;2011:954275.

22. Tan JK, O'Neill HC. Investigation of murine spleen as a niche for hematopoiesis. Transplantation 2010;89:140-145.

23. Tenen DG. Disruption of differentiation in human cancer: AML shows the way. Nat.Rev. Cancer 2003;3:89-101.

24. Psaila B, Lyden D, Roberts I. Megakaryocytes, malignancy and bone marrow vascular niches. J.Thromb.Haemost. 2012;10:177-188.

25. Pallotta I, Lovett M, Rice W, Kaplan DL, Balduini A. Bone marrow osteoblastic niche: a new model to study physiological regulation of megakaryopoiesis. PLoS.One. 2009;4:e8359.

26. Bunting S, Widmer R, Lipari T et al. Normal platelets and megakaryocytes are produced in vivo in the absence of thrombopoietin. Blood 1997;90:3423-3429.

27. Avecilla ST, Hattori K, Heissig B et al. Chemokine-mediated interaction of hematopoietic progenitors with the bone marrow vascular niche is required for thrombopoiesis. Nat. Med. 2004;10:64-71.

28. Zhao M, Perry JM, Marshall H et al. Megakaryocytes maintain homeostatic quiescence and promote post-injury regeneration of hematopoietic stem cells. Nat.Med. 2014;20:1321-1326.

29. Kimoto M, Ando K, Koike S et al. Significance of platelets in an antimetastatic activity of bacterial lipopolysaccharide. Clin.Exp.Metastasis 1993;11:285-292.

30. Sanjuan-Pla A, Macaulay IC, Jensen CT et al. Platelet-biased stem cells reside at the apex of the haematopoietic stem-cell hierarchy. Nature 2013;502:232-236.

31. Libregts SF, Gutierrez L, de Bruin AM et al. Chronic IFN-gamma production in mice induces anemia by reducing erythrocyte life span and inhibiting erythropoiesis through an IRF-1/PU.1 axis. Blood 2011;118:2578-2588.

32. Meinders M, Kulu DI, van de Werken HJ et al. Sp1/Sp3 transcription factors regulate hallmarks of megakaryocyte maturation, and platelet formation and function. Blood 2014

33. Phillipsen D. Platelet biochemsitry. 1-1-2012.

34. De Cuyper IM, Meinders M, van d, V et al. A novel flow cytometry-based platelet aggregation assay. Blood 2013;121:e70-e80.

35. de Bruin AM, Voermans C, Nolte MA. Impact of interferon-gamma on hematopoiesis. Blood 2014;124:2479-2486.

36. Blajchman MA, Senyi AF, Hirsh J, Genton E, George JN. Hemostatic function, survival, and membrane glycoprotein changes in young versus old rabbit platelets. J.Clin.Invest 1981;68:1289-1294.

37. Kristinsson SY, Gridley G, Hoover RN, Check D, Landgren O. Long-term risks after splenectomy among 8,149 cancer-free American veterans: a cohort study with up to 27 years follow-up. Haematologica 2014;99:392-398.

38. Nagai Y, Garrett KP, Ohta S et al. Toll-like receptors on hematopoietic progenitor cells stimulate innate immune system replenishment. Immunity. 2006;24:801-812.

39. Sato T, Onai N, Yoshihara H et al. Interferon regulatory factor-2 protects quiescent hematopoietic stem cells from type I interferon-dependent exhaustion. Nat.Med. 2009;15:696-700.

40. Semple JW, Italiano JE, Jr., Freedman J. Platelets and the immune continuum. Nat.Rev. Immunol. 2011;11:264-274.

41. Andrews RK, Gardiner EE, Shen Y, Whisstock JC, Berndt MC. Glycoprotein Ib-IX-V. Int.J.Biochem.Cell Biol. 2003;35:1170-1174.

42. Massberg S, Brand K, Gruner S et al. A critical role of platelet adhesion in the initiation of atherosclerotic lesion formation. J.Exp.Med. 2002;196:887-896.

43. Suzuki-Inoue K, Fuller GL, Garcia A et al. A novel Syk-dependent mechanism of platelet activation by the C-type lectin receptor CLEC-2. Blood 2006;107:542-549.

44. Boulaftali Y, Hess PR, Getz TM et al. Platelet ITAM signaling is critical for vascular integrity in inflammation. J.Clin.Invest 2013;123:908-916.

Chapter 6

SUMMARY AND GENERAL DISCUSSION

SUMMARY AND GENERAL DISCUSSION

Platelets are blood circulating specialized subcellular fragments, which are produced by megakaryocytes. Platelets are essential for hemostasis and wound healing but also play a role in non-hemostatic processes such as the immune response or cancer metastasis. Considering the immediate precursors of platelets, normal megakaryocyte development is essential for normal platelet function. Although much is known about platelet development, some aspects of platelet production remain poorly understood.
Megakaryopoiesis is a complex process whereby the multipotent erythroid/megakaryocyte progenitors that commit their fate from hematopoietic stem cells (HSCs) differentiate into megakaryocytes. During maturation, megakaryocytes undergo several dramatic phenotypical changes including polyploidization and the development of a demarcation membrane system. The purpose of this thesis is to further elucidate novel mechanisms and aspects involved in megakaryopoiesis and the effect they have on platelet function, and how to assess with newly developed tests platelet functional characteristics.

Functional platelet testing

Platelets are essential for normal hemostasis.[1] Platelet function tests are used to diagnose and manage patients with bleeding problems, and in addition, they are also used for monitoring the efficacy of antiplatelet drugs or as point-of-care presurgical/perioperative tests when required. The first platelet functional test was developed in 1910 whereby bleeding time was measured after a small wound was made.[2] This test was the gold standard until the early 90s. Although this test seemed relatively easy to perform, great variability in test results were observed due to variability in skin thickness, blood vessel characteristics, temperature, localization of the incision, and handling.[3] Nowadays the most frequently used functional platelet test is light transmission aggregometry (LTA). The test is relatively easy to perform, but great quantities of blood are necessary to obtain a complete diagnostic picture and significant expertise is necessary to evaluate the results. It is based on the measurement of light transmission through a sample of platelet rich plasma, which will increase as platelets aggregate and the sample becomes more translucent. Since it is not recommended to concentrate the platelet count, samples from thrombocytopenic patients or infants remain difficult to test as results deviate from the normal values. Furthermore, the test is not reliable when the plasma is highly lipemic.[4] Although whole blood impedance aggregation tests can overcome the difficulties to measure highly lipemic samples, other limitations have been noted for both tests. For example, impedance aggregometry and LTA rely on the formation of big aggregates that require ultimately activation of αIIbβ3 integrin to form fibrinogen bridges between platelets, and therefore cannot distinguish between primary defects of either αIIbβ3 or α2β1 integrins, as has been shown with platelets from Glanzmann Thrombasthenia (defect in αIIbβ3) and LAD-III (defects in both αIIbβ3 or α2β1) patients, which appear equally defective using LTA or impendance aggregometry.[5] Therefore, novel methodologies are necessary that allow platelet functional testing in a reliable manner in thrombocytopenic

patients, or infants, and that allow to measure the contribution of single receptors to platelet aggregation.

In ***Chapter 2*** we describe our efforts to develop a novel flow cytometry based platelet aggregation assay (FCA) which is easy to perform, needs small quantities of blood and can discriminate between different receptor pathways. This test uses flow cytometry, and by differentially labelling and mixing back two populations of platelets, the aggregation of activated platelets can be measured as double colored events. Upon activation, platelets can bind to fibrinogen or directly to each other whereby small aggregates are formed. Thus, this method allows measuring microaggregates, the early steps during the aggregation process, while light transmission aggregometry relies on the formation of large aggregates for a positive test.

A vast advantage of this assay is the small amount of blood necessary, whereby both whole blood and platelet rich plasma can be used. Especially for diagnosing severe thrombocytopenic patients, or when animal models are used, the small quantity necessary for each test poses great advantages. Whereby for LTA one mouse has to be sacrificed to obtain sufficient platelets for one single test, FCA only requires 200µl of blood to perform aggregation tests with at least 6 different agonists. This means that the mouse can be kept alive, and makes the analysis of platelet aggregation in one mouse during time possible (i.e. development, aging, or during treatment).

The second benefit of this assay is the possibility to discriminate between the Clec2, α2β1, αIIbβ3, GPIb/V/IX and GPVI pathways by using different agonists. We have proven which receptors are involved in the process by applying a combination of agonists and antagonists. Therefore we know which receptors are involved following stimulation with a specific agonist, while in the LTA setting, b3 integrin is ultimately required for the formation of a big thrombus, and defects prior its activation or on b3 itself cannot be discriminated. By activating the platelets with a specific agonist, i.e. aggretin, collagen, PMA, botrocetin or convulxin they respond in a dose dependent manner. Besides measuring the maximal activation, this assay also allows us to evaluate the aggregation slope and relative aggregate size, which can give additional information about the capacity and speed of aggregation.

Van de Vijver et al,[6] described that by using FCA, a clear distinction – in contrast to LTA – could be made between Glanzmann Thrombasthenia and LAD-III patients, hence proving its functionality as a novel diagnostic tool.

Besides the use as a diagnostic tool, FCA has great potential in research settings. The possibility to adjust individual parameters involved during platelet aggregation (i.e. plasma type, shaking speed or the the study of a specific group of platelets involved in aggregation or interaction with other cell types using appropriate markers), provides the researches with many possibilities to adjust the test for specific applications.

Although this test has great advantages compared to other methods, a disadvantage is that, unlike with LTA, we are not able to identify a primary and secondary response when platelets are stimulated with ADP. Furthermore, our assay is based on micro-aggregation which is suggested by Maurer-Spurej et all to be different from thrombus formation, as microaggregation is induced by (early) signaling processes that are slightly different than those occurring during thrombus formation.[7]

In the meantime, new platelet analyzers have been developed, including the platelet function analyzer 100 (PFA-100), which measures aggregation of platelets in response to agonists at a well-defined shear rate.[8, 9]
Notwithstanding the increased use of PFA-100 in clinical biochemistry laboratories, our own novel aggregation method has proven to be functionally relevant as a diagnostic tool and has a great advantage in the research setting of testing samples of a very limited blood volume or with a very low platelet count. We have used this method to characterize platelet function in mouse models extensively, mouse models that were described in chapters 3-5, appendix 1-2 and others[10] and that would have been otherwise very difficult by using conventional methods: we were able to use the minimal number of mice required (reduction), and still we were able to characterize different pathways on these platelets, that would have been masked using conventional methods. However, although FCA has great advantages, to study all or specific aspects of platelet function, an integrative set of tests must be chosen which can address the underlying question regarding platelet functionality.

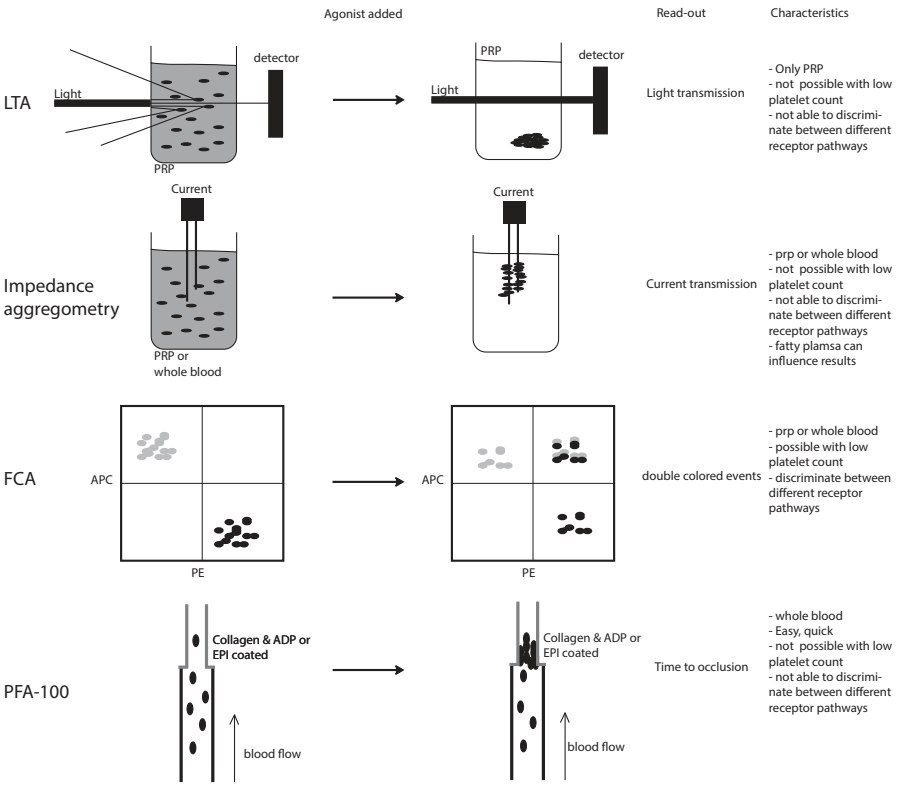

Figure 1. Overview of aggregation methods

This figure depicts a schematic view of aggregation methods used. On the top light transmission aggregometry is shown, where light transmission is increased when platelets form aggregates. The impedance aggregometry is based on a

decreased of current if platelets are activated and attach to the electrode. The FCA is based on flow cytometry where an increase in double colored events can be seen after platelet activation. PFA-100 is measuring the time to occlusion response to agonists at a well-defined shear rate.

MEGAKARYOPOIESIS

Megakaryopoiesis and thrombopoiesis, the maturation of a megakaryocyte which ultimately results in platelet production, is a highly regulated process. Megakaryocytes develop from HSCs through successive lineage commitment steps to ultimately differentiate into mature megakaryocytes ready to produce platelets. Transcription factors regulate gene expression, and the first significant advances in understanding the transcriptional basis of hematopoietic cell differentiation were made in the 1990s.[11] Unveiling the role of transcription factors essential during megakaryopoiesis and their transcriptional programs is vital to understand the process in health and disease.[12]

Pivotal steps in cell differentiation are linked to the activation of key transcriptional regulators. A number of transcription factors have been suggested to be involved in the regulation of megakaryopoiesis, either by positively or negatively regulating megakaryocyte specific genes. These factors include RUNX1, GATA1, ZFPM1, FLI1, c-MYB and NFE2.[13]

The use of genetic manipulated mouse models, genetic analysis of cellular processes, including differentiation, have allowed progress in understanding transcription during megakaryopoiesis. This knowledge is very relevant, since mutations in regulatory regions of genes, and not only in coding regions, could be the cause of inherited platelet disorders.

In ***Chapter 3***, we investigated the role of Sp1 and Sp3 transcription factors in megakaryopoiesis. Sp1 and Sp3 belong to the family of Specificity protein/Krüppel-like Factor (SP/KLF) transcriptional regulators, are characterized by three highly conserved zinc fingers, and recognize the widely distributed G-rich promoter elements which are present in the regulatory regions of many ubiquitously and tissue specific genes.[14]

Since neither Sp1 or Sp3 complete knock-out mice are viable,[15;16] conditional double Sp1 and Sp3|Pf4-cre mice were generated to investigate their role in megakaryopoiesis. Sp1-lox|Pf4-Cre nor Sp3|Pf4-Cre mice showed a phenotype, and since these transcription factors could be redundant in function, a double Sp1-lox::Sp3-lox|Pf4-Cre was used. These mice showed severe macrothrombocytopenia, altered platelet function and a defect in megakaryocyte maturation. Elaborate investigation on megakaryopoetic hallmarks, platelet functional assays and RNA-Seq in megakaryocytes and proteomics in platelets (OMICS) revealed new and unexpected targets involved in megakaryopoiesis.

RNA-Seq data indicated that upon removal of Sp1 and Sp3 in megakaryocytes, 440 genes were down regulated and 350 genes upregulated in dKO megakaryocytes. A close look at the promoter elements revealed a significant enrichment of the G-rich promoter element in downregulated genes, indicating that most genes are activated by Sp1 and Sp3 during megakaryopoiesis.

Sp1 and Sp3 are known to be involved in cell metabolism and a large portion of differentially expressed genes could be related to this. We could also identify a large proportion of genes which are known to be vital during megakaryopoiesis and thrombopoiesis.[17] Besides genes previously described to be important in megakaryopoiesis, our OMICS data revealed other genes/proteins whose contribution to megakaryopoiesis and platelet function has not been fully characterized yet.
One of these proteins is myosin-light-chain-kinase (Mylk), a protein previously described to be involved in thrombus formation in zebrafish.[18] We show that Mylk has a vital role in proplatelet formation and stabilization in megakaryocytes and that it is important for Clec2 and GpVI signaling during platelet aggregation. This suggests that although Sp1 and Sp3 are important as ubiquitous transcription factors, they also have an important cell-type specific function during megakaryopoiesis.
Based on these findings, we can hypothesize that the view of specific transcription factors which only determine differentiation or transcription factors which regulate housekeeping genes is superseded, indicating that transcription factors could be both involved during differentiation and regulate housekeeping genes. A more flexible view of transcription factors and their role during specific processes must be considered.

One of the first transcription factors characterized to be vital in megakaryopoiesis is Gata1.[19] In humans, GATA1 mutations lead to a variety of symptoms which can be summarized as dyserytropoietic anemia and thrombocytopenia, as a syndrome of platelets defective in the vWF receptor response (pseudo-Bernard-Soulier syndrome, or X-linked Bernard-Soulier syndrome), or as a lack alpha granules (pseudo-Gray Platelet syndrome, or X-linked Gray Platelet syndrome).
Gata1 is expressed in erythroid, megakaryocytic, mast and eosinophil lineages, dendritic cells as well as multipotent myeloid progenitors and Sertoli cells of the testis.[19-23] Gata1 mouse embryos die due to severe anemia, therefore analysis of its role during megakaryocyte development and platelet production in adult mice could not be examined in full knockout animals.
Different Gata1 targeted mouse models were created to investigate the role of Gata1 in megakaryocytes including the ΔneoΔHS and Gata1.05 mice[24]. Both mouse models showed severe macrothrombocytopenia, but neither KO model was restricted to the megakaryocytic lineage. Therefore we cannot exclude the impact on mast cells or eosinophils, and how that feeds back to hematopoietic production.
To circumvent this drawbacks, and in order to study the role of Gata1 in adult hematopoiesis, a pan-hematopoietic Gata1 KO mouse was created by crossing Gata1-lox mice with mice bearing an interferon-inducible Cre-transgene (Mx1-Cre mice) which resulted in almost complete deletion of the Gata1 gene, and overall reduction of Gata1 expression in the bone marrow to 20% compared to WT littermates. These mice showed anemia, a reduced platelet count and an increased number of splenic immature megakaryocytes.[25]
In ***Chapter 4*** we generated Gata1-lox|Pf4-Cre mice to investigate the function of Gata1 in a lineage-specific way. To create a mature megakaryocyte-specific Gata1 knockout mouse model, Gata1-lox mice were crossed with Pf4-Cre which allows gene recombination in late committed megakaryocytes.[26]

Both Pertuy et al and Calaminus et al showed that Pf4-Cre mice show some leakage regarding cell-specificity, and that recombination also occurs in a minor population of HSCs, circulating leukocytes, monocytes, macrophages and in epithelial cells of the colon.[27;28] This must be kept in mind when analyzing Pf4-cre mice.[28] While Gata1 is expressed at low levels in monocytes, it is not expressed in leukocytes, neither in macrophages, thus we exclude major effects from recombination of Gata1 in these lineages.

Our model confirms the previous reported phenotype including macrothrombocytopenia, aggregation defects upon stimulation with collagen and botrocetin (activating the α2β1/GPVI and GPIb/V/IX receptor respectively), and a reduced expression of CD42b, one of the subunits of the vWF receptor GPIb/V/IX.[29;30] Our new aggregation method, see Chapter 2, allowed us to distinguish between 5 distinct receptor pathways, i.e. GPIb/V/IX, α2β1, GPVI, Clec2 and α2bβ3. We noted a defect in aggregation upon stimulation with aggretin (Clec2) and convulxin (GPVI), which could not be explained by a decrease in receptor expression. Interestingly, both receptor pathways signal through spleen tyrosine kinase (Syk),[31] a signaling molecule critical during platelet activation. We show that in Gata1|Pf4-Cre KO megakaryocytes and platelets, Syk expression is reduced, and we confirmed Gata1 binding to the Syk promoter by chromatin immunoprecipitation assays in megakaryocytes, suggesting that Gata1 regulates Syk.

Syk knock-out mice generally do not survive beyond 1-5 days after birth due to severe hemorrhage,[32] and Abtahian et al showed that mice deficient in Syk show severe defects in the separation of lymphatic and blood vasculature.[33;34] Like Syk knock-out mice, Clec2 KO mice also have this problem, and it was suggested that the Clec2 receptor is crucial for this process.[35] Mice with megakaryocyte-specific Syk deletion, i.e. Syk-lox|Pf4-Cre mice, showed a similar phenotype compared to complete abrogation of Syk regarding lymph vessel separation during ontogeny although adult mice were born with normal platelet counts; these strongly suggests that Syk is required in megakaryocytes and platelets for normal lymphatic development, although it seems not to be involved or required for proper platelet number production (data not shown).[36]

Since Syk is essential in platelets for normal lymphatic development, and we show that Syk is directly regulated by Gata1, we can hypothesize that Gata1 is not only an essential factor for platelet production and function but that loss of Gata1 in the megakaryocyte lineage might influence lymphatic development during embryogenesis. We investigated lymphatic vessel separation in Gata1 KO embryos, however we did not see complete penetrance of the lymph vessel separation defect. Some mice presented with blood filled lymphatics, other did not (data not shown). We should also note that Syk is reduced, but not absent in these embryos. Furthermore, the fact that Gata1 is X-linked might be a factor influencing these results, since recombination efficiency together with X-inactivation might lead to the variation observed in mouse embryos (which were assessed on genotype but not on gender).

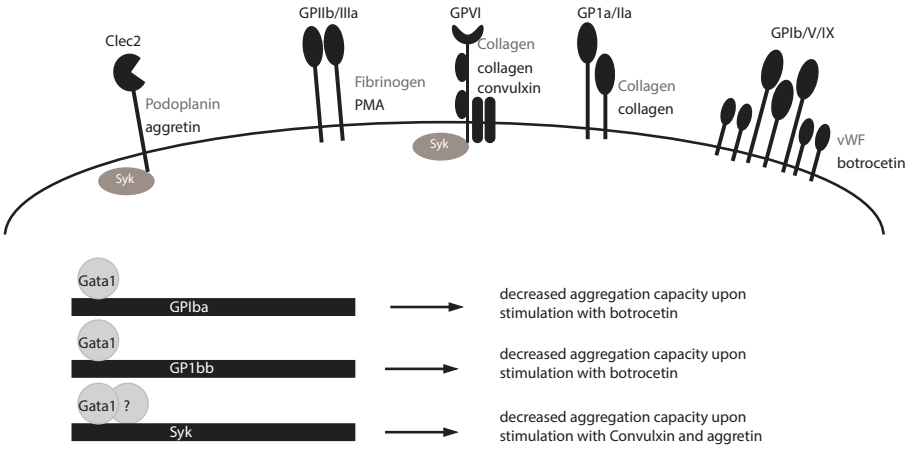

Figure 2. Schematic overview of Gata1 interaction

This diagram shows that Gata1 directly regulates Gp1ba and Gp1bb, thereby reducing its receptor expression on platelets, explaining a decreased aggregation capacity upon stimulation with its agonist (botrocetin). Gata1 is also is able to directly regulate Syk, although we cannot exclude that other transcription factors co-regulate its expression, since Syk levels were not completely abrogated in *Gata*1-KO mice.

Hematopoiesis sites and megakaryopoiesis

Hematopoiesis, the production of all blood cells, is a dynamic process during ontology by which the location of HSCs changes. During development HSCs first appear in the Aorta/Gonad/Mesonephros (AGM) region, then migrate to the fetal liver, spleen and eventually occupy the bone marrow around birth in human. It is recognized that the output of HSCs changes during development and is location dependent. The first HSCs are identified in the AGM, where HSC differentiation appears to be absent.[37] When HSCs reside in the fetal liver and the spleen, the output is mainly erythroid and megakaryocytic, and by occupying the bone marrow, myeloid output increases.[38] It has been suggested that the change of location, influences the development and differentiation capacity of the HSC, i.e. the microenvironment, also known as a niche, influences HSC differentiation.[39] In the same way, megakaryocytes are only capable to produce platelets when they reside in the bone marrow vascular niche, but not in the endosteal niche.[40] While steady state megakaryopoiesis in human occurs only in the bone marrow, is has been recognized that steady state megakaryopoiesis also occurs in the spleen in mice.

Hematopoietic stress, which can be induced by bleeding episodes, infection, inflammation, congenital disorders including thrombocytopenias, WBC deficiencies, anemia or overproduction of one of the hematopoietic lines, can expand the primary site of megakaryopoiesis to extramedullary locations. These locations include the spleen or the liver, i.e. hematopoietic locations during ontogeny. It has not been studied so far whether the splenic megakaryopoiesis produces platelets that are

functionally normal or different, or whether the process is necessary for recovery upon stress at all.

In ***Chapter 5*** we investigate platelet production and function upon different sorts of hematopoietic stress and evaluate the role of the spleen as extramedullary organ in such situations. We identified that during hematopoietic stress episodes, produced platelets have an altered phenotype, i.e. a decreased aggregation capacity when stimulated with specific agonists. In particular, when the stress causes severe thrombocytopenia, independently on whether the stress was acute (antibody-mediated platelet depletion) or chronic (CD70Tg sterile inflammation model), a 10-20% of the platelets had an increased expression of CD42b. The platelets with an increased CD42b expression where produced by splenic megakaryocytes which showed also a strongly increased expression of CD42b on their surface as compared to bone marrow megakaryocytes. Moreover, these CD42b^{bright} platelets were absent in splenectomized mice upon acute severe hematopoietic stress (platelet-depletion model). To investigate whether the spleen is a vital extramedullary organ during hematopoietic stress episodes in the mouse, the mice were splenectomized prior to inducing acute platelet depletion. Splenectomized mice displayed a normal platelet recovery time compared to WT mice, indicating that the spleen is not vital during the hematopoietic stress episodes for platelet count recovery, and that the platelet production can be covered by the bone marrow itself (although we cannot exclude extramedullary production in other sites than the spleen).

When looking at the aggregation profile of platelets in the different stress models used, we noted an alteration in aggregation capacity. Depending on the severity, time span and cause of hematopoietic stress, specific alterations upon stimulation with the different agonists was seen. Acute severe thrombocytopenia causes a specific aggregation defect, i.e. only upon stimulation with aggretin and convulxin. In contrast, chronic hematopoietic stress causes a decreased aggregation capacity when stimulated with PMA, botrocetin, convulxin, collagen or aggretin. However, splenectomized mice suffering from acute severe hematopoietic stress show an aggregation defect upon stimulation with aggretin, convulxin and botrocetin. The difference between splenectomized mice and WT, regarding the defect upon botrocetin stimulation specifically, could be explained by the loss of the platelet population expressing CD42b at high levels derived from splenic megakaryocytes. We cannot exclude that the differences found are only due to altered platelet formation, while other components might be involved, such as different priming of platelets during circulation or an altered function inherent to platelet size, since platelets formed under hematopoietic stress have an increased platelet volume.

Increased platelet volume and number is also reported in patients after splenectomy.[41] It has been reported that splenectomized patients have an increased risk of bacterial infections, which could be explained by de host defense the spleen exerts.[42] Besides this, we have shown that during inflammatory conditions, the spleen increases platelet output and these platelets have a different phenotype, including an increased CD42b expression. It has been shown that CD42b may promote neutrophil extravasation and can activate neutrophils, which could mean that these platelets produced from the splenic megakaryocytes could be more suited to activate neutrophils and loss of this population increased the risk on infections.

General conclusion and future perspectives

In this thesis I have contributed to the development of a novel platelet aggregation test. This has proven to be very useful in order to assess platelet functionality in samples with low platelet counts and to discern platelet aggregopathies; not only that, it has ease enormously the study of platelet function in mouse models. This test has shown a number of possible applications during my thesis period. I foresee that this test could be further optimized and many more applications could be implemented: for example in drug testing on platelet functionality, to study the effect of plasma factors on platelet functionality, to study platelet interactions with other blood cell types, and as a prognosis test, for example, before transfusion is performed.

Patients that suffer from thrombocytopenia either genetic or acquired, receive platelet transfusions when there is bleeding or when there is a risk for bleeding. Bone marrow transplantations are considered in severe conditions. Understanding the cause of the thrombocytopenia may pose alternatives for the improvement of the treatment options for patients suffering from platelet disorders. Nowadays, with the advancement on high throughput sequencing, and the international efforts made to characterize the genomes of healthy and non-healthy individuals, we are getting closer to the identification of genes causative of disease.

Our studies also suggest that the platelet and megakaryocytic research fields must communicate with each other and bridge, in order to advance in the understanding of clinical complications related to platelet function. Not only that, the demand to find ways to generate platelets in vitro for transfusion purposes would benefit enormously if the molecular steps during megakaryopoiesis are unraveled. The production of megakaryocytes for platelet products from donor iPS cells would lower the risks of unwanted side effects during treatment with allogenic products. Autologous iPS-derived megakaryocytes or platelets could also be manipulated to serve the needs of the patient in the near future.

In addition, we have observed that megakaryopoiesis and platelet production and function varies in situations of hematopoietic stress. In particular, when the hematopoietic stress leads to severe thrombocytopenia, a subpopulation of platelets expressing high levels of CD42b appears in the blood. We were able to link the origin to these platelets to the spleen, since they were not found in splenectomized mice going through the same induced hematopoietic stress. With our aggregation test, we could observe that the aggregation profile of platelets produced upon stress is slightly different than that of platelets in the steady state, and we hypothesize that this functional difference might have a consequence for the hemostatic and non-hemostatic functions of platelets. This concept needs further investigation, because if platelets are produced with a different phenotype, and for that they have a specific function in the stress response, we might learn from that physiological event, and try to manipulate platelets accordingly for therapeutic purposes, such as exacerbated immune responses or autoimmunity, cancer metastasis and vascular disease/wound healing being all non-hemostatic functions which platelets have been recently linked to.

REFERENCE LIST

1. George JN. Platelets. Lancet 2000;355:1531-1539.
2. Duke WW. The relation of blood platelets to hemorrhagic disease. By W.W. Duke. JAMA 1983;250:1201-1209.
3. Panzer S, Jilma P. Methods for testing platelet function for transfusion medicine. Vox Sang. 2011;101:1-9.
4. Rand ML, Leung R, Packham MA. Platelet function assays. Transfus.Apher.Sci. 2003;28:307-317.
5. van d, V, De Cuyper IM, Gerrits AJ et al. Defects in Glanzmann thrombasthenia and LAD-III (LAD-1/v) syndrome: the role of integrin beta1 and beta3 in platelet adhesion to collagen. Blood 2012;119:583-586.
6. van d, V, De Cuyper IM, Gerrits AJ et al. Defects in Glanzmann thrombasthenia and LAD-III (LAD-1/v) syndrome: the role of integrin beta1 and beta3 in platelet adhesion to collagen. Blood 2012;119:583-586.
7. Maurer-Spurej E, Devine DV. Platelet aggregation is not initiated by platelet shape change. Lab Invest 2001;81:1517-1525.
8. Kundu SK, Heilmann EJ, Sio R et al. Description of an in vitro platelet function analyzer--PFA-100. Semin.Thromb.Hemost. 1995;21 Suppl 2:106-112.
9. Paniccia R, Priora R, Alessandrello LA, Abbate R. Platelet function tests: a comparative review. Vasc.Health Risk Manag. 2015;11:133-148.
10. Fujita R, Takayama-Tsujimoto M, Satoh H et al. NF-E2 p45 is important for establishing normal function of platelets. Mol.Cell Biol. 2013;33:2659-2670.
11. Shivdasani RA, Orkin SH. The transcriptional control of hematopoiesis. Blood 1996;87:4025-4039.
12. Kaushansky K. Historical review: megakaryopoiesis and thrombopoiesis. Blood 2008;111:981-986.
13. Geddis AE. Megakaryopoiesis. Semin.Hematol. 2010;47:212-219.
14. Suske G, Bruford E, Philipsen S. Mammalian SP/KLF transcription factors: bring in the family. Genomics 2005;85:551-556.
15. Marin M, Karis A, Visser P, Grosveld F, Philipsen S. Transcription factor Sp1 is essential for early embryonic development but dispensable for cell growth and differentiation. Cell 1997;89:619-628.
16. Bouwman P, Gollner H, Elsasser HP et al. Transcription factor Sp3 is essential for post-natal survival and late tooth development. EMBO J. 2000;19:655-661.
17. Li L, He S, Sun JM, Davie JR. Gene regulation by Sp1 and Sp3. Biochem.Cell Biol. 2004;82:460-471.
18. Tournoij E, Weber GJ, Akkerman JW et al. Mlck1a is expressed in zebrafish thrombocytes and is an essential component of thrombus formation. J.Thromb.Haemost. 2010;8:588-595.
19. Orkin SH, Shivdasani RA, Fujiwara Y, McDevitt MA. Transcription factor GATA-1 in megakaryocyte development. Stem Cells 1998;16 Suppl 2:79-83.

20. Fujiwara Y, Browne CP, Cunniff K, Goff SC, Orkin SH. Arrested development of embryonic red cell precursors in mouse embryos lacking transcription factor GATA-1. Proc.Natl. Acad.Sci.U.S.A 1996;93:12355-12358.

21. Martin DI, Zon LI, Mutter G, Orkin SH. Expression of an erythroid transcription factor in megakaryocytic and mast cell lineages. Nature 1990;344:444-447.

22. Zon LI, Yamaguchi Y, Yee K et al. Expression of mRNA for the GATA-binding proteins in human eosinophils and basophils: potential role in gene transcription. Blood 1993;81:3234-3241.

23. Ito E, Toki T, Ishihara H et al. Erythroid transcription factor GATA-1 is abundantly transcribed in mouse testis. Nature 1993;362:466-468.

24. Takahashi S, Komeno T, Suwabe N et al. Role of GATA-1 in proliferation and differentiation of definitive erythroid and megakaryocytic cells in vivo. Blood 1998;92:434-442.

25. Gutierrez L, Tsukamoto S, Suzuki M et al. Ablation of Gata1 in adult mice results in aplastic crisis, revealing its essential role in steady-state and stress erythropoiesis. Blood 2008;111:4375-4385.

26. Tiedt R, Schomber T, Hao-Shen H, Skoda RC. Pf4-Cre transgenic mice allow the generation of lineage-restricted gene knockouts for studying megakaryocyte and platelet function in vivo. Blood 2007;109:1503-1506.

27. Calaminus SD, Guitart AV, Sinclair A et al. Lineage tracing of Pf4-Cre marks hematopoietic stem cells and their progeny. PLoS.One. 2012;7:e51361.

28. Pertuy F, Aguilar A, Strassel C et al. Broader expression of the mouse platelet factor 4-cre transgene beyond the megakaryocyte lineage. J.Thromb.Haemost. 2015;13:115-125.

29. Shivdasani RA, Fujiwara Y, McDevitt MA, Orkin SH. A lineage-selective knockout establishes the critical role of transcription factor GATA-1 in megakaryocyte growth and platelet development. EMBO J. 1997;16:3965-3973.

30. Ludlow LB, Schick BP, Budarf ML et al. Identification of a mutation in a GATA binding site of the platelet glycoprotein Ibbeta promoter resulting in the Bernard-Soulier syndrome. J.Biol.Chem. 1996;271:22076-22080.

31. Watson SP, Herbert JM, Pollitt AY. GPVI and CLEC-2 in hemostasis and vascular integrity. J.Thromb.Haemost. 2010;8:1456-1467.

32. Cheng AM, Rowley B, Pao W et al. Syk tyrosine kinase required for mouse viability and B-cell development. Nature 1995;378:303-306.

33. Abtahian F, Guerriero A, Sebzda E et al. Regulation of blood and lymphatic vascular separation by signaling proteins SLP-76 and Syk. Science 2003;299:247-251.

34. Sebzda E, Hibbard C, Sweeney S et al. Syk and Slp-76 mutant mice reveal a cell-autonomous hematopoietic cell contribution to vascular development. Dev.Cell 2006;11:349-361.

35. Suzuki-Inoue K, Inoue O, Ding G et al. Essential in vivo roles of the C-type lectin receptor CLEC-2: embryonic/neonatal lethality of CLEC-2-deficient mice by blood/lymphatic misconnections and impaired thrombus formation of CLEC-2-deficient platelets. J.Biol. Chem. 2010;285:24494-24507.

36. Finney BA, Schweighoffer E, Navarro-Nunez L et al. CLEC-2 and Syk in the megakaryocytic/platelet lineage are essential for development. Blood 2012;119:1747-1756.

37. Godin I, Garcia-Porrero JA, Dieterlen-Lievre F, Cumano A. Stem cell emergence and hemopoietic activity are incompatible in mouse intraembryonic sites. J.Exp.Med. 1999;190:43-52.

38. Golub R, Cumano A. Embryonic hematopoiesis. Blood Cells Mol.Dis. 2013;51:226-231.

39. Martinez-Agosto JA, Mikkola HK, Hartenstein V, Banerjee U. The hematopoietic stem cell and its niche: a comparative view. Genes Dev. 2007;21:3044-3060.

40. Pitchford SC, Lodie T, Rankin SM. VEGFR1 stimulates a CXCR4-dependent translocation of megakaryocytes to the vascular niche, enhancing platelet production in mice. Blood 2012;120:2787-2795.

41. Wehmeier A, Scharf RE, Schneider W. Influence of splenectomy on platelet morphometry and function. Klin.Wochenschr. 1990;68:847-852.

42. Bohnsack JF, Brown EJ. The role of the spleen in resistance to infection. Annu.Rev.Med. 1986;37:49-59.

Appendix 1

THE MICROTUBULE PLUS-END TRACKING PROTEIN CLASP2 IS REQUIRED FOR HEMATOPOIESIS AND HEMATOPOIETIC STEM CELL MAINTENANCE

The microtubule plus-end tracking protein CLASP2 is required for hematopoiesis and hematopoietic stem cell maintenance

Cell Rep. 2012 Oktober

Drabek K, Gutiérrez L, Vermeij M, Clapes T, Patel SR, Boisset JC, van Haren J, Pereira AL, Liu Z, Akinci U, Nikolic T, van Ijcken W, van den Hout M, Meinders M, Melo C, Sambade C, Drabek D, Hendriks RW, Philipsen S, Mommaas M, Grosveld F, Maiato H, Italiano JE Jr, Robin C, Galjart N

Cell Reports
Report

The Microtubule Plus-End Tracking Protein CLASP2 Is Required for Hematopoiesis and Hematopoietic Stem Cell Maintenance

Ksenija Drabek,[1,12,13] Laura Gutiérrez,[1,6,12] Marcel Vermeij,[2] Thomas Clapes,[1,3] Sunita R. Patel,[7] Jean-Charles Boisset,[1,3] Jeffrey van Haren,[1] Ana L. Pereira,[1,8] Zhe Liu,[1] Umut Akinci,[1] Tatjana Nikolic,[4] Wilfred van IJcken,[5] Mirjam van den Hout,[5] Marjolein Meinders,[6] Clara Melo,[8] Clara Sambade,[9] Dubravka Drabek,[1] Rudi W. Hendriks,[4] Sjaak Philipsen,[1] Mieke Mommaas,[11] Frank Grosveld,[1] Helder Maiato,[8,10] Joseph E. Italiano, Jr.,[7] Catherine Robin,[1,3] and Niels Galjart[1,*]
[1]Department of Cell Biology and Genetics
[2]Department of Pathology
[3]Erasmus Stem Cell Institute
[4]Department of Pulmonary Medicine
[5]Erasmus Center for Biomics
Erasmus MC, P.O. Box 2040, 3000 CA Rotterdam, The Netherlands
[6]Department of Blood Cell Research, Sanquin Research and Landsteiner Laboratory, Academic Medical Centre, University of Amsterdam, Plesmanlaan 125, 1066 CX Amsterdam, The Netherlands
[7]Hematology Division, Brigham and Women's Hospital and Harvard Medical School, Boston, MA 02115, USA
[8]Chromosome Instability & Dynamics Laboratory-Instituto de Biologia Molecular e Celular
[9]Cancer Biology, IPATIMUP, and Medical Faculty of Porto
[10]Department of Experimental Biology
Faculdade de Medicina, Universidade do Porto, 4200-465 Porto, Portugal
[11]Center for Electron Microscopy, Department of Molecular Cell Biology, Leiden University Medical Center, 2300 RA Leiden, The Netherlands
[12]These authors contributed equally to this work
[13]Present address: Department of Oncogenomics, Academic Medical Center, University of Amsterdam, Meibergdreef 15, P.O. Box 22700, 1105AZ Amsterdam, The Netherlands
*Correspondence: n.galjart@erasmusmc.nl
http://dx.doi.org/10.1016/j.celrep.2012.08.040

SUMMARY

Mammalian CLASPs are microtubule plus-end tracking proteins whose essential function as regulators of microtubule behavior has been studied mainly in cultured cells. We show here that absence of murine CLASP2 in vivo results in thrombocytopenia, progressive anemia, and pancytopenia, due to defects in megakaryopoiesis, in erythropoiesis, and in the maintenance of hematopoietic stem cell activity. Furthermore, microtubule stability and organization are affected upon attachment of *Clasp2* knockout hematopoietic stem-cell-enriched populations, and these cells do not home efficiently toward their bone marrow niche. Strikingly, CLASP2-deficient hematopoietic stem cells contain severely reduced mRNA levels of *c-Mpl*, which encodes the thrombopoietin receptor, an essential factor for megakaryopoiesis and hematopoietic stem cell maintenance. Our data suggest that thrombopoietin signaling is impaired in *Clasp2* knockout mice. We propose that the CLASP2-mediated stabilization of microtubules is required for proper attachment, homing, and maintenance of hematopoietic stem cells and that this is necessary to sustain *c-Mpl* transcription.

INTRODUCTION

Cells of the blood are generated in a complex process called hematopoiesis. Production begins with hematopoietic stem cells (HSCs), which are present in a very limited number in the adult bone marrow. HSC maintenance is achieved by self-renewal, whereas HSC differentiation eventually generates cells of all the blood lineages. Attachment, migration, and (a)symmetric cell division are important for the maintenance, proliferation, and differentiation of all hematopoietic cells, including HSCs. These processes are regulated by the microtubule (MT) cytoskeleton. MTs are dynamic polymers assembled from heterodimers of α- and β-tubulin. MTs perform many of their cellular tasks by changing their organization and stability in response to the needs of the cell. This process is largely controlled by MT-associated proteins. Some of these factors are localized specifically at the ends of growing MTs and are called "plus-end tracking proteins," or +TIPs (for review, see Galjart, 2010).

Mammalian CLASP1 and CLASP2 are +TIPs that can stabilize MTs in specific regions of the cell, thereby regulating both mitosis and interphase. In motile fibroblasts, for example, CLASP2 acts downstream of PI3K and GSK-3β to enhance MT stabilization at the leading edge and support directed motility (Akhmanova et al., 2001; Drabek et al., 2006). The C terminus of CLASP2 is required for association with the cell cortex, through LL5β and ELKS (Lansbergen et al., 2006), proteins that might form a PI3K-regulated cortical platform to which CLASPs attach distal MT ends. Cortex localization and clustering of LL5β

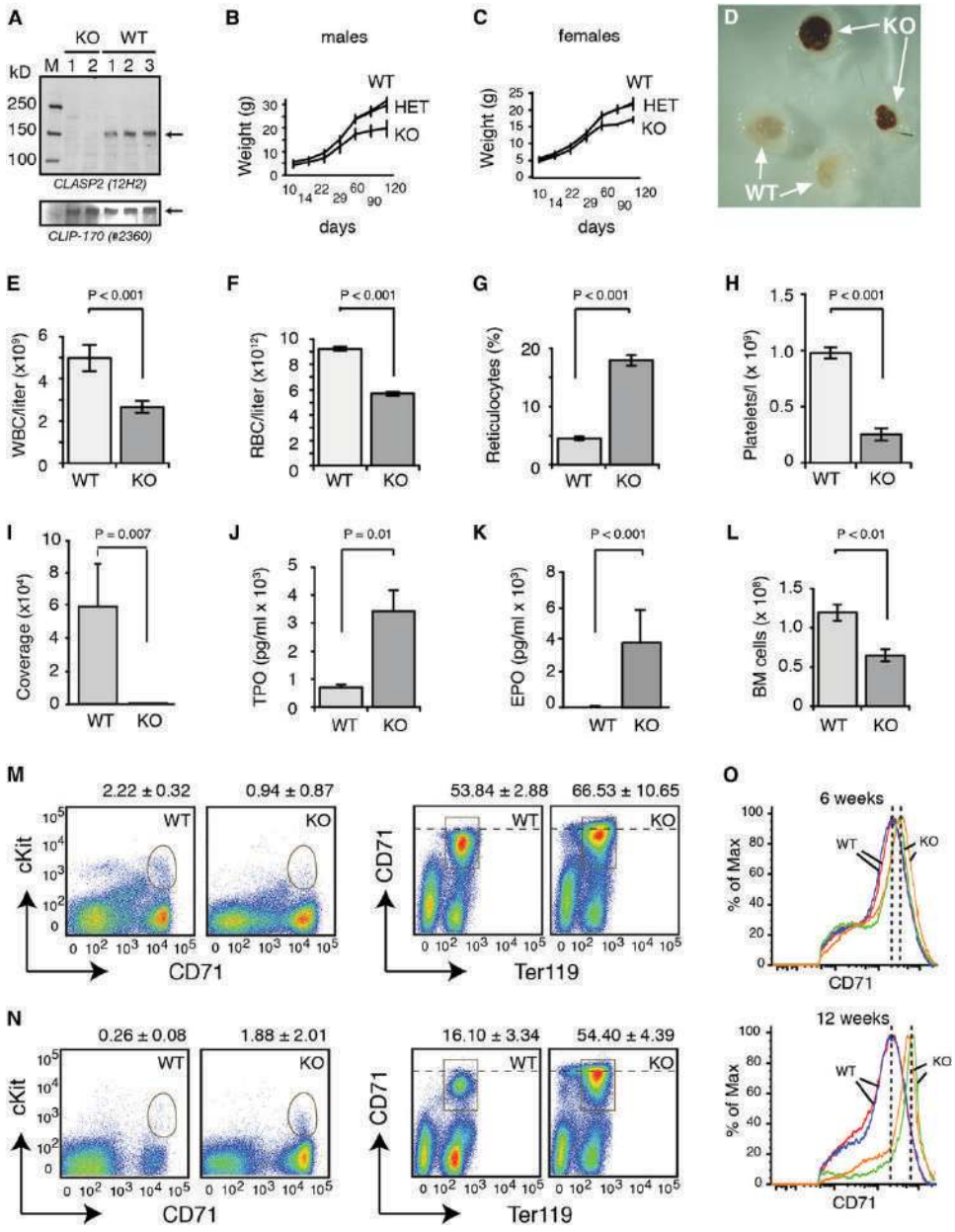

Figure 1. Hemorrhages, Pancytopenia, and Erythroid Defects in Clasp2 KO Mice

(A) Western blot analysis. Protein extracts from the bone marrow of WT and *Clasp2* KO mice were analyzed on western blot using anti-CLASP2 (12H2) and anti-CLIP-170 (#2360) antisera.

(B and C) Growth curves. Body weights of WT, heterozygous (HET), and homozygous *Clasp2* KO mice are shown at different time points. Groups consisted of 5 KO, 10 HET, and 9 WT males (B) and 4 KO, 14 HET, and 9 WT females (C).

(D) Hemorrhages in *Clasp2* KO mice. Ovaries from WT and *Clasp2* KO mice were isolated. In both KO ovaries, severe hemorrhages are present.

(E and F) WBC and RBC counts. Blood was isolated from 12 WT and 16 *Clasp2* KO mice.

(G) Reticulocyte counts. Blood from three WT and three *Clasp2* KO mice was deposited on glass slides. Approximately 2,000 RBCs were counted per mouse, and the percentage of reticulocytes was measured.

in epithelial cells are regulated by integrins and the cell-adhesion molecule laminin (Hotta et al., 2010), providing a link among cell adhesion, integrin signaling, CLASPs, and MTs.

To examine the in vivo role of CLASP2, we generated *Clasp2* knockout (KO) mice. These mice display multiple defects, including problems in megakaryopoiesis, erythropoiesis, and the maintenance of the HSC bone marrow pool. We show that the MT network is affected in CLASP2-deficient HSC-enriched bone marrow cells and that these cells do not home efficiently toward their niche. Interestingly, expression of *c-Mpl*, which encodes the thrombopoietin (TPO) receptor (Kaushansky, 2009), is reduced in CLASP2-deficient HSCs. Our data reveal a link between the mechanical action of CLASP2 at MT ends and the expression of a hematopoietic factor that is important for megakaryocyte development and HSC maintenance.

RESULTS

Pancytopenia in Clasp2 KO Mice

We disrupted the murine *Clasp2* gene (Figures S1A and S1B) and showed abrogation of CLASP2 expression (Figures 1A and S1). Matings between heterozygous *Clasp2* KO mice yielded less homozygous offspring than expected (29% wild-type [WT], 50% heterozygous, and 22% homozygous *Clasp2* KOs in 729 mice counted). The body weight of homozygous *Clasp2* KO mice was approximately 30% lower than that of WT and heterozygous littermates (Figures 1B and 1C). Patho-anatomic examination of adult *Clasp2* KO mice revealed severe anomalies in male and female reproductive organs but no gross alterations in other tissues (data not shown). These results indicate that CLASP2 plays a role in germ cell development as well as in multiple somatic tissues.

We observed hemorrhages in different *Clasp2* KO organs, including the reproductive system (in 50% of the animals; Figure 1D) and stomach (in 67% of the mice). Petechiae, small red spots caused by a minor hemorrhage, were found in the brain, bladder, and lymph nodes (in 20%, 17%, and 11% of the KOs, respectively). Furthermore, white blood cell (WBC) and red blood cell (RBC) numbers were reduced in *Clasp2* KO blood (Figures 1E and 1F), as were hematocrit and hemoglobin levels (data not shown). By contrast, we detected more reticulocytes in *Clasp2* KOs (Figure 1G), indicating that immature RBCs are extruded into the blood to compensate for the erythrocyte deficiency.

Platelets were also reduced in *Clasp2* KOs (Figure 1H). Because a reduction in platelet number is by itself not sufficient to explain a bleeding phenotype, we analyzed whether defects in the endothelium that lines the blood vessels could explain the internal bleedings, but we detected no obvious endothelial damage in hematoxylin/eosin-stained sections of *Clasp2* KO mice (data not shown). Because platelets need to adhere in order to form a clot, we examined platelet adhesion to collagen under physiological shear rate. Strikingly, adhesion was almost completely inhibited in CLASP2-deficient platelets (Figure 1I), indicating that this underlies the hemorrhages in *Clasp2* KO mice. Taken together, our data reveal a severe pancytopenia in *Clasp2* KO mice.

TPO is a major regulator of platelet homeostasis in vivo (Kaushansky, 2009), whereas erythropoietin (EPO) controls the levels of RBCs (Richmond et al., 2005). TPO values were about four times higher, and EPO levels were even more increased in *Clasp2* KO mice compared to WT littermates (Figures 1J and 1K, respectively). These results indicate that the thrombocytopenia and anemia are sensed by the *Clasp2* KO mice; however, despite elevated TPO and EPO levels, platelet and RBC numbers are not restored to normal values. Furthermore, in addition to reduced WBC, RBC, and platelet numbers in the blood, we also observed fewer nucleated cells in the bone marrow of *Clasp2* KO mice (Figure 1L). We therefore investigated the various hematopoietic lineages in *Clasp2* KO mice in more detail.

CLASP2 Is Required for Erythropoiesis

During erythropoiesis, committed erythroid progenitors (burst-forming unit erythroid [BFU-E] and colony-forming unit erythroid [CFU-E]) differentiate toward the erythroblast stage, which develops further into enucleated reticulocytes and, finally, into mature erythrocytes, or RBCs. In case of anemia, erythroid progenitors relocate to the spleen and commence stress erythropoiesis in order to increase RBC output in the blood. As a result, the spleen increases in size. Clonogenic culture assays showed reduction of bone marrow-derived BFU-E and CFU-E colonies in the absence of CLASP2 (Figure S1F). By contrast, in the spleen, a slight increase in the number of these colonies was observed (Figure S1G), indicative of stress erythropoiesis.

Further analysis of the erythroid system revealed a significant decrease in early c-kit$^+$CD71$^+$ erythroblasts in the *Clasp2* KO bone marrow, whereas the amount of later-stage CD71$^+$ TER119$^+$ erythroblasts was similar to WT (Figure 1M). By contrast, in the *Clasp2* KO spleens, both early- and late-stage erythroblasts were increased (Figure 1N). Taken together, our data suggest that a CLASP2 deficiency limits erythroid

(H) Platelet counts. Blood was isolated from 18 WT and 22 *Clasp2* KO mice, and platelets were counted.
(I) Platelet adhesion to collagen under physiological shear rate. Whole blood from WT and *Clasp2* KO mice was perfused over collagen-coated slides. Adhered platelets were visualized with CD41-PE- or CD61-FITC-conjugated antibodies, and immunofluorescence coverage of slides was quantified.
(J and K) Cytokine production. TPO (J) and EPO (K) levels were determined in the serum of WT and *Clasp2* KO mice. TPO levels were measured in 12 WT and 10 KO mice; EPO levels were measured in 6 WT and 6 KO mice (SD indicated).
(L) Analysis of bone marrow. Nucleated cells were counted in bone marrow (BM) from seven WT and seven *Clasp2* KO mice. In (A)–(L), SEM is shown (unless stated otherwise) together with t test results.
(M and N) Erythroid differentiation. Early erythroid progenitors were identified by flow cytometry using c-kit and CD71 in bone marrow (M) and spleen (N) from WT and *Clasp2* KO mice. Single-flow cytometry plots are shown with the area outlined used to calculate c-kit$^+$/CD71$^+$ cells. Percentages (n = 6 in all groups, SD indicated) of cells are indicated above the plots.
(O) Age-dependent increase in CD71 expression. Cells of four WT and four *Clasp2* KO mice, of 6 and 12 weeks, were gated on the basis of the erythroid marker CD71. Vertical striped lines show approximate CD71 peak positions. % of Max, percentage of maximum.
See also Figure S1.

differentiation in the bone marrow. This induces stress erythropoiesis in the spleen, which is consistent with an increased spleen/body weight ratio in *Clasp2* KO mice (Figure S1E). Stress erythropoiesis is, however, not sufficient to compensate for the RBC loss in the blood (Figure 1F), which explains the highly increased EPO levels (Figure 1K).

Flow cytometry analysis showed increased amounts of CD71, the transferrin receptor, on the cell surface of CLASP2-deficient erythroblasts (Figures 1M–1O). Strikingly, CD71 expression was higher in 12-week-old than in 6-week-old *Clasp2* KO mice (Figure 1O). Because CD71 is a target of EPO (Sivertsen et al., 2006), the age-dependent increase in CD71 expression in *Clasp2* KO mice indicates that EPO levels also increase with age. EPO levels, in turn, correlate with severity of anemia. We therefore propose that lack of CLASP2 results in progressive anemia.

CLASP2 Is Required for Megakaryopoiesis

Histological sections suggested a deficit of megakaryocytes, the cells that give rise to platelets, in *Clasp2* KO bone marrow (Figures 2A and 2B). Flow cytometry analysis suggested impairment in all stages of megakaryopoiesis (Figures 2C and S2A). Megakaryocytes acquire high DNA ploidy levels by endomitosis, allowing them to grow very large and form many platelets from a single megakaryocyte. DNA staining indicated that *Clasp2* KO megakaryocytes skew toward a lower ploidy status (Figure 2D). Analysis in fetal liver-derived megakaryocyte cultures showed that *Clasp2* KO megakaryocytes were smaller than WT (Figures 2E and 2F). In addition, in bone marrow-derived cultures, 10-fold fewer megakaryocytes developed (Figure 2G), and the fraction of KO megakaryocytes with >8N DNA content was lower (Figure 2H). Furthermore, we observed a decrease in *Clasp2* KO megakaryocyte progenitor cells (colony-forming unit megakaryocyte [CFU-MK]) in clonogenic assays (Figure 2I). Thus, CLASP2 deficiency affects megakaryocytes at the level of progenitors and at later stages. The block in maturation leads to fewer and smaller megakaryocytes with reduced DNA content. Absence of CLASP2 did not appear to impede (pro)platelet formation (Figures S2B–S2E), indicating that CLASP2 is not involved in the final stages of megakaryopoiesis. Platelet activation upon thrombin stimulation was also not affected by the lack of CLASP2 (Figures S2F–S2M),

Because endomitosis requires the MT-based movement of chromosomes, we asked if CLASP2 localizes to the mitotic spindle machinery. Immunofluorescence analysis showed that in WT megakaryocytes from 6 day cultures, CLASP2 colocalizes with the CREST kinetochore marker (Figures 2J–2M). Thus, CLASP2 might have a role in endomitosis as a kinetochore protein. Although this is a novel finding, it is consistent with a role for CLASP2 at kinetochores in fibroblast mitosis (Pereira et al., 2006).

CLASP2 Is Required for HSC Maintenance and Homing

Flow cytometry analysis in HSC-enriched and early progenitor populations revealed a reduction in all fractions in *Clasp2* KO mice (Figures 3A and S3A–S3C), including $Lin^-/Kit^+/Sca1^+$ (LSK) cells, which contain both long- and short-term HSCs, and $CD48^-/CD150^+$ LSK cells, which are further enriched for long-term HSCs (Kiel et al., 2005). Thus, a deficiency of CLASP2 affects HSCs and early progenitors.

To examine whether the stem cell defect in *Clasp2* KO mice is due to malfunctioning HSCs themselves or to an abnormal stromal environment, we performed transplantation assays. We injected bone marrow cells derived from *Clasp2* KO mice and WT littermates into sublethally irradiated recipients and examined donor HSC progeny in the blood of recipient mice after short (i.e., 1 month) and long-term (i.e., 4 months) reconstitution. Bone marrow cells from the *Clasp2* KOs failed to fully reconstitute irradiated recipient mice even with the highest dose of cells injected (Figure 3B). By contrast, bone marrow cells from WT donors reconstituted efficiently, even when few cells were injected (Figure 3B). These data reveal a cell-autonomous HSC defect in *Clasp2* KO mice.

To examine whether CLASP2 plays a role in HSC homing in vivo, we isolated bone marrow cells from WT and *Clasp2* KO mice, loaded these with the fluorescent compound CFSE, and injected cells into sublethally irradiated recipients. Fifteen hours after injection, we examined the number of $CFSE^+$ LSK cells in the bone marrow of the recipient mice and compared this value to the number of original $CFSE^+$ LSK cells injected. The efficiency with which CLASP2-deficient LSK cells homed to their niche in recipient bone marrow was approximately half of that of WT cells (Figure 3C). We conclude that, akin to its role in persistent motility in fibroblasts (Drabek et al., 2006), CLASP2 is involved in the homing of LSK cells in vivo.

CLASP2 Deficiency Affects c-Mpl Transcription

To investigate whether the hematopoietic phenotype in CLASP2-deficient mice might be explained by a differential expression of CLASP1 and CLASP2, we examined *Clasp1* and *Clasp2* mRNA levels in different bone marrow fractions by RT-PCR. This revealed that *Clasps* are expressed at similar levels throughout the hematopoietic system (Figure S3D). Thus, CLASP1 and CLASP2 are not redundant in vivo.

We next investigated at a genome-wide level whether lack of CLASP2 affects distinct genes and/or signaling cascades. Next-generation sequencing of LSK-derived mRNA showed that many mRNAs, including *Actin*, *Clasp1*, and *Slam1* (CD150), were not affected by a lack of CLASP2 (Figures 3D and S3F; Table S1). However, the levels of *Meis1*, which encodes an important transcription factor for megakaryopoiesis and HSC survival (Hisa et al., 2004; Simsek et al., 2010), and of *c-Mpl*, which encodes the TPO receptor (Kaushansky, 2009), were severely reduced in the absence of CLASP2 (Figures 3D and S3F). Real-time PCR confirmed the reduction in *Meis1* (Figure S3E).

One reason for the reduced expression of *Meis1* and *c-Mpl* in LSK cells could be that long-term HSCs are underrepresented in the *Clasp2* KO. We therefore also sequenced $CD150^+$ LSK fractions, which are highly enriched for HSCs (Kiel et al., 2005). Whereas *Meis1* was only moderately affected in *Clasp2* KO $CD150^+$ LSK cells, *c-Mpl* expression was still severely decreased (Figure 3E). Moreover, the expression of *Prdm16*, an HSC marker (Forsberg et al., 2010) and target of c-Mpl in HSCs (Heckl et al., 2011), was also downregulated (Figure 3E). These results suggest that absence of CLASP2 leads to aberrant *c-Mpl* transcription and c-Mpl signaling.

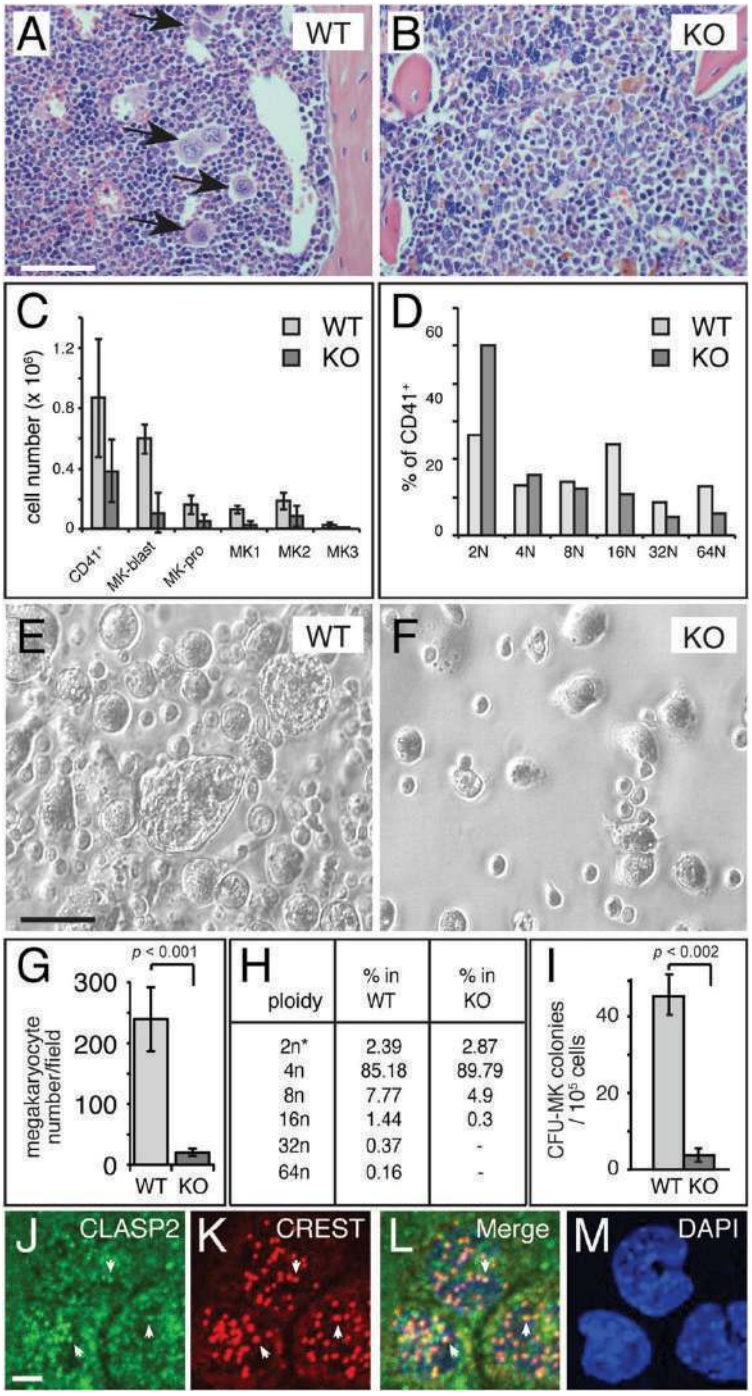

Figure 2. Megakaryocyte Defects in Clasp2 KO Mice

(A and B) Hematoxylin and eosin-stained sections of the bone marrow. (A) WT and (B) *Clasp2* KO bone marrow is shown. Megakaryocytes are indicated with arrows. Scale bar, 100 μm.

(C) Megakaryocyte differentiation in the bone marrow. Consecutive stages in megakaryocyte differentiation were analyzed by flow cytometry. MK-blast, megakaryoblast; MK-pro, megakaryocyte progenitor; MK1, MK2, and MK3, early and mature megakaryocytes. SD is indicated.

(D) DNA content in bone marrow megakaryocytes. Ploidy levels measured by flow cytometry in two WT and two *Clasp2* KO mice and expressed as percentages of total number of $CD41^+$ cells are presented. Average values are shown.

(E–H) Liquid megakaryocyte cultures. Phase-contrast images (E and F), megakaryocyte counts (G), and DNA content analysis (H) of fetal liver (E and F) and adult (G and H) megakaryocyte cultures from WT and *Clasp2* KO are presented. (G) SEM is indicated; t test reveals significant difference. (H) Ploidy levels in five WT and seven KO cultures expressed as percentages of total number of observed cells are demonstrated. Scale bar, 50 μm.

(I) CFU-MK progenitor assay. Number of colonies (per 50,000 cells seeded) counted after 10 days in culture is shown (SD is indicated; t test reveals significant difference).

(J–M) Localization of CLASP2 in megakaryocytes. WT cells were stained with CLASP2 antibodies (green), the kinetochore marker CREST6 (red), and DAPI (blue). Kinetochore association of CLASP2 is indicated by arrows. Scale bar, 3 μm.

See also Figure S2.

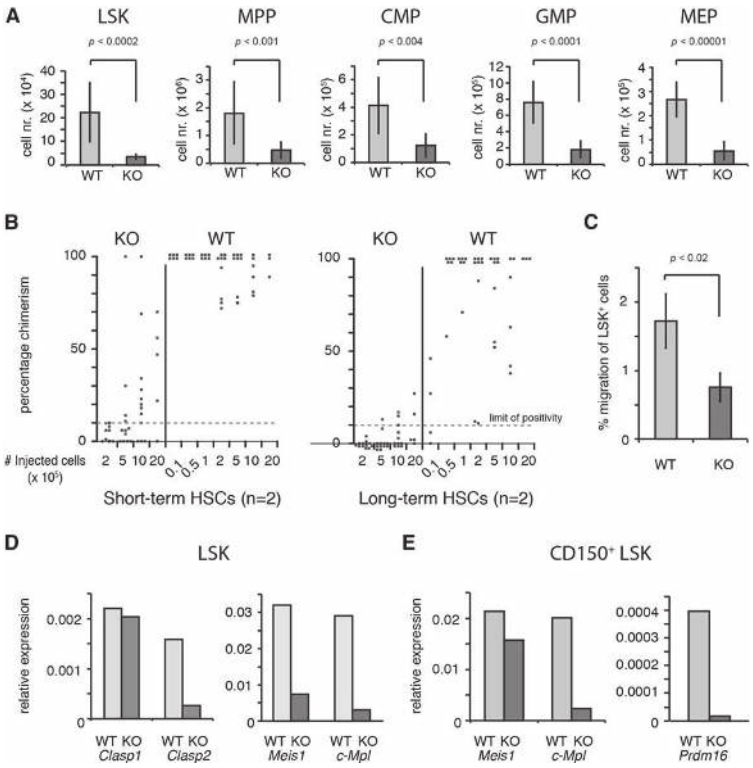

Figure 3. HSC and Progenitor Defects in Clasp2 KO Mice

(A) Analysis of HSC-enriched (LSK) and hematopoietic progenitor (MPP, CMP, GMP, MEP) cells from WT and *Clasp2* KO bone marrow is shown (see Figures S3A and S3B for flow cytometry examples). SD is indicated; t tests reveal significant differences. cell nr., cell number.

(B) In vivo hematopoietic repopulation analysis. Irradiated recipient mice were injected with bone marrow cells from adult *Clasp2* KO or WT mice. Analyses were performed at 1 month (short term) and 4 months (long term) post-transplantation (n = 2). Percentage of chimerism is indicated, with each dot representing a transplanted mouse. The number of cells injected per recipient is indicated below the graph. Mice showing greater than 10% donor chimerism (limit of positivity) in peripheral blood are considered as reconstituted.

(C) In vivo homing assay. CFSE-loaded bone marrow cells from two WT and two *Clasp2* KO mice were intravenously injected into the tails of irradiated recipient mice. $CFSE^+$ LSK numbers in WT and KO donor and recipient mice, at the onset and 15 hr after injection, respectively, were calculated (SD is indicated; t test reveals significant differences).

(D and E) Next-generation sequencing of RNA from WT and *Clasp2* KO LSK (D) or $CD150^+$ LSK (E) populations is shown. Expression of indicated genes is relative to *Actin*.

See also Figure S3 and Table S1.

CLASP2 Organizes the MT Network upon Cell Attachment

CLASP2 selectively regulates MT stabilization in motile fibroblasts (Akhmanova et al., 2001). Because fibroblast adherence also results in selective MT stabilization (Palazzo et al., 2004), we asked whether CLASP2 is involved in this process too. Indeed, CLASP2-deficient fibroblasts plated on a fibronectin-coated matrix contained less stable MTs compared to WT cells (Figure S4).

Next, we isolated WT and CLASP2-deficient HSC-enriched (LSK) cells, allowed them to attach, and examined the MT network and associated organelles using specific antibodies. EB1 staining revealed ample-growing MTs, which originated at the centrosome and circumnavigated the nucleus (Figures 4A–4C). No obvious difference was observed in the number of EB1 dots in WT and CLASP2-deficient HSC-enriched cells. Examination of the MT network using anti-α-tubulin antibodies revealed a cage-like organization in most of the WT cells, with MTs originating at the centrosome and surrounding the nucleus (Figures 4D and 4E). The Golgi network, as observed with anti-GM130 antibodies, was clustered around the centrosome; its organization was similar in WT and *Clasp2* KO HSC-enriched cells (Figures 4F and 4G).

In contrast to the Golgi apparatus, the distribution of stable MTs was significantly different in CLASP2-deficient HSC-enriched cells compared to WT cells (Figures 4H–4L). MT organization was also affected, i.e., approximately half of the CLASP2-deficient HSC-enriched cells contained a cage-like MT organization compared to WT cells (Figure 4M). Combined, our data suggest that CLASP2 is required for cell attachment and the subsequent stabilization of the MT network, as well as its organization, both in freshly isolated HSC-enriched cells as well as in cultured MEFs.

DISCUSSION

We show here that CLASP2 is essential for mouse hematopoiesis, acting at multiple steps in erythroid, megakaryocytic, lymphoid, and myeloid differentiation. Shortages in RBCs and platelets in *Clasp2* KO mice lead to increased EPO and TPO levels and induce a stress response. However, these reactions are insufficient, and thus, an enhanced replenishment by HSCs is required. Because CLASP2 is also necessary, in a cell-autonomous manner, for HSC maintenance, the stem cell pool becomes exhausted in *Clasp2* KO mice, explaining the progressive pancytopenia. This phenotype resembles that of patients with congenital amegakaryocytic thrombocytopenia, which starts as a severe thrombocytopenia at birth and then rapidly progresses to pancytopenia (Ballmaier and Germeshausen, 2009). Most patients carry a mutation in the *c-Mpl* gene.

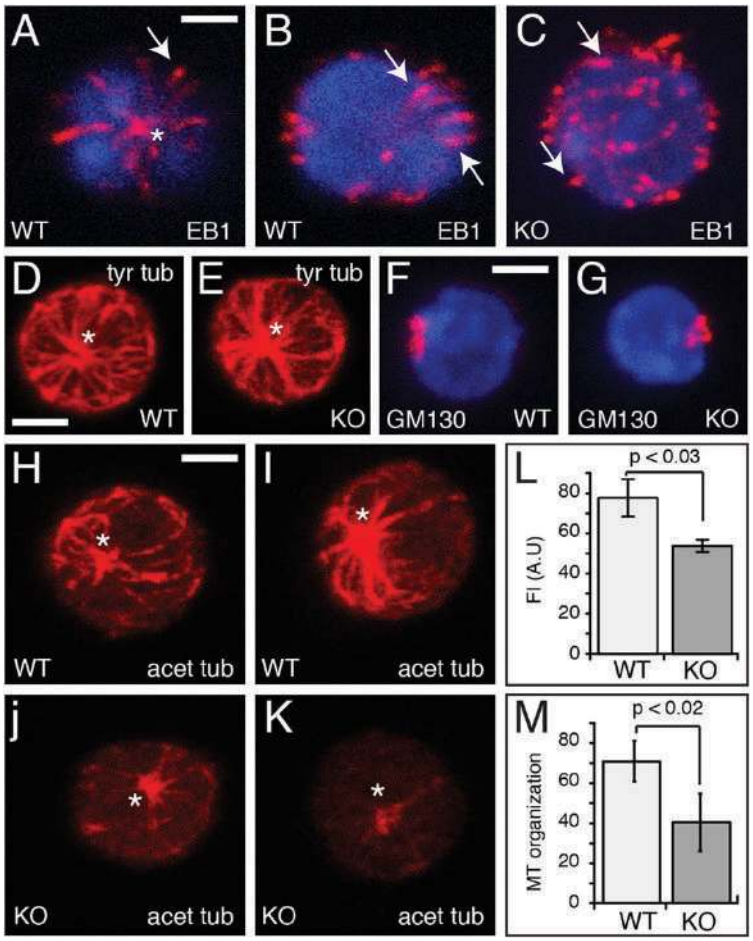

Figure 4. CLASP2 Stabilizes and Organizes MTs in HSC-Enriched Cells

(A–K) Immunofluorescence analysis. HSC-enriched cells from WT and *Clasp2* KO mouse bone marrow were deposited on poly-L-lysine-coated coverslips, incubated for 30 min, and stained with antibodies against EB1 (A–C), tyrosinated tubulin (tyr tub) (D and E), GM130 (F and G), and acetylated tubulin (acet tub) (H–K). Maximum intensity projections of cells are shown, except in (A) and (B), where bottom and top projections, respectively, of the same cell are shown. Centrosomes are indicated by asterisks. Arrows indicate EB1-comets, decorating the ends of growing MTs. Scale bars, 2 μm.

(L and M) Quantification of MT stability and organization. The amount of stable MTs per HSC-enriched cells, and of HSC-enriched cells with a "cage-like" MT network, was measured using fluorescence intensity (FI) of antibodies (SD is indicated; t tests reveal significant differences). AU, arbitrary unit.

See also Figure S4.

Strikingly, one of the most downregulated genes in *Clasp2* KO HSC-enriched fractions is *c-Mpl*. Thus, a major molecular mechanism underlying the HSC maintenance defect in *Clasp2* KO mice might be impaired TPO signaling through c-Mpl.

How is it possible that CLASP1, which is similar to CLASP2 and also expressed in the hematopoietic system, cannot compensate for a CLASP2 deficiency? One explanation is that CLASP levels are critical, such that in the absence of CLASP2, there is not enough CLASP1 to compensate for a lack of CLASP2. Alternatively, CLASP2 might be recruited by signaling pathways that do not act on CLASP1, and vice versa. Recent work has indeed shown that CLASP1, and not CLASP2, is important for maintaining spindle position and a correct cell division axis in human cells (Samora et al., 2011). CLASPs may therefore coexist in cells, but distinct cascades, acting through phosphorylation (Kumar et al., 2009), might selectively affect their activity toward MTs.

Our data show that despite their round shape and small cytoplasm attached HSC-enriched cells are polarized, with centrosome and Golgi located at one side of the nucleus and the plus ends of MTs emanating toward the other side. Both in these cells and in fibroblasts, CLASP2 stabilizes and organizes the MT network. Furthermore, CLASP2 is required for the proper attachment of fibroblasts, HSC-enriched cells, and platelets, indicating a general role for this protein in cell attachment. It remains to be shown whether an integrin-LL5-CLASP2-MT connection is operative in these systems as it is in epithelial cells (Hotta et al., 2010). We hypothesize that in the absence of CLASP2, long-term HSCs do not recognize their bone marrow niche anymore because of faulty attachment and/or migration, turn off *c-Mpl* transcription due to deregulated signaling and thereby lose stem cell potential.

EXPERIMENTAL PROCEDURES

Miscellaneous Assays

We have obtained all the necessary permissions from local and national review boards for the mice used in our research. Gene targeting and immunohistochemistry techniques (Hoogenraad et al., 2002), generation of CLASP2-deficient fibroblasts and immunofluorescent staining assays (Drabek et al., 2006), and standard molecular biology techniques (Sambrook et al., 1989) have been described. See Extended Experimental Procedures for details.

Hematological Analyses

Hematological assays were performed in peripheral blood, platelets, bone marrow, spleen, thymus, and lymph nodes. Where needed, cells were sorted by flow cytometry and analyzed with FlowJo software. For in vivo HSC analysis, total bone marrow cells from adult WT and *Clasp2* KO male mice were intravenously injected into irradiated recipients. After 1 and 4 months, donor chimerism was analyzed by semiquantitative PCR on peripheral blood. For

the in vivo homing assay, bone marrow cells from WT and *Clasp2* KO mice were labeled with CFSE, analyzed by flow cytometry to estimate the percentage of $CFSE^+$ LSK cells (time point 0 hr), and intravenously injected into irradiated recipients. After injection (15 hr), bone marrow cells were collected, and the number of $CFSE^+$ LSK cells was again determined. The fraction of LSK cells homing into the bone marrow was calculated by dividing the number of donor $CFSE^+$ LSK cells at 15 hr by the number of $CFSE^+$ LSK cells injected at 0 hr. See Extended Experimental Procedures for details.

Genome-wide Transcriptome Analyses

RNA was isolated from LSK and $CD150^+$ LSK fractions from WT and *Clasp2* KO mice and sequenced using the Illumina platform. See Extended Experimental Procedures for further details.

SUPPLEMENTAL INFORMATION

Supplemental Information includes Extended Experimental Procedures, four figures, and one table and can be found with this article online at http://dx.doi.org/10.1016/j.celrep.2012.08.040.

LICENSING INFORMATION

ACKNOWLEDGMENTS

We would like to thank Reinier van der Linden for help with flow cytometry. This work was supported by The Netherlands Organization for Scientific Research (ALW and ZonMw), a VENI grant (863.09.012) to L.G., the Dutch Cancer Society (KWF) and Cancer Genomics Center (CGC), an EC integrated project (LSHG-CT-2003-503259), NIH grant HL68130, grants PTDC/SAU-GMG/099704/2008 and PTDC/SAU-ONC/112917/2009 from Fundação para a Ciência e a Tecnologia of Portugal (COMPETE-FEDER), the Human Frontier Research Program, and the 7th framework program grant PRECISE from the European Research Council.

Received: January 30, 2012
Revised: July 9, 2012
Accepted: August 31, 2012
Published online: October 18, 2012

REFERENCES

Akhmanova, A., Hoogenraad, C.C., Drabek, K., Stepanova, T., Dortland, B., Verkerk, T., Vermeulen, W., Burgering, B.M., De Zeeuw, C.I., Grosveld, F., and Galjart, N. (2001). Clasps are CLIP-115 and -170 associating proteins involved in the regional regulation of microtubule dynamics in motile fibroblasts. Cell *104*, 923–935.

Ballmaier, M., and Germeshausen, M. (2009). Advances in the understanding of congenital amegakaryocytic thrombocytopenia. Br. J. Haematol. *146*, 3–16.

Drabek, K., van Ham, M., Stepanova, T., Draegestein, K., van Horssen, R., Sayas, C.L., Akhmanova, A., Ten Hagen, T., Smits, R., Fodde, R., et al. (2006). Role of CLASP2 in microtubule stabilization and the regulation of persistent motility. Curr. Biol. *16*, 2259–2264.

Forsberg, E.C., Passegué, E., Prohaska, S.S., Wagers, A.J., Koeva, M., Stuart, J.M., and Weissman, I.L. (2010). Molecular signatures of quiescent, mobilized and leukemia-initiating hematopoietic stem cells. PLoS One *5*, e8785.

Galjart, N. (2010). Plus-end-tracking proteins and their interactions at microtubule ends. Curr. Biol. *20*, R528–R537.

Heckl, D., Wicke, D.C., Brugman, M.H., Meyer, J., Schambach, A., Büsche, G., Ballmaier, M., Baum, C., and Modlich, U. (2011). Lentiviral gene transfer regenerates hematopoietic stem cells in a mouse model for Mpl-deficient aplastic anemia. Blood *117*, 3737–3747.

Hisa, T., Spence, S.E., Rachel, R.A., Fujita, M., Nakamura, T., Ward, J.M., Devor-Henneman, D.E., Saiki, Y., Kutsuna, H., Tessarollo, L., et al. (2004). Hematopoietic, angiogenic and eye defects in Meis1 mutant animals. EMBO J. *23*, 450–459.

Hoogenraad, C.C., Koekkoek, B., Akhmanova, A., Krugers, H., Dortland, B., Miedema, M., van Alphen, A., Kistler, W.M., Jaegle, M., Koutsourakis, M., et al. (2002). Targeted mutation of Cyln2 in the Williams syndrome critical region links CLIP-115 haploinsufficiency to neurodevelopmental abnormalities in mice. Nat. Genet. *32*, 116–127.

Hotta, A., Kawakatsu, T., Nakatani, T., Sato, T., Matsui, C., Sukezane, T., Akagi, T., Hamaji, T., Grigoriev, I., Akhmanova, A., et al. (2010). Laminin-based cell adhesion anchors microtubule plus ends to the epithelial cell basal cortex through LL5alpha/beta. J. Cell Biol. *189*, 901–917.

Kaushansky, K. (2009). Molecular mechanisms of thrombopoietin signaling. J. Thromb. Haemost. *7*(*Suppl 1*), 235–238.

Kiel, M.J., Yilmaz, O.H., Iwashita, T., Yilmaz, O.H., Terhorst, C., and Morrison, S.J. (2005). SLAM family receptors distinguish hematopoietic stem and progenitor cells and reveal endothelial niches for stem cells. Cell *121*, 1109–1121.

Kumar, P., Lyle, K.S., Gierke, S., Matov, A., Danuser, G., and Wittmann, T. (2009). GSK3beta phosphorylation modulates CLASP-microtubule association and lamella microtubule attachment. J. Cell Biol. *184*, 895–908.

Lansbergen, G., Grigoriev, I., Mimori-Kiyosue, Y., Ohtsuka, T., Higa, S., Kitajima, I., Demmers, J., Galjart, N., Houtsmuller, A.B., Grosveld, F., and Akhmanova, A. (2006). CLASPs attach microtubule plus ends to the cell cortex through a complex with LL5beta. Dev. Cell *11*, 21–32.

Palazzo, A.F., Eng, C.H., Schlaepfer, D.D., Marcantonio, E.E., and Gundersen, G.G. (2004). Localized stabilization of microtubules by integrin- and FAK-facilitated Rho signaling. Science *303*, 836–839.

Pereira, A.L., Pereira, A.J., Maia, A.R., Drabek, K., Sayas, C.L., Hergert, P.J., Lince-Faria, M., Matos, I., Duque, C., Stepanova, T., et al. (2006). Mammalian CLASP1 and CLASP2 cooperate to ensure mitotic fidelity by regulating spindle and kinetochore function. Mol. Biol. Cell *17*, 4526–4542.

Richmond, T.D., Chohan, M., and Barber, D.L. (2005). Turning cells red: signal transduction mediated by erythropoietin. Trends Cell Biol. *15*, 146–155.

Sambrook, J., Fritsch, E.F., and Maniatis, T. (1989). Molecular Cloning: A Laboratory Manual, Second Edition (Cold Spring Harbor, NY: Cold Spring Harbor Laboratory Press).

Samora, C.P., Mogessie, B., Conway, L., Ross, J.L., Straube, A., and McAinsh, A.D. (2011). MAP4 and CLASP1 operate as a safety mechanism to maintain a stable spindle position in mitosis. Nat. Cell Biol. *13*, 1040–1050.

Simsek, T., Kocabas, F., Zheng, J., Deberardinis, R.J., Mahmoud, A.I., Olson, E.N., Schneider, J.W., Zhang, C.C., and Sadek, H.A. (2010). The distinct metabolic profile of hematopoietic stem cells reflects their location in a hypoxic niche. Cell Stem Cell *7*, 380–390.

Sivertsen, E.A., Hystad, M.E., Gutzkow, K.B., Døsen, G., Smeland, E.B., Blomhoff, H.K., and Myklebust, J.H. (2006). PI3K/Akt-dependent Epo-induced signalling and target genes in human early erythroid progenitor cells. Br. J. Haematol. *135*, 117–128.

Supplemental Information

EXTENDED EXPERIMENTAL PROCEDURES

Antibodies and Reagents

For immunofluorescence studies and Western blot analysis, we used monoclonal anti-CLASP1 and −2 antibodies (Maffini et al., 2009), rabbit polyclonal antibodies #2358 against CLASP2 (Akhmanova et al., 2001), antiserum #2360 against CLIP-170 (Coquelle et al., 2002), antiserum #2221 against CLIP-115 and –170, antiserum #2238 against CLIP-115 (Hoogenraad et al., 2002), and anti-EB3 antisera (Stepanova et al., 2003). The anti-CREST6 antibodies were a kind gift of Dr. Y. Mimori-Kiyosue (KAN Research Institute, Kyoto, Japan). The following antibodies were purchased: anti-GFP antibodies (Abcam and Santa Cruz, Roche), mouse monoclonal antibodies against α-tubulin and acetylated alpha-tubulin (Sigma), and actin (Chemicon). Secondary antisera were alkaline phosphatase-labeled anti-rabbit and anti-mouse antibodies (Sigma), and FITC-conjugated goat anti-rabbit IgG and Alexa594-conjugated goat anti-human antisera (Molecular Probes).

For flow cytometry analysis we used the following antibodies: Ter119 Pacific Blue or PerCP-Cy5.5 conjugated (eBiosciences), CD41 PE, CD71 PE conjugated or biotinylated, c-kit APC or APC-Cy7 conjugated, Lineage cocktail APC conjugated, CD3e-biotin, B220-biotin, CD11b-biotin, Gr1-biotin, CD16/CD32 PE conjugated, CD127 biotin, CD34 Pacific Blue, Alexa Fluor 647 (eBiosciences) or PerCp-Cy5.5, Sca1 PE-Cy7, streptavidin APC-Cy7, PE-Cy5, PerCP-Cy5.5 or Pacific Blue (Invitrogen) conjugated. Antibodies were from BD Biosciences unless otherwise indicated. Hoechst 33342 (Invitrogen) was used to stain dead cells.

Generation of Clasp2-Deficient Mice and MEFs

Targeting techniques and the procedures for selection of ES cells and generation of KO mice (Akhmanova et al., 2005; Hoogenraad et al., 2002) have been described. Targeting efficiency in ES cells was very low (1/800). The positive ES cell clone contained a correct karyotype and was injected into blastocysts. One of four chimeras gave germline transmission and was mated into the C57BL/6 background to generate inbred *Clasp2* heterozygous and homozygous KO mice. The generation of CLASP2-deficient MEFs has been described (Drabek et al., 2006).

Fibroblast Adhesion Assay

MEF adhesion experiments were essentially carried out as published (Palazzo et al., 2004). For IF analysis of the cell adhesion of MEFs, coverslips were coated with 25 μg/ml fibronectin or poly-L-ornithin (Invitrogen) and cells were examined 90 min after adhesion. Attachment on poly-L-ornithin does not lead to stable MT formation, neither in WT fibroblasts nor in CLASP2-deficient cells (data not shown).

To test adhesion capacity, a colorimetric assay was used. Briefly, trypsinized and resuspended cells were plated in 96-well plates coated with fibronectin of poly-L-ornithin (30,000 cells per well). Cells were fixed 90 min after adhesion, washed and stained with Crystal Violet (0.5%) for 10 min. Plates were washed with water and air-dried. Absorbance was read at 570 nm using a plate reader. This adhesion assay revealed that *Clasp2* KO MEFs do not attach as efficiently as WT cells (data not shown).

Immunofluorescence Analysis

For IF analysis of megakaryocytes, cells were cultured under the conditions described below. After 6 days of culture cells were centrifuged onto poly-L-lysine-coated coverslips at 400 rpm for 5 min, fixed for 15 min in ice-cold methanol/1mM EGTA and permeabilized with 0.5% Triton X-100. After blocking with 1% bovine serum albumin (BSA) in PBS, slides were incubated with a 1:300 dilution of primary antibodies, for one hour at room temperature. After washing, cells were incubated with FITC-conjugated goat anti-rabbit IgG (1:100) and/or Alexa594-conjugated goat anti-human (1:300) antibodies, again for one hour at room temperature. Cells were counterstained with DAPI to visualize nuclear DNA. Controls were processed identically, except for the omission of the primary antibody, and did not give a detectable signal (data not shown).

For IF analysis of HSC-enriched cells, bone marrow single cell suspensions from *Clasp2* KO mice and WT littermates were stained with Lineage cocktail APC, c-kit APC-Cy7 and Sca1 PE-Cy7 conjugated antibodies. The HSC-enriched cells were sorted in the FACSAria (BD Biosciences). Cells were concentrated by centrifugation and then spotted in a small volume (∼10 μl) onto poly-L-lysine (Invitrogen) coated coverslips. Cells were allowed to adhere to the glass at 37°C for ∼30 min in StemPro®-34 SFM supplemented with B-27 Serum-Free Supplement and 1% Penicillin/Streptomycin/L-glutamine solution (Invitrogen). Cells were fixed and incubated with antibodies as described previously (Drabek et al., 2006). IF image acquisition was carried out as described (Akhmanova et al., 2005; Boisset et al., 2010). In Figures 4L and 4M, the fluorescence intensity (FI) of maximum intensity projections (MIPs) of cells, stained with anti-acetylated tubulin antibodies (which represents the amount of stable MTs) was quantified by placing exactly fitting ROIs around the cells and measuring the average FI (11 WT and 12 KO cells analyzed). Note that the difference between WT and KO is actually underestimated because in the WT MIP the FI is saturated in many areas of the cell (due to the stacking of the images), whereas this is not the case in KO cells. To quantify MT organization, cells with a "cage-like" MT network (see Figures 4D, 4E, and 4I), as identified with antibodies against tyrosinated tubulin and acetylated tubulin, were quantified in different microscopic slides containing WT (WT) or *Clasp2* KO HSC-enriched cells (>300 WT and KO cells analyzed).

Hematological Analysis

Peripheral blood samples were taken from the retro-orbital venous plexus using EDTA-coated tubes. Blood counts were determined with a Vet'ABC counter (SCIL, Viernheim, Germany).

The analysis of erythropoietin (EPO) levels in plasma was performed using the Quantikine mouse/rat EPO immunoassay (BD Biosciences, Franklin Lakes, NJ). Thrombopoietin (TPO) levels were determined in serum by ELISA (Quantikine Mouse TPO Immunoassay; R&D Systems), according to the manufacturer's instructions. Serum levels from each mouse were measured in duplicate. Values were imported into Aabel (Gigawiz) for graphical representation and statistical analysis.

Colony forming unit- and burst forming unit-erythroid (CFUe and BFUe) assays were performed by culturing $2x10^5$ cells per 35mm dish in methylcellulose media (MethoCult M3234, Stem Cell Technologies, Vancouver, Canada) supplemented with 4U/ml human recombinant EPO, (Janssen-Cilag, Issy-les-Moulineaux, France), 100ng/ml murine recombinant stem cell factor (SCF), 20 μg/ml iron-saturated human transferrin, $2x10^{-4}$ M hemin (Sigma) and 1% Penicillin/Streptomycin/L-glutamine solution (Invitrogen, Gaithersburg MD). Colony numbers were determined after 3 days (CFUe) or 8 days (BFUe) of culture on triplicate dishes.

Megakaryocytes were cultured from 13.5 day fetal livers in DMEM (GIBCO), supplemented with 10% fetal bovine serum, 2 mM L-glutamine and 1% tissue culture supernatant from a murine TPO producer cell line (Villeval et al., 1997). After 3 days of culture, megakaryocytes were enriched on a BSA gradient as described previously (Italiano et al., 1999). Megakaryocytes from three WT and three *Clasp2* KO mice were counted after 6 days of culture in at least 5 microscopic fields of each culture. For proplatelet formation analysis, cultures were analyzed on day 5 by phase contrast microscopy.

For the megakaryocyte progenitor cell assay (CFU-MK assay) bone marrow cells from 2 WT and 2 *Clasp2* KO mice were collected by flushing femurs and tibias of *Clasp2* KO or WT mice with Iscove's MDM containing 2% fetal bovine serum. Serum-free collagen assays were performed with a MegaCult TM -C kit (StemCell Technologies Inc.; Vancouver, Canada). A combination of human recombinant growth factors was used as a source of megakaryocyte (MK) colony-stimulating activity: 1.1 mg/ml collagen, 1% bovine serum albumin (BSA), 10 g/ml bovine pancreatic insulin, 200 g/ml iron-saturated human transferrin, 50 ng/ml thrombopoietin, 10 ng/ml interleukin 6, and 10 ng/ml interleukin 3. Cultures were prepared according to the manufacturer's instructions. The final culture mixture of 1.5 ml was dispensed into the two wells (0.75 ml each) of a chamber slide and incubated in humidified 5% CO_2 incubator at 37°C. After 10 days of incubation, slides were fixed in cold acetone (15 min), stained, and CFU-MK colonies were counted. CFU-MKs were identified by the detection of acetylcholinesterase activity of megakaryocytes. A CFU-MK colony was defined as a cluster of three or more MK cells detected by light microscopy.

To measure the DNA content of cultured megakaryocytes, individual single-cell suspensions were made from bone marrow harvested from the femurs of 5 WT and 7 *Clasp2* KO mice. Cells were cultured using the conditions described above. After the second day of culture, megakaryocytes were purified on a BSA gradient, cultured for one more day, and prepared for flow cytometry analysis. In short, harvested cells were fixed in ice-cold 70% ethanol for 48 hr, centrifuged and resuspended in PBS. Cells were subsequently stained with propidium iodide (PI) in a triton/RNase solution for 30 min at room temperature, and the DNA content was measured using a FACScan flow cytometer (Becton Dickinson). The proportion of cells in each ploidy class was determined by integrating the area under each peak. Lymphocytes from the spleen were used as 2n/4n control.

To measure the DNA content of freshly isolated bone marrow megakaryocytes, mouse bone marrow single cell suspensions were incubated with anti-CD41-PE (BD PharMingen, San Diego) for 1 hr on ice in PBS/1%BSA. Cells were then washed with 10 volumes PBS/1%BSA and spun at 1000 rpm for 5 min. Cells were resuspended in Cytofix/Cytoperm solution (Cytofix/Cytoperm, BD Biosciences) and incubated 30 min on ice. Cells were spun at 1000 rpm for 5 min, resuspended in 80% EtOH and incubated 30 min at −20°C. Cells were spun at 1000 rpm for 5 min and resuspended in PBS containing 50 μg/mL Hoechst 33342, 0.1% Triton X-100 and 50 μg/mL RNase and incubated for 1hr at RT. Samples were analyzed on a flow cytometer (LSR-II, BD Biosciences) and analyzed with FlowJo software. Megakaryocytes were identified as CD41-positive cells and Hoechst 33342 staining intensity was used as a measure of DNA ploidy.

Platelet Adhesion and Morphology

For platelet adhesion assays, whole blood was perfused over collagen-coated (Horm-Collagen type I, 100 μg/ml) slides at a shear rate of 1300^{s-1}. Whole blood volume corresponding to the same circulating platelet number was perfused, after which adhered platelets were washed with PBS for 5 min. Platelets were then labeled with CD41 PE or CD61 FITC conjugated antibodies and photos were taken at 200x magnification with an EVOS microscope. Coverage (fluorescence) was quantified with ImageJ software.

For morphology assays platelets were separated from whole blood by sequential centrifugation (Schwer et al., 2001). Platelets from the resulting platelet rich plasma (PRP) were allowed to rest for 30 min at 37°C, before fixation. To examine cell shape, platelets were fixed with an equal volume of 8% PFA for 20 min and centrifuged onto poly-L-lysine (Sigma) coated coverslips, or fixed in 1% glutaraldehyde in platelet buffer (145 mM NaCl, 10 mM HEPES [pH 7.4], 10 mM glucose, 0.2 mM Na_2HPO_4, 5 mM KCl) for 20 min and moved to a coverslip chamber. Images were obtained using 63x differential interference contrast objective equipped with a 1.5X optivar.

Long-Term Transplantation Assay and Analysis

For in vivo HSC analysis, total bone marrow cells (cell doses are indicated in Figure 3) from adult WT and *Clasp2* KO male mice were intravenously injected into irradiated (9 Gy split dose, ^{137}Cs-source) female recipients. After 1 and 4 months, donor chimerism (*YMT*) was analyzed by semiquantitative PCR on peripheral blood. Signal quantitation was by DNA normalization (*myogenin*) and *YMT* control DNA dilutions (0, 1, 3, 10, 30, 60 and 100%).

In Vivo Homing Assay

Bone marrow (BM) cells were flushed from the tibiae and femura of WT and *Clasp2* KO mice with PBS/10% FBS. The mononuclear cells (MNC) were isolated after Ficoll-Hypaque gradient, washed and counted. Cells were then labeled with the cytoplasmic dye carboxyfluorescein diacetate succinimidyl diester (CFSE, Invitrogen) according to manufacturer's instructions (concentration: 4 μM). More than 99% of the cells were positively stained, with a fluorescence intensity ranging between 10^4 and 10^5 arbitrary units. Part of the $CFSE^+$ cells was further stained with specific antibodies and analyzed by flow cytometry (BD Biosciences, FACS Aria III) to estimate the percentage of $CFSE^+$ LSK cells in the cell suspension (this time point was designated 0h). Two doses of $CFSE^+$ MNC (5×10^6 and 12×10^6) were intravenously injected into irradiated (900 rads) adult C57Bl/6 recipients. Fifteen hours after injection (15h), the BM cells from each recipient were collected from both femurs and tibias and MNC were isolated after Ficoll. The number of $CFSE^+$ LSK cells (i.e., from donor origin) that homed into the BM was determined by flow cytometry similar to the 0h time-point. The percentage of WT and *Clasp2* KO LSK cells homing into the BM was calculated by dividing the number of donor ($CFSE^+$) LSK at 15h by the number of $CFSE^+$ LSK injected at 0h and multiplying this value with 100.

Smarter RNA-Seq-Based Gene Expression Analysis on HSC-Enriched Cells

For RNA sequencing of LSK fractions, cells were pooled from 2 WT mice, and 2 *Clasp2* KO mice. For RNA sequencing of $CD150^+$ LSK fractions, cells were individually isolated from 2 WT mice, and 2 *Clasp2* KO mice. Total RNA (100 pg for LSK, 500 pg for $CD150^+$ LSK) of each sample was isolated and converted to cDNA using the Smarter ultra low RNA kit (Clontech). The cDNA was used in the TrueSeq DNA sample prep kit (Illumina v3) to prepare an indexed sequencing library. Samples were sequenced for 36 bp on a HiSeq 2000 using Illumina v3 chemistry.

Illumina BaseCall results were demultiplexed using NARWHAL (Brouwer et al., 2011). The reads were aligned using Tophat (Trapnell et al., 2009) against the UCSC mm9 reference genome, using Ensembl genes.gtf annotation provided by Illumina iGenomes (http://www.illumina.com). For *Clasp2* KO LSK mRNA we obtained 45.7 million reads, of which 83.4% aligned back to the reference genome, for WT LSK mRNA we obtained 45.8 million reads with 81.7% alignment, for *Clasp2* KO $CD150^+$ LSK mRNA we obtained 71.7 million reads, with 84.9% alignment, and for WT $CD150^+$ LSK mRNA we obtained 39.7 million reads with 82.4% alignment. FPKM (Fragments Per Kilobase transcript per Million mapped reads) expression levels were calculated by Cufflinks (Trapnell et al., 2010).

Real-Time PCR

RNA was pooled from 7 WT and 7 *Clasp2* KO mice. Flow cytometry was used to isolate the LSK fraction (WT LSK: 0.66 ± 0.23% of live cells, KO LSK: 0.13 ± 0.09 of live cells, $p < 0.02$ t test). Real time PCR was performed as described (van de Nobelen et al., 2010) to quantify *Actin* (forward primer: 5′-AGGTCATCACTATTGGCAAC-3′, reverse primer: 5′-AGAGGTCTTTACGGATGTCA-3′) and *Meis1* (forward primer: 5′-TCACACAGTGGGGATAACAG-3′, reverse primer: 5′-ACGCTTTTTGTGACGCTTTT-3′) levels. PCR was performed using Platinum Taq, (Invitrogen, cat no. 10966-034) and the Real-time PCR CFX96 detection system (BIO-RAD).

SUPPLEMENTAL REFERENCES

Akhmanova, A., Hoogenraad, C.C., Drabek, K., Stepanova, T., Dortland, B., Verkerk, T., Vermeulen, W., Burgering, B.M., De Zeeuw, C.I., Grosveld, F., and Galjart, N. (2001). Clasps are CLIP-115 and -170 associating proteins involved in the regional regulation of microtubule dynamics in motile fibroblasts. Cell *104*, 923–935.

Akhmanova, A., Mausset-Bonnefont, A.L., van Cappellen, W., Keijzer, N., Hoogenraad, C.C., Stepanova, T., Drabek, K., van der Wees, J., Mommaas, M., Onderwater, J., et al. (2005). The microtubule plus-end-tracking protein CLIP-170 associates with the spermatid manchette and is essential for spermatogenesis. Genes Dev. *19*, 2501–2515.

Boisset, J.C., van Cappellen, W., Andrieu-Soler, C., Galjart, N., Dzierzak, E., and Robin, C. (2010). In vivo imaging of haematopoietic cells emerging from the mouse aortic endothelium. Nature *464*, 116–120.

Brouwer, R.W., van den Hout, M.C., Grosveld, F.G., and van Ijcken, W.F. (2011). NARWHAL, a primary analysis pipeline for NGS data. Bioinformatics.

Bulinski, J.C., and Gundersen, G.G. (1991). Stabilization of post-translational modification of microtubules during cellular morphogenesis. Bioessays *13*, 285–293.

Coquelle, F.M., Caspi, M., Cordelières, F.P., Dompierre, J.P., Dujardin, D.L., Koifman, C., Martin, P., Hoogenraad, C.C., Akhmanova, A., Galjart, N., et al. (2002). LIS1, CLIP-170's key to the dynein/dynactin pathway. Mol. Cell. Biol. *22*, 3089–3102.

Drabek, K., van Ham, M., Stepanova, T., Draegestein, K., van Horssen, R., Sayas, C.L., Akhmanova, A., Ten Hagen, T., Smits, R., Fodde, R., et al. (2006). Role of CLASP2 in microtubule stabilization and the regulation of persistent motility. Curr. Biol. *16*, 2259–2264.

Hoogenraad, C.C., Koekkoek, B., Akhmanova, A., Krugers, H., Dortland, B., Miedema, M., van Alphen, A., Kistler, W.M., Jaegle, M., Koutsourakis, M., et al. (2002). Targeted mutation of Cyln2 in the Williams syndrome critical region links CLIP-115 haploinsufficiency to neurodevelopmental abnormalities in mice. Nat. Genet. *32*, 116–127.

Italiano, J.E., Jr., Bergmeier, W., Tiwari, S., Falet, H., Hartwig, J.H., Hoffmeister, K.M., André, P., Wagner, D.D., and Shivdasani, R.A. (2003). Mechanisms and implications of platelet discoid shape. Blood *101*, 4789–4796.

Italiano, J.E., Jr., Lecine, P., Shivdasani, R.A., and Hartwig, J.H. (1999). Blood platelets are assembled principally at the ends of proplatelet processes produced by differentiated megakaryocytes. J. Cell Biol. *147*, 1299–1312.

Kiel, M.J., Yilmaz, O.H., Iwashita, T., Yilmaz, O.H., Terhorst, C., and Morrison, S.J. (2005). SLAM family receptors distinguish hematopoietic stem and progenitor cells and reveal endothelial niches for stem cells. Cell *121*, 1109–1121.

Maffini, S., Maia, A.R., Manning, A.L., Maliga, Z., Pereira, A.L., Junqueira, M., Shevchenko, A., Hyman, A., Yates, J.R., 3rd, Galjart, N., et al. (2009). Motor-independent targeting of CLASPs to kinetochores by CENP-E promotes microtubule turnover and poleward flux. Curr. Biol. *19*, 1566–1572.

Palazzo, A.F., Eng, C.H., Schlaepfer, D.D., Marcantonio, E.E., and Gundersen, G.G. (2004). Localized stabilization of microtubules by integrin- and FAK-facilitated Rho signaling. Science *303*, 836–839.

Patel, S.R., Richardson, J.L., Schulze, H., Kahle, E., Galjart, N., Drabek, K., Shivdasani, R.A., Hartwig, J.H., and Italiano, J.E., Jr. (2005). Differential roles of microtubule assembly and sliding in proplatelet formation by megakaryocytes. Blood *106*, 4076–4085.

Schwer, H.D., Lecine, P., Tiwari, S., Italiano, J.E., Jr., Hartwig, J.H., and Shivdasani, R.A. (2001). A lineage-restricted and divergent beta-tubulin isoform is essential for the biogenesis, structure and function of blood platelets. Current Biology *11*, 579–586.

Stepanova, T., Slemmer, J., Hoogenraad, C.C., Lansbergen, G., Dortland, B., De Zeeuw, C.I., Grosveld, F., van Cappellen, G., Akhmanova, A., and Galjart, N. (2003). Visualization of microtubule growth in cultured neurons via the use of EB3-GFP (end-binding protein 3-green fluorescent protein). J. Neurosci. *23*, 2655–2664.

Trapnell, C., Pachter, L., and Salzberg, S.L. (2009). TopHat: discovering splice junctions with RNA-Seq. Bioinformatics *25*, 1105–1111.

Trapnell, C., Williams, B.A., Pertea, G., Mortazavi, A., Kwan, G., van Baren, M.J., Salzberg, S.L., Wold, B.J., and Pachter, L. (2010). Transcript assembly and quantification by RNA-Seq reveals unannotated transcripts and isoform switching during cell differentiation. Nat. Biotechnol. *28*, 511–515.

van de Nobelen, S., Rosa-Garrido, M., Leers, J., Heath, H., Soochit, W., Joosen, L., Jonkers, I., Demmers, J., van der Reijden, M., Torrano, V., et al. (2010). CTCF regulates the local epigenetic state of ribosomal DNA repeats. Epigenetics Chromatin *3*, 19.

Villeval, J.L., Cohen-Solal, K., Tulliez, M., Giraudier, S., Guichard, J., Burstein, S.A., Cramer, E.M., Vainchenker, W., and Wendling, F. (1997). High thrombopoietin production by hematopoietic cells induces a fatal myeloproliferative syndrome in mice. Blood *90*, 4369–4383.

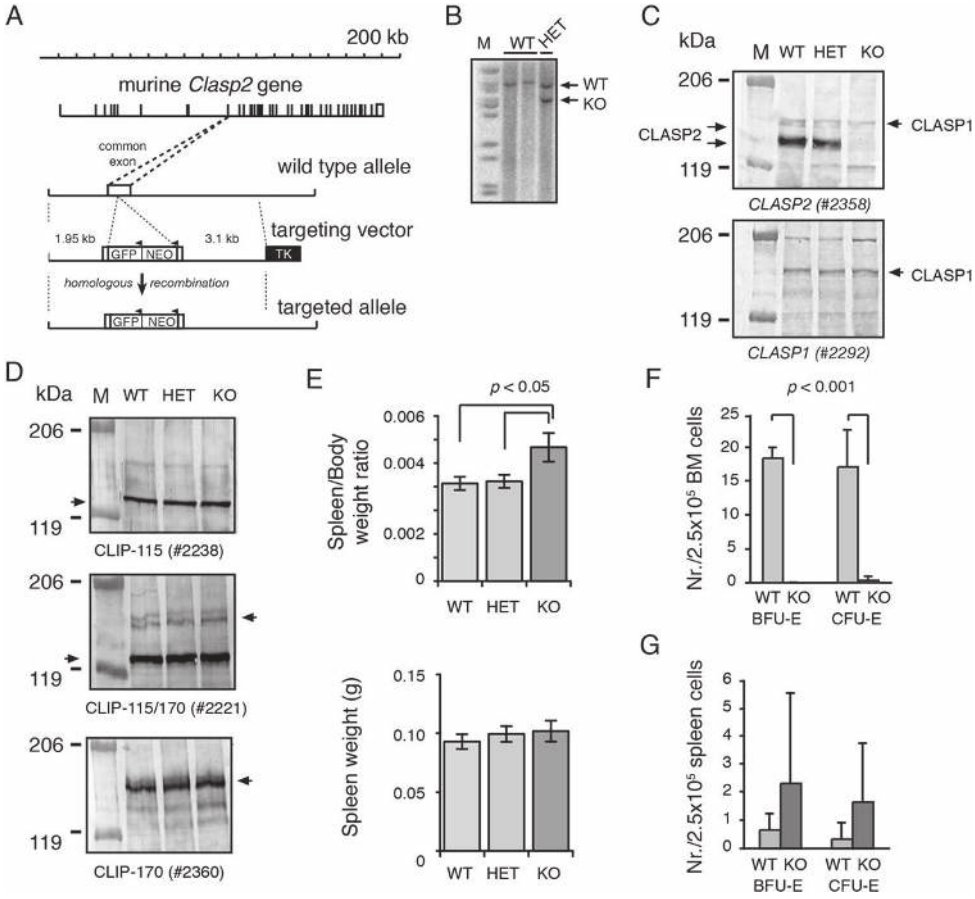

Figure S1. Targeted Inactivation of the Clasp2 Gene and Hematopoietic Analyses, Related to Figure 1

(A) Outline of the targeting strategy. The murine *Clasp2* gene spans about 200 kb and contains approximately 40 exons (indicated by vertical lines). The second exon common to all known isoforms of CLASP2 was interrupted by insertion of an EGFP-loxP-pMC1NEO-loxP cassette; the GFP sequence is followed by a translational stop, and the *neomycin resistance* gene (NEO) is transcribed in the opposite direction to *Clasp2*. LoxP sites (indicated by arrowheads) surround the *neomycin resistance* gene. The targeting vector contains 1.95 kb of 5′ end and 3.1 kb of 3′end homology and a *thymidine kinase* (*TK*) gene at the 3′ end for counter selection. The targeted *Clasp2* allele (*Clasp2* KO) is presented at the bottom.

(B) Southern blot analysis. EcoRI-digested ES-cell DNA, from WT mice and heterozygous *Clasp2* KO mice (HET), was analyzed with a *Clasp2*-specific probe. WT and *Clasp2* KO bands are indicated. This analysis verifies homologous recombination.

(C) Western blot analyses on brain extracts of WT, heterozygous (HET) and homozygous (HOM) *Clasp2* KO mice, using rabbit antibodies against CLASP2 (#2358) and CLASP1 (#2292). The large arrows indicate CLASP2 isoforms, whereas the small arrows indicate CLASP1. CLASP2 is most abundantly expressed in the brain (Akhmanova et al., 2001). Hence, we performed the western blot analysis on this tissue to demonstrate that the targeting of the *Clasp2* gene ablated the expression of protein. In WT brain lysates proteins of approximately 140 kDa and 170 kDa were detected, representing the different CLASP2 isoforms (Akhmanova et al., 2001). In extracts of homozygous *Clasp2* KO mice these isoforms were not detected, while reduced levels were present in heterozygous mice. A CLASP2 deficiency does not influence CLASP1 expression. CLASP2 is also absent in fibroblasts derived from *Clasp2* KO mice (Drabek et al., 2006). We conclude that our targeting strategy successfully abrogates CLASP2 expression.

(D) Western blot analyses on brain extracts of WT, heterozygous (HET) and homozygous (HOM) *Clasp2* KO mice, using antibodies against CLIP-115 (#2238, #2221), and CLIP-170 (#2221, #2360). Arrows on the left side of the blots indicate CLIP-115, arrows to the right hand side indicate CLIP-170. A CLASP2 deficiency does not influence CLIP expression.

(E) Spleen weight analysis. Whole body and spleen weight of 21 WT mice, and 16 heterozygous (HET) and 22 homozygous *Clasp2* KO mice was measured. Both the spleen/body weight ratios (upper panel) as well as the spleen weights (lower panel) are displayed. A t test revealed a significant difference ($p < 0.05$) between WT and KO, and between HET and KO. SEM is shown.

(F and G) Clonogenic progenitor assays. BFU-E and CFU-E colony assays were performed with bone marrow cells (BM, F) and spleen cells (G). Average and SD are depicted ($n > 3$ in both groups). t test was applied to calculate significant differences.

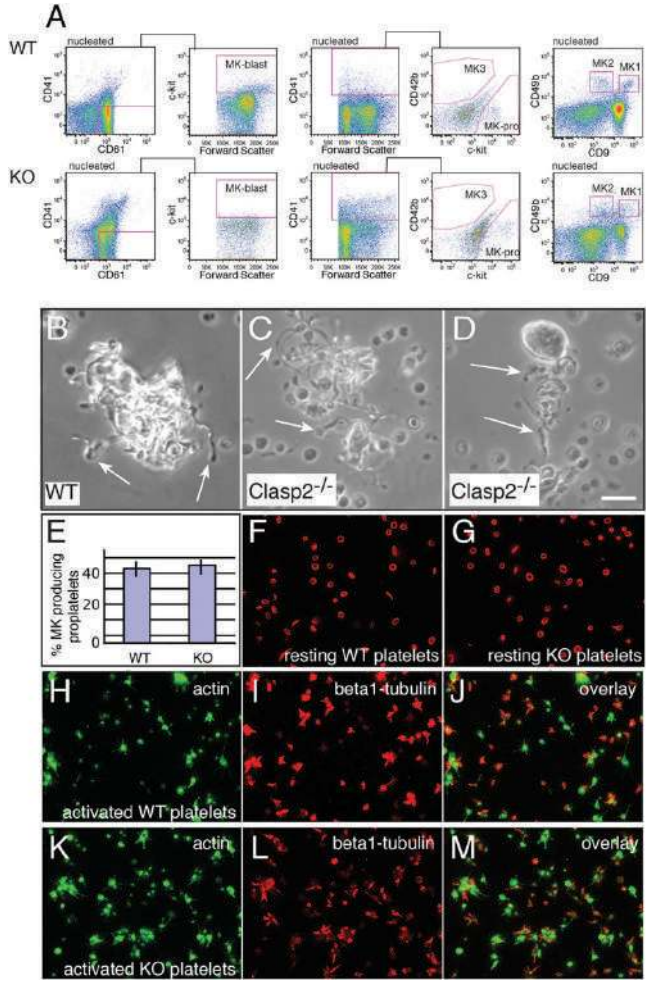

Figure S2. Megakaryocyte Analysis, Related to Figure 2

(A) Flow cytometry analysis of bone marrow cells from WT and *Clasp2* KO mice aimed at describing megakaryocyte differentiation.

(B–D) Differential-interference-contrast (DIC) micrographs of proplatelet networks. Megakaryocytes use a MT-based mechanism to convert their cytoplasm into long, branched proplatelets, which remodel into platelets. MT polymerization is necessary to support the enlarging proplatelet mass, which occurs before megakaryocytes shed their platelets (Patel et al., 2005). Although MTs play a crucial role in platelet biogenesis, the MT-based proteins that are involved have not yet been identified. Since CLASP2 is present in proplatelets, as are its interaction partners CLIP-115 and −170 (not shown), EB1 and −3 (Patel et al., 2005), we examined whether CLASP2 deficiency resulted in defects in the formation of proplatelets. Using a megakaryocyte liquid culture system (Italiano et al., 1999) we observed proplatelets, emanating from WT (B) as well as from *Clasp2* KO (C, D) megakaryocytes. The CLASP2-deficient proplatelets exhibited the normal beaded morphology observed in WT cultures. Furthermore, ultrastructural analysis of the bone marrow by electron microscopy (EM) showed the presence of megakaryocytes in *Clasp2* KO mice, which contained demarcating membranes and dense granules (data not shown).

(E) Proplatelet production. The percentage of proplatelet-producing megakaryocytes in WT and *Clasp2* KO cultures was determined. Megakaryocytes lacking CLASP2 exhibit normal proplatelet production. SD is shown.

(F and G) Immunofluorescence microscopy of resting platelets. Platelets from WT (F), or *Clasp2* KO (G) mice were labeled with antibodies to beta-1 tubulin. In several thrombocytopenias associated with mutations in cytoskeletal proteins platelets are large and have an abnormal shape. The normal disc-shape of the platelet is maintained by a marginal band of MTs (Italiano et al., 2003). As CLASP2 is a regulator of the MT network, it might influence the marginal band. We therefore analyzed the shape and cytoskeletal structure of platelets from *Clasp2* KO mice. Circulating platelets from *Clasp2* KO mice exhibited the normal discoid shape. Furthermore, the diameter and the circumference occupied by MT coils were similar in platelets from WT and *Clasp2* KO mice. Magnification is 600x.

(H–M) Immunofluorescence microscopy of activated platelets. Platelets were labeled with phalloidin (green, H, K), which is a marker for F-actin, and with antibodies to beta-1 tubulin (red, I, L). Panels (J) and (M) show merged images. Platelets were from WT (H-J), or *Clasp2* KO (K-M) mice. *Clasp2* KO platelets, activated with thrombin, spread and formed lamellipodia and filopodia, like WT platelets. Thus, absence of CLASP2 does not significantly impede platelet activation. Magnification is 600x.

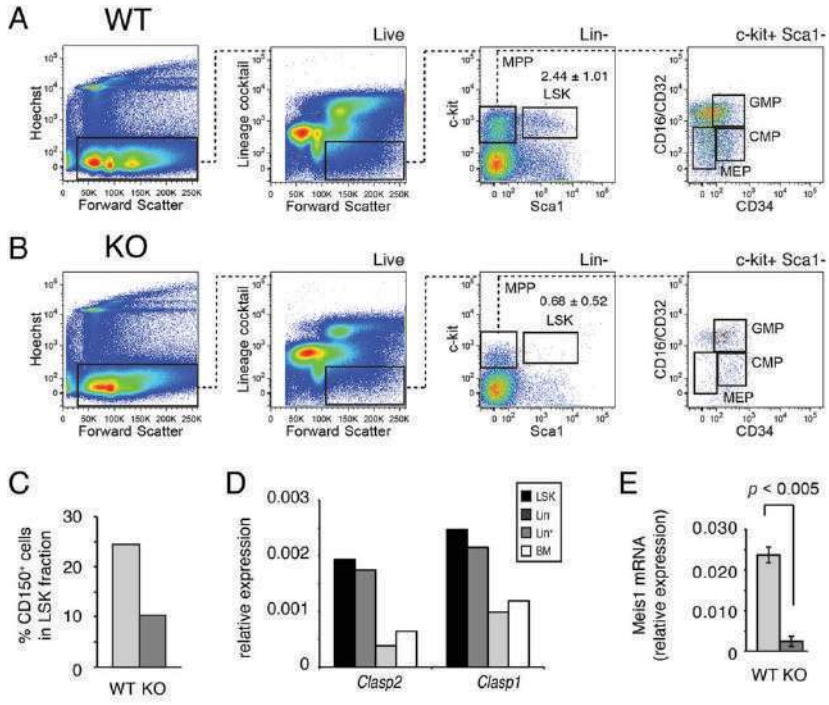

F

KO vs. WT	gene description	gene symbol	Relative expression in LSK: Wild type	Relative expression in LSK: Clasp2 KO
1.2	Actin, beta	actin	3893.79	4469.8
1.1	CLIP associating protein 1	Clasp1	8.6	9.07232
0.19	CLIP associating protein 2	Clasp2	6.17089	1.18101
1.3	Forkhead box O1	Foxo1	3.31938	4.2393
0.75	Programmed cell death 6 interacting protein	Pdcd6ip	11.9261	8.96515
0.92	Upstream binding protein 1	Ubp1	12.4909	11.4774
1.10	Signaling lymphocytic activation molecule family member 1 (CD150)	Slamf1	3.35993	3.69298
0.50	Kit oncogene	Kit	62.3816	31.1284
0.49	Lymphocyte antigen 6 complex, locus A	Ly6a	255.47	123.952
0.27	Meis homeobox 1	Meis1	124.505	33.1521
0.12	Myeloproliferative leukemia virus oncogene	Mpl	113.564	13.4887
0.093	E26 avian leukemia oncogene	Ets2	5.27636	0.491225
26	Spi-B transcription factor (Spi-1/PU.1 related)	Spib	0.0998163	2.62336

Figure S3. A Role for CLASP2 in HSC Maintenance, Related to Figure 3

(A and B) Characterization of HSC-enriched and progenitor cell populations. Representative gating strategy used to sort by flow cytometry LSK ($Lin^-/Sca\text{-}1^+/Kit^+$) cells, MPPs (myeloid pluripotent progenitors), CMPs (common myeloid progenitors), GMPs (granulocyte-macrophage progenitors), MEPs (megakaryocyte-erythrocyte progenitors) in the bone marrow of WT (A) and *Clasp2* KO (B) mice. The percentage of LSK^+ fractions (i.e., the HSC-enriched cells) in WT and KO mice is shown.

(C) Characterization of cell populations highly enriched for HSCs. Bone marrow cells from 2 WT and 2 *Clasp2* KO mice were sorted by flow cytometry as in (A), with the exception that the Lin^- cocktail contained CD48, and that CD150 was used in addition to Sca-1 and Kit. The percentage of $CD150^+LSK$ cells, which is highly enriched for long term HSCs (Kiel et al., 2005) is shown (average values).

(D) *Clasp1* and *Clasp2* expression in the hematopoietic system. Total RNA was isolated from the LSK^+, Lin^-, and Lin^+ fractions, as well as from total bone marrow, of WT mice. Real time PCR was performed using *Clasp1* and *Clasp2* specific primers.

(E) Quantification of *Meis1* mRNA. Total RNA was isolated from the LSK fraction of 7 WT mice and 7 *Clasp2* KO mice. Expression of *Meis1* is shown relative to *Actin*, as determined by real time PCR (3 experiments, SD indicated, t test reveals significant differences).

(F) Next generation sequencing of LSK-derived mRNA. Total RNA was isolated from the LSK^- fraction of 2 WT mice, and 2 *Clasp2* KO mice. Deep sequencing reveals up- and downregulated genes in KO versus WT (relative expression was calculated with the aid of Cufflinks (right hand columns). The ratio of KO to WT is shown on the left. A list of selected genes is shown (not affected, up-, or downregulated) to confirm that the deep sequencing results are valid, and to show deregulation of interesting genes (see Table S1 for complete analysis). For example, as expected, *Clasp2* expression is severely affected in KO samples, whereas the expression of the two genes that are up- and down-stream of the (targeted) *Clasp2* locus (*Pdcd6ip* and *Ubp1*) is not affected by the insertion of an EGFP-loxP-pMC1NEO-loxP cassette. In addition, the relative expression of *Clasp1* (as compared to *Actin*), determined with deep sequencing (~0.0023 (i.e., ~9 divided by ~4000)), is very similar to that measured by real time PCR (see Figure S3D). The relative expression of *Meis1* in WT and KO samples is also very similar in the deep sequencing (Figure S3E) and real time PCR experiments (Figure S3D).

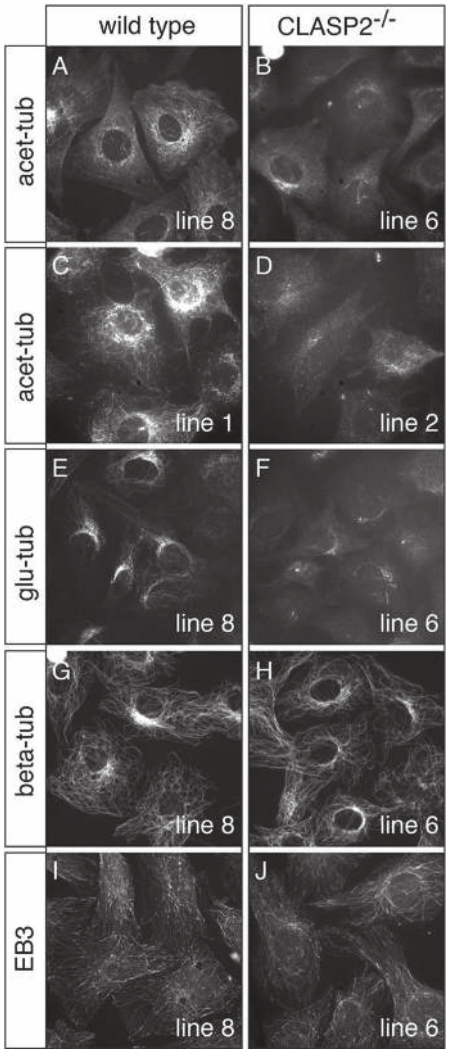

Figure S4. Fibronectin-Induced MT Stabilization Is Inhibited in Clasp2 KO MEFs, Related to Figure 4

We plated two WT (lines 1 and 8) and two *Clasp2* KO (lines 2 and 6) mouse embryonic fibroblast (MEF) cell lines (Drabek et al., 2006) on fibronectin-coated glass coverslips and examined the appearance of focal adhesions and stable MTs 90 min after plating using immunofluorescence analysis. Upon adherence to fibronectin, both WT cells and *Clasp2* KO cells formed focal adhesions, as detected with an antibody against phosphorylated focal adhesion kinase (FAK-pY397, data not shown). Neither of the two *Clasp2* knock out MEF lines (B, D, F) form stable MTs as efficiently as the WT lines (A, C, E), as measured with two different markers for stable MTs (Bulinski and Gundersen, 1991), i.e., anti-acetylated (acet) tubulin and anti-detyrosinated (glu) tubulin antibodies. Moreover, *Clasp2* KO MEFs adhered less efficiently to a fibronectin-coated surface than WT cells (data not shown). *Clasp2* knock out MEFs did form a normal MT array (G, H) and EB3 was localized at the ends of MTs in *Clasp2* knock out fibroblasts (I, J). As a further control we tested adult dermal fibroblast lines instead of MEFs, and obtained a similar result, i.e., CLASP2 is required for the formation of stable MTs upon cell attachment (data not shown). Furthermore, we were able to rescue the MT stabilization defect in *Clasp2* KO MEFs by expressing GFP-CLASP2 (data not shown).

Appendix 2

CONTROLS MEGA-KARYOCYTE PROTEIN HOMEOSTASIS AND PROPER PLATELET FUNCTIONALITY

ATAXIN2 CONTROLS MEGAKARYOCYTE PROTEIN HOMEOSTASIS AND PROPER PLATELET FUNCTIONALITY

S. Zeddies*, M. Meinders^, S. Podliesna*, F. di Summa*, E. Damrath#, M. Halbach#, G. Auburger#, L. Gutiérrez^, M. von Lindern*, D.C. Thijssen-Timmer *

* *Department Hematopoiesis, Sanquin Research and Landsteiner Laboratory, Academic Medical Centre, University of Amsterdam, Amsterdam, The Netherlands*

^ *Department Blood Cell Research, Sanquin Research and Landsteiner Laboratory, Academic Medical Centre, University of Amsterdam, Amsterdam, the Netherlands*

\# *Experimental Neurology, Goethe University Medical School, Frankfurt am Main, Germany*

Running Head: ATXN2 regulates protein homeostasis
Corresponding author: Daphne C. Thijssen-Timmer
Department of Hematopoiesis Sanquin Research
Plesmanlaan 125
1066CX Amsterdam
Phone: +31 20 5123525
FAX: +31 20 5123474

Number of words: 4000
Abstract word count: 171
Number of figures: 4 plus 2 supplemental figures
Number of tables: 2 supplemental tables
Number of references: 44
Category: Platelets and Thrombopoiesis

Key Points

- ATXN2 controls protein synthesis and decay during megakaryopoiesis
- ATXN2 loss results in a platelet aggregation defect

ABSTRACT

Multinucleated megakaryocytes accumulate large quantities of mRNA encoding, among others, proteins associated with the cytoskeleton, various platelet-specific granules, and membranes. To produce thousands of functional platelets per megakaryocyte, protein synthesis in the maturing megakaryocyte is likely to require strict spatio-temporal control. We observed that the RNA-binding protein ATAXIN2 (ATXN2) is differentially expressed during megakaryopoiesis. Here, we show that ATXN2 regulates protein homeostasis in megakaryocytic cells, which is needed to obtain functional platelets.

Atxn2-deficient mice contained normal platelet counts, but platelet aggregation was decreased upon activation of the αIIbβ3-integrin and Clec-2 receptor. Silencing ATXN2 in human megakaryocytic cells decreased overall protein synthesis and caused lower total protein content. ATXN2 associates with PABP and DDX6, proteins that control mRNA stability and translation. We subsequently profiled nontranslated subpolysomal RNA, and actively translated polysomal RNA following ATXN2 knockdown in megakaryocytic cells. ATXN2 mainly affected polysome recruitment of transcripts encoding proteins implicated in protein metabolism in general. Our results indicate that ATXN2 is involved in protein metabolism during megakaryopoiesis and is needed for proper platelet functionality.

INTRODUCTION

Megakaryopoiesis encompasses the differentiation of a hematopoietic stem cell towards mature megakaryocytes that subsequently undergo cytoskeletal remodelling, and ultimately release platelets into the blood stream[1]. Compared to many other differentiation processes, megakaryopoiesis contains several unique features, one of the most striking being endomitosis[2]. During this incomplete cell division, the nuclear content of the cell is doubled without subsequent cytoplasmic separation[3-5]. Incomplete division is repeated and as a result, mature megakaryocytes contain polylobulated nuclei up to 128N. It is believed that the increase in nuclear material allows for the accumulation of large amounts of mRNA[6]. Many of the proteins synthesized from this increased mRNA pool are then packaged into cellular organelles called alpha granules[7]. When mature megakaryocytes reorganize their cytoskeleton, alpha granules are actively transported and accumulate in the newly formed proplatelets. Ultimately, proplatelets are shed into the bloodstream where they circulate as mature, anucleate, platelets[8;9]. Upon vascular damage, platelets interact with proteins of the subendothelial lining. This triggers signalling cascades, resulting in the activation and subsequent adhesion and spreading of platelets at the side of damage and the release of alpha granule contents[10].

To understand the complex mechanism of megakaryocyte differentiation including protein production and alpha granule synthesis, we performed gene expression profiling in human megakaryocytic cells. Among putative novel regulators of megakaryopoiesis we detected ATAXIN2 (ATXN2).

Recently, ATXN2 has also been found to play a role in hematological disorders. Genome-wide association studies revealed single nucleotide polymorphisms in the *ATXN2* locus which associate with an increased risk for thrombotic antiphospholipid syndrome or autoimmune disease[11-13].

ATXN2, encoded at the genomic locus SCA2[14;15] is a 140 kDa protein that has mainly been studied as a polyglutamine repeat protein in the context of spinocerebellar ataxia type 2 (SCA2)[16] and amyotrophic lateral sclerosis (ALS)[13;17-19].

Considerable progress has been made deciphering the mechanism involved in aggregate formation of polyQ-expanded ATXN2 protein in neurodegenerative disease[20], but the function of physiological ATXN2 remains elusive. Several studies indicated that ATXN2 is involved in regulating mRNA translation. First, structural

and functional analysis revealed domains involved in mRNA binding and translational regulation[21;22]. Next, ATXN2 has been described to associate with stress granules[23], the rough endoplasmic reticulum[24] and polyribosomes[25].
Lastly, ATXN2 was reported to promote microRNA-mediated mRNA breakdown[26;27]. In addition to a role in translation, ATXN2 may control receptor endocytosis, actin filament regulation and protein exocytosis[28-31]. The observed effects may be due to regulation of translation of key factors in these processes; however this has not been investigated yet.
Several studies used murine models to elucidate the function of Atxn2. *Atxn2* deficient mice present with smaller litters, a segregation distortion with more male than female offspring and increased body weight[32;33]. Brain phenotypes were subtle in *Atxn2* knockout mice, suggesting that polyQ-expanded ATXN2 has stronger or converse effects than the loss of ATXN2.
We hypothesize that ATXN2 controls mRNA translation in megakaryocytes during the accumulation of large amounts of transcripts encoding proteins required for platelet production. Mice lacking Atxn2 expressed normal numbers of platelets that were, however, defective in aggregation. Knockdown of ATXN2 in human megakaryopoietic cells reduced overall protein synthesis. Polysome profiling indicated that loss of ATXN2 alters translation of transcripts encoding proteins involved in protein synthesis and degradation. Thus, ATXN2 regulates general protein homeostasis in megakaryocytes, a process which is crucial for the production of fully functional platelets.

METHODS

Blood analysis

Blood was drawn from Atxn2 knockout (*Atxn2*$^{-/-}$)[33]. and wildtype (*WT*) animals by retro orbital puncture using heparin-coated glass capillaries (Hirschmann, Eberstadt, Germany), and collected in heparin-coated vials. Blood parameters were determined on a scil Vet abc Plus+ instrument (scil animal care, Oostelbeers, the Netherlands). Platelet rich plasma (PRP) was separated by centrifuging the blood 15 min at 50g.

Mouse femur preparation and flow cytometry

Mice were anaesthetised using Isofluran (Baxter, Unterschleissheim, Germany) and sacrificed by perfusion with 4% paraformaldehyde. Following perfusion, femurs were isolated, crushed and bone marrow was resuspended in PBS + 0.1% HSA. Bone marrow suspensions were then passed through a cell strainer (VWR, Amsterdam, the Netherlands) and counted on a Casy Cell Counter (Roche, Woerden, the Netherlands). Cells were then stained with cMpl (Santa Cruz), Clec-2 (AbD Serotec, Pucheim, Germany), CD9-PE (Abcam), CD61-FITC, CD41-PE, KIT PerCPCy5.5, (BD Biosciences); CD42a-FITC, CD42b-DL649, CD42c-FITC, CD42d-FITC (Emfret); CD31 PECy7 (Abcam) using a 1:1000 dilution for all antibodies. Flow cytometry based platelet aggregation assays were performed as previously described[34]. Receptor surface expression was measured using a flow cytometer

(LSRII + HTS, BD Biosciences) and data was analyzed with FlowJo software version 9.2 (Tree Star Inc., Ashland, OR, USA).

Human CD34⁺ cultures

Peripheral blood stem cells were provided by the Sanquin Laboratory for Cell Therapy and obtained from leukapheresis material of healthy donors or donors in disease remission from Hodgkin lymphoma, multiple myeloma or breast cancer. For megakaryocyte cultures, $CD34^+$ cells were cultured in CellGro medium (CellGenix, Frankfurt, Germany) supplemented with TPO (N-plate, Amgen, Breda, the Netherlands and IL-1β (PeproTech, Heerhugowaard, the Netherlands). At designated time points, cultures were either sorted for CD34 and CD41 expression, using the antibodies specified above, on an Aria II cell sorter (BD Biosciences). For phenotype analysis, cells were fixed with 1% PFA, washed with PBS + 0.05% BSA + 0.05M EDTA and incubated with CD34 PeCy7, CD41 APC or CD42b APC (all BD Biosciences). Samples were measured with flow cytometry (LSRII + HTS, BD Biosciences).

Lentiviral knockdown constructs

The lentiviral knock down vector SIN.PPT.CMV.GFP.U3*Nhe*1 was the kind gift of N.A Kootstra (Academic Medical Center, Amsterdam, The Netherlands). We cloned a cassette containing the short hairpin RNA (shRNA) sequence under the control of a U6 promoter. The shRNA sequences used against *ATXN2* were:

sh93
GCCAAGACATATAGAGCAGTA
sh95
CCGAAGTGTGATTTGGTACTT
and as a non-targeting *shRNA* control (*shc002*)
CAACAAGATGAAGAGCACCAA was used.
All cloned short hairpins were verified by sequencing.

Lentivirus production and lentiviral transduction

Lentiviral particles were produced in 293T cells using the third generation system as described before[35]. Transductions were carried out as described before[35]. Cells were then seeded into megakaryocytic liquid cultures or used for colony formation assays. Megacult colony formation assay (Stem Cell Technologies, Grenoble, France) and Colony Gel colony formation assay (Cell Systems, Frankfurt, Germany) were carried out according to the manufacturer's specifications. ClickIt total protein synthesis determination assay was performed according to the manufacturer's specifications with an adjusted incubation time of one hour for AHA (LifeTechnologies).

Immunoprecipitation and immunodetection

Immunoprecipitation was carried out with $CD34^+/CD41^+$ immature megakaryocytes. Cells were lysed in solubilization buffer (20mM Tris pH 8.0, 137mM NaCl, 2mM EDTA, 10% Glycerol, 1% NP-40), supplemented with protease inhibitor cocktail (Roche, Woerden, The Netherlands) and 25U/ml benzonase (Merck,Darmstadt, Germany). 5µl of ATXN2 antibody (BD Biosciences) or IgG control antibody

(Sanquin, Amsterdam, The Netherlands) was added to the lysate and incubated overnight at 4°C. The next day, sepharose beads (Pierce, Rockford, IL, USA) were added and incubated for at least 6 hours. Beads were then washed three times with solubilization buffer and eluted using SDS sample buffer. Samples were loaded on a 10% precast gel (Thermo Scientific, Waltham, MA, USA) and transferred onto nitrocellulose membranes using iBlot (Invitrogen, Bleiswijk, The Netherlands). Membranes were probed with ATXN2 (BD Biosciences), DDX6 (Novus Biologicals, Littleton, CO), PABP (Abcam, Cambridge, GB) and TIA-1 (Santa Cruz, Heidelberg, Germany). Secondary anti mouse-HRP antibody or anti rabbit-HRP antibody (both Dako, Glostrup, Denmark) was applied and membranes were developed by Enhanced Chemiluminescence (Pierce, Rockford, IL, USA).

Polysome profiling and microarray

Lysate of $7x10^6$ Meg-01 cells was loaded on 7-46% sucrose gradients (10ml SW40 tubes UltraClear, Beckman, Woerden, The Netherlands). Gradients were spun at 35,000rpm for 3 hours (Beckman) and harvested as 17 fractions of 600µl. RNA was isolated as described[36]. Fractions 1-8 were combined as subpolysomal RNA; fractions 9-17 as polysomal RNA. RNA was cleaned up using the Qiagen Micro kit according to the manufacturer's protocol (Qiagen, Venlo, The Netherlands). Microarray was performed at Service XS (Leiden, The Netherlands). Samples were hybridised to the Illumina Human HT-12 v4 expression beadarray (Illumina, San Diego, CA). *The data discussed in this manuscript have been deposited in NCBI's Gene Expression Omnibus and are accessible through GEO Series accession number GSE63297.* R version 2.15.3 (www.r-project.org) and Bioconductor version 2.11 (www.bioconductor.org) were used for quality control and normalisation of the Illumina arrays. The Bioconductor package "lumi" is used for loading the Illumina data into R. VSN normalization is applied on the data using the 'lumiN' function.

To maximize detection, no genes were excluded from the analysis. eBayes option was used to estimate the 'average' gene variability and to bring both high and low variability genes closer to the mean. The Benjamini Hochberg FDR values are calculated using the 'multtest' library (function: 'mt.rawp2adjp'). The q- values are calculated utilizing the 'qvalue' package. The Bioconductor 'lumiHumanAll.db' and the 'GO.db' packages are used to get the most up-to-date annotations for the GO enrichment and other analysis. For the GO enrichment analyses, the calculated p-values are used together with the GO-annotations. Gene Set Enrichment Analysis (GSEA) (http://www.broadinstitute.org/gsea) is provided by the Broad Institute. The t-values are used to do a GSEAPreranked test to determine which biological pathways are significant in the underlying microarray experiment. The biological pathways are obtained from the MSigDB database.

RESULTS

Atxn2 deficiency causes a platelet aggregation defect

To investigate whether Atxn2 is required for megakaryopoiesis, or for hematopoiesis in general, we first investigated the blood cell composition in *Atxn2* deficient

(*Atxn2*$^{-/-}$) mice compared to wildtype (*WT*) animals. Platelet count, mean platelet volume as well as red and white blood cell counts were not significantly changed between *Atxn2*$^{-/-}$ and *WT* animals (Figure 1A). To measure the efficiency of platelet aggregation, platelets from *Atxn2*$^{-/-}$ and *WT* mice were activated with four specific agonists and microaggregation was measured by flow cytometry following a time course. Addition of botrocetin, which induces signaling via the GPIb(CD42b)/GPV(CD42d)/GPIX(CD42a) vWF receptor complex was comparable between Atxn2$^{-/-}$ and WT platelets. Likewise, addition of collagen, which binds GPVI and integrin α2β1, was normal. Strikingly, aggregation of *Atxn2*$^{-/-}$ platelets was significantly reduced compared to *WT* platelets upon addition of the αIIbβ3 integrin (CD41, CD61) agonist PMA and the Clec-2 agonist Aggretin A (Figure 1B). Aggregation was not completely ablated in the Atxn2$^{-/-}$ platelets compared to WT; moreover, it still followed the same kinetics. To investigate whether the decreased aggregation could be due to diminished receptor surface expression, we analyzed resting platelets from *Atxn2*$^{-/-}$ and *WT* mice by flow cytometry for expression of the most abundant platelet receptors. Expression of all tested antigens was normal on *Atxn2*$^{-/-}$ platelets compared to *WT* with the exception of a 30% decrease in CD31 (PECAM) (Figure 1B-C). Reduced receptor expression therefore does not explain the reduction in aggregation. These findings suggest that other factors might be involved to account for the reduced aggregation observed in *Atxn2*$^{-/-}$ mice.

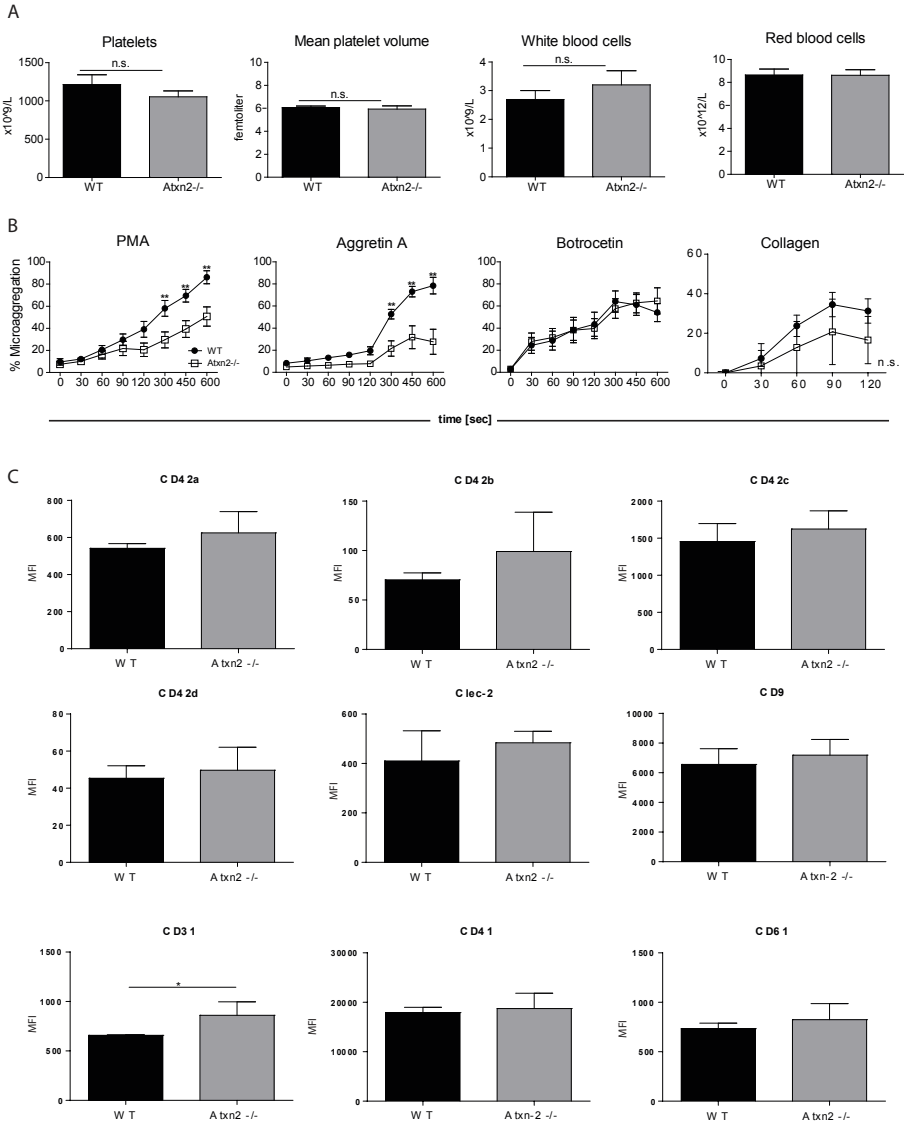

Figure 1) ATXN2 deficiency causes a platelet aggregation defect.

A) Blood cell counts after retroorbital sampling from from *WT* or *Sca2*$^{-/-}$ mice, n=8 n.s.: not significant.

B) Aggregation of platelets from *WT* or *Sca2*$^{-/-}$ mice, activated with PMA, Aggretin, botrocetin or collagen and incubated for designated times measuring percentage of aggregation over time, n=5, ** p<0.01.

C) Platelet receptor surface expression measured with flow cytometry on *WT* or *Sca2*$^{-/-}$ platelets in resting state, n=5, * p<0.05

Atxn2 deficiency does not alter megakaryocytic differentiation

As platelets are derived from megakaryocytes, we next investigated at which stage Atxn2 expression influences megakaryocytic differentiation. Flushed femurs from *WT* and *Sca2*$^{-/-}$ animals yielded similar numbers of total bone marrow cells (Figure 2A). When bone marrow cell suspensions were analyzed for megakaryocytes using multicolour flow cytometry, the percentage of megakaryocytes (CD9^{+}/c-kit^{+}) was not significantly changed in Sca2$^{-/-}$ mice compared to *WT* (Figure 2B). Furthermore, no differences in the expression of the megakaryocytic surface markers CD42b, CD61 were detected on bone marrow MK (Figure 2C). Also, when bone marrow megakaryocytes were analyzed for their differentiation state according to side scatter distribution and surface marker expression, no differences between *WT* and *Atxn2*$^{-/-}$ mice were found (Supplemental Figure 1).

To address the impact of ATXN2 on megakaryopoiesis in more detail, we first determined the physiological expression of the ATXN2 protein in distinct stages of human megakaryocyte development: CD34^{+}/CD41^{-} hematopoietic stem and progenitor cells (HSPC), CD34^{+}/CD41^{+} immature megakaryocytes, and mature CD34^{-}/CD41^{+} megakaryocytes. ATXN2 expression increased from CD34^{+}/CD41^{-} to immature CD34^{+}/CD41^{+} megakaryocytes and sharply decreased again during differentiation to CD34^{-}/CD41^{+} megakaryocytes (Figure 2D). Next we depleted ATXN2 using lentiviral knockdown technology in CD34^{+} HSPC that were cultured towards the megakaryocytic lineage. Knockdown using two different short hairpins specific for ATXN2 (sh93 and sh95) almost completely abolished ATXN2 protein expression in CD34^{+} HSPC compared to short hairpin controls (shc002) (Figure 2E). Following 5 days of culture towards the megakaryocytic lineage, the distribution of CD34^{+} HSPC, CD34^{+}/CD41^{+} immature megakaryocytes and CD41^{+} mature megakaryocytes was similar in *ATXN2* knockdown cells transduced with either sh93 or sh95 compared to short hairpin controls (shc002) (Figure 2F). When transduced CD34^{+} cells were seeded into semisolid medium promoting the formation of megakaryocytic colonies, *ATXN2* knockdown or shc002 gave rise to similar numbers of CD41^{+} megakaryocytic colonies (Figure 2G). We also examined the possible effect of ATXN2 knockdown on the commitment towards erythroid and granulocyte-monocyte progenitors, by plating single cell - single well transduced CD34^{+} cells into conditioned semisolid medium. Compared to shc002, cells depleted for ATXN2 showed the same distribution of burst-forming unit erythroid (BFU-E), colony-forming unit erythroid (CFU-E), colony forming unit granulocyte macrophage (CFU-GM) and colony forming unit granulocyte, erythrocyte, macrophage (CFU-GEMM) (Figure 2H). Taken together, lack of ATXN2 does not influence hematopoietic lineage fate or early megakaryocytic differentiation in our human CD34^{+} in vitro system.

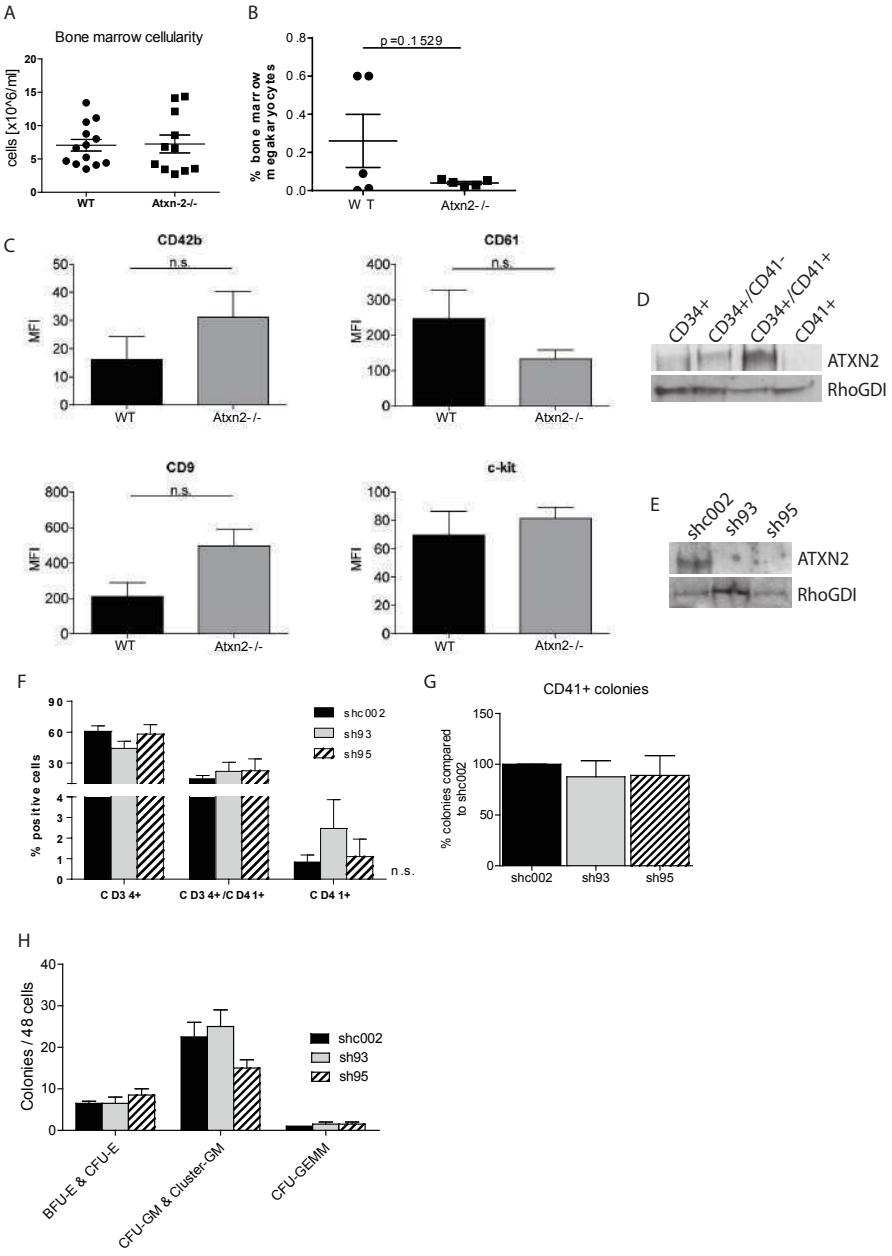

Figure 2) ATXN2 deficiency does not alter megakaryocytic differentiation.

A) Bone marrow cellularity. Cell count was determined on bone marrow from *WT* or *Sca2*$^{-/-}$ femurs, n=8

B) Percentage of bone marrow megakaryocytes identified as CD9^{+}/c-kit^{-} cells found in total bone marrow cells.

C) Expression of megakaryocyte surface proteins from *WT* or *Sca2*$^{-/-}$ mice. Flow cytometry was performed on cells isolated from femur, n=5.
D) Western Blot depicting ATXN2 expression during megakaryopoiesis. CD34^{+} cells derived from mobilized peripheral blood (MPB) were cultured in the presence of TPO and IL-1β and cell sorting was performed after 7 days of culture to obtain CD34^{+}/CD41^{-} and CD34^{+}/CD41^{+} fractions. Subsequent culture of the CD34^{+}/D41^{+} fraction resulted in a sample of terminally differentiated CD41^{+} cells. Immunodetection was carried out with ATXN2 and RhoGDI as a loading control. Representative image from n=3.
E) Lentiviral knockdown efficiency in CD34^{+} cells. CD34^{+} cells were transduced with shc002, sh93 or sh95. 48hours after transduction cells were sorted for GFP expression and cultured for an additional three days before lysis Immunodetection with ATXN2 and RhoGDI as loading control. Representative image from n=3.
F) Liquid megakaryocyte culture using CD34^{+} cells. Cells were transduced with sh93, sh95 or shc002 and cultured towards megakaryocytes in a liquid culture with TPO and IL-1β. Flow cytometry using monoclonal antibodies against CD34, CD41 and CD42b was used after 5 days of culture to assess differentiation. N=3, n.s.: not significant.
G) Megakaryocytic colony formation assay. CD34^{+} cells were transduced with shc002, sh93 or sh95 and seeded into semisolid medium promoting megakaryocytic colony formation. After two weeks of culture, CD41^{+} colonies were counted, shc002 set to 100%, n=3.
H) Colony formation assay to investigate hematopoietic lineage fate after ATXN2 knockdown. CD34+ cells were transduced with shc002, sh93 or sh95 and plated out single cell single well into semisolid medium. After two weeks, the amount of burst forming unit erythroid (BFU-E) and colony forming unit erythroid (CFU-E) as well as colony forming unit granulocyte macrophage (CFU-GM) and colony forming unit granulocyte, erythrocyte, macrophage (CFU-GEMM) were counted, n=3.

ATXN2 associates with proteins involved in mRNA storage and decay

The ATXN2 protein contains several domains facilitating binding to mRNA and other proteins (Figure 3A)21;23;25. Therefore, we investigated if interactions with known binding partners are also found in megakaryocytic cells, and whether ATXN2 may be associated with actively translated mRNA. The human megakaryoblastic cell line Meg-01 was used to separate mRNA in polyribosomal, translated, and subpolysomal, untranslated, RNA (Figure 3B). The RPL11 protein, which is part of the 60S ribosomal subunit, was prominently present in the subpolysomal fractions 5-7 of the gradient that contained the bulk of the total RNA as 60S ribosomal subunit plus 80S monoribosome (Figure 3B). Compared to RPL11, ATXN2 was only detectable in the first fractions of the gradient. These first fractions contain untranslated RNA and free proteins suggesting that most of ATXN2 is either not associated with RNA, or associates with untranslated RNA (Figure 3B). Immunoprecipitations demonstrated association of ATXN2 with poly(A) binding protein (PABP) and the RNA helicase DDX6 in immature primary human megakaryocytes (Figure 3C). The DDX6-PABP complex is known to be involved in miRNA-mediated mRNA decay[37]. mRNA targeted for degradation or translational silencing associates with GW182 (an RNAse and marker for P- bodies) or TIA1 (an RNA-binding protein and marker for stress granules). Neither GW182 nor TIA1 associated with

the ATXN2/PABP/DDX6 complex (Figure 3C). Taken together, our results show that ATXN2 associates with untranslated RNA and forms complexes with proteins involved in miRNA-mediated decay.

Given the association with untranslated mRNA and miRNA-mediated decay, we next investigated whether loss of ATXN2 impacts on protein synthesis. Meg-01 cells were transduced with shRNA constructs targeting ATXN2 (sh93 and sh95) or scrambled control (shc002) (Figure 3D). Compared to shc002, expression of sh93 or sh95 decreased total protein content by almost 50% whereas total RNA concentrations were not affected (Figure 3E). Incubation of transduced cells with a methionine analog to label newly synthesized protein revealed significantly lower methionine incorporation upon ATXN2 knockdown compared to shc002. Incorporation measured as mean fluorescence intensity was reduced by 50% with sh93 and by 70% with sh95 (Figure 3F). These results show that loss of ATXN2 results in decreased total protein content in megakaryocytic cells, caused by decreased de novo protein synthesis.

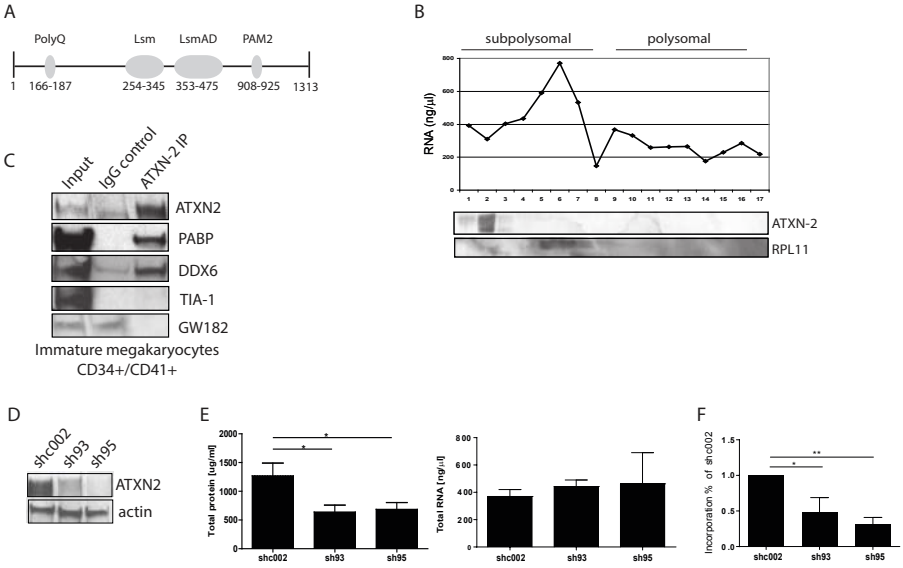

Figure 3. ATXN2 associates with proteins of mRNA storage and decay.

A) Schematic representation of functional domains within ATXN2.
B) Polysome profiling. Meg-01 cell lysate was separated by sucrose gradient centrifugation. Fractions were analysed for RNA concentration and immunodetection of ATXN2.
C) Immunoprecipitation using ATXN2 antibody in immature megakaryocytes. Membranes were probed for PABP, DDX6 and TIA-1.
D) Total protein and total RNA content measured in Meg-01 cells after ATXN2 knockdown compared to shc002.
E) De novo protein synthesis was measured by flow cytometry as incorporation of a methionine analogue after transduction of Meg-01 cells with shATXN2 or SH002 expressing virus. n=5, ** $p<0.01$.

ATXN2 controls the generation of proteins implicated in protein homeostasis

The global reduction in protein synthesis suggests that translation of most transcripts is reduced. However, not all transcripts may be affected equally. To investigate which transcripts are under control of ATXN2, polyribosome profiling was performed on Meg-01 cells transduced with either shc002 or sh95 to analyze changes in the composition of untranslated and translated mRNA compared to shc002 (Figure 4A). Fractions 1-8 were pooled as subpolysomal mRNA, while fractions 9-17 were pooled as polysomal RNA (Figure 4A). The RNA was hybridised to an Illumina beadchip array. To analyze global changes in protein expression, we focused our subsequent analysis on polysomal-bound mRNA and compared polysome-bound mRNA after ATXN2 knockdown with shc002. ANOVA analysis identified 172 transcripts differentially expressed in the polysomal fraction in three independent experiments. We calculated the fold change in expression between mRNAs in ATXN2 knockdown cells compared to cells transduced with shc002 for subpolysomal fractions as well and performed non- hierarchical, Euclidian clustering (Figure 4B-C, Supplemental Table 1). Due to poor hybridisation results, the subpolysomal fraction of shc002 and sh95 from one experiment was excluded from further analysis.

Clustering analysis based on the polysomal fractions revealed 9 clusters that we ordered in 6 functional groups (Figure 4C). Following ATXN2 knockdown, some transcripts were either up- or down-regulated in both polysomal and subpolysomal RNA (group C, n=37; group F, n=21). However, in group A (n=43) transcripts were increased in the polysomal fraction compared to subpolysomal expression and in group E (n=18) active translation in the polysomal fraction was reduced. Groups B and D contain transcripts that hardly changed in the subpolysomal fraction but were up- (B, n=44) or down-regulated (D, n=9) in polysomal mRNA suggesting a combination of transcriptional and translational regulation. Thus, ATXN2 knockdown altered the presence of specific transcripts in the polysomal, translated fraction compared to shc002.

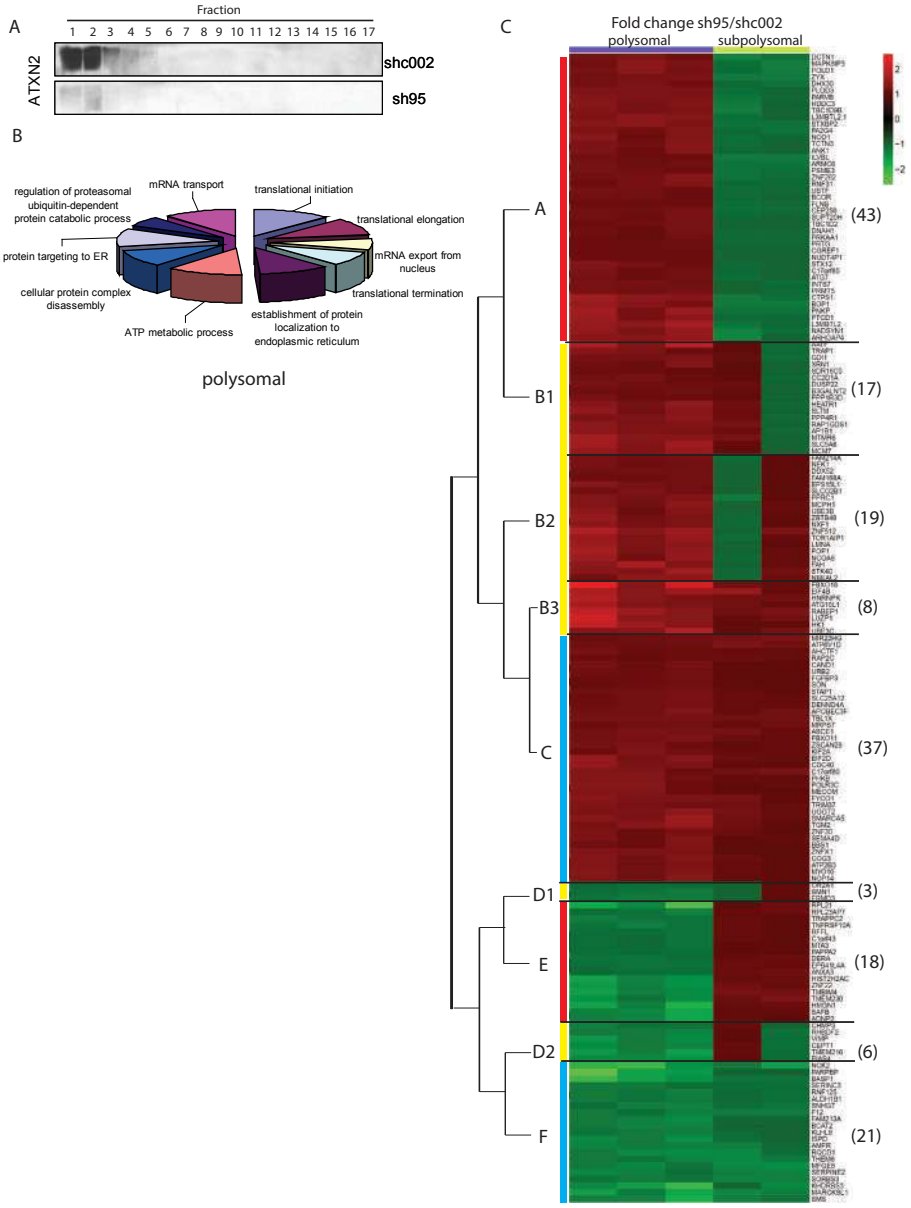

Figure 4. ATXN2 controls the generation of proteins implicated in protein homeostasis.

A) Polysome profiling after ATXN2 knockdown in Meg-01 cells. Meg-01 cells were transduced with shc002 or sh95, lysed, and spun down over a sucrose gradient. RNA concentrations of fractions were measured and samples for determining ATXN2 knockdown efficiency were taken. RNA from subpolysomal fraction 1-8 was pooled as was RNA from polysomal

fraction 9-17. After pooling, RNA from pooled fractions was loaded on an Illumina Beadchip for expression profiling.

B) ErmineJ analysis of polysomal fractions from polysome profiling.

C) Heatmap showing fold increase (red) or decrease (green)of mRNAs after ATXN2 knockdown compared to shc002. Polysomal fractions (in blue) and subpolysomal fractions (in yellow) are shown after hierarchical clustering.

Gene set enrichment analysis showed that *ATXN2* knockdown lead to a significant correlation with processes involved in mRNA turnover and translation, affecting processes as translation initiation ($p= 10^{-12}$), translation termination ($p=10^{-12}$) and regulation of proteasomal ubiquitin-dependent protein catabolic process ($p= 10^{-12}$) (Supplemental Figure 2, Supplemental Table 2). Differentially expressed polysomal fractions also showed a significant positive correlation with both the mRNAs expressed in platelets[38] and the Reactome translation pathway (Supplemental figure 2, Supplemental Table 2). However, when comparing the amount of shared RNAs, only 45 of the 172 selected transcripts were shared with the platelet enriched transcripts, whereas 153 of the 172 mRNAs were shared with the Reactome translation pathway. This indicates that ATXN2 knockdown impacts not just platelet specific transcripts but also general translation. Of note, the subpolysomal fraction showed a negative correlation to the platelet transcriptome[38] and the Reactome translation pathway (Supplemental figure 2, Supplemental Table 2).
In conclusion, our results show that ATXN2 knockdown altered the composition of the translated, polysomal mRNA fraction in megakaryocytic cells thereby changing protein translation and degradation processes.

DISCUSSION

Here, we analyzed how the RNA-binding protein ATXN2 impacts on protein homeostasis during megakaryopoiesis. ATXN2 is highly expressed in the first phase of megakaryopoiesis when cells become endomitotic and more translationally active. This suggests that ATXN2-dependent regulation of mRNA processing or translation may be involved in the generation of protein-dense, functional platelets. Mice lacking Atxn2 contained normal numbers of megakaryocytes and platelets. However, platelet aggregation in response to specific agonists was reduced. Strikingly, the protein content of ATXN2 depleted megakaryocytes was almost 2-fold decreased, whereas mRNA levels were not significantly changed. The low protein content of ATXN2 depleted megakaryocytes was associated with a 50% reduction in protein synthesis in combination with increased translation of proteins involved in ubiquitination and protease degradation. Before platelet shedding, megakaryocytes accumulate proteins in alpha granules that are crucial for platelet function. Failure to accumulate these proteins may underlie the aggregation defect observed in mouse platelets.

Expression of all major platelet surface receptors was unchanged compared to WT which suggests that the reduced aggregation upon PMA and Aggretin A could be due to other factors. ATXN2 interacts with PABP and DDX6 in HEK 293T cells,

SH-SY5Y cells and also in megakaryocytes[23]. The same study also showed that in a yeast-2-hybrid screen, ATXN2 binds directly to DDX6 through its Lsm domain[23]. While the presented data are convincing, the timing and functionality of this binding remain elusive. DDX6 participates in miRNA mediated decay and recruits the CCR4/NOT complex to mRNA to cause deadenylation, which subsequently leads to reduced translation and destabilisation of mRNA[37]. However, DDX6 exerts its effect downstream of GW182 which has to bind to the target mRNAs first to induce miRNA mediated decay. GW182 binds to the PAM2 motif of PABP, occupying the same structure that also ATXN2 binds to[39]. This concurrence for the PAM2 motif means that binding of both GW182 and ATXN2 to PABP is impossible, reflected in our findings that upon immunoprecipitation with ATXN2, GW182 could not be co-precipitated. However, since ATXN2 is outcompeted by GW182 to induce RNA decay, the question remains why binding between ATXN2 and DDX6 occurs during the progression of mRNA decay. Direct or indirect interaction of ATXN2 with PABP and DDX6 may either enhance or inhibit the recruitment of CCR4/NOT by DDX6.

Recently, ATXN2 was shown to bind to AU-rich elements thereby promoting RNA stability and translation[22]. We also analyzed the occurrence of AU-rich elements in the various clusters observed in the microarray but could not detect any correlation. Still, the interaction of ATXN2 with DDX6 may suggest protection from RNA decay by DDX6. We found that protein synthesis was reduced upon loss of ATXN2, which also suggests a positive role of ATXN2 in translation regulation. The unresolved question is whether ATXN2 binds PABP/DDX6 in presence or absence of mRNA. It is currently unknown if ATXN2 sequestersPABP/DDX6 and prevents mRNA binding, or whether it binds mRNA and thereby inhibits PABP/DDX6 function on the same transcript.

Amongst the transcripts that we found increased in the polysomal, translated fraction after ATXN2 knockdown were members of the ubiquitination pathway such as the E3 ubiquitin ligase UBEC3 and the F-box protein FBXO18. During megakaryopoiesis, proteins and specific RNAs are actively transported into the developing platelets[40;41]. In a recent RNA sequencing study of human platelets, several RNAs coding for ubiquitination proteins were detected, including UBEC3 and FBXO18[42]. Taking into consideration that platelets are capable of de novo protein synthesis and contain functional proteasomes[43] it is therefore possible that the impaired aggregation observed in Atxn2$^{-/-}$ mice is caused by increased ubiquitin-mediated protein degradation. This hypothesis is reinforced by observations that integrin αIIbβ3 (CD41/CD61) has been shown to directly bind an E3 ubiquitin ligase and that protein ubiquitination takes place in activated platelets[44], placing protein decay directly downstream of the integrin signalling that was decreased in Atxn2$^{-/-}$ mice.

In a recent publication, Yokoshi and colleagues show that ATXN2 binds to AU- rich elements thereby promoting RNA stability and translation[22]. Using microarray analysis we identified transcripts of which translation was reduced upon ATXN2 knockdown which indeed could indicate faster mRNA decay, but most transcripts

showed increased translation upon ATXN2 knockdown. This seems contradictory with the conclusion that ATXN2 stimulates mRNA translation. It is therefore also possible that the transcripts with increased polysome recruitment upon ATXN2 knockdown are not those regulated by ATXN2, but are positively controlled by mechanisms that remain intact, or even increase upon loss of ATXN2.
Our results clearly demonstrate a role for ATXN2 during megakaryopoiesis and provide the first evidence for the importance of proper protein accumulation for platelet reactivity. Still, there seems to be a discrepancy between the physiological role of ATXN2 and the pathogenicity caused by mutant polyglutamine ATXN2. It was assumed that the clinical manifestations of neurodegenerative diseases are caused by the accumulation of the mutant protein in the cytoplasm of affected neurons, rendering the protein dysfunctional, a state comparable to a loss of function in mice with ablation of *Atxn2*. However, two independent ATXN2 knock out mice strains have been generated, both of which show diverse, but rather subtle, phenotypes[32;33]. It is especially striking that even though mutant ATXN2 was discovered as a protein causing neurodegenerative disease, loss of the physiological protein does not cause severe effects in murine brain[33]. Recent studies showed that mutant ATXN2 does not accumulate by itself, but in complexes containing PABP[20]. Combined with our results showing that loss of ATXN2 results in declined de novo protein synthesis and decreased total cellular protein content, a strong relationship of ATXN2 with protein homeostasis emerges. It is therefore possible that degeneration of affected neurons in SCA2 patients is the result of deregulated protein synthesis caused by the accumulation of PABP-ATXN2 complexes. This aggregation would eventually deprive the cells of essential proteins, leading to impaired neuron functionality. If indeed this hypothesis can be confirmed is beyond the scope of this manuscript but the contribution of ATXN2 to regulation of protein homeostasis may provide new leads to unravel the mechanism behind SCA-2.

ACKNOWLEDGEMENTS

This work was funded by Sanquin Blood Supply, grant PPOC-09-023, The Netherlands Genomics Initiative (NGI-MEC), EuroSCA (LSHM-CT-2004-503304) and the DFG (AU96/14-1).

Authorship contributions and disclosures
SZ, MM, SP, FdS, ED and MH performed experiments, SZ and DCT designed and analyzed experiments and wrote the paper, GA revised the manuscript and provided materials, LG and MM analyzed data and revised the manuscript, MvL analyzed experiments and revised the manuscript. The authors declare no competing financial interests.

Abbreviations List
ATXN2: ATAXIN-2
CLEC-2: C-type lectin-like receptor 2
WT: Wildtype mice

BFU-E: burst-forming unit erythroid
CFU-E: colony-forming unit erythroid
CFU-GM: colony-forming unit granulocyte macrophage
CFU-GEMM: colony forming unit granulocyte, erythrocyte, macrophage
HSPC: hematopoietic stem and progenitor cell
TIA-1: T-cell restricted intracellular antigen-1
DDX6: DEAD-box helicase 6
PABP: poly(A)-binding protein C1
PMA: phorbol myristate acetate

REFERENCE LIST

1. Machlus KR, Italiano JE, Jr. The incredible journey: From megakaryocyte development to platelet formation. J.Cell Biol. 2013;201:785-796.
2. Lordier L, Bluteau D, Jalil A et al. RUNX1-induced silencing of non-muscle myosin heavy chain IIB contributes to megakaryocyte polyploidization. Nat.Commun. 2012;3:717.
3. Lordier L, Jalil A, Aurade F et al. Megakaryocyte endomitosis is a failure of late cytokinesis related to defects in the contractile ring and Rho/Rock signaling. Blood 2008;112:3164-3174.
4. Lordier L, Bluteau D, Jalil A et al. RUNX1-induced silencing of non-muscle myosin heavy chain IIB contributes to megakaryocyte polyploidization. Nat.Commun. 2012;3:717.
5. Geddis AE, Fox NE, Tkachenko E, Kaushansky K. Endomitotic megakaryocytes that form a bipolar spindle exhibit cleavage furrow ingression followed by furrow regression. Cell Cycle 2007;6:455-460.
6. Zimmet J, Ravid K. Polyploidy: occurrence in nature, mechanisms, and significance for the megakaryocyte-platelet system. Exp.Hematol. 2000;28:3-16.
7. Blair P, Flaumenhaft R. Platelet alpha-granules: basic biology and clinical correlates. Blood Rev. 2009;23:177-189.
8. Richardson JL, Shivdasani RA, Boers C, Hartwig JH, Italiano JE, Jr. Mechanisms of organelle transport and capture along proplatelets during platelet production. Blood 2005;106:4066-4075.
9. Thon JN, Italiano JE. Visualization and manipulation of the platelet and megakaryocyte cytoskeleton. Methods Mol.Biol. 2012;788:109-125.
10. Broos K, Feys HB, De Meyer SF, Vanhoorelbeke K, Deckmyn H. Platelets at work in primary hemostasis. Blood Rev. 2011;25:155-167.
11. Ochoa E, Iriondo M, Bielsa A et al. Thrombotic antiphospholipid syndrome shows strong haplotypic association with SH2B3-ATXN2 locus. PLoS.One. 2013;8:e67897.
12. Orru V, Steri M, Sole G et al. Genetic variants regulating immune cell levels in health and disease. Cell 2013;155:242-256.
13. Auburger G, Gispert S, Lahut S et al. 12q24 locus association with type 1 diabetes: SH2B3 or ATXN2? World J.Diabetes 2014;5:316-327.
14. Imbert G, Saudou F, Yvert G et al. Cloning of the gene for spinocerebellar ataxia 2 reveals a locus with high sensitivity to expanded CAG/glutamine repeats. Nat.Genet. 1996;14:285-291.
15. Nechiporuk T, Huynh DP, Figueroa K et al. The mouse SCA2 gene: cDNA sequence, alternative splicing and protein expression. Hum.Mol.Genet. 1998;7:1301-1309.
16. Pulst SM, Nechiporuk A, Nechiporuk T et al. Moderate expansion of a normally biallelic trinucleotide repeat in spinocerebellar ataxia type 2. Nat.Genet. 1996;14:269-276.
17. Elden AC, Kim HJ, Hart MP et al. Ataxin-2 intermediate-length polyglutamine expansions are associated with increased risk for ALS. Nature 2010;466:1069-1075.

18. Nihei Y, Ito D, Suzuki N. Roles of ataxin-2 in pathological cascades mediated by TAR DNA-binding protein 43 (TDP-43) and Fused in Sarcoma (FUS). J.Biol.Chem. 2012;287:41310-41323.

19. Lahut S, Omur O, Uyan O et al. ATXN2 and its neighbouring gene SH2B3 are associated with increased ALS risk in the Turkish population. PLoS.One. 2012;7:e42956.

20. Damrath E, Heck MV, Gispert S et al. ATXN2-CAG42 sequesters PABPC1 into insolubility and induces FBXW8 in cerebellum of old ataxic knock-in mice. PLoS.Genet. 2012;8:e1002920.

21. Albrecht M, Golatta M, Wullner U, Lengauer T. Structural and functional analysis of ataxin-2 and ataxin-3. Eur.J.Biochem. 2004;271:3155-3170.

22. Yokoshi M, Li Q, Yamamoto M et al. Direct Binding of Ataxin-2 to Distinct Elements in 3' UTRs Promotes mRNA Stability and Protein Expression. Mol.Cell 2014;55:186-198.

23. Nonhoff U, Ralser M, Welzel F et al. Ataxin-2 interacts with the DEAD/H-box RNA helicase DDX6 and interferes with P-bodies and stress granules. Mol.Biol.Cell 2007;18:1385-1396.

24. van de Loo S, Eich F, Nonis D, Auburger G, Nowock J. Ataxin-2 associates with rough endoplasmic reticulum. Exp.Neurol. 2009;215:110-118.

25. Satterfield TF, Pallanck LJ. Ataxin-2 and its Drosophila homolog, ATX2, physically assemble with polyribosomes. Hum.Mol.Genet. 2006;15:2523-2532.

26. McCann C, Holohan EE, Das S et al. The Ataxin-2 protein is required for microRNA function and synapse-specific long-term olfactory habituation. Proc.Natl.Acad.Sci.U.S.A 2011;108:E655-E662.

27. Sudhakaran IP, Hillebrand J, Dervan A et al. FMRP and Ataxin-2 function together in long-term olfactory habituation and neuronal translational control. Proc.Natl.Acad. Sci.U.S.A 2014;111:E99-E108.

28. Nonis D, Schmidt MH, van de Loo S et al. Ataxin-2 associates with the endocytosis complex and affects EGF receptor trafficking. Cell Signal. 2008;20:1725-1739.

29. Drost J, Nonis D, Eich F et al. Ataxin-2 modulates the levels of Grb2 and SRC but not ras signaling. J.Mol.Neurosci. 2013;51:68-81.

30. Ralser M, Nonhoff U, Albrecht M et al. Ataxin-2 and huntingtin interact with endophilin-A complexes to function in plastin-associated pathways. Hum.Mol.Genet. 2005;14:2893-2909.

31. Satterfield TF, Jackson SM, Pallanck LJ. A Drosophila homolog of the polyglutamine disease gene SCA2 is a dosage-sensitive regulator of actin filament formation. Genetics 2002;162:1687-1702.

32. Kiehl TR, Nechiporuk A, Figueroa KP et al. Generation and characterization of Sca2 (ataxin-2) knockout mice. Biochem.Biophys.Res.Commun. 2006;339:17-24.

33. Lastres-Becker I, Brodesser S, Lutjohann D et al. Insulin receptor and lipid metabolism pathology in ataxin-2 knock-out mice. Hum.Mol.Genet. 2008;17:1465-1481.

34. De Cuyper IM, Meinders M, van d, V et al. A novel flow cytometry-based platelet aggregation assay. Blood 2013;121:e70-e80.

35. Zeddies S, Jansen SB, di SF et al. MEIS1 regulates early erythroid and megakaryocytic cell fate. Haematologica 2014

36. Joosten M, Blazquez-Domingo M, Lindeboom F et al. Translational control of putative protooncogene Nm23-M2 by cytokines via phosphoinositide 3- kinase signaling. J.Biol. Chem. 2004;279:38169-38176.

37. Mathys H, Basquin J, Ozgur S et al. Structural and biochemical insights to the role of the CCR4-NOT complex and DDX6 ATPase in microRNA repression. Mol.Cell 2014;54:751-765.

38. Gnatenko DV, Dunn JJ, McCorkle SR et al. Transcript profiling of human platelets using microarray and serial analysis of gene expression. Blood 2003;101:2285-2293.

39. Kozlov G, Safaee N, Rosenauer A, Gehring K. Structural basis of binding of P-body-associated proteins GW182 and ataxin-2 by the Mlle domain of poly(A)-binding protein. J.Biol.Chem. 2010;285:13599-13606.

40. Italiano JE, Jr., Richardson JL, Patel-Hett S et al. Angiogenesis is regulated by a novel mechanism: pro- and antiangiogenic proteins are organized into separate platelet alpha granules and differentially released. Blood 2008;111:1227-1233.

41. Cecchetti L, Tolley ND, Michetti N et al. Megakaryocytes differentially sort mRNAs for matrix metalloproteinases and their inhibitors into platelets: a mechanism for regulating synthetic events. Blood 2011;118:1903-1911.

42. Rowley JW, Oler AJ, Tolley ND et al. Genome-wide RNA-seq analysis of human and mouse platelet transcriptomes. Blood 2011;118:e101-e111.

43. Nayak MK, Kumar K, Dash D. Regulation of proteasome activity in activated human platelets. Cell Calcium 2011;49:226-232.

44. Brophy TM, Raab M, Daxecker H et al. RN181, a novel ubiquitin E3 ligase that interacts with the KVGFFKR motif of platelet integrin alpha(IIb)beta3. Biochem.Biophys.Res. Commun. 2008;369:1088-1093.

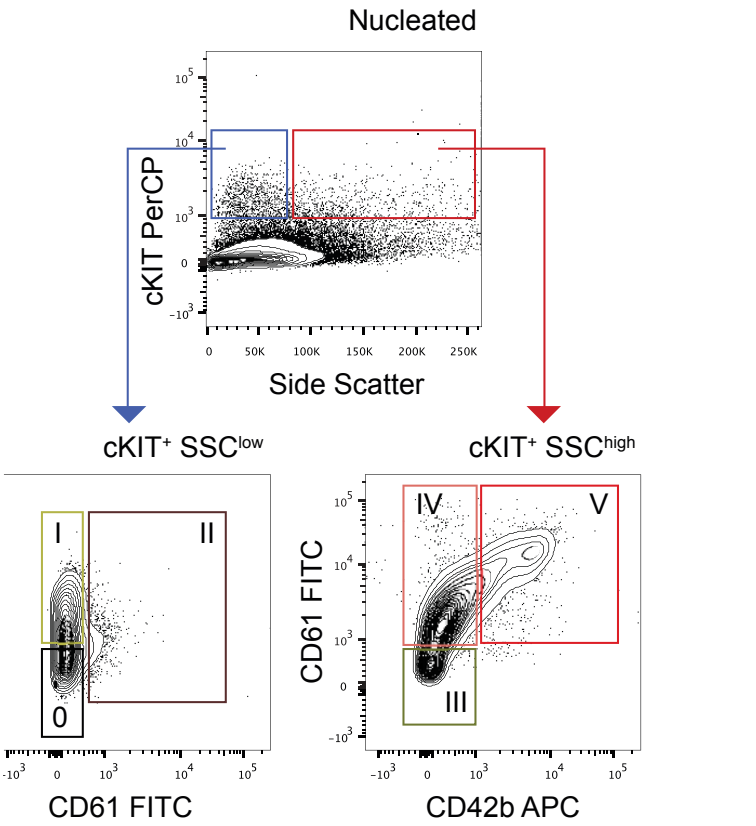

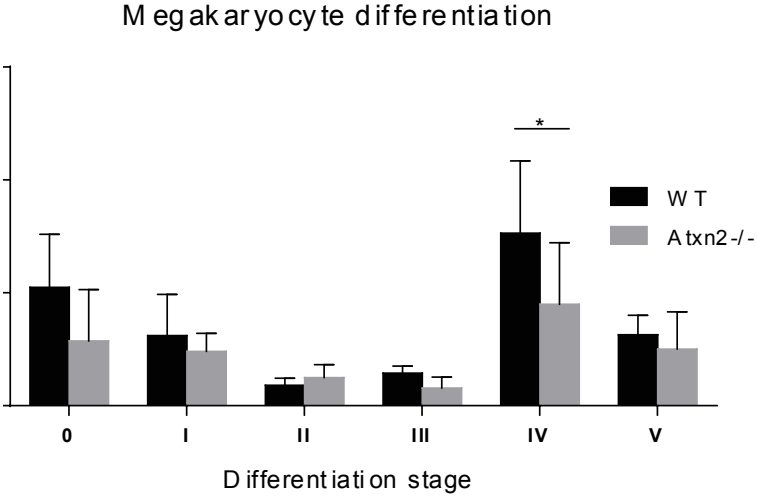

Supplementary Figure 1

Supplemental figure 2

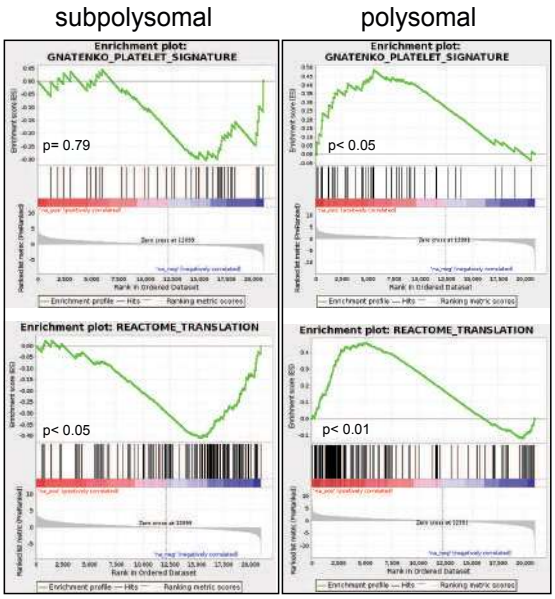

Supplementary Figure 2

Addendum

SAMENVATTING NL
PORTFOLIO
DANKWOORD

NEDERLANDSE SAMENVATTING

Bloedplaatjes, ook wel trombocyten genoemd, zijn kleine cellen in het bloed die voornamelijk betrokken zijn bij snelle, efficiënte bloedstolling. Een tekort aan bloedplaatjes, genaamd trombocytopenie, kan leiden tot ernstige bloeding. Daarnaast is recentelijk gebleken dat ze ook een rol spelen bij afweerreacties.
Bloedplaatjes worden geproduceerd door megakaryocyten, grote, meerkernige cellen die in de mens voornamelijk in het beenmerg, maar in de muis ook in de milt, te vinden zijn. Megakaryocyten ontstaan door differentiatie van hematopoietische stamcellen (HSCs). HSCs zijn voorlopercellen die alle verschillende bloedcomponenten kunnen voortbrengen waaronder rode bloedcellen, witte bloedcellen en bloedplaatjes. De productie van de verschillende bloedcomponenten is afhankelijk van specifieke signalen. Deze signalen bestaan uit hormonen, cytokines en chemokines.
Transcriptiefactoren functioneren als een schakelaar in het DNA: binding van een transcriptiefactor aan een specifieke DNA sequentie zorgt voor meer of minder eiwitproductie. Dergelijke signalen kunnen transcriptiefactoren aan of uit zetten en daarmee de productie van specifieke eiwitten reguleren.
Dit proefschrift beschrijft het onderzoek dat wij hebben gedaan naar een aantal transcriptiefactoren die essentieel blijken te zijn voor de normale ontwikkeling van megakaryocyten. We hebben geconstateerd dat de omgeving waarin de megakaryocyt zich bevindt, van invloed is op hun uiterlijk (fenotype, eiwit-opmaak) en de functionaliteit van bloedplaatjes. Aangezien we met hele kleine bloedmonsters of bloedmonsters met buitnegwwon lage aantallen bloedplaatjes te maken hadden, hebben we daarvoor een nieuwe aggregatie methode ontwikkeld om die functionaliteit van plaatjes goed te kunnen meten.

SAMENVATTING

Bloedplaatjes hebben een aantal essentiële receptoren op hun oppervlakte, onder andere GpVI, Clec2, GPIb/V/IX and GPIIbIIIa, die externe signalen kunnen doorgeven die aanleiding geven tot hun activatie en aggregatie. In ***Hoofdstuk 2*** hebben we een nieuwe aggregatiemethode ontwikkeld die onderscheid kan maken tussen de activatie door deze verschillende receptoren. Daarnaast zijn voor deze methode minder bloedplaatjes nodig dan in de aggregatietest die op dit moment gebruikt wordt voor diagnostiek. Dit is voornamelijk voordelig voor patiënten die lijden aan ernstige trombocytopenie en baby's waarvan niet zo eenvoudig voldoende bloed voor de standaardtesten te verkrijgen is. Ook is deze methode erg geschikt om de aggregatiecapaciteit van bloedplaatjes van muizen mee te testen, omdat deze test slechts weinig bloed vereist.

In ***Hoofdstuk 3*** beschrijven we de rol van de transcriptiefactoren Sp1 en Sp3 in de megakaryopoiese van muizen. Voor dit hoofdstuk is een muis gebruikt met specifiek in megakaryocyten een defect in zowel Sp1 als Sp3. Ons onderzoek wees uit dat Sp1 en Sp3 essentieel zijn voor een normale megakaryocyt ontwikkeling

en plaatjes functionaliteit: de eerder genoemde muis leidt aan ernstige trombocytopenie, een defect in plaatjesfunctionaliteit en heeft een andere ontwikkeling van hun membraanopbouw. Uit eiwit-analyse bleek dat dit komt doordat Sp1 en Sp3 de aanwezigheid van een aantal megakaryocyt- en plaatjes-specifieke eiwitten reguleert, waaronder Mylk, dat essentieel is voor een normaal functionerende megakaryopoiese. Dit hoofdstuk bewijst dat transcriptiefactoren zowel betrokken kunnen zijn bij de regulatie van zogeheten standaard "huishoud-genen" als ook die van cel-specifieke processen.

In ***Hoofdstuk 4*** onderzoeken we de functie van Gata1 in de megakaryopoiese van muizen. Muizen die specifiek in megakaryocyten een deficiëntie hebben in Gata1, lijden aan ernstige trombocytopenie. Ook functioneren hun bloedplaatjes minder na stimulatie van de receptoren Clec2 en GpVI. In dit hoofdstuk verklaren we dit door aan te tonen dat de aanwezigheid van het signaleringsmolecuul Syk, nodig voor activatie van plaatjes via Clec2 en GpVI, direct gereguleerd kan worden door Gata1. Daarnaast zien we tijdens megakaryocytaire ontwikkeling in afwezigheid van Gata1 een nieuwe subgroep megakaryocyten ontstaan. We hebben niet kunnen identificeren of deze nieuwe groep een specifieke functie heeft.

In ***Hoofdstuk 5*** hebben we onderzoek gedaan naar de invloed van de omgeving op megakaryocyt ontwikkeling en plaatjes functie. In de muis bevinden megakaryocyten zich zowel in het beenmerg als in de milt. Normaal gesproken leveren de megakaryocyten in het beenmerg de grootste bijdrage aan de plaatjesproductie. Wij laten in dit hoofdstuk zien dat onder verschillende omstandigheden van hematopoiëtische stress, zoals bij een acute of ontsteking, de bijdrage van megakaryocyten in de milt aan de plaatjesproductie sterk toeneemt. Daarnaast laten wij zien dat de plaatjes die in dit geval geproduceerd worden door de milt megakaryocyten een ander fenotype en functie hebben. Dit zou kunnen betekenen dat deze plaatjes in geval van hematopoiëtische stress anders functioneren.

PORTFOLIO

Name PhD student: Meinders M.
PhD period: 1-9-2010 t/m 1-9-2-14
Name PhD supervisor: Gutierrèz L.

1. PHD TRAINING

	Year	Workload *(Hours/ETCTS)*
Specific courses		
- PHD training course atherosclerosis and thrombosis de hartstichting,	2010	1.2
- Article 9, proefdierkunde	2010	3.9
- Animal handling, general course on mouse techniques	2010	1
- Animal handeling, orbita and check puncture	2011	0.5
- Platelets summer school, Birmingham	2011	1.1
- Anatomy of the house mouse AMC	2012	1.2
- Platelets 2014 Educational Course	2014	0.5
- Mouse techniques, splenectomy	2014	1
Seminars, workshops and master classes		
- Weekly department lectures	2010-	4
- Biweekly Sanquin-wide lectures	2014	2
- Master Class Joe Italiano	2010-	0.1
- Workshop EU-plan Maastricht	2014	0.1
- Master Class Andy Weirich	2010 2012 2013	0.1
Presentations		
- Poster presentation (Papendal) *Defining the role of Caprin 2 in mega karyopoiesis/hematopoiesis*	2010	
- Poster presentation Sanquin Science day *Defining the role of Caprin 2 in mega karyopoiesis/hematopoiesis*	2010	
- Poster presentation course platelets (Birminham, UK) *A new technique to follow proplatelet formation*	2011	
...		

...

- Poster Presentation EU plan (Maastricht) *A new technique to follow proplatelet formation*	2012	
- Poster presentation Sanquin Science day *Sp1/Sp3 double knockout mouse model: A transcription-dependent Bernard-Soulier syndrome phenocopy*	2012	
- Oral presentation Sanquin wide *Diving into murine fetal and adult megakaryopoiesis*	2012	
- Oral presentation ISBT (Amsterdam) *Sp1/Sp3 double knockout mouse model: A transcription-dependent Bernard-Soulier syndrome phenocopy*	2013	
- Poster Presentation ISTH (Amsterdam) *A novel flow cytometry-based platelet aggregation assay*	2013	
- Oral presentation Sanquin wide *Analysis of megakaryocyte-specific Sp1/Sp3 double KO mice reveals transcription program hallmarks during megakaryopoiesis that recapitulate single-gene congenital megakaryocyte pathologies*	2014	
- Oral presentation Platelets (Israel) *Sp1/Sp3 transcription factors regulate hallmarks of megakaryocyte maturation, and platelet formation and function*	2014	
- Poster presentation Platelets (Israel) *Platelet formation under hematopoietic stress*	2014	

(Inter)national conferences		
- Microscopy (Leuven)	2012	1
- EU plan (Maastricht)	2012	1
- ISBT (Amsterdam)	2013	1
- ISTH (Amsterdam)	2013	1
- Platelets 2014 (Israel)	2014	1.2

2. TEACHING

	Year	Workload *(Hours/ETCTS)*
Lecturing		
- Invited lecture, voorlichting biomedical students	2013	
Supervising		
- Rotation Student, 4 weeks (Bachelor)	2011	6
- Rotation Student, 12 weeks (Bachelor)	2012	18

3. PUBLICATIONS

	Year
Peer reviewed	
- The microtubule plus-end tracking protein CLASP2 is required for hematopoiesis and hematopoietic stem cell maintenance. *Drabek K, Gutiérrez L, Vermeij M, Clapes T, Patel SR, Boisset JC, van Haren J, Pereira AL, Liu Z, Akinci U, Nikolic T, van Ijcken W, van den Hout M, Meinders M, Melo C, Sambade C, Drabek D, Hendriks RW, Philipsen S, Mommaas M, Grosveld F, Maiato H, Italiano JE Jr, Robin C, Galjart N.*	2012
- A novel flow cytometry-based platelet aggregation assay. *Meinders M De Cuyper IM, , van de Vijver E, de Korte D, Porcelijn L, de Haas M, Eble JA, Seeger K, Rutella S, Pagliara D, Kuijpers TW, Verhoeven AJ, van den Berg TK, Gutiérrez L.*	2013
- Sp1/Sp3 transcription factors regulate hallmarks of megakaryocyte maturation, and platelet formation and function. *Meinders M, Kulu DI, van de Werken HJ, Hoogenboezem M, Janssen H, Brouwer RW, van Ijcken WF, Rijkers EJ, Demmers JA, Krüger I, van den Berg TK, Suske G, Gutiérrez L, Philipsen S.*	2014

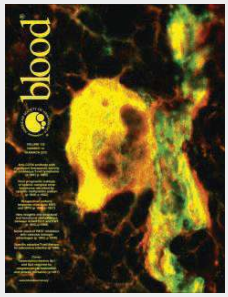

Image used for cover of Blood
March 18, 2015

DANKWOORD

En dan is je boekje bijna klaar, alleen het dankwoord nog. Een niet-onbelangrijk stuk van mijn thesis omdat ik het zeker niet alleen heb kunnen doen. Ik wil dan ook iedereen bedanken die mij zowel in als buiten het lab heeft geholpen.

Als eerste ***Laura***, wat een eer was het om jouw eerste PhD student te mogen zijn. Ondanks de rumoerige periodes, en de incidentele spraakverwarringen gedurende mijn onderzoek, ben je mij altijd blijven steunen. Ik ben je ontzettend dankbaar voor alle inzet en begeleiding. Een begeleider hebben die zonder te zeuren nachten doorwerkt om de stukken zo snel mogelijk gecorrigeerd te hebben is uniek en ik ben je dan ook erg dankbaar. Ik hoop dat je een mooie toekomst tegemoet gaat in de wetenschap. Muchas Gracias!

Taco, als mijn promoter wil ik je bedanken voor alle werkbesprekingen en de richting die je aan mijn project hebt gegeven. Waar mijn focus lag op het onderzoek in de muizen, zorgde jij ervoor dat ik de link met de patient niet vergat. Dankjewel voor alle werkbesprekingen en alle kennis die je gedeeld hebt.

Timo, als student kwam ik solliciteren voor een stageplek op jouw afdeling. Hierbij heb ik een geweldige tijd gehad, ik was dan ook erg blij toen ik werd aangenomen als promotiestudent op jouw afdeling. Ik wil je bedanken voor de kans die je mij gegeven hebt en natuurlijk voor alle input die heeft bijgedragen aan mijn project.

En dan mijn paranimfen
Edit, aka E, jeetje wat heb ik een geluk gehad dat ik jou heb leren kennen gedurende mijn stage, en nog beter tijdens mijn promotie-onderzoek. De vele koffie-dates, zowel op sanquin als daarbuiten en de leuke vakanties die we hebben gehad hebben er zeker toe bijgedragen dat ik kan terug kijken op een geweldige promotietijd. Ik ben dan ook vereerd dat je vandaag naast me staat! Ik verheug me op alle komende koffidates (zowel in real-life als via skype) en weekendjes weg.

Mark, de muizenman. Ondanks dat je in Hoorn woonde - maar wie gaat daar dan ook wonen - was het nooit een probleem om om 7 uur te beginnen. De vele uren in het muizenhuis zijn dan ook van onschatbare waarde geweest voor mijn proefschrift en ik ben je hier dan ook enorm dankbaar voor. Maar natuurlijk ook voor de vele koffiepauzes, de vrimibo's en de leuke uitstapjes die we hebben gehad. Ik hoop dat we er vanavond dan ook nog een mooi feestje van gaan maken!

Dan de plaatjesgroep (en natuurlijk een klein beetje de DCs)
Maaike, bijna tegelijk begonnen en we gingen gezamenlijk door dezelfde fases gedurende onze projecten. Met jouw hulp kon ik het allemaal in perspectief plaatsen en kon ik het allemaal een beetje relativeren. Dankjewel hiervoor.

Iris, onnavolgbaar, altijd wat te vertellen, en vooral erg gezellig, dankjewel voor de leuke tijd.

En ***Annie***, ondanks dat je al in mijn eerste jaar vertrok heb ik veel aan je gehad. Ik hoop dan ook dat we contact houden en dat we nog een paar goede borrels gaan drinken.

BTT, mijn kamergenoten, ***Eric***, ***Richard*** en ***Mya***, dankjewel voor de gezellige tijd op de kamer!

De ***RBC-groep***, mede dankzij jullie leuke werkbesprekingen is de tijd voorbij gevlogen. Ik zie jullie misschien nog terug op een rode bloedcellen congres.

Robin, nogmaals bedankt voor het voordragen aan Ash. Ik had deze positie nooit gevonden zonder jou.

BCR, geweldige collega's, ik heb zo genoten van alle squash uurtjes, survival runs, bbq's in het park en gesprekken op het lab. Ik kan zeker terugkijken op een geweldige tijd mede dankzij jullie.

Sietse, het weekje schrijven op Texel was zeker de moeite waard, zowel veel gewerkt als veel geleerd van vogels ;). Nog een paar loodjes en dan ben je klaar.

Roel, jou zie ik nog wel terug op een paar goede feestjes!

Ida en ***Christine***, ondanks dat jullie pas in mijn laatste jaar bij Sanquin kwamen, heb ik erg genoten van de gesprekken en de goede adviezen. Veel succes beiden bij Sanquin de komende tijd.

MCBers, de borrels waren zeker niet hetzelfde zonder jullie!

En ***Jeffrey***, wat was het fijn om in de laatste maanden te weten dat er nog iemand was die dezelfde stress ervoer. Heel succes over twee dagen! Je gaat het geweldig doen.

Centrale Faciliteit, dank jullie wel voor de flexibiliteit. Altijd op zoek naar een oplossing als ik weer eens 20 platen moest facsen. Ik had het zeker niet gered zonder jullie.

De ***dierverzorgens in het muizenhuis*** en ***Marleen*** in het bijzonder. Dankjewel voor het uitstekend verzorgen van al mijn dieren en de flexibiliteit. Het was nooit een probleem als ik weer eens last-minute iets nodig had of hulp kon gebruiken tijdens de operaties. Dankjewel hiervoor.

Group-Ash. I never thought I could feel at home so fast in a new country and in a new lab. I feel blessed to be part of your group.

Dan mijn lieve vrienden en familie
Floor, ***Marloes*** en ***Marlon***. Ondanks dat ik jullie niet zo vaak zie als ik zou willen,

zijn jullie er al die jaren voor mij geweest. Of het nou 'schrijfweekjes' waren in Italië of Turkije, uitwaaien in Scheveningen of een dagje naar de sauna, het heeft er zeker toe bijgedragen dat ik weer met een frisse blik aan het werk kon.

US dames 1 en 2. Dank jullie wel voor jullie begrip en geduld. Nooit was het een probleem als ik weer eens te laat op training kwam of chagrijnig was van een lange dag werk. Omdat we het niet vaak over werk hadden, kon ik het heerlijk loslaten tijdens trainen, de wedstrijden en natuurlijk tijdens de borrels en feestjes erna. Deze leuke en gezellige groep is zeker iets wat ik ga missen in Bristol.

Jenny, dankjewel dat je de lay-out van mijn boekje wilde verzorgen. En natuurlijk voor alle fijne gesprekken, feestjes en goede adviezen.

Nienke, mijn grote zus. Tijdens de meest stressvolle periode in mijn promotie traject kon ik altijd bij je terecht. Of het nou voor een snel kopje koffie was op zaterdag ochtend of samen eten. Ik baalde er dan onwijs van toen je vertelde dat je naar Indonesië vertrok. Gelukkig is de afstand niet zo groot dankzij viber/skype en ben je ook blijven steunen gedurende de laatste periode tijdens onze ontbijt gesprekken. Vind het dan ook heel fijn dat je voor deze dag terug bent gekomen.

En dan last but zeker not least, ***mama en papa***, ik wil jullie bedanken voor de onvoorwaardelijke steun en de ongetemde interesse. Al moet het soms onnavolgbaar geweest zijn wat ik deed, jullie hebben altijd geprobeerd het te begrijpen en keer op keer weer gevraagd wat ik nou exact aan het doen was. Bedankt voor alles.